AN INVESTIGATION INTO PASSENGER CAR STRUCTURAL DYNAMIC BEHAVIOR AND ITS RELATIONSHIP TO RIDE COMFORT

ZAHIR HANOUF

THESIS SUBMITTED IN FULFILMENT FOR THE DEGREE OF DOCTOR OF PHILOSOPHY

FACULTY OF ENGINEERING AND BUILT ENVIRONMENT
UNIVERSITY KEBANGSAAN MALAYSIA
BANGI

2014

KAJIAN MENGENAI PERILAKU DINAMIK STRUKTUR KERETA PENUMPANG DAN HUBUNGANNYA DENGAN KESELESAAN PENUNGGANGAN

ZAHIR HANOUF

TESIS YANG DIKEMUKAKAN UNTUK MEMPEROLEH IJAZAH DOKTOR FALSAFAH

FAKULTI KEJURUTERAAN DAN ALAM BINA
UNIVERSITI KEBANGSAAN MALAYSIA
BANGI

2014

DECLARATION

I hereby declare that the work in this thesis is my own except for quotations and summaries which have been duly acknowledged.

15 May 2014

ZAHIR HANOUF
P36303

ACKNOWLEDGMENTS

I would like to thank Allah for providing this opportunity to pursue my studies as well as for instilling the patience and perseverance to successfully complete my Ph.D.
The research was done in the Department of mechanical Engineering, University Kebangsaan Malaysia Kuala Lumpur and International Islamic University Malaysia, under the supervision of Prof. Dr. Mohd. Jailani Mohd. Nor (UKM) and Assoc. Prof. Dr. Waleed F. Faris (IIUM).

I would like to express my sincere gratitude to my supervisor Prof. Dr. Mohd. Jailani Mohd for his patience, encouragements, kindness, guidance and concern, throughout the research. His esteemed opinions on my research have been extremely helpful in successfully completing my thesis.

My deep appreciation and earnest thanks to my co-supervisor Assoc. Prof. Dr. Waleed F. Faris from Mechanical Engineering Department IIUM for his kind assistance with my research work. With his help, my research work certainly became easier to complete as planned.

I am grateful to Mr Nik Zahir Mohd Idris and Bahtiar Affandi from S&V Teknik (Malaysia) Sdn Bhd for providing me the equipment and advising me conducting my experiments and doing analysis.

I would also thank all staff in our group specially Dr Mohammad Hosseini Fouladi Captain Othman and Dian Darina Indah. I have learned a lot from you and I am always grateful for your time, patience and knowledgeable information you shared with me. Moreover, special gratitude goes to Kartini Ahmad from Department of mathematics CFS IIUM for translating the abstract into Bahasa Malaysia. My sincere appreciation is also extended to all colleagues from department of mathematics CFS IIUM.

This acknowledgment is would not be complete without thanking my wife, who constantly encouraged me, and was always supportive and understanding of my time constraints completing my Ph.D. My whole hearted appreciation to my beautiful daughters Wissal, Iatissam, Hanin and Ra'afa.

Finally, I also would like to thank the most important people in my life, my mother, father, brothers, sisters and other family members specially Benchabane Abdelmoumen who have provided their support and patience throughout this time.

ABSTRACT

Dynamic characterization of vehicle structures is a crucial step in NVC analysis and helps in refining the vibration and noise in new vehicles, which is becoming a marketing edge as well. Therefore understanding dynamic behavior of each structural part of the vehicle is a major requirement in improving the NVC characteristics of a vehicle. The main focus of this research is to investigate structural dynamic behavior of a passenger car using modal analysis part by part technique and apply this method to derive the interior noise sources. In the first part of this work computational modal analysis part by part tests were carried out to identify the dynamic parameters of the passenger car. Two softwares were used to carry out these tests namely VPG 3.2 and LS-Dyna. Finite elements models of the different parts of the car are constructed using VPG 3.2 software. Ls-Dyna pre and post processing was used to identify and analyze the dynamic behavior of each car components panels. These tests had successfully produced natural frequencies and their associated mode shapes of such panels like trunk, hood, roof and door panels. In the second part of this research, experimental modal analysis part by part is performed on the selected car panels to extract modal parameters namely frequencies and mode shapes. The study establishes the step-by-step procedures to carry out experimental modal analysis on the car structures, using single input excitation and multi-output responses (SIMO) technique. To ensure the validity of the results obtained by the previous method an inverse method was done by fixing the response and moving the excitation and the results found were absolutely the same. Finally, comparison between results obtained from both analyses showed good similarity in both frequencies and mode shapes. Conclusion drawn from this part of study was that modal analysis part-by-part can be strongly used to establish the dynamic characteristics of the whole car. Furthermore, the developed method is also used to show the relationship between structural vibration of the car panels and the passengers' noise comfort inside the cabin. Two analysis techniques were used for this matter, namely signal analysis and modal analysis. The main goal of these techniques is to identify the dominating frequencies inside the passenger car and then diagnose the structural vibration components that can be the sources of the interior noise. The results showed that the dominating peaks inside the passenger cabin is associated with the resonance of the front suspension system at 62 Hz and the resonance of the cross roof beam at 163 Hz and 173 Hz. These frequencies are in the frequency range of the passenger's discomfort. Even though, there is an arguing among researchers in the open literature review regarding the frequency range of discomfort, still the most researchers are agreed that the frequency range of discomfort can be either less than 100Hz or less than 200 Hz which is strongly agreed with the findings of this study. This study is conducted on a Malaysian passenger car, because studies on noise and vibration comfort in Malaysian automotive industry still in its infancy stage. Most researches conducted in Malaysia are concentrated on the measurement of the comfort or discomfort inside the cabin by using surveys. However, there is a lack of research about determination of the sources of noise and vibration that affects the passenger's discomfort. Therefore, it is important that both methods should be investigated in order to identify the sources of discomfort and how they affect the passenger's comfort, especially Malaysia has its own automotive industry. This studycan be considered as an important preliminary effort to understand the effect of noise and vibration towards Malaysian passengers comfort.

ABSTRAK

Pencirian dinamik struktur kenderaan merupakan langkah penting dalam analisis NVH dan ianya membantu memperbaiki getaran dan hingar kenderaan baru yang merupakan salah satu faktor pemasaran. Oleh itu, memahami perilaku dinamik dari setiap bahagian struktur kenderaan ada keperluan utama untuk memperbaiki ciri-ciri NVH kenderaan. Fokus utama kajian ini adalah untuk menyiasat perilaku struktur dinamik kereta penumpang secara ujikaji dan teori analisis ragaman. Pada bahagian pertama kajian, ujian teori analisis ragaman telah digunakan bagi mengenal pasti parameter-parameter dinamik kereta menggunakan analisis ragaman bahagian-demi-bahagian. Dua perisian telah digunakan untuk melakukan ujian ini. Model unsur terhingga untuk setiap bahagian kereta telah dibangunkan menggunakan perisian VPG 3.2. Perisian Ls-dyna pula telah digunakan untuk menganalisis perilaku dinamik panel-panel komponen kereta. Ujian ini telah berjaya menghasilkan frekuensi tabii dan bentuk-bentuk mod bersekutu untuk badan, penutup enjin, bumbung dan panel pintu kereta. Seterusnya di bahagian kedua kajian ini, analisis ragaman ujikaji telah dijalankan pada panel kereta untuk mengekstrak parameter ragaman iaitu frekuensi dan bentuk mod. Tesis ini menetapkan prosedur langkah demi langkah dalam melakukan analisis ragaman ujikaji pada struktur kereta menggunakan kaedah pengujaan tunggal dan sambutan-pelbagai. Untuk memastikan kesahihan keputusan yang diperoleh dengan kaedah terdahulu, kaedah songsang dijalankan dengan menetapkan sambutan dan mengerakkan pengujaan dan keputusan yang didapati adalah sama. Akhir sekali, perbandingan yang diperoleh dari kedua-dua analisis menunjukkan persamaan rapat pada kedua-dua frekuensi dan bentuk mod. Kesimpulan yang boleh diambil dari kajian ini adalah analisis ragaman bahagian-demi-bahagian boleh digunakan dengan baik untuk membandingkan kaedah analisis ragaman secara teori dan ujikaji dalam menentukan parameter dinamik untuk keseluruhan kereta. Kajian ini juga menunjukkan hubungan antara getaran struktur dan keselesaan hingar penumpang di dalam kabin. Dua teknik analisis telah digunakan iaitu analisis isyarat dan analisis ragaman. Tujuan utama teknik-teknik tersebut adalah untuk mengenal pasti sumber komponen getaran struktur yang menyumbang kepada hingar dalaman. Keputusan menunjukkan puncak-puncak dominan di dalam kabin penumpang adalah bersekutu dengan salunan sistem ampaian depan pada 62 Hz dan salunan alang silang bumbung pada 163 Hz dan 173 Hz, Dalam literatur wujud perselisihan antara penyelidik mengenai julat frekuensi ketidakselesaan. Walau bagaimanapun kebanyakan penyelidik bersetuju bahawa julat frekuensi ketidakselesaan boleh kurang dari 100 Hz atau kurang dari 200 Hz. Ini bersesuaian dengan penemuan dalam kajian ini. Kajian telah dilakukan ke atas kereta penumpang Malaysia kerana kajian keselesaan dan ketidakselesaan adalah pada peringkat awal dalam industri automotif Malaysia. Kebanyakan penyelidikan dalam Malaysia tertumpu kepada pengukuran keselesaan dan ketidakselesaan dalam kabin menggunakan soal-selidik. Sebaliknya ada kekurangan penyelidikan mengenai sumber hingar dan getaran yang memberi kesan kepada ketidakselesaan penumpang. Oleh itu adalah mustahak untuk faktor ketidakselesaan, penentuan sumber dan kesan mereka ke atas ketidakselesaan penumpang diselidik secara serentak terutamanya dalam industri automotif Malaysia. Kajian ini boleh dianggap sebagai kajian permulaan yang mustahak dalam usaha untuk memahami kesan hingar dan getaran kepada keselesaan penumpang Malaysia.

CONTENTS

LIST OF FIGURES

LIST OF TABLES

LIST OF ABRIVIATION

CAD	Computer-Aided Design
CAE	Computer aided engineering
DDS	Data Dependent Systems
DFT	Digital Fourier Transform
DOF	Degree -of -freedom
EMA	Experimental analysis
FE	Finite element
FEA	Finite element analysis
FEM	Finite element method
FFT	Fast Fourier Transform
FRF	Frequency response function
LDV	Laser Doppler vibrometer
LSTC	Livermore Software Technology Cooperation
MAC	Modal assurance criteria
MPP	Massively Parallel Processing
NCAC	National Crash Analysis Centre)
NCAP	New Car Assessment Program
NVH	Noise, vibration and harshness
ODS	Operational deflection Shapes
RES	Real part of the eigen value of squeal mode
SAE	Society of Automotive Engineers
SDOF	Single degree of freedom
SPH	Smooth Partial Hydrodynamic
SPM	Substructure's modal parameters
VPG	Virtual Proving Ground
1D	One-dimensional
2D	Two-dimensional
3D	Three-dimensiona

CHAPTER 1

INTRODUCTION

1.1 MOTIVATION

The size of requirement for industrial vehicles excelling in comfort and reliability has become very large for the last few decades. Due to the demands of high speed operation and the use of light weight and flexible structures in modern machinery, static measurements of stress/strain properties are not sufficient. One of the main areas that should be considered when investigating comfort and reliability of a vehicle is the structural vibration measurements and analysis of its components. This is leads to the improvement of its vibro-acoustic quality as we know that structural vibration has a strong relationship with the interior noise.

Vehicle structures are one essential part of the development targets in automotive industries. Researchers are looking at different perspectives in them such as material used, strength, crashworthiness, and noise and vibration. Understanding the dynamic behavior of a vehicle and getting control of it requires the identification of each structural component of the vehicle such as door, trunk, etc.

Knowing dynamic characteristics of a vehicle components such as natural frequencies, mode shapes and damping ratios are essential for vehicle structural safety evaluation, longer fatigue life, comfort and structural health monitoring. By knowing the dynamic behavior of a structure under its natural frequencies, we could determine the location of damaged parts of the structure before it starts causing losses of life, because damaged structure tends to exhibit excessive deformation under the same magnitude of excitation. Also by knowing the dynamic characteristics of a structure, engineers can design better structures.

Weight, stiffness and damping of the structure have a strong effect on the natural frequencies and mode shapes, which they can determine where these natural frequencies and mode shapes will exist. For that reason, we have to look into these frequencies and know how they affect the vibration behavior of the structure when a force excited it.

Understanding the mode shapes and knowing how the structure vibrating when excited by an input, helps engineers to design good structures with improved vibration. Therefore, most of the developments of the structural vibration analysis tools in the new era of engineering came about due to the need to solve vibration problems. Modal analysis in both methods (experimental and computational) is one of the useful tools that provide an understanding of structural dynamic characteristics, operating condition and performance criteria that makes design of optimal dynamic behavior or solving structural dynamics problems in the existing designs.

In the worldwide, no researches have been conducted to identify the dynamic characteristics of the whole passenger car by comparing the experimental and computational modal analysis. In this investigation we have developed a new technique to compare the two methods is called modal analysis part by part. This technique has been extended to find the relationship between the structural vibration and the interior noise and also to identify the main contributor to the interior noise. However, there is much work has been done on vehicle components using experimental or computational modal analysis only or both. Also there is some researches conducted on the whole car, but by using experimental modal analysis only or computational modal analysis only, but not both as shown in the open literature review in the next chapter.

The typical automotive system of this project was a local passenger car which is large demanded in the market. To be competitive in the market, its noise and vibration comfort should be compatible with the customer's quality requirements.

1.2 PROBLEM STATEMENT

Noise and vibration comfort in automotive industry has become a competitive target for car selling. The more refined the car is, the more selling potential it will be. In improving noise, vibration and comfort (NVC) characteristics of a vehicle, it is a must to understand the dynamic behavior and characteristics of each structural part of the vehicle. This issue has been lacking in the open scientific literature. The only available information is modal analysis of the body-in-white and chassis but the individual structural components for the whole car still not studied yet. It has been researched and studied for decades how computational and experimental modal analysis methods are used to solve noise and vibration problems in automotive and also the importance of the combination between them in order to provide a comprehensive understanding of the dynamic characteristics of vehicles prior and after manufacturing which is leading to improve their noise, vibration and comfort. However, this method has been used successfully for simple structure. However, for complex structure like cars still under investigation, because of no good linearity between the excitation force and the response force which for sure affect the quality of the results. Therefore, to solve this problem we have developed a new method. This method is based on modal analysis part by part and was validated by a comparison between experimental and computational modal analysis. It helps us to identify easily the individual structural component of the vehicle that can be radiate high vibration or contribute to the interior noise and then getting control of it.

In this work, we are addressing this point by detailed study for a specific passenger car model as a case study using modal analysis part by part. In addition, the same method has been used to investigate the relationship between the structural vibrations of the car components with the interior noise and comfort.

1.3 RESEARCH SCOPE

The aim of this research is to implement an accurate and reliable method to investigate the dynamic characteristics of a complex structure, hence assures easier and faster implementation. In the first part of this work computational and experimental modal analysis part-by-part is utilized to determine and analyze the dynamic characteristics of a specific vehicle structure. Only few vehicle panels are considered in this study in order to find its natural frequencies and their corresponding mode shapes. The developed method is validated by comparing the results obtained from experimental modal analysis and computational modal analysis techniques.

The second part of this study carried out signal analysis and modal analysis part by part techniques to quantify noise and vibration comfort interior the vehicle cabin. Signal analysis technique is accomplished to discover the dominant noise component inside a stationary vehicle compartment. Contribution of the engine vibration and the engine sound to the interior noise is identified. It was found that the engine vibration is the main contributor to the interior noise. Afterward, contour of sound pressure level over horizontal cross-sectional plane close to the passenger's ear is investigated to estimate the dominating noise frequencies inside the passenger cabin. This was carried out under front random excitation and rear random excitation.

Modal analysis part by part method was applied to determine the dynamic characteristics of every component of the vehicle body panel that would be expected to contribute to the interior noise.

Finally, a comparison between signal analysis and modal analysis results showed a good relationship between the structural vibration and the passenger's comfort inside the passenger cabin.

1.4 RESEARCH OBJECTIVES

This study aiming to:

1. Investigate the dynamic characteristics of a vehicle structure using modal analysis part-by-part.
2. Validate and verify modal analysis part-by-part method through comparing the experimental and computational results.
3. Develop the relationship between structural vibration and the interior noise comfort.
4. Apply modal analysis part-by-part in order to derive the interior noise sources.

1.5 THESIS STRUCTURE

This research is divided into seven main Chapters.

Chapter 1 discusses motivation, problem statement and the objectives of the study.

Chapter 2 describes the literature review of the previous studies. It covers the review of some of the journal articles, proceedings and publications which are related to the objectives of this study.

Chapter 3 presents theoretical background of the modal analysis which is the core of this research and ride comfort of passenger cars and finally the human response to noise and vibration.

Chapter 4 presents the methodology of computational and experimental modal analysis which explains the instrumentations and techniques used in the experiments in order to obtain accurate results. Moreover, it presenting and discussing computational results to be compared latter with experimental results.

Chapter 5 presenting and discussing experimental modal analysis results of the car panels and its comparison with computational modal analysis results.

Chapter 6 introduces a study to determine the relationship between structural vibration and the passenger comfort inside the passenger car. It presents the use of the signal analysis and modal analysis to evaluate the sources of the interior noise.

Chapter 7 covers general discussions and conclusions drawn based on the results of the analysis and finally give some recommendations for further work in the area.

CHAPTER 2

LITERATURE REVIEW

2.1 INTRODUCTION

Vibration analysis is an important part in any designing process of vehicles. Researchers and automotive manufacturers have invested and spent a lot of money over the last decades to improve and enhance the vibro-acoustics performance of their product. Large numbers of researches have been carried out regarding the performance, the response of components to static and dynamic loads, crashworthiness, safety and others. Particularly, with the growing of simulation capability usage by using computer aided engineering analysis in combination with prototype development and testing. This chapter listed some literatures deemed to be significant to this research that is conducted on structural dynamic of a passenger car using computational and experimental modal analysis. Based on the research scope and objectives of this work, three sections are introduced in this literature review, namely; computational modal analysis, experimental modal analysis and combination between computational and experimental modal analysis.

2.2 COMPUTATIONAL MODAL ANALYSIS FOR VEHICLE STRUCTURES

Because of the significant of dynamic behavior of engineering structures, it becomes important to design them with proper consideration of dynamics. Finite element analysis as a computational derived by theoretical consideration has provided engineers with good design tool, especially when dynamic properties need to be analyzed. This numerical analysis requires rigorous theoretical guidance to ascertain meaningful outcomes in relation to structural dynamics. An important part of dynamic finite element analysis is computational modal analysis. Computational modal analysis method played an important role in understanding car components dynamics by finding their frequencies and the corresponding mode shapes prior their realization.

By the early 70's, Finite Element Analysis (FEA) was limited to expensive mainframe computers generally owned by the aeronautics, automotive, defense, and nuclear industries. Since the rapid decline in the cost of computers and the phenomenal increase in computing power, FEA has been developed to an incredible precision. Present day supercomputers are now able to produce accurate results for all kinds of parameters. There is a lot of researches conducted in the last decade provide a comprehensive source of information. This information can be used as a guideline to make this work more successful. The following are samples of researches performed on structural dynamic analysis of vehicles using computational modal analysis method.

A computational modal analysis was used to investigate the dynamic characteristic of a truck chassis design to determine the relationship between road excitations and the vibration and strength of the truck chassis. The responses of the truck chassis which include stress distribution and displacement under various loading condition were also investigated. There are two types of structural analysis carried out; normal mode analysis to determine the natural frequencies and mode shapes, and the linear static stress analysis to look into the stress distribution and deformation pattern of the chassis under static load. Different boundary conditions were used for each analysis. In normal mode analysis, free-free boundary conditions were applied to the truck chassis model, with no constraint applied to the chassis model. For static analysis, the boundary conditions are used to represent the real operation environment of the truck chassis. In normal mode analysis, no load was applied to the truck chassis model. In static mode -when the truck is stationary- the loads from the weights of the components like cab, engine, gear box, fuel tank, exhaust and payload were applied to the mounting brackets of the components. It was found that the road excitation is the main disturbance to the truck chassis as the chassis natural frequencies lie within the road excitation frequency range. Furthermore, the determination of the suitable mounting locations of components such as engine and suspension system was possible from the mode shape (Teo & Roslan 2007). Another work was also carried out by (Kassahun 2008) on static and dynamic analysis of a commercial vehicle structure (van body). The method used was finite element modeling and analysis for which the inputs were obtained from quarter car model analysis. The dynamic analysis includes only modal and random response analysis of the structures. In the dynamic analysis, damping properties of the structure were not considered, only the damping due to shock absorber of the vehicle was included in the analysis. The analysis was carried out for the main load bearing structure of the vehicle, i.e., chassis side frames and cross members, steel frames of the van body structure, and cab. The effect of the engine was taken into account by distributing its weight into the side frames of the chassis. The responses to static loads and random excitation caused by road roughness were determined. Components and~~,~~ particularly areas which are much affected by the different loads were indentified. A further method was reported and validated by (Abrams 2008) using an engine as a structural member of a formula of Society of Automotive Engineers (SAE) (race car chassis. A modal analysis was used with a beam mesh of the chassis to provide relative comparison; with and without structural support from an engine. It was also used to validate the assumption that chassis stiffness would increase an increase of chassis stiffness. Results confirmed that providing structural support at engine mounting points of the chassis increased the stiffness and changed the first elastic mode of vibration from bending to torsion. Additionally, a static analysis was used to measure chassis deflection~~,~~ and established a decrease in deflection when structural support was provided at the engine mounting points of the chassis. This report’s conclusion indicated that using the engine as structural member significantly improves the stiffness of the chassis.

In a different study (Zhanwang & Chen 2000), finite element model for Mini-car Changan Star 6350 using SDRC/I-DEAS was developed. The model was imported to MSC. Patran to generate the mesh and the dynamic analysis of the model was accomplished using MSC.Nastran. The analysis included modal analysis of the load bearing structures, the chassis and the body structure frame, in which the first 100 natural frequencies were determined in torsion and bending modes, and transient dynamic analysis of the structures due to road loads that were introduced in the form of acceleration excitations. Results show good consistency with experimental results, therefore, ability of Mini car to meet dynamic design requirements was confirmed. The implementation of FE methods for dynamic analysis of heavy trucks was presented by

(Johansson & Gustavsson 2000). The proposed approach involves the development of FE model of the vehicle and its subsystems, i.e. frame, superstructure, engine, cab, axles and chassis suspensions, and steering system. In addition, modeling problems such as size reduction, global motion and centrifugal forces, lateral tire model and gyroscopic moments were also taken into account. There was a focus on the analysis of the road, wheel, brake, and driveline induced vibrations, static load cases and fatigue life prediction. An example was presented which shows the lateral and vertical acceleration of the cab structure due to periodic excitation of axle due to wheel run out. It was concluded that, FE-based complete vehicle analysis has the advantage to cover broad range of analyses with one type of model.

The optimization of light weight bus side structures was reported recently (Lan et al. 2004). The optimization targeted the reduction of the number as well as weight of different parts in the whole body structure. For this purpose, two scenarios, with and without supporting structures between longitudinal waist beams of the side frame were considered. The FE-model for the structure without the supporting structure was developed using the computer package UG and mesh generated in MSC.Patran, while the FE Analysis was completed using ANSYS. The deflections and stresses under static loading case were determined, modal analyses were performed too. All the results obtained were compared with experimental results. In addition, sensitivity analysis, selecting different important component dimensions, and light weight optimization were studied. The study was stated that the structure with support enables significant alleviation of body weight and satisfactory performance requirements were achieved. Recently, a comparative study was conducted between analytical and numerical methods for modeling automotive dissipative silencers with mean flow (Kirby 2009). The study was based on the assumption that equivalent numerical techniques are more computationally expensive than analytical techniques. The validity of this assumption was investigated and the relative speed and accuracy of two analytic methods were compared to two numerical methods for a uniform dissipative silencer that contains a bulker acting porous material separated from a mean gas flow by a perforated pipe. The numerical methods were developed in this investigation with a view to speeding up transmission loss computation, and were based on a mode matching scheme and a hybrid finite element method. The results presented in this study demonstrate excellent agreement between analytic and numerical models provided a sufficient number of propagating acoustic modes were retained. However, the numerical mode matching method was shown to be the fastest method, significantly outperforming an equivalent analytic technique. Moreover, the hybrid finite element method was demonstrated to be as fast as the analytic technique. The conclusion of this study was that both numerical techniques deliver fast and accurate predictions and was capable of outperforming equivalent analytic methods for automotive dissipative silencers. The possible causes of the failure of an exhaust system for heavy duty commercial trucks and the possible solutions were examined in a recent study (Vascncellose et al. 2003). The researchers describe the use of computer simulation supported by experimental data on the design process of the exhaust system, with regard to structural behavior. A finite element model was generated including the complete vehicle and the exhaust system. Static and dynamic analyses were performed in MSC.Nastran software simulating different loading conditions and system configurations. The results obtained assured the structural integrity of the modified exhaust system when implemented on the vehicle and also contribute to a better understanding of this system behavior and its structural strength. Generally, it was verified that numerical models validated with experimental data are a powerful tool during the development phases of a new vehicle, reducing project time and costs.

The load transfer paths in the cabin structures of heavy-duty trucks under static loading were investigated by (Hiroaki et al. 2003). The results were applied to reduce vibration in cabins. In a preliminary simulation using a simple model, it was shown that the floor panel vibration was closely related to the stiffness of the front cross-member of the floor structure. The load path analyses using the finite element method showed that the low stiffness of the front cross-member was caused by discontinuities and non uniformities in the load paths. In addition, a numerical modeling approach for investigating the onset of squeal in a drum brake system was proposed few years back (Jinchun et al. 2006). The brake system model was based on the modal information extracted from finite element models for individual brake components. The component models of drum and shoes were coupled by the shoe lining material which was modeled as springs located at the centroids of discretized drum and shoe interface elements. The developed multi degree of freedom coupled brake system model is a linear non-selfadjoint system. Its vibrational characteristics were determined by a complex eigen-value analysis. The study showed that both the frequency separation between two system modes due to static coupling and their associated mode shapes played an important role in mode merging. Mode merging and veering were identified as two important features of modes exhibiting strong interactions, and those modes were likely candidates that lead to coupled-mode instability. Techniques were developed for a parameter sensitivity analysis with respect to lining stiffness and the stiffness of the brake actuation system. In a new research work (Jae-Yeol Park & Singh 2010). The effect of spectrally varying mount properties (including stiffness and damping) was examined analytically on the dynamics of power train motions under torque excitation. This work is an extension of (Jeong and Singh 2000) and (Park and Singh 2008). To overcome the deficiency of the direct inversion method (limited to only the frequency domain analysis), two methods were developed that described the mount elements via a transfer function (in Laplace domain) or analogous mechanical model. New analytical formulations were verified by comparing the frequency responses with numerical results obtained by the direct inversion method (based on Voigt type mount model). Eigensolutions and transient responses of a spectrally varying mounting system were also predicted from new models. Based on complex eigenstructure, new coupling indices, including modal kinetic energy fractions, were defined for each method. Complex eigenvalue problem formulation with spectrally varying properties provides a closer match with measured natural frequencies than the real eigensolution with frequency-independent mounts. Given spectral variance in the mount properties, a simple roll mode decoupling scheme was suggested for the power train isolation system. Finally, an axiom for torque roll axis decoupling was provided by employing direct and adjoint eigenvalue problems.

A method for calculating steady state displacement response and force transmission at the wheel axle of a pneumatic tire-suspension system due to a steady state force or displacement excitation at the tire to ground contact point was also reported (Kung et al. 1986). The method required the frequency responses (or receptances) of both tire-wheel and suspension units. The frequency response of the tire-wheel unit was obtained by using modal expansion method. The natural frequencies and mode shapes of the tire-wheel unit were obtained by using a geometrically non-linear ring type, thin shell finite element of laminate composite. The frequency response of the suspension unit was obtained analytically. These frequency responses were used to calculate the force-input and the displacement-input responses at the wheel axle. This method allows the freedom of designing a vehicle and its tires independently and still achieving optimum dynamic performance.

Finally, an interesting approach for a Reduced Beam and Joint Modeling approach to optimize and analyze global vehicle body dynamics, specifically bending and torsion modes was developed currently (Donders et al. 2009). This is a concept of Computer-Aided Engineering (CAE) modeling approach based on predecessor FE models, which can be used to improve the fundamental body noise, vibration and harshness behavior (global modes) by means of beam and joint modifications. Modifications in the body beam-like sections and in the joints were analyzed using body reduced modal model. This small-sized model was used to quickly and accurately optimize the low-frequency vehicle performance. The modifications were considered with respect to the existing (predecessor) model. Equivalent beam properties were estimated from the body FE model; modifications in the beam-like sections were implemented with beam elements from a standard FE library. The joint modifications were considered through static super elements: stiffness formulations between the end points of the joint connected to the beam layout. The validity of the approach was first demonstrated on simple example models. An industrial vehicle body in white (BIW) application case was subsequently presented. A beam and joint layout was created, and used for a fast sensitivity analysis to identify suitable modifications to improve the global modes. Next, two application cases were presented. First, a fast optimization analysis was performed to optimize the global body modes. Subsequently, suitable physical modifications were identified and applied to the full FE model; it was shown that the effect of these physical modifications is accurately predicted with fast sensitivity analysis. In summary, a static Beam Force Analysis strategy can be used to provide complementary insight in the vehicle body design in an early design stage, which can be employed to improve the static body performance.

As can be seen the above researches focus on the finite element analysis of vehicles and their different components, i.e. engine, steering system, superstructure, cab and axles and chassis suspensions. Different computer packages such as ANSYS, ADAMS, DADS, MSC.patran/MSC.Natran and IDEAS were used to develop the virtual models of vehicles and their components in order to perform the required analysis the method still recognized as an acceptable tool for designing simple structural design. However, the confidence in the results for complex structures still questionable because of several simplifications in the model. Therefore, certainty in the computational results most often depends on the experience of the analyst who builds the finite element model. In this research a new techniques is implemented to feel this gape is called modal analysis part by part. Moreover the validation of this method can be validated by comparing computational and experimental results.

2.3 EXPERIMENTAL MODAL ANALYSIS FOR VEHICLE STRUCTURES

Experimental modal analysis is the process of determining the modal parameters (natural frequencies, mode shapes and damping factors) of a linear system. One common reason for experimental modal analysis is the verification or correction of the results of computational modal analysis approach. Below are some reviews on the application of experimental modal analysis in automotive.

In a case study work, (Verboven et al. 2006) authors presented the assessment of nonlinear distortions in modal testing and analysis of vibrating automotive structures. New developments for the nonparametric processing of modal test data were presented. The application of the presented methods was studied for the case of a typical modal test of body-in white structure. The car body was suspended by means of steel cables connected to the car body through four sets of three springs connected at the front and back part of the body. Multiple-input testing was realized using two shakers in the front part where the applied loading was measured using PicoCoulomB (PCB) force sensors. Multiple responses were measured using PCB accelerometers and the results presented for this specific study used two of the observed responses (one sensor at the coupling of multiple parts by means of welding and screw joints, the other on a side panel). The measurements were controlled using MATLAB software in combination with a National Instruments data-acquisition board (with synchronized 2 generators and 16 channels). It was found that nonparametric estimation of multivariable frequency response functions can be more easily based on an "errors-in-variables" stochastic framework. Moreover, the application of a well-chosen multi sine excitation permits improvement of the data quality, as well as the detection, qualification and quantification of nonlinear distortions during Frequency Response Function (FRF) measurements. Also, the study suggested that, to make the presented techniques available for multi-input modal testing, attention is paid to the design of optimal multi-input excitations by maximizing the Fisher information matrix as well as minimizing the crest factor of the applied excitation.

Another study was conducted to explore sensitivity analysis methods to determine the dominant modal parameters of substructures of a brake system for brake squeal suppression analysis (Guan et al. 2006). The sensitivity analysis of the positive real part of the eigenvalue of squeal mode (RES) to substructures' modal parameters (SMP) was explored and the corresponding formulae were derived. The sensitivity analysis method can effectively determine the dominant modal parameters influencing the squeal occurrence in a regular way. These dominant modal parameters were then set to be the target of structural modification attempted to eliminate the squeal mode. Sensitivity analysis of a typical squealing disc brake was performed. The study showed that a modified rotor or a modified bracket can be used to eliminate the squealing and latter verified experimentally. On the other hand, the determination of the modal parameters of a disc-brake rotor was investigated using the Data Dependent Systems (DDS) methodology. The rotor causes the vibration induced disc-brake squeal phenomenon. The study presented results from an experimental investigation to show how structural modification can be used to change the modal parameters of the rotor. The modal parameters from both the DDS method and from a Fourier analyzer based modal analysis package were presented. Each rotor was modeled with 60 points on three equally spaced diameters. For an unmodified free-free rotor (resting on packing foam) the DDS results indicated that a 60th degrees and order model was required, whereas a structurally modified disc-brake rotor required a 76th degrees and order model. The study indicated how the disc-brake rotor can be modified to reduce the squeal propensity in selected frequency ranges (Pandit and Jacobson 1988). An alternative modal parameter identification technique applied to large complex structures with multiple steady sinusoidal excitations suggested that the force amplitudes are proportional to each other, and the phases are either coincident or opposite. The frequency response function does not exist in the usual sense in these circumstances. Therefore, the Laplace Transform of the response was taken as the function to be curve-fitted directly according to the principle of superposition for linear systems. Some advanced measures for improving the accuracy of the identified parameters were used. The application of this technique to some aircraft, and comparison with conventional ground vibration testing approaches, showed that the accuracies are comparable and that there is a significant reduction in the time required for testing by this technique. The technique does not require any prior knowledge of the test article, shaker placement, nor "fine turning" to a resonant state, (Jiang et al. 1990).

Two interesting papers have investigated the possible causes of failure and the pre-processing of the data acquired by different components. The first study identified the possible causes of the failure and proposed possible solutions of an exhaust system for heavy duty commercial trucks (Vascncellose et al. 2003). In this investigation the authors describe the use of computer simulation supported by experimental data on the design process of the exhaust system, with regard to structural behavior. A finite element model was generated including the complete vehicle and the exhaust system. Static and dynamic analyses were performed in MSC.Nastran software simulating different loading conditions and system configurations. The results obtained assured the structural integrity of the modified exhaust system when implemented on the vehicle and also contribute to a better understanding of this system behavior and its structural strength. Generally, it was verified that numerical models validated with experimental data are a powerful tool during the development phases of a new vehicle, reducing project time and costs. The second study investigates the applicability of a non-parametric exponential time-window in the pre-processing of data acquired with arbitrary excitation to improve the modal parameters of an engine sub-frame of a car (Verboven et al. 2005). The sub-frame was supported by elastic chords in order to approximate the free–free conditions. Time histories of 256 K samples were measured for the two applied forces and 23 responses (accelerations in vertical or +Z direction) using a random noise excitation in a frequency band 0–1024 Hz with a sampling rate of 2048 Hz. Since this sub-frame structure is characterized by a low damping Hanning window was applied to reduce possible effects of leakage. Also this paper presented a mixed nonparametric-parametric approach that minimizes the effects of measurement errors introduced by both the effects of leakage and measurement noise. At the end of this research the authors concluded that engineers are often interested in obtaining the modal parameters for reasons of physical interpretation and applications of numerical model updating and modification prediction. Several possible approaches for the reduction of effects of leakage on the estimated modal parameters have been studied and compared with techniques proposed in the literature. The comparison between different approaches, showed the how to improve modal parameter.

A successful implementation of modal control to arbitrary curved panels using experimentally evaluated mode shapes was demonstrated (Hurlebaus et al. 2008). The identification of the modal control parameters from a measured data base was of interest. The test object on which the proposed modal concept is implemented was a modern roaster car body. The floor panel has been selected for the experimental setup. Since, for such structures, the evaluation of modal parameters from numerical calculations of local modes is complicated because the results strongly depend on proper boundary conditions of the truncated structure. Thus, the modal data was identified using experimental modal analysis. The transformation of the experimentally measured mode shapes into closed-form analytical formulations and the extraction of modal input and output factors for sensors and actuators were used to connect experimental modal analysis with modal control theory. The implementation of the input and output factors in a modal state space formulation resulted in a modal filter for the point sensor array and a retransformation filter for the segmented actuator patches. In this study, PVDF film was used for sensors and actuators. The modal controller was implemented on a digital controller board, and experimental tests with the floor panel and center panel of a car body were carried out to validate the proposed concept. Finally, the reduction obtained in structural vibrations, which also leads to a reduction in acoustic radiation, was quite significant.

2.4 COMBINED MODAL ANALYSIS FOR VEHICLE STRUCTURES

Today's vehicles are typically more complex in terms of design and materials. Therefore, the structural analysts must make their design with accurate and realistic models and the experimentalist must be able to accurately define a structure's dynamic response to specify input forces. Nowadays experimental and computational modal analysis tools are available to assist researchers in this field. The analysts today use sophisticated finite element programs to help in the designing and understanding of complex structures like vehicles. The experimentalists also owned sophisticated experimental modal analysis equipments that support them in quantifying and understanding the dynamic behavior of a complex structure. However, there is a lack of communication between analysts and experimentalists due to misunderstanding of each other's terminology and methods of problem solution. Therefore, the combination between computational and experimental modal analysis is a must to understand the vehicle behavior and achieve better quality products. The following shows a literature review of the past work done in the field of modal analysis of various car components using experimental and computational modal analysis.

An early study combining the two approaches, described experimental and analytical modal analysis of the body of a 2 passenger cabriolet concept car "Ethos1"designed by Pininfarina. The study discusses the specific problems in a modal test on such a car body of extruded aluminum profiles. An experimental modal model was correlated with an MSC/NASTRAN analytical model, and a diagnosis is made to improve the analytical model. The correlation between analytical and experimental techniques gave an indication of the importance of a pre-test analysis to define proper excitation locations for the experimental modal test. An error localization method was performed to where and how the FE model should be modified to get closer in agreement with the test results (Brughman et al. 1995). Another important study was conducted to illustrate how to use the analytical mode shapes obtained from finite element analysis (FEA) to scale experimental mode shapes. The study also showed that analytical models having relatively few finite elements in them can yield mode shapes that correlate well with experimental mode shapes, and are therefore adequate for scaling the experimental shapes. A straightforward least squared error method is introduced for scaling the experimental shapes. The study also illustrates how FEA models of various sizes will still yield accurate results. The accuracy of results was again verified by overlaying synthesized and experimental FRFs, (Schwarz & Richardson 2006).

Various other studies were presented by many investigators focusing on different components and helped in the rapid progress of this field. Among those of particular significance the investigation of the dynamic performance of truss core sandwich structures based on modal analysis experiments (Binchao et al. 2008). A homogenization technique was introduced for three-dimensional (3D) pyramidal truss-core sandwich panels, which then used to establish a two-dimensional (2D) single-layer sandwich model so that the effective elastic constants as well as the dynamic characteristics of the sandwich can be determined. Full finite element simulations on 3D truss-core sandwiches were subsequently carried out. The validity of the analytical and numerical predictions was checked out using experimental measurements on pyramidal truss-core sandwich cantilevers. On the other hand, the vibro-impact phenomenon in a gear shift cable was the subject of another experimental and numerical study (Leib et al. 2010). The study was on the nonlinear dynamic behavior of a gear shift cable and more specifically of the associated tizzing phenomenon. A gear shift cable was composed of an inner wire that can slide freely in an outer composite housing. When undergoing harmonic excitation, the inner wire interacts with the housing. Hammer and swept sine shaker tests were first used to estimate the characteristics of the two main components. It was shown that the behavior of the outer housing was nonlinear and depends on the amplitude of the excitation. The assembled gear shift cable is then set up on the shaker and the nonlinear vibro-impacting phenomenon was studied. Finally a finite element model, based on the Euler Bernoulli beams and the Rayleigh damping coefficients, proves to offer good correlation with the measured data for different excitation frequencies. A period doubling bifurcation was observed both experimentally and numerically. Brughman et al. (1993) also applied Finite Element Analysis (FEM) and Experimental Modal Analysis (EMA) correlation and validation techniques to a body –in white, namely the 1991 GM Saturn four door Sedan. The FEM model of this car consisted of 46830 DOF's (Degree of Freedom) (half model). A multi-point experimental modal analysis (EMA) survey was executed for 360 response

DOF's. Classical techniques for correlation analysis such as Modal Assurance Criterion (MAC) were applied. The study introduces as well a variation of the MAC calculation that enables a better identification of regions of difference between FEM and EMA. Error localization methods have been applied to identify the regions of the FEM model causing most of the discrepancies between FEM and EMA. A FEM model updating procedure was executed to reduce the difference between FEM and EMA to acceptable limits. Another study addressed the development of a finite element model for a 1/10 scale crane rig in the laboratory. The purpose of the study was to predict the dynamic behavior of the scale crane rig based on the relevant features of the developed finite element model. The finite element modeling and experimental modal testing for the 1/10 scale crane rig were first carried out. The modal testing was undertaken to measure the natural frequencies and the corresponding mode shapes of the scale crane model, and then a comparison between the last results and those obtained from the finite element model was made. The modal parameters (natural frequencies and the corresponding mode shapes of the scale crane model) were determined using the Leuven Measurement Systems (LMS) modal testing software. Two kinds of mechanical coupling for the force transducer and the tested structure (the scale crane model) for achieving the better experimental outcome were used. The two types of the mechanical coupling were the tubular type and the double–side screw type. The practical decision was made to use the double-side screw coupling. The finite element model was then modified, according to the experimental results, using various techniques. It has been found that the new modified finite element model, by replacing the conventional infinite rigidity for the ground-fixed nodes by the appropriate stiffness for the translational and rotational springs, can predict the vibration characteristics of the experimental crane rig with satisfactory accuracy. It has also been found that the type of coupling between the load cell and the tested structure significantly affects the results of modal testing (Jia-Jang 2004). A more advanced study established an 8 degree-of-freedom (DOF) vehicle model to investigate the vertical vibration characteristics of an exhaust system excited by road surface inputs. The simplifications of the exhaust system relevant to the vehicle model was discussed in detail, including the steps of exhaust modal analysis, definition of mass element, exhaust partitioning, parameter acquisition, and simplified exhaust validation. The vehicle model was developed based on a half-vehicle model, simulated using MATLAB/SIMULINK, and validated by comparing the simulation and experiment on various road profiles. The results showed that the vehicle model effectively represents the dynamics of the vehicle characteristic in vertical vibration (Li et al. 2008).

A three-dimensional finite element (FE) model of a multilayered hull turret assembly of an armored vehicle were generated from major components such as the armored hull, turret and a 105 mm cannon models which were independently developed in PATRAN3 and assembled using rigid-link elements in the ADINA nonlinear dynamic FE code. Comparison of the eigenfrequencies and mode shapes with those from the experimental modal analysis results indicated poor agreement at all modes where the computational eigenfrequencies were substantially higher than the experimental values. This is because of several component masses attached to the experimental model which were not accounted for and proved to be rather difficult to include explicitly in the computational model due to modeling complexity. An implicit modeling approach with respect to missing component masses was adopted to rectify the problem using concentrated masses attached to corresponding nodes and uniformly distributed in the associated area in which these components are actually attached to the hull ± turret assembly. Distribution of these masses can significantly influence the mass while the stiffness remains relatively unaffected. Significant improvement in correlation between computational and experimental modal analyses resulted from this approach, which accounted for most experimental component masses omitted from the computational model (Gupta 1999).

Elegant ways were developed for coupled use of FEA and EMA. For instance, this coupling use of the two methods was used to investigate the dynamic behavior of an injection pump (Yasar et al. 2005). Authors performed analytical and experimental investigations for an injection pump, focusing on the dynamic behavior of the bearing housing. With the aim of quantifying the compliance of calculated natural frequencies and corresponding mode shapes with their measured counterparts, a series of correlation and sensitivity analyses has been performed by Sulzer Innotec using the specific tool. It was attempted, to update a finite element model of the whole pump using the algorithms integrated in the correlation software, selecting significant parameters and specifying their uncertainties. The first correlations EMA-FEA using the results of

ANSYS as well as those obtained with the simplified ABAQUS FE model were fairly good. The real modes were extracted from operational displacement shapes using conversion features of the correlation software before further treatment. The experimental results were based on a modest number of measurement points only. The quality of updating was highly dependent on the significance and completeness of the test. The correlation between EMA & FEA was visualized in form of MAC (modal assurance criterion) matrices. The iterative updating procedure has brought remarkable enhancement of the FE model, even for a limited number of modes. In general, the agreement obtained for FEA/EMA proved to be practically sufficient.

An investigation to examine in detail the vibration characteristics of a typical radial flow impeller with a tapered blade was carried out by (Ziaei 2005). In this investigation both experimental and analytical techniques have been used. A 3D solid element model was built and its convergence was verified by applying by mesh refinement and two mass distributions methods-lumped and consistent mass contribution to each of the FE models and comparing the differences between the predicted natural frequencies in the two data sets. A pre-test plan was performed before conducting a modal test in order to select the proper suspension points, driving point(s) and response points on the impeller. Modal analysis was carried out on the hammer testing results. The results showed good agreement between the FE model using solid elements and measured natural frequencies. However, some modes were not accurately predicted the constant blade thickness by using FE model. The measurements on the impeller as a demonstration of the circumferential line scan technique using a laser Doppler vibrometer (LDV) was also carried out, enabling the backplate modes to be described in terms of their nodal diameter components. The nodal diameters versus natural frequencies graph was then compared with the same results obtained from FE and hammer testing and showed good agreement. Finally, a parametric study was conducted on disc thickness, blade thickness, blade trailing, leading edge profiles and blade mistuning. It was found that the effect of varying disc thickness on the lower modes of the impeller was not significant. However, a significant shift in the natural frequencies resulted in higher modes. It was also found that the parametric study of natural frequencies versus blade thickness showed that the relationship is virtually proportional for the low frequency range, while for the higher modes it shows some decline. It was concluded that varying the blade leading edge position has a substantial effect on the modal frequencies.

The following two papers deal with the development for structural dynamic of aircraft fuselage and the implementation of finite element methods to analyze and evaluate minivan body structure. In the first study, the ability to extend the valid frequency range for finite element based structural dynamic predictions using detailed models of the structural components and attachment interfaces was examined for several stiffened aircraft fuselage structures (Ralph et al. 2000). This extended dynamic prediction capability is needed for the integration of mid-frequency noise control technology. Beam, plate and solid element models of the stiffener components were evaluated. Attachment models between the stiffener and panel skin range from a line along the rivets of the physical structure to a constraint over the entire contact surface. Normal mode predictions for different finite element representations of components and assemblies were compared with experimental results to assess the most accurate techniques for modeling aircraft fuselage type structures. In the second study (Jin Yi-Min 2000), the analysis involved static, dynamic, fatigue, crashworthiness, optimization and design sensitivity analysis. The static analysis was conducted taking into account the bending and torsion loads. The dynamic analysis comprised two sources, tire unbalance and engine excitation and the corresponding NVH analyses was carried out. In the paper the strength analysis in both torsion and bending case and modal analysis results were presented. The FE analysis was accomplished through the use of MSC.Nastran. The results obtained for the dynamic analysis were compared with experimental test results and found to be in good agreement.

2.5 CONCLUSION

According to the open literature review above much work has been done on vehicle components such as engine, exhaust system, cabin structure, chassis suspension, bearing structure, power train system and drum brake system using either experimental modal analysis or computational modal analysis or both. In addition there is also some work has been done on the whole car but with using the experimental modal analysis only or computational modal analysis only. The researchers discussed how computational and experimental modal analysis methods are used to solve noise and vibration problems and come out with the importance of the combination between them in order to provide a comprehensive understanding of the dynamic characteristics of vehicles prior and after manufacturing which leading to improve the noise and vibration comfort. In this study we develop an accurate method to analyze the dynamic characteristics of whole car using modal analysis part by part in order to solve the noise and vibration problems of a passenger car in easy way and less errors. The confidence in the results for complex structures still questionable because of the several simplifications and assumptions applied on the structure. The main assumption involved in modal analysis is that the structural system is linear, i.e., structural displacements are directly proportional to applied loads. In practical structures this condition is not always met especially for big and complex structures. Nonlinearities can complicate the analysis and tend to introduce errors into the data reduction and curve-fitting estimates of natural frequencies. Errors can range from small errors where minor non-linearities are present to large errors where the non-linear effects are substantial, such as in structures with assembled components with different designs.

CHAPTER 3

THEORETICAL BACKGROUND

3.1 INTRODUCTION

This chapter introduces all the background information needed to conduct the study. Based on the research objectives, three sections are introduced here, namely; general definitions and terminology of noise and vibration, modal analysis and ride comfort of cars.

3.2 GENERAL DEFINITIONS AND TERMINOLOGY

Vibrations occur in elastic systems that consist of one or more masses connected to each other or to a fixed member by springs. A vibration is the motion of a body or system that is repeated after a given interval of time known as a period. The number of cycles of motion per unit of time is called the frequency. The maximum displacement of the body or some part of the system form the equilibrium position is the amplitude of the vibration at that point.

There are two general types of vibration, namely, rectilinear and torsional.

• Rectilinear vibrations: appear in two forms:

-The longitudinal is the axial compression and extension of bars and wires; and includes the compression and extension of coil springs.

-The transverse such as the motion of beams is perpendicular to their centerlines.

•Torsional vibration: is one of oscillation or twisting as in shafts.

If the body or system is given an initial displacement from the equilibrium position and released, it will vibrate with a definite frequency known as its natural frequency. The vibration is said to be free, since no external forces act upon it after the initial displacement. The body vibrates with decreasing amplitude until it comes to rest. This reduction in amplitude is caused by a loss of the total energy in the system; known as damping and may be due to friction; fluid resistance etc. For some applications, a dashpot or Rubbing friction may be added to increase the damping effect. If the amount of damping is very large; the body may not vibrate but may merely creep back to the equilibrium position and its motion is said to be periodic. Under some conditions, as in an unbalanced machine, the body or system forced vibration occurs. If the frequency of this external force is the same as the natural frequency, resonance taking place. The body or system then vibrates with large amplitudes, which result in high stresses and possible interference of parts. When resonance occurs in rotating shafts (because of unbalance), the speed of rotation is known as the critical speed.

Vibrations may be classified as transient or steady state. A transient vibration is a temporary condition that disappears with time, such as free-damped vibrations. A steady - state vibration is one in which the motion is repeated exactly in each cycle, as in a forced vibration.

Many bodies or systems are able to vibrate in more than one manner and have more than one natural frequency. Systems having a continuous mass and elasticity, such as wire or beam of appreciable weight, have an infinite number of natural frequencies. Each of them is accompanied by its own mode or shape of vibration curve.

The number of degrees of freedom is equal to the number of coordinates required to specify completely the displacement of the body or system at any time. If the motion of the body is constrained so that it can vibrate in only one manner, or mode, it is said to have a single degree of freedom; if in two modes, two degrees of freedom; and so on. A single rigid body, such as a block supported on springs, could have six degrees of freedom. There are three directions of translation, or rectilinear motion and three of rotations, or torsional motion possible about the principal axes. The natural frequency of each mode of vibration is independent of the frequency of the others. Thus, if a weight less cantilever beam having a rectangular cross section and a mass at the tip is displaced downward and released, it will vibrate in a vertical plane with a certain natural frequency. If the beam is displaced outward and released, it will vibrate in a horizontal plane with a different natural frequency. However, if the beam is displaced both downward and outward before being released, both vibrations will occur simultaneously without affecting each other in either frequency or amplitude. The resultant motion of the beam will be the vector sum of these independent motions. In the systems, having more than one degree of freedom the action becomes more complex, and coupling action may take place between the various modes.

3.3 MODAL ANALYSIS

3.3.1 Introduction

In the past two decades, modal analysis has become the widest acceptance in the quest for determining, improving and optimizing dynamic characteristics of engineering structures, leading to higher comfort, and better performance.

The modal analysis enables engineers to get a better understanding of structural dynamic problems. Not only has been recognized in automotive and aeronautical engineering, but has also discovered profound applications for civil and building structures, biomechanical problems, acoustical instruments and nuclear plants. Typical examples include: Analysis of a car body, car components (engine, suspension, exhaust, brake), a fully equipped car –analysis of aircraft by Ground Vibration Tests of aircraft components (landing gear, control surfaces, engines..), in-flight testing in view of aero-elasticity stability (flutter).

In the process industry: analysis of pumps, compressors, piping systems, shafts and bearings, turbine blades, machinery foundations, high precision equipment-civil engineering studies related to bridges, dams, high-rise buildings, off-shore platforms.

Audio and household systems such as washing machine, loudspeaker, CD-drive, computer rack. In all these applications, it is the purpose to obtain adequate system models to perform troubleshooting as well as system optimization in terms of mission-critical functional performance parameters such as safety, stability, fatigue life, vibration comfort, interior and exterior noise etc.

The increasing demand of comfort, safety and reliability upon contemporary vehicles either defined by government regulations or accrued by consumers. These demands have created new challenges to the scientific understanding of engineering structures. Where the vibration of the structure is of concern, the challenge lies on better understanding its dynamic properties using analytical, numerical or experimental modal analysis or combination of them. Modal Analysis is used in a vast range of applications including:

- Ensuring that resonances are away from excitation frequencies
- Prediction of the dynamic behavior of components and assembled structures
- Optimization of the structure's dynamic properties (mass, stiffness,damping)
- Prediction of the forces from measured responses
- Prediction of the responses due to complex excitation
- Prediction of the effect of structural modifications
- Inclusion of damping in Finite Element Models
- Updating of Finite Element Models
- Damage detection and assessment

Modal Analysis ranges from simple mobility tests with impact hammers to multi-shaker testing of large and complex structures with hundreds of response accelerometers (B&K).

3.3.2 The concept of modal analysis

Modal analysis is the process of determining the dynamic characteristics of a system in forms of natural frequencies, damping factors and mode shapes, and using them to formulate a mathematical model for its dynamic behavior. The formulated mathematical model is referred to us the modal model of the system and the information for the characteristics is known as its modal data.

The dynamics of a structure are physically decomposed by frequency and position. This is clearly evidenced by the analytical solution of partial differential equations of continuous systems such as beams and strings. Modal analysis is based upon the fact that the vibration response of a linear time-invariant dynamic system can be expressed as the linear combination of a set of simple harmonic motions called the natural modes of vibration. The natural modes of vibration are inherent to a dynamic system and are determined completely by its physical properties (mass, stiffness, damping) and their special distributions. Each mode is described in terms of its modal parameters: natural frequency, the modal damping factor and characteristic displacement pattern, namely mode shape. The mode shape may be real or complex. Each corresponds to a natural frequency. The degree of participation of each natural mode in the overall vibrations determined both by properties of the excitation sources and by the mode shape of the system. Modal analysis embraces both theoretical (analytical) and experimental techniques.

3.3.3 Experimental modal analysis

Experimental modal analysis (EMA) or modal testing is a non-destructive testing strategy based on vibration responses of the structures (Kaewunruen and Remennikov. 2005). Because of the increasing importance of a preferable precise estimation of the model parameters, the computer aided measurement and analysis of dynamical properties of components play a more and more decisive role. The actual structural dynamical behavior can merely be investigated experimentally. The Experimental Modal Analysis (EMA) is one of the most important measurement procedures in this area.

Over the past decade, the experimental modal analysis (EMA) has become an effective means for identifying, understanding, and simulating dynamic behavior and responses of structures. Two of the techniques widely used in modal analysis are based on an instrumented hammer impact and shaker excitation. By using signal analysis, the vibration response of the structures to the excitation is measured and transformed into frequency response functions (FRFs) using Fast Fourier Transformation (FFT) technique. Subsequently, the series of FRFs are used to extract such modal parameters as natural frequency, damping, and corresponding mode shape. These modal parameters are required to avoid resonance in structures affected by external dynamic loads.

In application, numerous investigations related to automotive engineering, aeronautical engineering, and mechanical engineering; have been reported (He and Fu 2001). In recent years, experimental modal analysis has received wide acceptance in structural engineering application, particularly for identification of modal properties of bridges (Salane & Baldwin 1990) damage detection of structures using modal data (Friswell 1995) and (Liu 1999), structural health monitoring (Cremona 2004), dynamic FEM updating (Friswell 1995), active vibration control (He and Fu 2001), dynamic buckling of structures (Souza & Assaid 1991). Applications of modal testing to structural members also involve with determining modal properties of a variety of structural beams (Chowdhury 1999) and (Salzmann 2002) or with identifying the connection rigidity of the structures (Kohoutek 1995).etc.

The practice of experimental modal analysis involves measuring the FRFs or impulse responses of a structure. The FRF measurement can simply be done by asserting a measured excitation at one location of the structure in the absence of other excitations and measure vibration responses at one or more location(s). The excitation can be of a selected frequency band, stepped sinusoid, transient, random or white noise. It is usually measured by a force transducer at the driving point while the response is measured by accelerometers or other probes. Both the excitation and response signals are fed into an analyzer which is an instrument responsible for computing the FRF data.

In general, experimental modal analysis involves three phases: test preparation, frequency response measurements and modal parameter identification.

3.3.4 Test preparation

Test preparation involves selection of a structure’s support, type of excitation force(s), location(s) of excitation, hardware to measure force(s) and responses; determination of a structural geometry model which consists of points of response to be measured; and identification of mechanisms which could lead to inaccurate measurement.

3.3.5 Structure's supports

A structure is often connected to its surroundings. Therefore, its dynamic characteristics are determined by the boundary conditions as well as by itself. Analytically, boundary conditions can be specified in a completely free or completely constrained sense. In testing practice, however, it is generally not possible to fully achieve these conditions. The free condition means that the structure is, in effect, floating in space with no attachments to ground and exhibits rigid body behavior at zero frequency. The airplane in the air is an example of this free condition. Physically, this is not realizable, so the structure must be supported in some manner. The constrained condition implies that the motion, (displacements/rotations) is set to zero. However, in reality most structures exhibit some degree of flexibility at the grounded connections. In modal testing, the structure is often fixed to much more rigid and heavier object such as a concrete floor. It is only when we are convinced that the boundary condition is rigid enough not to affect the frequency range of interest, can we be confident with the FRF data measurement.

3. 3.6 Classification of excitation force

The excitation method is important for conducting accurate modal testing. The decision on excitation is based first on the optimum method for accurate measurement data that suit test objectives and the structure. It is therefore important for modal analyst to appreciate all available excitation methods to be able to select the most suitable one for testing. The following are the most common important excitation methods.

a) **Sinusoidal excitation**: Sinusoidal excitation method is the most traditional way for modal testing. Today, it is still the most popular one. The force contains one single frequency at a time and excitation sweeps from one frequency to another with a given step, allowing the structure to engage in one harmonic vibration at a time. This excitation is effective for exciting a structure with high vibration level, for characterizing nonlinearity of a structure, and for exciting normal vibration modes of a damped structure. Single input sinusoidal excitation could be very time-consuming, despite its superior effectiveness. The advent of multi-input multi-output (MIMO) testing partially rectified this problem. With the ability to perform real time FRF estimation on many channels, sinusoidal excitation becomes a fast as well as reliable excitation method for modal testing.

b) Random excitation: The force signal for random excitation is an ergodic, stationary random signal with Gaussian distribution. It contains all frequencies within the frequency range. For a structure that behaves nonlinearity, random excitation has the tendency to linearize the behaviour from the measurement data. The frequency response function derived from random excitation measurement will then be the linearized FRF. This FRF though failing to provide more information on the nonlinearity is actually a very useful function as it is perceived as the best FRF estimated for the structure. It correctly models the amount of energy dissipation of the structure during vibration. However, this linear model is best only for a particular force spectral density. Therefore, we may have a series of linearized FRFs for varying excitation force levels

c) Pseudo random excitation: The force signal in this excitation is an ergodic, stationary random signal that consists of discrete frequencies formed by integer multiples of the frequency resolution used by the Fourier transforms. It is a periodic signal with random amplitude and phase distribution. This excitation has eliminated the leakage problem at random excitation commonly encounters. It usually results in more accurate FRF data for modal analysis. Nevertheless, pseudo random excitation requires a special device to generate such a unique force signal and it requires more time than random excitation to implement.

d) Impact excitation: The time domain force signal for impact excitation is a pulse with uncontrollable frequency contents. The impact excitation is relatively simple excitation technique compared with shaker excitation. It is convenient to use and very portable for field and laboratory tests. Because of no physical connection between the excitation and the structure, impact test avoids t he problem of interaction between them. The main disadvantages of impact excitation are the difficulty to control either the force level or the frequency range of the impact. This could affect the signal to noise ratio in the measurement, thus resulting in quality data.

e) Location of excitation: The behavior of structures is often investigated by exerting external force on the structure and measuring its response. The structural excitation is typically performed using shakers and impactors. Shakers are attached devices, while impactors are not (although they make contact for a short period of time).

f) Impact hammer: Impact hammer is used to excite the test structure in order to measure a response to impact. It consists of an ICP quartz force sensor that converts impact force into an electrical signal that is then transferred through a cable connected to the end of the handle for analysis. The test structure is excited with a uniform force at all resonant frequencies located within the manufacturer specified operating range of frequencies. The impact signal is applied to the structure for only a fraction of the sample period. Its shape significantly influences the frequency content of the measured response, which may be modified by the use of mass extenders and hammer tips of varying hardness. For example, a soft hammer tips will produce a relatively long impact pulse and consequently a narrow frequency band is excited. Hard hammer tips produce a relatively short impact pulse and result in the excitation of a wide frequency range. A hammer tip that is too soft will not produce enough excitation at higher frequencies. Consequently the structure will not respond to the excitation at higher frequencies and a low coherence at these frequencies can be expected. A hammer tip that is too hard will produce too much excitation at higher frequencies. Consequently eigen modes above the frequency range of interest are excited. This causes a bad overall coherence especially near anti-resonances and at lower frequencies (Dave and David 1984).

g) Shaker Testing: The most useful shakers for modal testing are the electromagnetic shown in (often called electro dynamic) and the electro hydraulic (or, hydraulic) types. With the electromagnetic shaker, (the more common of the two), force is generated by an alternating current that drives a magnetic coil. The maximum frequency limit varies from approximately 5 kHz to 20 kHz depending on the size; the smaller shakers having the higher operating range. The maximum force rating is also a function of the size of the shaker and varies from approximately 2 lbf to 1000 lbf; the smaller the shaker, the lower the force rating. With hydraulic shakers, force is generated through the use of hydraulics, which can provide much higher force levels – some up to several thousand pounds. The maximum frequency range is much lower though – about 1 kHz and below. An advantage of the hydraulic shaker is its ability to apply a large static preload to the structure. This is useful for massive structures such as grinding machines that operate under relatively high preloads which may alter their structural characteristics.

To minimize the problem of forces being applied in other directions, the shaker should be connected to the load cell through a slender rod, called a stinger, to allow the structure to move freely in the other directions. This rod has a strong axial stiffness, but weak bending and shear stiffnesses. Infect, it acts like a truss member, carrying only axial loads but no moments or shear loads.

The method of supporting the shaker is another factor that can affect the force imparted to the structure. The main body of the shaker must be isolated from the structure to prevent any reaction forces from being transmitted through the base of the shaker back to the structure. This can be accomplished by mounting the shaker on a solid floor and suspending the structure from above. The shaker could also be supported on a mechanically isolated foundation. Another method is to suspend the shaker, in which case an inertial mass usually needs to be attached to the shaker body in order to generate a measurable force, particularly at lower frequencies. Figure 3.1 illustrates the different types of shaker setups. (Brown et al 1977).

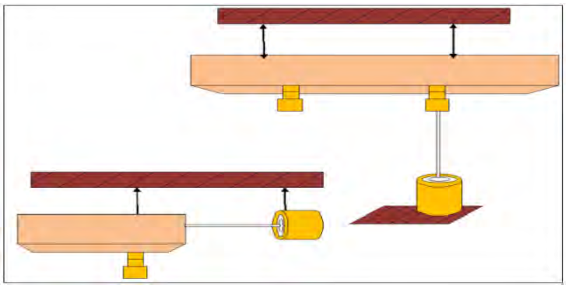

Figure 3.1 Test support mechanism

3.3.7 Frequency response function

The Frequency Response Function (FRF) is a fundamental measurement that isolates the inherent dynamic properties of a mechanical structure. Experimental modal parameters (frequency, damping, and mode shape) are also obtained from a set of FRF measurements. The FRF describes the input-output relationship between two points on a structure as a function of frequency, as shown in Figure 3.2. Since both force and motion are vector quantities, they have directions associated with them. Therefore, an FRF is actually defined between a single input DOF (point &direction), and a single output DOF.

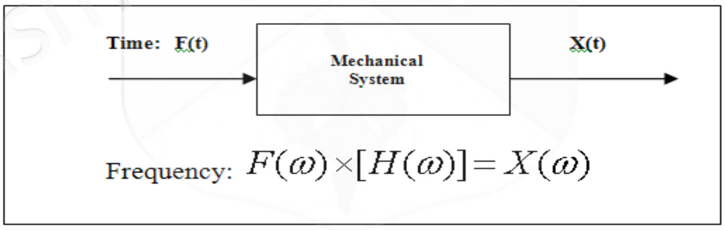

Figure 3.2 Block Diagram of an FRF

An FRF is a measure of how much displacement, velocity, or acceleration response a structure has at an output DOF, per unit of excitation force at an input DOF. Figure 3.2 also indicates that an FRF is defined as the ratio of the Fourier transform of an output response $X(\omega)$ divided by the Fourier transform of the input force $F(\omega)$ that caused the output.

3.3.8 Frequency response model

Consider a linear system as represented by the diagram in Figure 3.3.

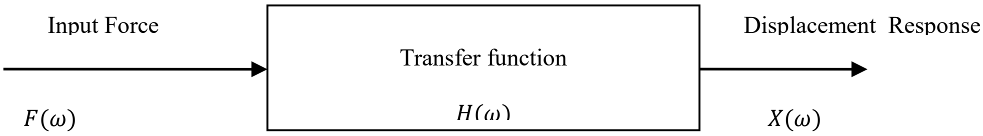

Figure 3.3 Linear System

$F(\omega)$ is the input force as a function of the angular frequency $\omega, H(\omega)$ is the transfer function. $X(\omega)$ is the displacement response function. Each function is a complex function, which may also be represented in terms of magnitude and phase. Each function is thus a spectral function. There are numerous types of spectral functions. For simplicity, consider each to be a Fourier transform. The relationship in Figure 3.3 can be represented by the following equations:

$$H(\omega) = \frac{X(\omega)}{F(\omega)}$$

Depending on whether the response motion is measured as displacement, velocity, or acceleration, the FRF and its inverse can have a variety of names as shown in Table 3.1.

Table 3.1 Frequency Response Function Names.

Dimensions	Names
Dsplacement/Force	Admitance,ComplianceorReceptance
Velocity/Force	Mobility
Acceleration/Force	Accelerence or Inertance
Force/Displacement	Dynamic stiffness
Force/Velocity	Mechanical Impedance
Force/Acceleration	Apparent Mass or Dynamic Mass

3.3.9 Presentation and characteristics of frequency response functions

Because of the complexity of the frequency response function, it cannot be fully displayed on a single two dimensional plot. However, it can, be presented in several formats, each of which has its own uses. The response variables discussed previously were displacement, velocity or acceleration. Acceleration is currently the accepted method of measuring modal response.

One method of presenting the data is to plot the polar coordinates, magnitude and phase versus frequency as illustrated in Figure 3.4. At resonance, when $\omega = \omega_n$, the magnitude is a maximum and is limited only by the amount of damping in the system. The phase ranges from 0° to 180° and the response lags the input by 90° at resonance.

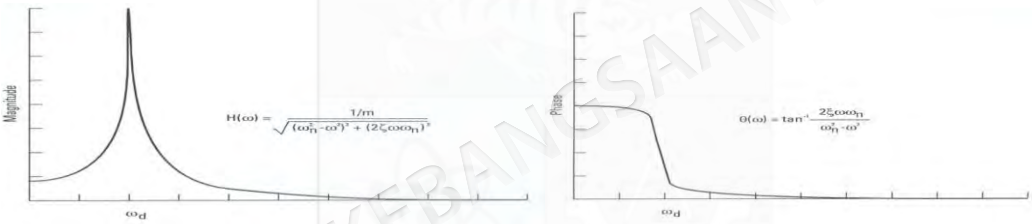

Figure3.4 Frequency response polar coordinates

Source: Hewlett-Packard Co, 1986.

Another method of presenting the data is to plot the rectangular coordinates, the real part and the imaginary part versus frequency. For a proportionally damped system, the imaginary part is maximum at resonance and the real part is 0, as shown in Figure 3.5.

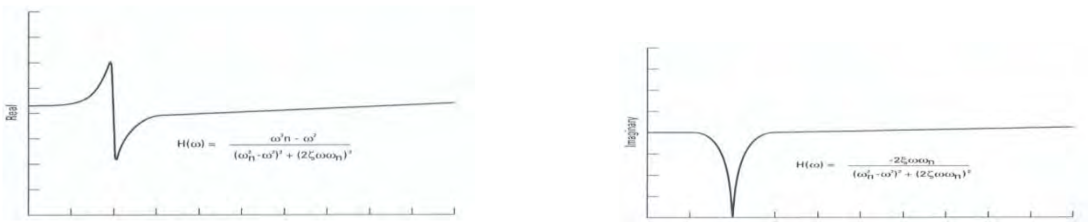

Figure3.5. Frequency response rectangular coordinate

Source: Hewlett-Packard Co, 1986.

A third method of presenting the frequency response is to plot the real part versus the imaginary part. This is often called a Nyquist plot or a vector response plot. This display emphasizes the area of frequency response at resonance and traces out a circle, as shown in Figure 3.6. By plotting the magnitude in decibels vs logarithmic (log) frequency, it is possible to cover a wider frequency range and conveniently display the range of amplitude. This type of plot also has some useful parameter characteristics which are described in the following plots.

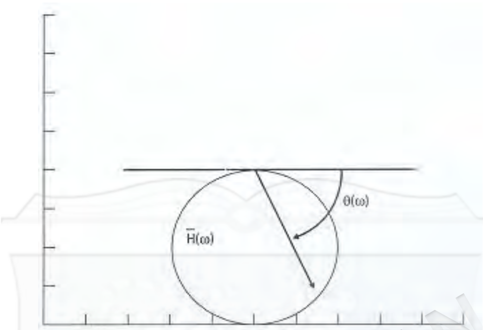

Figure 3.6 Nyquist plot of frequency response
Source: Hewlett-Packard Co, 1986.

When $\omega << \omega_n$ the frequency response is approximately equal to the asymptote shown in Figure 3.7. This asymptote is called the stiffness line and has a slope of 0, 1 or 2 for displacement, velocity and acceleration responses, respectively.

When $\omega >> \omega_n$ the frequency response is approximately equal to the asymptote also shown in Figure 3.7. This asymptote is called the mass line and has a slope of -2, -1 or 0 for displacement velocity or acceleration responses, respectively.

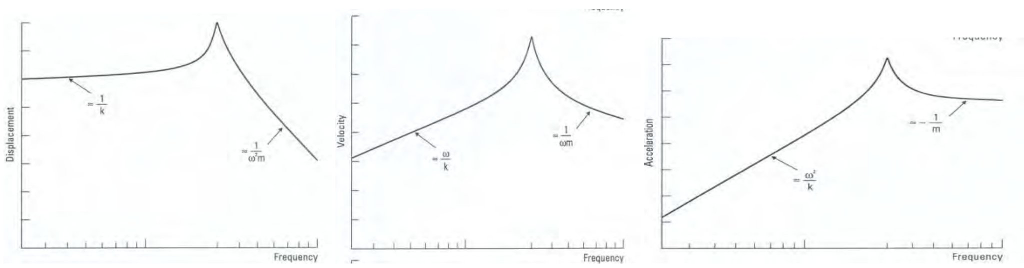

Figure 3.7 Different forms of frequency response
Source: Hewlett-Packard Co, 1986.

The various forms of frequency response function based on the type of response variable are also defined from a mechanical engineering viewpoint. They are somewhat intuitive and do not necessarily correspond to electrical analogies. These forms are compliance, mobility and accelerance as summarized in the previously.

3.3.10 Frequency response and transfer functions relationship

The transfer function is a mathematical model defining the input-output relationship of a physical system. Figure 3.8 shows a block diagram of a single input-output system.

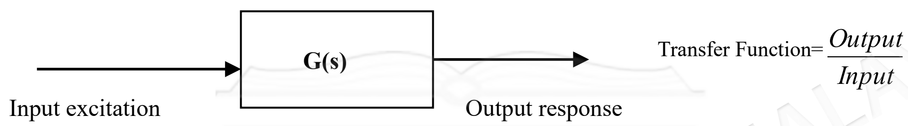

Figure 3.8 Single input-output system

System response (output) is caused by system excitation (input). The casual relationship is loosely defined as shown in Figure 3.8. Mathematically, the transfer function is defined as the Laplace transform of the output divided by the Laplace transform of the input. The frequency response function is defined in a similar manner and is related to the transfer function. Mathematically, the frequency response function is defined as the Fourier transform of the output divided by the Fourier transform of the input. These terms are often used interchangeably and are occasionally a source of confusion. This relationship can be further explained by the modal test process. The measurements taken during a modal test are frequency response function measurements. The parameter estimation routines are, in general, curve fits in the Laplace domain and result in the transfer functions. The curve fit simply infers the location of system poles in the s-plane from the frequency response functions as illustrated in Figure 3.9. The frequency response is simply the transfer function measured along the $j\omega$ axis as illustrated in Figure 3.10

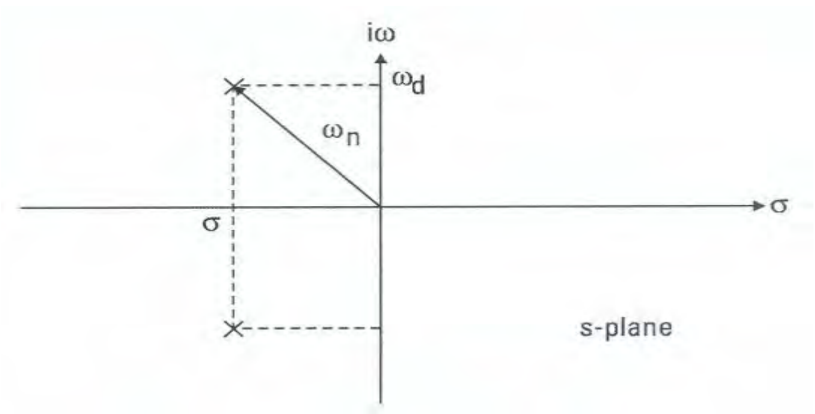

Figure3.9 S-plane representation

Source: Hewlett-Packard Co, 1986.

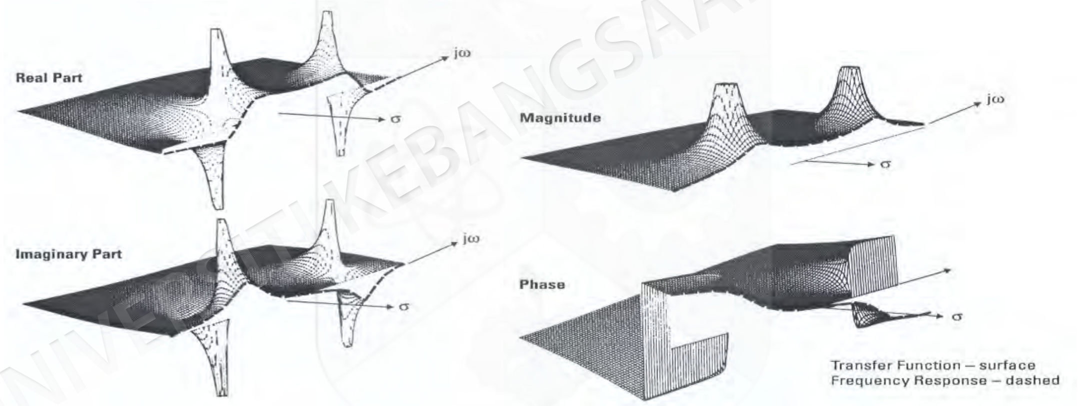

Figure3.10. 3-D Laplace representation

Source: Hewlett-Packard Co, 1986.

3.3.11 Measurement method and test configurations

There are a number of methods available to measure the frequency response functions to perform modal parameters. The most important differences between these methods are in the number of inputs and outputs and in the excitation method used. The common input output methods are single input single output (SISO) and the multiple input multiple output (MIMO) methods. The two most common excitation methods are excitation using an impact hammer and excitation using an electrodynamical shaker. Each of the above methods has specific advantages and disadvantages that determine which measurement method should be used in the specific case. Advantages and disadvantages of each method are discussed in (Allemang 1999), and (Ewins 2000). The experimental setup of the frequency response functions measurement required few major factors. These include the type of structure to be tested; the level of results desired the support fixture and the excitation mechanism. Figure 3.11 shows a diagram of a basic test system configuration.

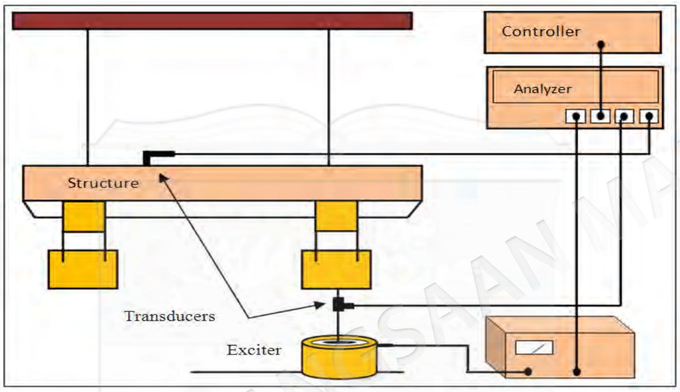

Figure 3.11 General Test configuration

The controller or computer is the important device in the test system, which is the operator's communication link to the analyzer. It can be configured with various levels of memory, displays and data storage. The modal analysis software usually resides here, as well as any additional analysis capabilities such as structural modification and forced response.

The analyzer provides the data acquisition and signal processing operations. It can be configured with several input channels, for force and response measurements, and with one or more excitation sources for driving shakers. Measurement functions such as windowing, averaging and Fast Fourier Transforms (FFT) computation are usually processed within the analyzer.

For making measurements on simple structures, the exciter mechanism can be as basic as an instrumented hammer. This mechanism requires a minimum amount of hardware. An electrodynamic shaker may be needed for exciting more complicated structures. This shaker system requires a signal source, a power amplifier and an attachment device. The signal source, as mentioned earlier, may be a component of the analyzer. Transducers, along with a power supply for signal conditioning, are used to measure the desired force and responses. The piezoelectric types, which measure force and acceleration, are the most widely used for modal testing. The power supply for signal conditioning may be voltage or charge mode and is sometimes provided as a component of the analyzer, so care should be taken in setting up and matching this part of the test system.

3.3.12 Modal parameters estimation

In the previous sections several techniques for making frequency response measurements for modal analysis were presented. In this section we show the different ways in which modal parameters can be obtained. Modal parameters are most commonly identified by curve fitting a set of FRFs. They can also be identified by curve fitting an equivalent set of Impulse Responses, or inverse response functions. Figure 3.12 shows an example of FRF curve fitting.

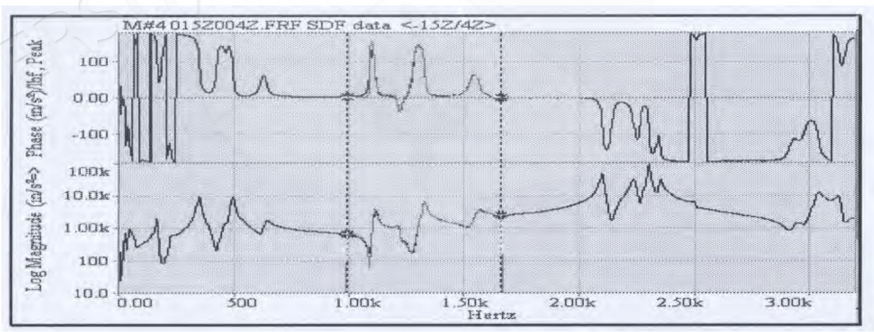

Figure3.12 A curve Fitting Example

Source: Brian & Mark 1999

3.3.13 Curve fitting methods

The choice of the modal parameter estimation method is a very important step in the estimation process. There are three properties on which the choice of a method can be based. The first property is a 'single degree of freedom'-method or a 'multiple degree of freedom'-method, the second property is a local or a global method and the third property is whether the measurements are in the frequency domain or in the time domain (Schrijver 2005).

SDOF is short for a Single degree of Freedom or single mode method. Similarly, MDOF is short for a Multiple Degree Of Freedom, or multiple mode method. SDOF methods estimate modal parameters one mode at a time. MDOF, Global, and Multi-Reference methods can simultaneously estimate modal parameters for two or more modes at a time. Local methods are applied to one FRF at a time. Global and Multi-Reference methods are applied to an entire set of FRFs at once. Local SDOF methods are the easiest to use, and should be used whenever possible. SDOF methods can be applied to most FRF data sets with light modal density (coupling). MDOF methods must be used in cases of high modal density. Global methods work much better than MDOF methods for cases with local modes. Multi-Reference methods can find repeated roots (very closely coupled modes) where the other methods cannot.

3.3.14 Local SDOF (single mode) methods

The three most commonly used curve-fitting methods for obtaining modal parameters are shown below. These methods are based on applying an analytical expression for the FRF to measured data. (Richardson 1975)

a) Modal Frequency as Peak Frequency: The peak frequency in the FRF is used as the modal frequency. This peak frequency is not exactly equal to the modal frequency but is a close approximation, especially for lightly damped structures. The resonance peak should appear at the same frequency in almost every FRF measurement. It won’t appear in those measurements corresponding to nodal lines (zero magnitude) of the mode shape see Figure3.13.

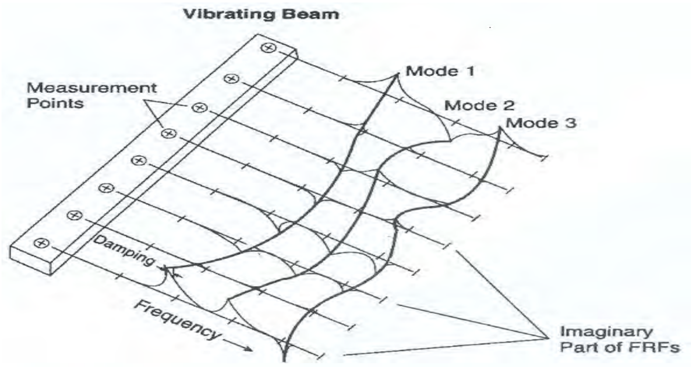

Figure 3.13 Curve Fitting FRF Measurements
Source: Brian & Mark 1999

b) Modal Damping as Peak Width: The width of the resonance peak is a measure of modal damping. The peak width should be the same for all FRF measurements, meaning that modal damping is the same in every FRF measurement.

c) Mode Shape from Quadrature Peaks: In this curve fitting method the peak values of the imaginary part of (displacement/force) or (acceleration/force) FRFs are taken as components of the mode shape. From (velocity/force) FRFs, the peak values of the real part are used as mode shape components. Hence, using the simplest Local SDOF curve fitting methods, all three modal parameters (frequency, damping, and mode shape) can be extracted directly from a set of FRF measurements.

3.3.15 Local MDOF methods

The two most popular Local MDOF curve fitting methods are Complex Exponential and the Rational Fraction Polynomial methods.

a) Complex Exponential (CE): A set of impulse response data is normally obtained by applying the Inverse FFT to a set of FRF measurements. The advantage of this method is that can handles many modes, fast and numerically stable. Its disadvantage is that must be over specifying number of modes and delete computational modes and the leakage of the time domain.

b) Rational Fraction Polynomial (RFP): This method applies the rational fraction polynomial expression directly to an FRF measurement. Its advantage is that it can be applied over any frequency range of data, and particularly in the vicinity of a resonance peak.

3.3.16 Global and multi-reference methods

Both the complex exponential and rational fraction polynomial methods have been implemented as Global and Multi-reference methods also. The details are given by (Formenti & Richardson 1985; 1986) and (Vold & Rocklin. 1982).

3.3.17 Modes

Modes (or resonances) are important properties of a structure. Resonances are determined by the material properties (mass, stiffness, and damping properties), and boundary conditions of the structure. Each mode is defined by a natural frequency, modal damping, and a mode shape. If either the material properties or the boundary conditions of a structure change, its modes will change. For instance, if mass is added to a structure, it will vibrate differently because its modes have changed. At or near the natural frequency of a mode, the overall vibration shape of a machine or structure will tend to be dominated by the mode shape of the resonance.

3.3.18 Mode shape

In the study of vibration in engineering, a mode shape describes the expected curvature (or displacement) of a surface vibrating at a particular mode. The mode shape is multiplied by a function that varies with time, thus the mode shape always describes the curvature of vibration at all points in time, but the magnitude of the curvature will change. The mode Shape is dependent on the shape of the surface as well as the boundary conditions of that surface.

3.3.19 Coherence

Coherence is a function of the energy of the output signal caused by the input signal. It is a function of frequency, and its value ranges from zero to one. A coherence of less than one may be caused by unmeasured inputs or multiple energy sources, the presence of noise, or a nonlinear system relating the input to the output. The coherence function is typically used to ensure the quality of the frequency response function measurements. For a high value of coherence in particular frequency range, the output is caused by the input and the frequency response function estimate is valid for that range of frequencies.

3.4 RIDE COMFORT OF PASSENGER CARS

Nowadays people are most complaining about the discomfort inside the passenger cars. Mainly, this discomfort is caused by the noise and vibration pollutions. These pollutions are transmitted to human and affect them in different ways. Transmission of vibration depends on many factors such as frequency and the direction of the input and characteristics of the output. Furthermore, sound would be analyzed by human brain based on its frequencies and amplitudes. Transmission of noise has various effects on the comfort, performance and health of the passengers; it would also cause permanent hearing damage. These effects depend on the strength and duration of exposure and psychological characteristics of the human body (Taylor 1971).

Hence, noise and vibration analysis is necessary prior and after the identification of their sources. Various studies were conducted on noise and vibration quality inside the passenger car in order to achieve the vehicle noise and vibration comfort in different operation conditions (Thomas et al. 1991; Ishiyama and Hashimoto 2000; Farina and Bozzoli 2002; Repik 2003; Genuit 2004; Lee et al. 2005; Mohd Nor et al. 2006; Nahvi et al. 2006). Therefore it is a fundamental requirement to study dynamics of the car components to obtain an accurate description of its structural vibration, which has a strong relationship with the interior comfort.

Usually, in vehicle refinement there is a chain of mechanical noise and vibration consists of source, transfer path and receiver. The first step is to discover the sources of excitations. After that engineers would plan appropriate strategies to eliminate the sources or attenuate them to international standard level.

In motion, cars sweep a wide range of vibrations that can be sensed by the driver and influence him and his driving as well. The excitation sources for these vibrations can be road roughness, tire/wheel assembly, driveline excitation, engine excitation, aerodynamic forces, and transmission excitation. Usually, road roughness and engine vibration will be the major source that excites the car body through tire/wheel assembly and suspension system. The vibration of the car body components will be contributed to the interior noise in the form of structure borne noise. Other sources contribute least because of their own design that their vibrations will be transmitted through longer routes until it will reach the occupants.

Till now the main tests for ride comfort subjective and the objective testing is not yet developed in a standardized way. The main three areas of research in ride comfort are human response to vibration, vehicle response to excitation, and ways of testing and evaluating the ride comfort. In this section, we are going to focus more on passenger cars.

3.4.1 Human response to vibrations.

In general, the human response to vibrations is quite complex. This is mainly due to the distinctive features of every human being and the different sensitivity. Research in this area had started longtime back and still growing but no final word have been said, which opens the way to more active and creative research.

Goldman divided the human response level into three thresholds (Goldman 1948):

- Threshold of perception (level 1) – detectable using sensory measurement.
- Threshold of discomfort (level 2) – Stimulus is intense enough so that the subject feels a tinge of discomfort or unpleasantness due to pain, muscular effort or any other source.
- Threshold of tolerance (level 3) – the subject is unwilling to tolerate the stimulus further due to pain, extreme discomfort or merely lack of desire to cooperate. He

conducted a test where all subjects were standing, seated or lying down on a vibrating body with the direction of vibration along any of the three principal body axes for the duration of exposure of few minutes. Results showed that differences due to the direction of application of the vibration were smaller than statistical variations. Therefore data were grouped without directional factor with the assumption that direction was secondary importance. Also, it was concluded that level 1 has a minimum acceleration near 5 Hz and the sensory receptors are most sensitive near 250 Hz.

Human vibration must be defined in terms of: the nature of the forcing function, the source of vibratory energy, the path between the source and the human, and the posture and characteristics of the receiver (subject). (Pradko 1965) developed a technique to identify and measure whole body human response to vibration and to describe properly the performance potential of man in vibrational environment and to predict his response.

Measurable changes in human equilibrium are caused by input vibration and such changes may appear in physical performance capabilities – ability to concentrate, ability to communicate and visual acuity. The author gave detailed discussion on the experimental setup for vertical, pitch, roll, vertical and pitch, pitch and roll, and vertical, pitch and roll modes. Subjects were evaluated from eight different experimental positions – standing (erect and knee bent), seated (relaxed and braced), reclining and walking (normal walk, fast walk and running).

Pitch vibration affects human tolerance significantly more than do roll and vertical vibration, pitch tolerance does not change appreciably with increased frequency, whole body tolerance of random vibration in the vertical mode is significantly greater than sinusoidal tolerance, whole body vibration endurance is greatly increased for vertical motion when space orientation is removed when the vibratory path is applied completely or partially to the head, the vibration tolerance is decreased to a minimum level, and acceleration tolerance is greatly influenced by the direction and duration of the force vector and the measurement technique employed to record effects.

Human response in a vibratory environment can be determined through measurement of input conditions only. Absorbed Power concept is an advantageous method in identifying human reaction to vibration (Pradko 1966). Many studies are conducted by various researchers on tolerance and comfort for sinusoidal vibration and some comparison between sinusoidal and random vibrations. In random vibration, many frequencies may be present simultaneously or at least within some specified bandwidth. Therefore for the purpose of calculation and experimental work, the concept of acceleration density is used, where the total summation of acceleration amplitudes over a frequency spectrum yields the mean square value of the acceleration. It is literally defined as:

Power Spectral Density, $PSD = \lim_{B \to 0} \frac{a^2}{B}$

Where a= rms value of the random acceleration

B = Band width or range of frequencies under consideration.

The power spectral density (PSD) curve is a plot of the acceleration density of each component frequency (g^2/cps) versus frequency over the spectrum of interest. They used transfer function for acceleration to predict human mechanical response to vibration and proposed the transfer function for acceleration.

Comparison between analytical results from the transfer function with experimental measurement of subjective response shows good correlation. Correlations also were shown in the case of square wave and white noise input. Further tests were conducted to validate the advantage of absorbed power. They concluded that transfer function statements may be used to determine absorbed power for random vibration condition, and subjective human response may be accurately described by absorbed power.

Whole body human response to mechanical vibration below 60 Hz can be determined through measurement of input condition only using the concept of absorbed power. This technique does not require information on the frequency spectrum and can identify human response with single numerical distinctness (Pradko and Lee 1966).The absorbed power technique was compared to others, especially Power Spectral Density

(PSD) and found that PSD and others statistically describe the vibrational input to the occupant but failed to identify his subjective response to that environment. The important assumption and establishment for the technique is that human behaves as a linear system, at least within the bounds of interest. The human response displays linear characteristics to vibration under physical equilibrium, transfer function statements accurately describe human response to random vibration, and absorbed power describes human response quantitatively and is sensitive to time.

The absorbed power method can be used analytically to determine human response to vibration for periodic and random environments. Vibration in real world occurs as a time function, which can be periodic or aperiodic (Lee et al 1968). When human is exposed to a vibration, human impression can be considered as a two step procedure: first the physical motion or mechanical response, then the subjective response - a psychological impression.

Human physical response was shown to have nearly linear characteristics and can be treated under proper constraints as quasilinear. The subjective response is nonlinear. The physical response is comparable to an elastic system – having both transient and steady-state components of vibration distinguishable. As vibration is received by the human, it is transferred and distributed throughout the body, and is modified by the inertia, damping, and the elastic restoring force of the connective muscle tissue and the skeletal structure. Different organs or portions of human body would have different magnitude of vibration transmitted from the original input. In studying the vibration transmission from one part of body to another, there is no single accepted point of reference for measurement. Transmissibility or the frequency response is referred to the ratio of the steady-state response of the excited mass to the motion of the exciting mass, i.e. the ratio of the output to the input. Extensive testing has shown that the rate of flow of energy become the parameter that characterizes the interaction of the vibrating human and environment. This is termed as average "absorbed power".

In general, a muscular person has a lower absorbed power than a more obese person of the same body weight. A contoured seat generally would produce lower absorbed power. Absorbed power is a scalar quantity, therefore for multi-degree of freedom systems, the individual values can be simply added for a single quantitative and qualitative measure of vibration. Finally, the authors provided tables of absorbed power constants for the four different vibration inputs and concluded that absorbed power method can accurately measures vibration severity for short period of exposure but a relation need to be established to take into account for long term exposure.

Another experimental technique was developed is known as the *floating reference*. It used to compare the subjective response of seated subjects to sinusoidal vibrations (Donati et al. 1983). They found that subjects are more sensible to random than to sinusoidal vibration, significant differences with the ISO 2631 were observed and discussed, and floating reference has significant advantage to constant reference.

Using seated subjects exposed to vertical and lateral vibration, females are more sensitive to vibration than males at 3.15, 4.0 and 5.0 Hz for 0.75ms^{-2} r.m.s reference and at 5.0 Hz for 0.25 ms^{-2} r.m.s reference and increasing sensitivity to vibration acceleration at frequencies above 2 Hz.

By involving the determination of a comfort contour using octave bands of random vibrations centered on 0.5, 1.0, 2.0 and 4.0 Hz it found that the magnitude of equivalent comfort using random stimuli is lower than using sinusoidal stimuli, i.e. subjects are more sensitive to random motion than sinusoidal motion, but not very significant different, with an average of 7% lower. (Corbridge & Griffin 1986). For lateral vibration using sinusoidal vibration there is no significant differences at any of the frequencies between the two groups and maximum sensitivity to lateral vibration occurred in the range 1.25 – 2.0 Hz.

Equivalent discomfort contours for whole-body vibration produced by vibration in the fore-and-aft, lateral and vertical axis directions have been obtained by carrying a vibration test until it gives discomfort equivalent to some standard or i.e. using the method of adjustment (Fairley &Griffin 1988). A discussion on the shortcomings of the method of adjustment is presented and several approaches were made to minimize the errors. The Wilcoxon signed-ranks test was used to test whether there were significant differences between the actual discomfort (experimental) and the discomfort predicted by the three procedures of linear sum ($n = 1$), root-sums-of-squares ($n = 2$) and the worst component ($n = \infty$). Two experiments were conducted. Experiment 1 showed that the root-sums-of-squares procedure gave the best predictions while the linear-sum has over estimated the discomfort and the worst component have underestimated. There was no apparent difference between frequencies. Experiment 2 also showed that the root-sums-of-squares give better result than the other two. However, there were some significant differences between the root-sums-of-squares predictions and the actual discomfort. It is worth to note that the root-sums-of-squares procedure is also the one suggested by the International Standard ISO 2631 Amendment 1 and the British Standard BSI 6841.

Furthermore, vertical vibration effect writing and holding cup ability. Considerable difficulties are experienced when attempting to write while exposed to whole-body vibration (Corbridge & Giffin 1991). Authors are also discovered the effect of vibration on drinking ability and found that subjects were less affected by yaw vibration than roll or pitch and were less affected by motion in the horizontal axes than in the vertical. Finally, they concluded that adding sinusoidal vibration of duration 10s and frequency range of 3.15 to 8 Hz will increase the writing difficulty and affect the writing performance. This is fairly consistent with the frequency weightings defined by ISO 2631 and BS 6841 which indicate maximum sensitivity to vibration acceleration in the frequency range of 4 to 8 Hz, the reference magnitude and frequency had little effect on subjects holding a cup of liquid. However, adding sinusoidal vibration especially from 3.15 to 5 Hz produce considerable difficulty and that at 4 Hz the most sensitive to vertical vibration.

Biodynamic human response to whole body vibration can be categorized using four biodynamic response functions: driving Point Mechanical Impedance (DPMI), apparent Mass (APMS), transfer Mechanical Impedance (TMI), and seat-to-head Transmissibility (STHT). While the first three functions often used to describe *to the body* biodynamic function, STHT instead, describes the vibration transmitted through the body. In vertical direction, the STHT curve has two resonant frequencies: near 5Hz – corresponds to whole body resonance, near 14 Hz – corresponds to upper body resonance, and in some cases third resonance corresponds to foot resonance. In fore and aft, the STHT curve has one resonant frequency, corresponds to the whole body resonance and in multi-directional vibration the STHT curve has 2 resonant frequencies in the fore and aft direction. The platform-seat-human system is nonlinear in the fore and aft direction and the increase in seat-backrest angle changes the resonant frequency and increases the STHT magnitude, phase and coherency. In the vertical vibration, subjects are very sensitive to low-frequency random vibration (less than 1 Hz), less sensitive to narrowband random vibration (1.25 Hz to 5 Hz) and least sensitive to frequency above 5 Hz and in the fore and aft vibration, subjects are very sensitive to vibration below 0.8 Hz, less sensitive to the frequency range of 1 – 5 Hz and least sensitive to frequency above 5 Hz. Also, subjects are more sensitive to random, multi-directional vibration than one-directional and equivalent comfort curves for multi-directional random vibrations are 15 to 20 percent lower than for one-directional vibrations. (Demic et al. 2002).

3.4.2 Vehicle response to excitations

Vehicle response to excitations is usually analyzed in two approaches. First approach is using discrete modeling. This approach breaks down the car into lumped systems of masses, springs, and dampers are the most popular among researchers due to its simplicity and it is argued that it gives reasonable results with minimum computation effort. The second approach is using what is known in dynamics as continuous modeling. In this approach, the car is taken completely including its geometry into consideration. The main tool for this approach is Finite Element Method. This approach is becoming popular in industries but the main disadvantages are the computational effort and the need for an expertise in using FEM. As mentioned earlier, discrete system approach is still the most common among researchers.

Stone and Demetriou have described a detail derivation of a full car vehicle model with 6-DOF using the Newtonian approach (Stone et al. 2000). This model is able to simulate the effect of suspension (ride) as well as braking and steering (handling) in all three translational motions (vertical, forward and side), pitch, roll and yaw (heave) directions. General assumptions in deriving the model, which are common assumptions, are provided, that are: the vehicle mass may be lumped into a single mass which is referred to as the sprung mass, the vehicle center of gravity is located above the roll and pitch centers, the vehicle suspension springs will not be allowed to top out during maneuvering; the suspension springs will always be in compression, aerodynamic lift and drag force, and tire rolling resistance are neglected, the vehicle remains grounded at all times, i.e. the four tires never lose contact with the ground, and the deflections in the pitch and roll planes are small, and may be simplified with small angle approximation.

Gillespie and Karamihas (2000) studied quarter car model under effect of road roughness. They found that quarter car models to be adequate for discriminating the roughness of the road on a scale that correlates well to the public judgment of its severity.

Type of suspension element has significant effect on the vehicle suspension system performance. Researchers introduced a solution of the vehicle dynamics problem by studying the effect of various types of suspension element on the vehicle suspension system performance. Load carrying capacity of a vehicle rear suspension can be solved using stiff suspension spring system or a twin spring suspension system, a fully active suspension system can improve the vehicle performance criteria significantly but at a high cost, the tire damping has a very small effect on the vehicle ride comfort, when the tire stiffness parameter is increased, the systems have higher wheel resonance peaks in the dynamic tire load response (Soliman et al. 2001).

3.4.3 Ride comfort testing

Ride comfort testing is the sum of all measures which maintain and improve the well-being of a person and reduce his fatigue during traveling (Von Eldik 1966). It consists of:

- Riding Comfort – the comfort experienced in the road or rail vehicle itself.
- Local Comfort – the comfort experienced at stations, interchange points, and airports.
- Organizational Comfort – such as good connections, reliability of service and custom clearance.

In this study we dealt only with the Riding Comfort we focus only on the mechanical vibration problems. There are generally two types of tests for comfort criteria, which are Objective and Subjective tests. Objective test is related to medical test in which human fatigue is considered as a criterion. Several investigations were discussed and can be concluded that it is very difficult to establish good relation between fatigue and the vibration characteristics of the vehicle. Subjective test is widely used in comfort criteria and a reasonably good correlation has been established between comfort criteria and the vehicle‘s vibration characteristics. Several criteria proposed by various researchers were discussed like Reiher-Meister Criteria, Jacklin-Liddel Criteria, Janeway Criteria, Sperling Criteria, Mauzin-Sperling Criteria, and Dieckmann Criteria. These criteria were compared carefully and modified classification of limits for different groups of vibrations were later introduced. However the limits are still disputable.

Riding comfort is a subjective experience resulting from whole body (or nearly whole body) vibration to which a person is subjected when riding in a motor vehicle over an uneven course.

Human response to vehicle vibration assessment can be categorized into four different approaches: subjective ride measurement – the traditional technique which employs a trained ride jury. Suitable to compare of more than one vehicle, shake table analysis, ride simulator tests – either an actual vehicle body is mounted on a hydraulic actuating mechanism or Computer Simulation facilities, and ride measurements in vehicles – on-the-road measurement (Van Deusen 1968). It was found that the cross modality technique is a meaningful method of measuring subjective ride sensation in a vehicle. The importance of spectral composition in subjective testing is for the meaningful result, and direction of vibration affects the feel. Thus, variance of acceleration in each frequency band and covariance between directions should be tabulated to quantify riding comfort in actual vehicles.

The evaluation of travelling comfort can be a function of cab isolation parameters. The technique/criteria recommended by SAE for the 'measurement of whole body vibration of the seated of agricultural equipment – SAE J1013', can be used to evaluate the capability of cab isolation systems for ride travelling improvement of on-highway tractors (Allen 1975). The author used an analog computer model to simulate various suspension parameters and described the test setup and data acquisition. He concluded that by modifying the suspension elements at the back of the cab, no improvement in the vertical ride can be obtained and some improvement in the longitudinal ride can be obtained but at the expense of lost in vertical ride.

Dempsey et al. (1979) conducted experimental work to develop criteria for ride quality prediction in a noise-vibration environment where subjects are seated on an apparatus that resemble the interior of modern jet transport and asked to evaluate the comfort by comparing the test vibration to a reference. They observed that addition of noise to the vibration environment generally increases the discomfort responses, increasing acceleration at each noise level/octave band combination generally increasing discomfort level, rating of discomfort level increases linearly with vibration acceleration when noise is absent, and loses its linearity as noise is increases, and logarithmic value of the rating of discomfort level increases linearly with noise level. They also came out with a set of constant discomfort curves or criteria curves for human response to the combined environment.

3.5 SUMMARY

In the first part of this study we gave some basic definitions on vibration, because we believe that are important for any reader or researcher to understand before start any study related to noise and vibration. The second part covered the theory of modal analysis which is the core of this research. The last part is a reviewed study on ride comfort of cars. Three main categories were involved, human response to vibrations, vehicle response to vibrations, and ride comfort testing. It was found how these responses affect the vehicle occupants and how to evaluate the ride comfort of passenger car. In general the human response to noise and vibrations is quit complex. This is mainly due to the distinctive features of every human being and different sensitivity. Thus, more researches need to be conducted on these areas to solve this problem. The main complexity of these fields is that the three categories are interrelated and influencing each other.

CHAPTER 4

METHODOLOGY OF COMPUTATIONAL AND EXPERIMENTAL MODAL ANALYSIS

4.1 INTRODUCTION

The main objective of this chapter is to raise awareness and generate discussion about the research methodology to identify the natural frequencies and mode shapes of the car structure using experimental and computational modal analysis part by part. Modal analysis was utilized as a tool to find the dynamic properties of the passenger car namely natural frequency, mode shape and damping. Computational modal analysis part by part results are also presented in this chapter to be validated by experimental modal analysis part by part method in the next chapter.

4.2 COMPUTATIONAL MODAL ANALYSIS

Computational modal analysis part by part was conducted using FEA technique. It is a computer simulation technique used in engineering analysis. It uses a numerical technique called finite element method (FEM). It is the core and heart of all computer-aided engineering software and has revolutionized the way we solve and optimize engineering problems. In general, there are three phases in any computer-aided engineering task are pre-processing, analysis Solver and Post-Processing.

4.2.1 Ls-dyna

It is a multi-purpose, explicit and implicit FEM program used to analyze linear, non-linear static and dynamic behavior of structures. It is actively developed by Livermore Software Technology Cooperation (LSTC), in California, USA. LSTC was found in

1986. However, the beginning of LS-DYNA is traced back to the early 70′s. Furthermore, LS-DYNA provides many features making it a very powerful tool to solve a broad spectrum of applications, i.e. from easy to very complex problems. Some of the significant features in LS-DYNA are: full definition of contact area, large library of constitutive models, large library of element types and others (Carlos 2006). Beside of these features there are different implicit solvers and capabilities for working with the Arbitrary Lagrange Eulerian (ALE) method, Smooth Particle Hydrodynamics (SPH) thermal solver and coupled fluid dynamics. These capabilities allow the user to solve different problem with fluids and structure.

It's origins and core-competency lies in highly nonlinear transient dynamic finite element analysis using explicit time integration. It is capable of nonlinear dynamics, rigid body dynamics, eigenvalue analysis, fluid-structure interaction, crack propagation, fully automated contact analysis, implicit spring-back, multi-physics coupling, thermal analysis and adaptive re-meshing.

Typical applications include crashworthiness simulations, occupant and pedestrian safety, airbag modeling, metal forming, building safety, biomechanics (human FE models), material modeling of composites and ceramics, bird-strike analysis, drop tests of home appliances such as cell phones, PDAs, electric razors etc and many more.

4.2.2 CAD model proposed for project

The simulation results of any Finite element analysis depend on many variables. The most important ones are:

1. CAD Model.
2. Boundary Conditions and Initial Loading
3. Assumptions made

CAD models are the starting point for any analysis, and in this experiment the car of interest is a Proton Perdana V6 2001. Since no CAD model exists of this car we had to make use of what we have in terms of the available FEA models. The available

Models can be used for this investigation are from NCAC (National Crash Analysis Centre) as shown in figure 4.1:

	2001 Ford Taurus, Detailed model (1,057,113 elements) Date posted: 2008 May 12
	Dodge Neon, Detailed model (272,485 elements) Date posted: 2006 Jul 3
	Ford Taurus, Modified model (28,400 elements) Date posted: 2000 Oct 21

Figure 4.1 Available car models from NCAC

Source: www.ncac.gwu.edu

4.2.3 Model specification of 2001 Ford Taurus

Table 4.1 shows the specifications of the Ford Taurus car model 2001.

Table 4.1 2001 Ford Taurus specifications (NCAC)

	FE Model	**Test Vehicle**
Weight(kg)	1665	1776
Engine Type	3.0L V6	3.0L V6
Tire size	P215/60R 16	P215/60R 16
Attitude (mm)	F-705	F-713
As delivered	R-672	R-692
Wheelbase(mm)	2755	2755
CG(mm) Rearward of front wheel C/L	1035	1101

The following figure shows the detailed FE model of Ford Taurus car.

- Detailed Model can be used for all impact scenarios.
- Interiors trims are added to the model
- Material data derived from coupon testing
- Validated to Frontal NCAP

Number of Parts	778
Number of Nodes	936258
Number of Shells	805505
Number of Beams	4
Number of Solids	99486
Number of Elements	1057113

Figure 4.2 2001 Ford Taurus detailed model (NCAC)

Source: www.ncac.gwu.edu

4.2.4 Model specification of Dodge Neon

Model specifications of Dodge Neon car are given in Table 4.2. Two types of specifications are given; FE model specifications and test vehicle specifications. The model is shown in Figure 4.3.

Table 4.2 Dodge Neon specifications (NCAC)

	FE Model	**Test Vehicle**
Weight (Kgs)	1333	1354
Engine Type	2.0L I4	2.0L I4
Tire size	P185/65R15	P185/65R14
Attitude (mm)	F-675	F-660
As delivered	R-665	R-676
Wheelbase (mm)	2648	2642
CG (mm) Rearward of front wheel C/L	1046	1022

Figure 4.3 Dodge Neon model (NCAC)

Source: www.ncac.gwu.edu

4.2.5 Model specification of Proton Perdana V6 2001

The Model of the Proton Perdana V6 2001 is shown in Figure 4.4 and the specifications in Table 4.3.

Figure 4.4 Model of the Proton Perdana V62001

Table 4.3 shows the specifications of Proton Perdana car. This model will be used to conduct experimental modal analysis and compared with results obtained from computational modal analysis.

Table 4.3 Model specifications of Proton Perdana

Dimensions and Weight	
Overall length	4615 mm
Overall Width	1730 mm
Overall Height	1400 mm
Wheelbase	2635 mm
Front Track	1510 mm
Rear Track	1505 mm
Kerb Weight	1300 kg
Engine Capacity	2.0 L 4 G 63 I 4(1995-2000)

4.2.6 Conclusion:

The closest model to the Proton Perdana is the Dodge Neon model, though it has a slightly longer wheel base and has a slightly more kerb weight. The model has been modified to meet the Proton Perdana car model. This model should be the simulation model used to compare with the experimental modal analysis results of the actual Proton Perdana car.

The Ford Taurus is a larger car with a larger engine and the results may not be the same. But if given the time, we can run the same analysis on the Taurus as well to see the difference in results.

4.2.7 Computational modal analysis part by part methodology

The initial tests were carried out using Ansys Workbench since the knowledge of LS-Dyna was a lot less. This was the greatest problem we faced: the problem of carrying out modal analysis, but with which software and how. The following were the FEA software available:

• LS-PrePost -LS-Dyna.

• Ansys V11 and Ansys Workbench.

• Virtual Proving Ground 3.2 (VPG 3.2).

The methodology involved in Ansys V11 or Ansys workbench were relatively simpler and easier to follow as the documentation provided was reliable and robust. There are numerous tutorials available with the software and are also available online. Therefore it was a lot easier to do simple Modal Analysis on any structure that we can draw or we can import, but the problem remained that Ansys was not compatible completely with Ls-Dyna Keyword files. The model shown above is of this nature.

VPG 3.1/3.2 is very capable software with a lot of libraries that contain vehicle related components and used Ls-Dyna as its Processor and solver. The only problem was that VPG had terrible documentation where the manual had referenced nearly everything to the LS-Dyna Manual. Though this software had the capability to read LS-Keyword files we could not make full use of it, though we later see how this software helped us finally to solve our problems. LS-Dyna also has a free Pre and Post processing software called LS-PrePost, we had to in the end use this software.

4.2.8 Modal analysis part by part method in LS-Dyna

Modal analysis methods offer an opportunity for tremendous cost savings compared to traditional explicit approaches to transient dynamic analysis. Modal methods approximate the structural response of a body by a linear combination of pre-computed mode shapes, eliminating the need for explicit element processing. LS-Dyna's modal analysis capability is combined with existing rigid body features to offer the additional advantage of large rigid body motion with superimposed linear modal response.

An LS-Dyna modal analysis is performed in two stages. In the first phase, the modes are computed and are output to a binary database. Later in the second stage, this database can be used as input to supply modes for the transient dynamic analysis. In this way, modes maybe computed only once and re-used for transient analyses of several loading cases.

To extract modes we had to remove unwanted parts and components that pose a problem to the modal analysis and make the problem larger. The modes are computed using implicit analyses. An eigenvalue analysis is used to compute Eigen modes, which are written to a binary database named “d3eigv”. This database is viewed using LS-PrePost. The following control cards are crucial for Modal analysis:

* CONTROL_IMPLICIT_GENERAL

* CONTROL_IMPLICIT_EIGENVALUE

* CONTROL_IMPLICIT_AUTO

* CONTROL_IMPLICIT_SOLVER

At first we tried doing the modal analysis for the whole car so that we will not have to do it for individual components. The problem was that this model was designed for crash test and has several other parameters attached to the car model that is irrelevant to the modal analysis. Afterwards, we have discovered a new method is called modal analysis part by part. The technique is to extract each part from the original FEA model and then carry out modal analysis test. At first we used LS-PrePost to output the activated parts. This resulted in the geometry to be exported but the properties of the parts were not. There were a lot of things that were not exported in this procedure and made the task a lot more difficult. Material properties, shell thicknesses, element types, spot welds were all not exported. Therefore, the problem was again that we were able to get the geometry but not the properties. We then used different software where we could select parts and export the activated parts with their properties. This is where VPG 3.2 came in handy, we could select the parts we wanted and then later export it and still keep the properties intact. Later, we discovered other techniques to even keep the spot welds on our designated parts.

4.3 SIMULATION RESULTS AND OBSERVATIONS

4.3.1 Trunk panel results

The FE model of the trunk panel is shown in Figure 4.5. The frequencies of the panel are listed in Table 4.4, and the first six corresponding mode shapes are shown in Figures 4.6. The others mode shapes are given in Appendix A. The details discussion is given bellow.

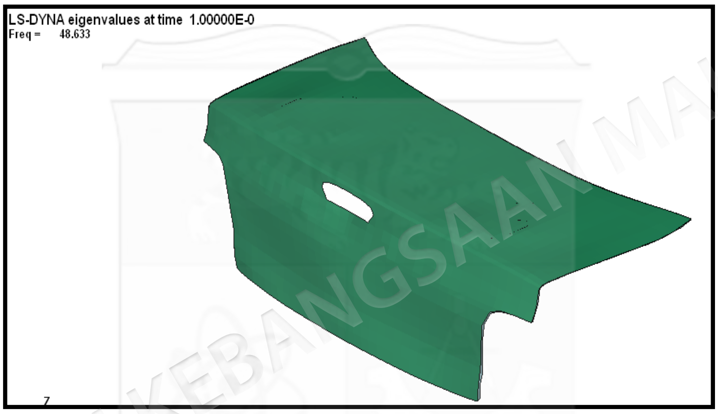

Figure 4.5 Car trunk panel

Table 4.4 Trunk panel frequencies

Mode no	Frequency
1st Mode	48.633
2nd Mode	71.94
3rd Mode	77.536
4th Mode	81.134
5th Mode	95.409
6th Mode	101.09
7th Mode	105.43
8th Mode	116.74
9th Mode	120.68
10th Mode	133.81

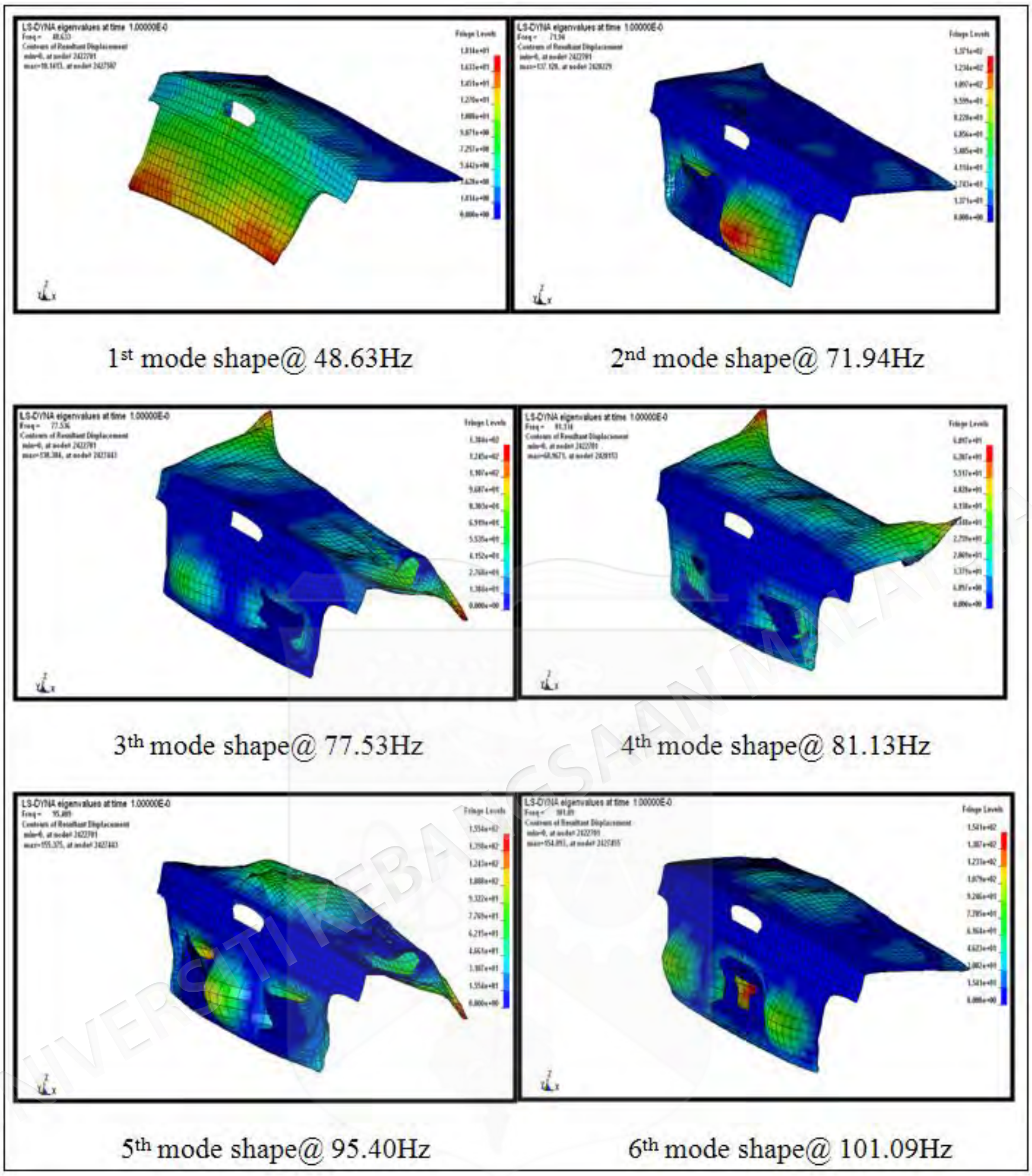

Figure 4.6 Simulation mode shapes for trunk panel

As shown in Figure 4.6, the first mode of vibration occurs at 48.63 Hz, the horizontal part appears to be not vibrating and the vertical part looks like flying freely with high amplitude at the bottom edge. The second mode of vibration occurs at 71.94 Hz, the vertical part of the trunk appears to be oscillating in a second bending mode as we can see clearly that the panel exhibit two nodes and three antinodes. However, the horizontal part does not show any significant vibration. The third mode of vibration looks like the second mode shape with less amplitude; the only difference is that the second mode shows vibration at the two corners of the horizontal part of the trunk. At the fourth mode the two antinodes of the vertical part are vibrating in phase and opposite to the two antinodes of the horizontal part. At the fifth mode the panel shows third bending mode at both vertical and horizontal parts of the panel with high amplitude. The sixth mode was at 101.09 Hz, it is quite similar to the fifth mode, with low amplitude, while the horizontal part does not show significant vibrations. The other modes are shown in Appendix A. At the seventh mode both vertical and horizontal parts of the trunk shows second bending mode. The eighth mode of vibration occurs at 116.74 Hz, the horizontal part of the trunk oscillates in torsional mode as we can see clearly that each two opposite corners vibrating in phase (twisting motion) and the vertical part shows second bending mode. The ninth mode of vibration occurs at frequency 120.68 Hz, both parts of the trunk vibrate in phase with a first bending mode. Also we can see that the vertical part vibrates with high amplitude compare to the horizontal part. The last mode of vibration occurs at 133.81 Hz, only the horizontal part of trunk vibrates with third bending mode.

4.3.2 Hood panel results

Figure 4.7 shows the hood panel FE model. Table 4.5 presents the natural frequencies of the hood panel and the first six corresponding mode shapes are shown in figures 4.8. The others mode shapes are given in Appedix A. Afterwards, the discussion of the results will be explained bellow in details.

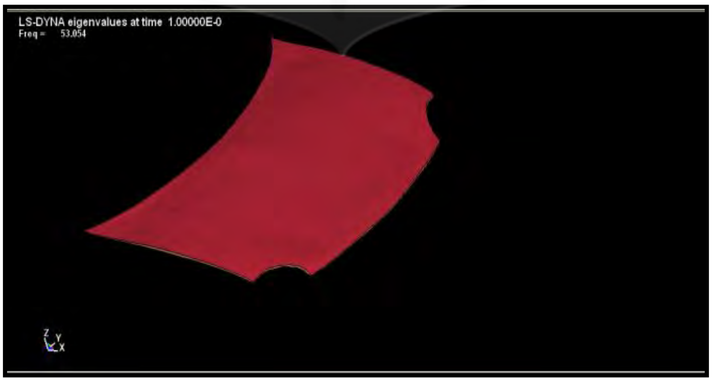

Figure 4.7 Car hood panel

Table 4.5 hood panel frequencies

Mode no	Frequency
1st Mode	53.054
2nd Mode	58.83
3rd Mode	76.084
4th Mode	84.153
5th Mode	86.802
6th Mode	100.87
7th Mode	102.89
8th Mode	107.78
9th Mode	117.59
10th Mode	125.68

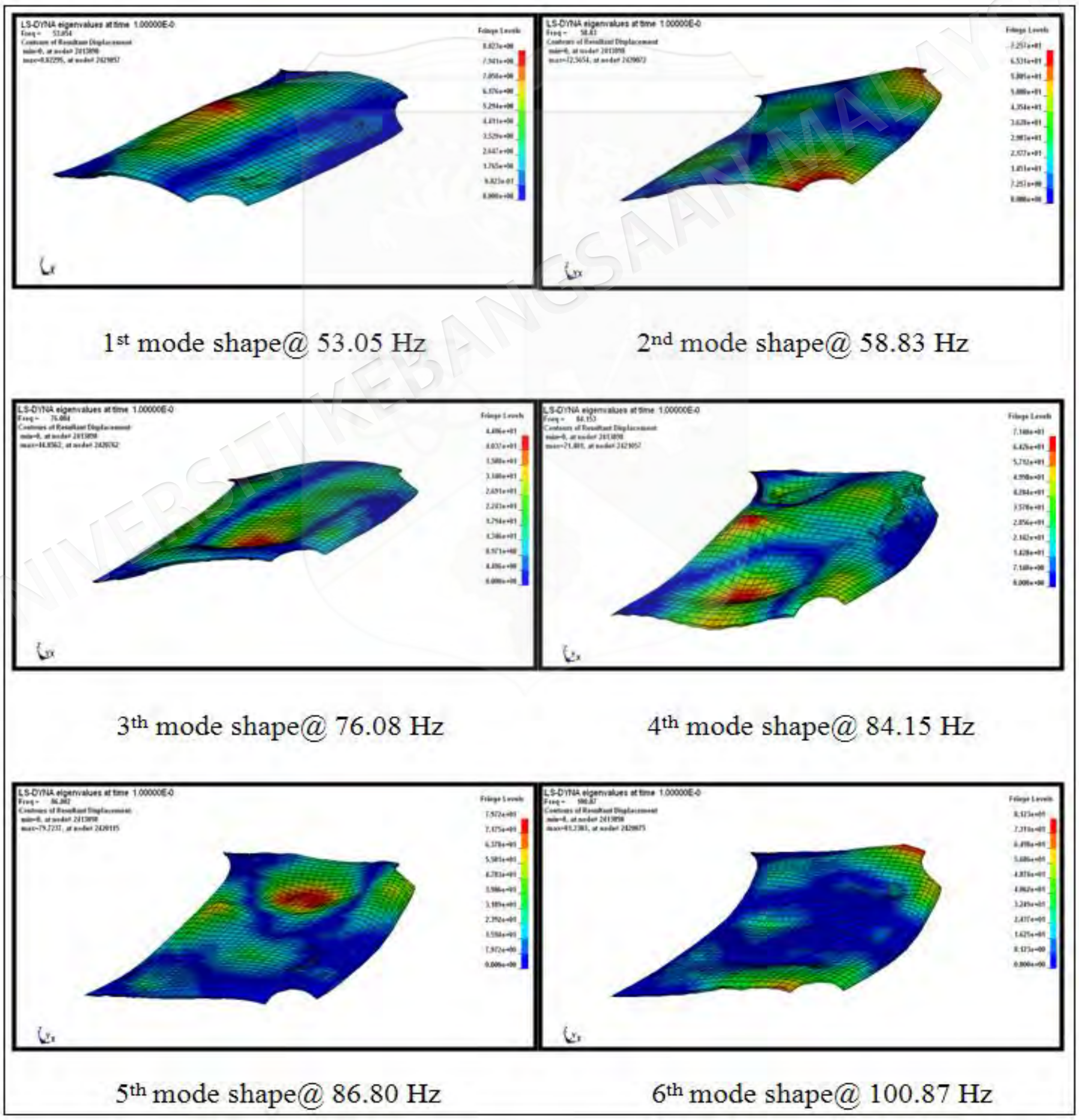

Figure 4.8 Simulation mode shapes for hood panel

As shown in figure 4.8 the first mode of the vibration occurs at 53.05 Hz, and appears to be a simple bending mode. The second mode occurs at 58.83 Hz, and it is a torsional mode, each two opposite corners are vibrating in phase. At the third mode the hood panel shows second bending mode, and occurs at 76.08 Hz. The fourth mode of vibration occurs at 84.15 Hz. It looks like a tortional mode as each two opposite corners are vibrating in phase. The fifth mode occurs at 86.8 Hz, and appears to be a second bending mode. There are two antinodes, one on the right side and the other one on the left side. The left antinode has high amplitude compare to the right one. The sixth mode of vibration occurs at 100.87 Hz. At this mode the two front corners of the hood are vibrating freely and the two rear corners are not, it looks like flying mode. Appendix A shows the others mode shapes. At the seventh mode, the panel appears to be in torsional mode, the two rear antinodes present high amplitude of vibration compared to the two front antinodes. The eighth mode of vibration occurs at 107.78 Hz. It shows high vibration on the left and right sides, and looks like flying mode. The ninth mode of vibration occurs at 117.6 Hz, and appears to be a third vertical bending mode. The last mode of vibration occurs at 125.7 Hz and only the left side of the hood is vibrating.

4.3.3 Roof panel results

The FE model of the roof panel is shown in figure 4.9. The frequencies of the panel are listed in table 4.6, and the first six corresponding mode shapes are shown in figures 4.10, the others in Appendix A. The discussion of the results is given bellow.

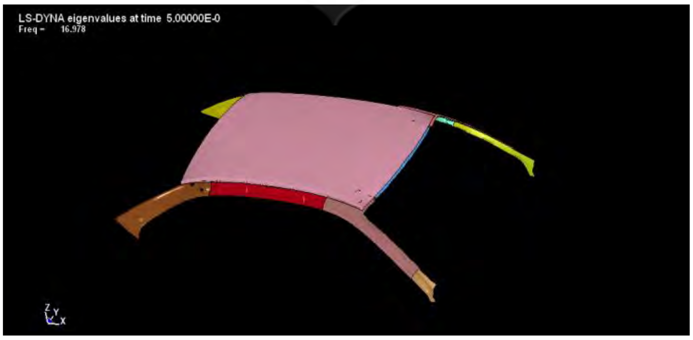

Figure 4.9 Car roof panel

Table 4.6 Car roof panel frequencies

Mode no	Frequency
1st Mode	16.978
2nd Mode	32.88
3rd Mode	38.331
4th Mode	73.574
5th Mode	75.439
6th Mode	76.429
7th Mode	97.818
8th Mode	100.5
9th Mode	102.93
10th Mode	104.56

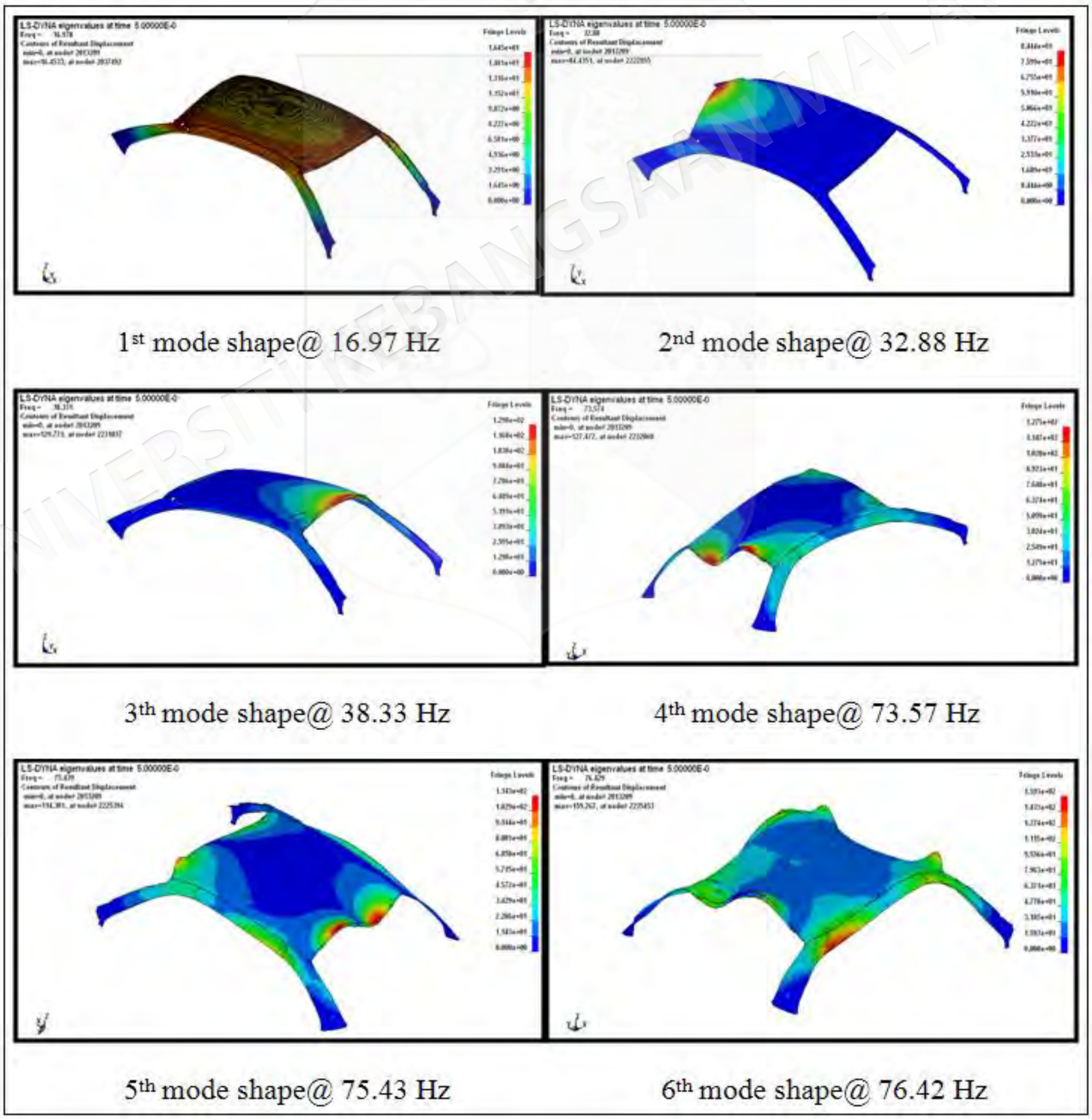

Figure 4.10 Simulation mode shapes for roof panel

The first mode of vibration occurs at 16.97 Hz. The roof appears to be in rigid body mode. The second mode occurs at 32.88 Hz. The roof at this mode shows a first bending mode at the rear part of the roof. Probably the mode results from the first bending mode of the rear frame. The third mode of vibration occurs at 38.33 Hz, and it is a first bending mode. This is also most probably resulted from the vibration of the front frame of the roof. Modes 4, 5 and 6 are close to each other (73.6 Hz, 75.4 Hz and 76.4 Hz respectively). All are showing same second bending mode at the rear part of the roof. Most probably the rear beam is the main contributor to the second bending mode. The seventh and eighth modes have similar behavior and also their frequencies are close (97.81 Hz and 100.5 Hz) respectively. They show first bending mode at the left and right sides the roof. The ninth mode occurs at 102.9 Hz. At this mode the roof shows a third bending mode at the rear frame of the roof with high amplitude at the middle antinode. The last mode was at natural frequency 104.5 Hz. It shows second bending mode at the front of the roof refer to Appendix A.

4.3.4 Door panel results

The FE model of the door panel is shown in figure 4.11, the natural frequencies are listed in table 4.7, the first six corresponding mode shapes are shown in figures 4.12 and the others mode shapes are given in Appendix A.The discussion of the results is also addressed bellow.

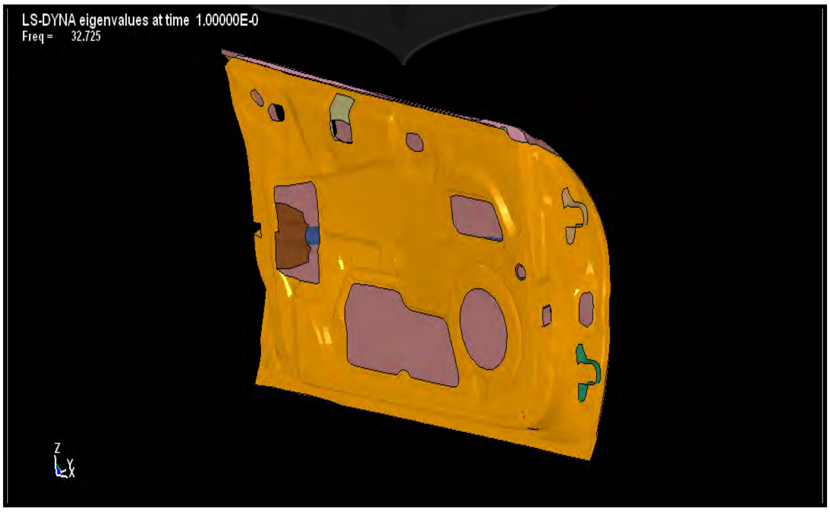

Figure 4.11 Front door panel

Table 4.7 Front door frequencies

Mode no	Frequency
1st Mode	32.725
2nd Mode	45.047
3rd Mode	55.71
4th Mode	64.924
5th Mode	74.015
6th Mode	74.355
7th Mode	86.525
8th Mode	94.882
9th Mode	99.37
10th Mode	105.45

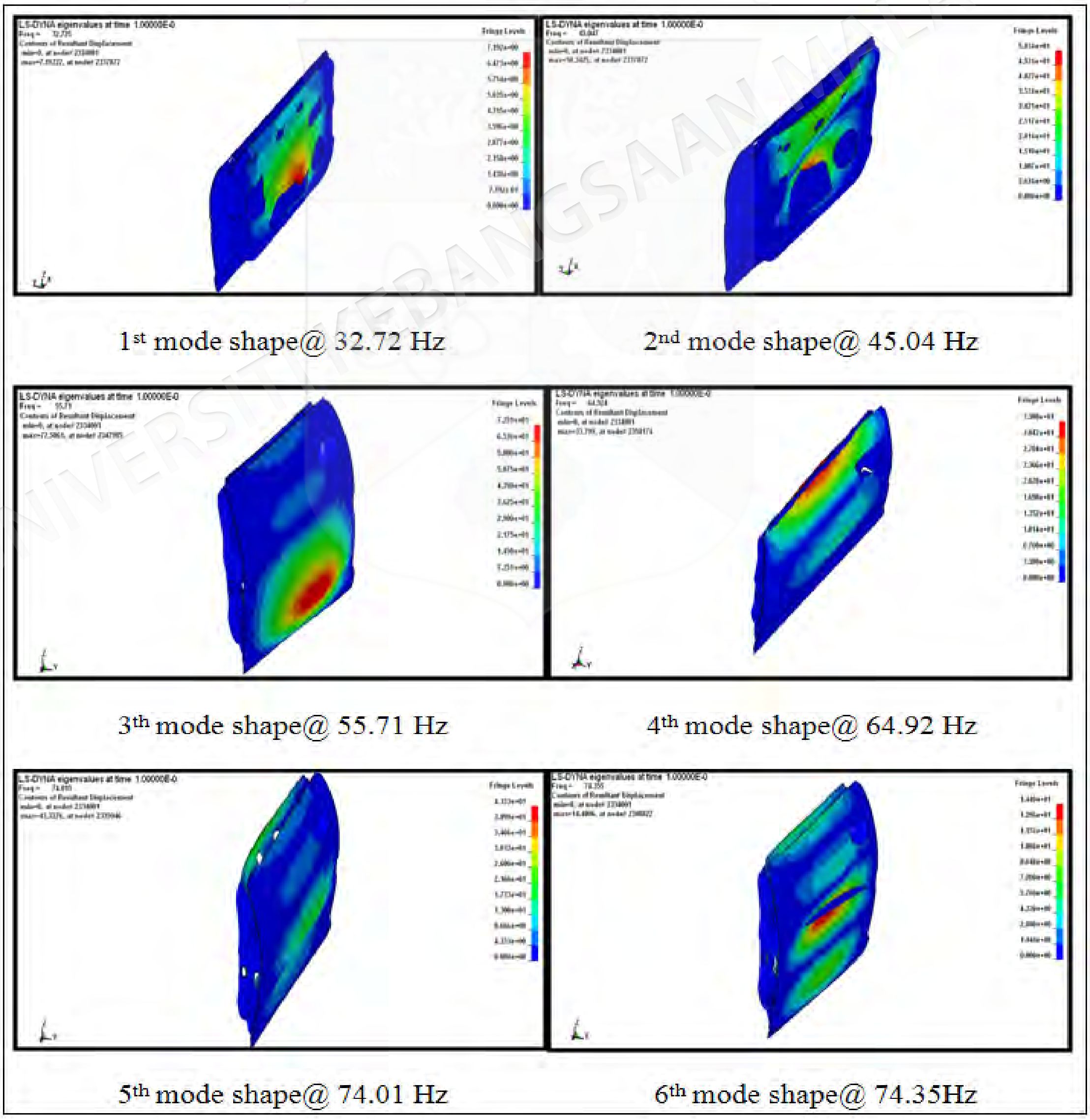

1st mode shape@ 32.72 Hz

2nd mode shape@ 45.04 Hz

3th mode shape@ 55.71 Hz

4th mode shape@ 64.92 Hz

5th mode shape@ 74.01 Hz

6th mode shape@ 74.35Hz

Figure4.12 Simulation mode shapes for door panel

The first two modes of the door panel occur at frequencies 32.72 Hz and 45.04 Hz respectively. The door panel does not show any significant vibration at these modes. It is only shows low vibration at the center. The third mode exhibits a first bending mode at the bottom half of the door panel at 55.71 Hz. The fourth mode occurs at 64.92 Hz. The door panel shows first bending mode at the upper half of the door panel. The fifth and sixth modes occur at 74.01 Hz and 74.3 Hz respectively. They are very close in frequencies, and both exhibit the same second bending mode at the bottom part of the door panel with low amplitude. At mode number 7 the door panel shows significant vibration at the inside part of the panel. The eighth mode occurs at 94.88 Hz. It shows first bending mode at the center of the door. This mode is resulted from the vibration of horizontal crossing beam as shown in the figure. At the ninth mode, the door shows more deformations at the bottom than the upper part of panel. The last mode was at 105.45 Hz. At this mode the door panel shows second bending mode at the bottom half. For mode shapes six and above refer to Appendix A.

4.3.5 Floor panel results

The FE model of the floor panel is shown in figure 4.13, the frequencies of the panel are listed in table 4.8, the corresponding first six mode shapes are shown in figures 4.14 and the others mode shapes are given in Appedix A. The results discussion is given bellow.

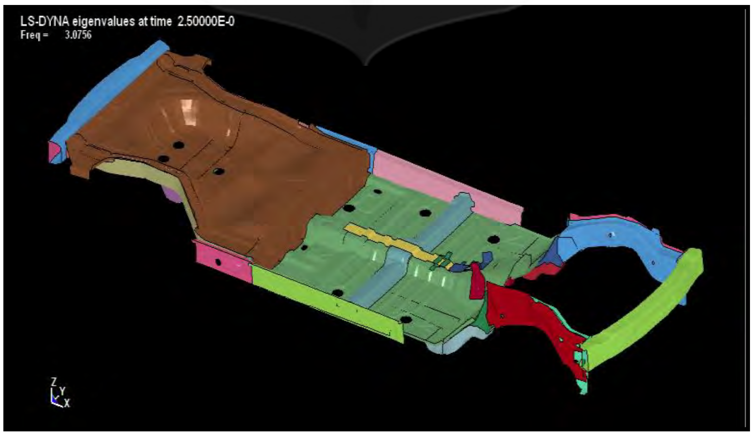

Figure4.13 Floor Pans and Chassis rails panel

Table 4.8 Floor panel frequencies

Mode no	Frequency
1st Mode	3.0756
2nd Mode	5.2638
3rd Mode	9.5924
4th Mode	12.793
5th Mode	16.274
6th Mode	18.156
7th Mode	21.325
8th Mode	24.638
9th Mode	28.368
10th Mode	31.51

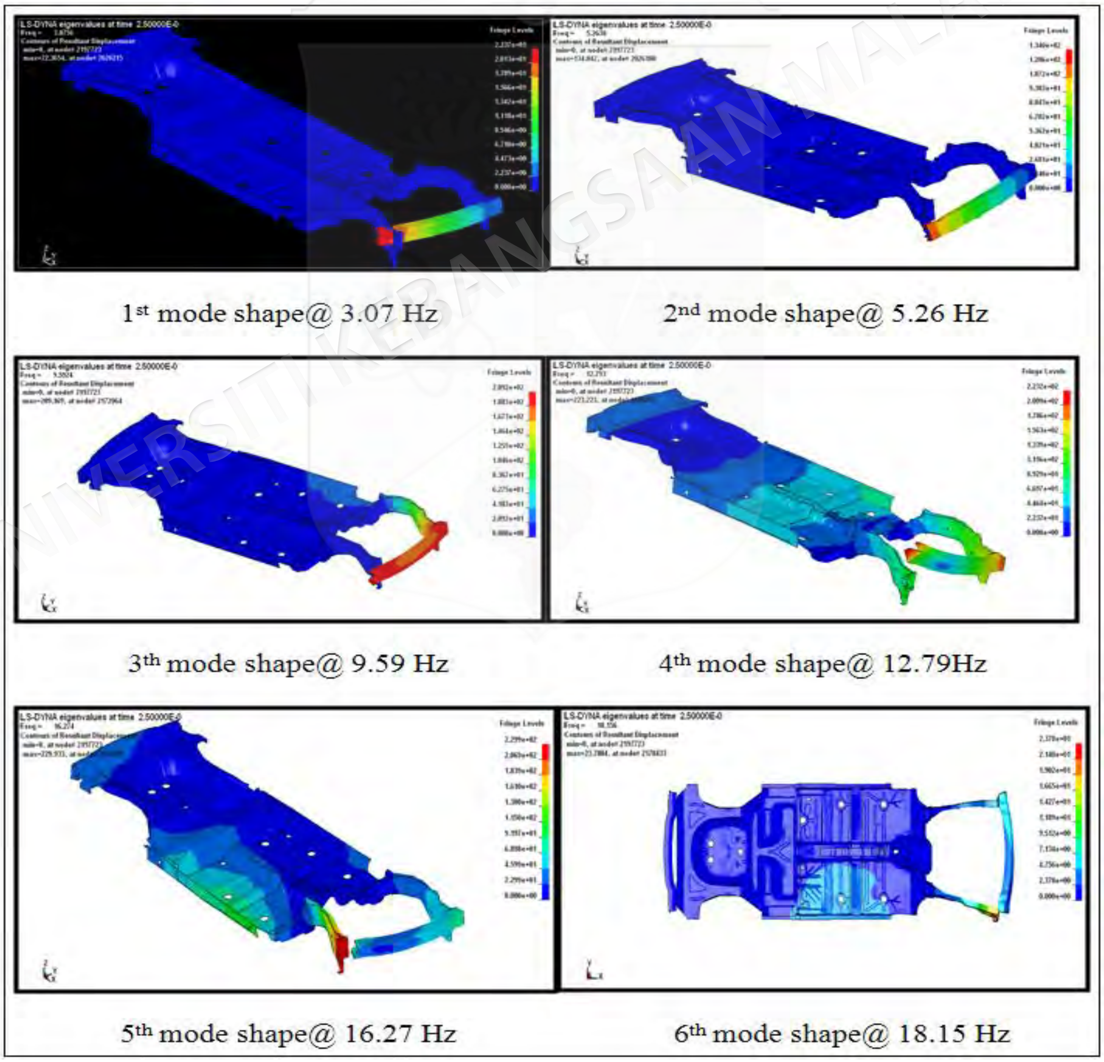

Figure 4.14 Simulation mode shapes for chassis panel

As shown in figure 4.14 and Appendix A. The first and second modes only the front steel panel vibrates. The third and fourth modes of vibration occur at 9.6 Hz and 12.79 Hz respectively. At these modes only the front steel and left valence are vibrating. The fifth and sixth modes were at 16.27 Hz and 18.15 Hz respectively, both modes exhibit the same deformations at the right valence side and right main panels. The mode shape at the seventh mode shows significant vibrations at the right valence side and less vibration at the left side of the main floor and the rear panel. The eighth mode of vibration occurs at 24.63 Hz, the main floor is vibrating symmetrically along the x-axis. The mode shape corresponds to the ninth mode shows significant deformation at the rear panel while the other parts do not show any significant vibration. The last mode of vibration shows torssional mode at the front of the panel.

4.4 EXPERIMENTAL MODAL ANALYSIS METHODOLOGY

In this section the experiments were performed to obtain the dynamic parameters (frequencies, mode shapes and damping) of the car panels. The current instrumentations and techniques used in the experiment are also discussed in details in order to improve the quality and accuracy of measurements.

4.4.1 Measurement preparation

Pre-preparations are very important. How well the pre-preparation we done, we will determine the betterment of the expected data in the experiment. There are several important considerations that must be taken into account before start the measurement in order to obtain accurate results such as identification of experimental model, checking the equipments of measurement, choosing the measuring method, mark the appropriate points on the physical geometry, choose the point of excitation and the positions of accelerometers on the object.

4.4.2 Description of experimental object and boundary conditions

The experimental object for this investigation is the body panels of Proton Perdana car (2.0 L 6A12 V6). The panels are: trunk, hood, roof and door panels. These panels are assembled with the whole car and the car was supported by its four wheels as shown in figure 4.15.

Figure 4.15 Proton Perdana car panels

Six accelerometers were mounted to the surface along each panel and the excitation was fixed at one point. Therefore, we have used single input multiple output (SIMO) method rather than single input single output (SISO) method to carry out results. The method is to fix the impact hammer excitation at one point and move the sequence of the six accelerometers over the all point on the structure and then finally we calculate the average transfer function of all points (Curve fitting). The first step for any experimental modal analysis is to consider the method of supporting the structure. In this project fixed boundary conditions was taken similar to the FEA boundary conditions. The constrained condition implies that the motion, displacement/rotation) is set to zero. However in reality most structures exhibit some degree of flexibility at the grounded connections (Guinchard 2007).

4.4.3 Measurement points and point of excitation

In this experiment, only degrees of freedom normal to the panel's surfaces were considered. The location of measurement points should be at the area where expect high response of the structure. In addition the curvature of panels in modal analysis does not affect the results in experimental modal analysis because the measurements are punctual. The measurement points for all panels are given in Figure 4.16 through Figure 4.23.

Figure 4.16 Distribution of the measurement points over the trunk panel

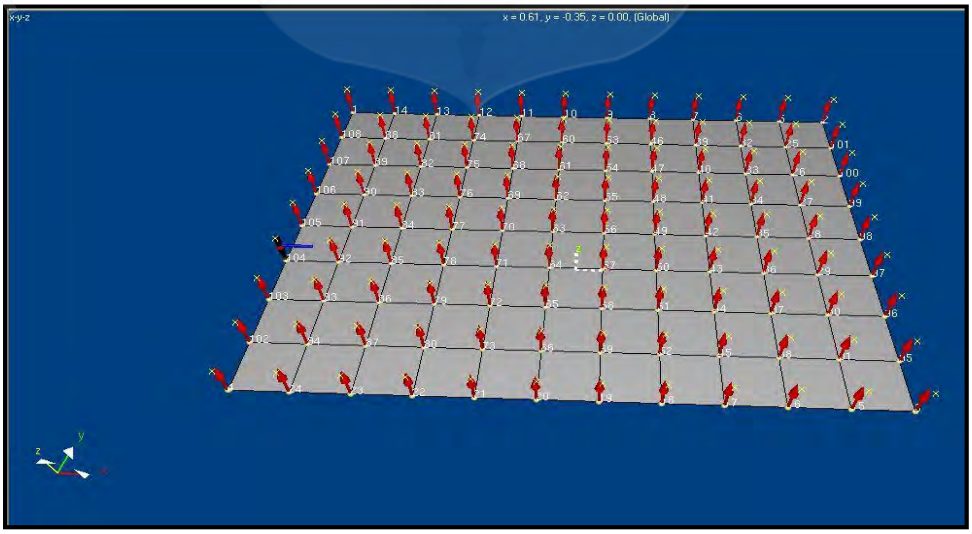

Figure 4.17 DOFs of the excitation and response forces of the trunk panel

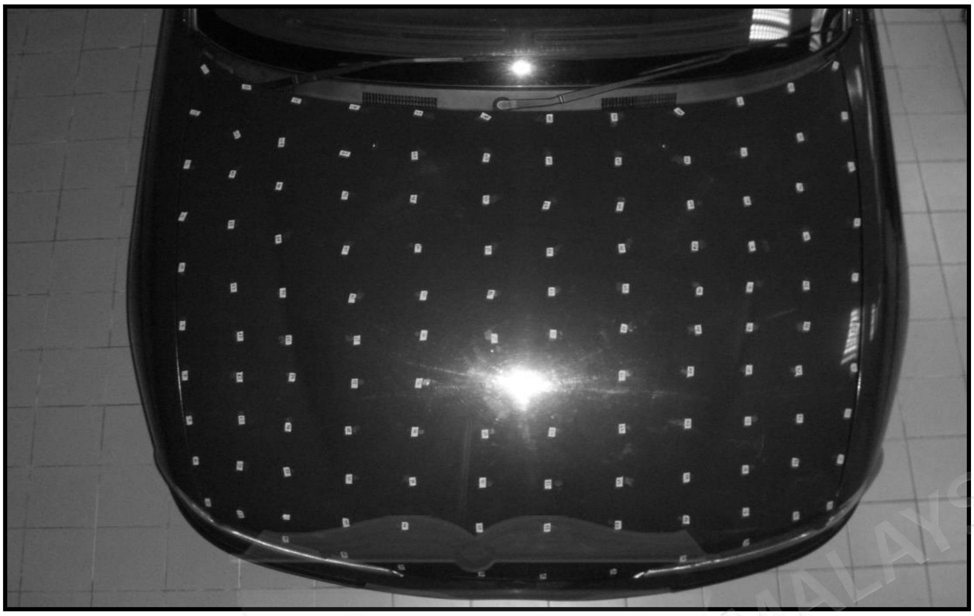

Figure 4.18 Distribution of the measurement points over the hood panel

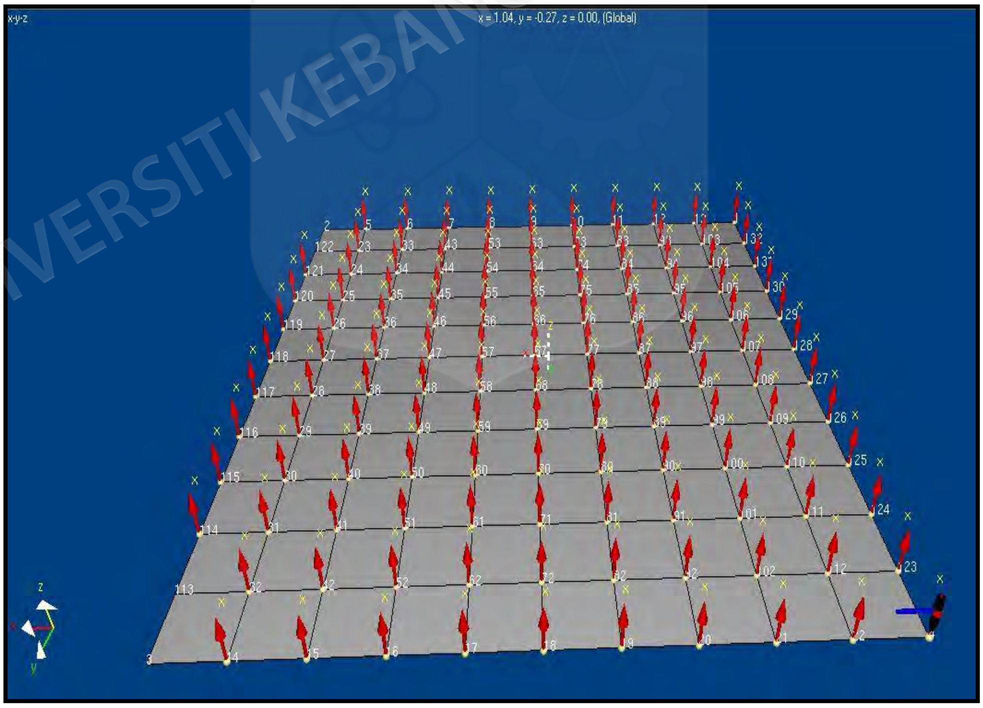

Figure 4.19 DOFs of the excitation and response forces of the hood panel

Figure 4.20 Distribution of the measurement points over the roof panel

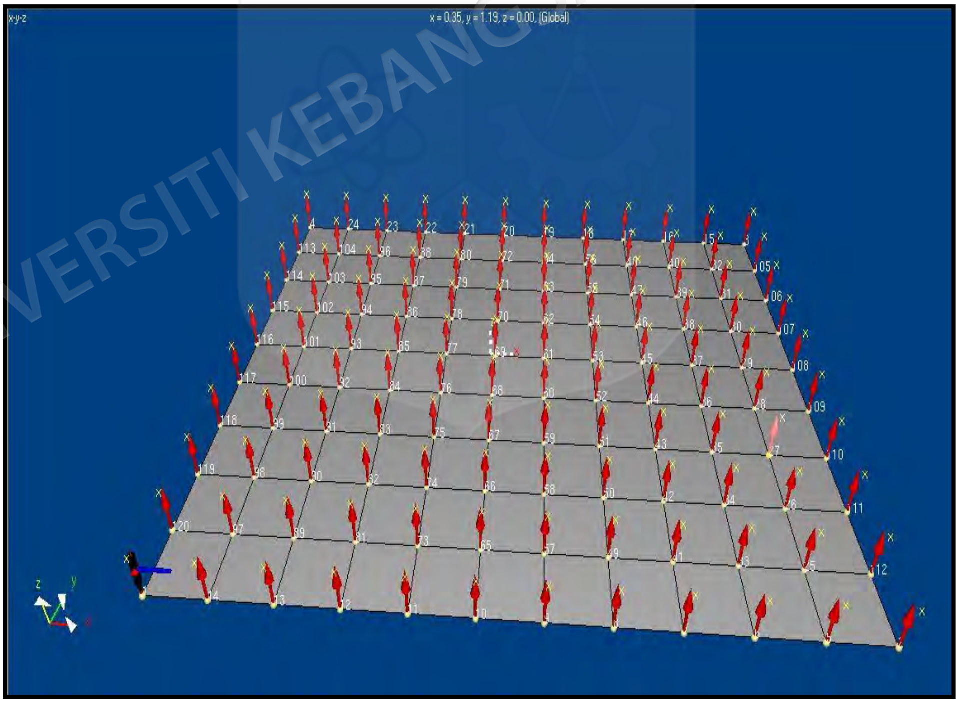

Figure 4.21 DOFs of the excitation and response forces of the roof panel

Figure 4.22 Distribution of measurement points over the door panel.

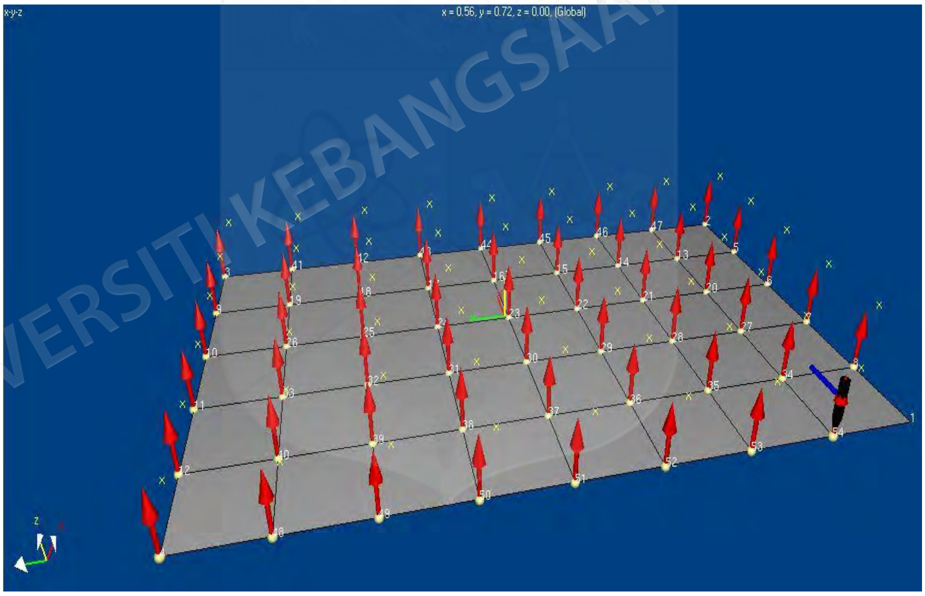

Figure 4.23 DOFs of the excitation and response forces of the door panel

The two main points that have to take in consideration when selecting measurement points are: the number of measurement points and the location of each measurement point. One thing that has to keep in mind when selecting the number of measurement points in experimental modal analysis is that there are enough points to cover all the desired mode shapes. When the measurement points chosen are minimal we may not see all the desired mode shapes. Also if too many points are chosen the measurement take an unnecessary long time. If the purpose of modal analysis is to identify the different mode shapes, then minimum points are probably sufficient. In the other hand if the purpose of the modal analysis is to validate a finite element (FEA) simulation than more points should be taken which is the case of this study. The location of measurement points should be at the area where we expect high response.

The measurement points for modal analysis of the car panels are shown in Figures 4.16 through Figure 4.23. These figures showed the distribution of the measurement points over the surface of panels. They are spaced equally over the surface of the panels. The location of the exciting point was chosen to be at the rigid area of the panel to ensure the excitation of all modes. Figures 4.17, 4.19, 4.21 and 4.23 show the excitation points of all panels.

For impact hammer excitation, usually the accelerometer is fixed and the hammer is moving around the structure. However, because we have enough accelerometers available we had fixed the impact hammer excitation and move the sequence of the six accelerometers around the structure see Figure 4.24. This gives a large corresponding

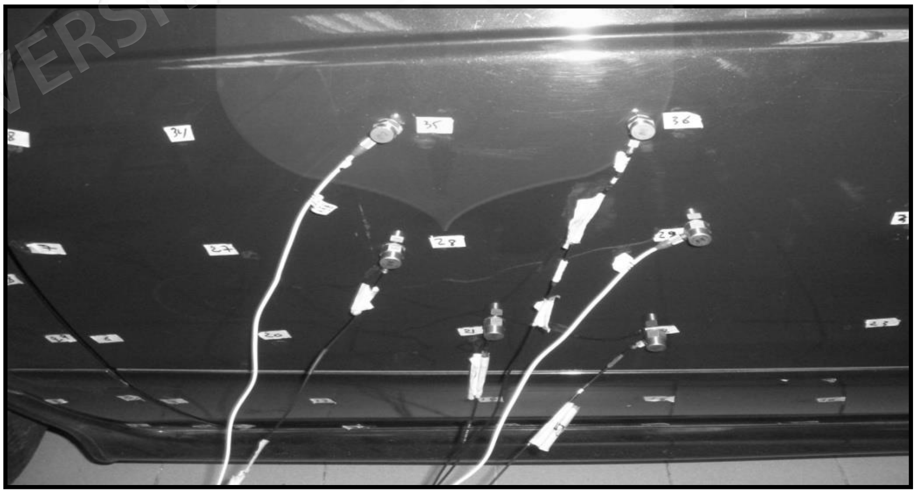

Figure 4.24 Location of the six accelerometers over the panel

mass loading. However, the mass loading for each DOF will subsequently be the same in all frequency response functions.

The primary assumption concerning the excitation of a linear structure is that the excitation must be measurable. Whenever the excitation is measured, this assumption simply implies that the measured characteristic properly describes the actual input characteristics. Mostly periodic input signals are generated by using shaker, and transient input signals are generated by using impact hammer. Figure 4.25 shows shakers and hammers used in experimental modal analysis. Figure 4.26 shows the popular excitation and response measurement methods.

Figure 4.25 Shakers & hammers used in experimental modal analysis
Source: Bruel & Kjaer 2006

Figure 4.26 Popular excitation and response measurement methods: top left: shaker, top right : impact hammer, bottom left: accelerometers, bottom right: laser vibrometer.

Source: Vander Auweraer 2004

Impact (Transient) deterministic signals are used in this study to determine the dynamic characteristics of the car panels. There are several periodic and non-periodic deterministic signals and also several non-deterministic signals. Table 4.9 shows the general list of most commonly signals used for frequency response function estimation (Allemang 1998).

Table 4.9 Various signals used in frequency response estimation

Name	Signal type
Swept Sine	Periodic deterministic
Periodic Chirp	Periodic deterministic
Impact (Impulse)	Non periodic (transient) Deterministic
Step Relaxation	Non periodic (transient) Deterministic
Pure Random	Ergodic, stationary random
Pseudo Random	Ergodic, stationary random
Periodic Random	Ergodic, stationary random
Burst Random	Both, transient deterministic and Ergodic, stationary random

The accuracy of the response depends to the choice of the response transducer and transducer mounting. Transducer used in this project is the piezoelectric accelerometer. Since transducer mounting technique and surface preparation can affect the amplitude of the frequency response, particularly at high frequencies care should be taken to ensure a flush mating with a smooth, flat surface. Nicks, scratches, or other deformations of the mounting surface or the transducer will affect frequency response (Mathews). For optimal measurement a thin layer of beeswax (applied to the base of the accelerometer before firmly pressing it on to the structure) has been used in this investigation. This alternative technique can lower the useful frequency range of the accelerometer, but it produces good results and rarely gives problems in modal analysis (Dossing 1988). For adhesively mounting accelerometers, the amount of adhesive thickness may play a critical role in achieving good frequency response.

For these experiments six single axis accelerometers were used as shown in Figure 4.27, so that six points could be measured at the same time. These accelerometers were B&K type 750-100, DeltaTron Sensors with 10 mV/ms-2 sensitivity. These accelerometers have a build-in charge amplifier and low-impedance voltage output and they were attached to the panels using Bees Wax.

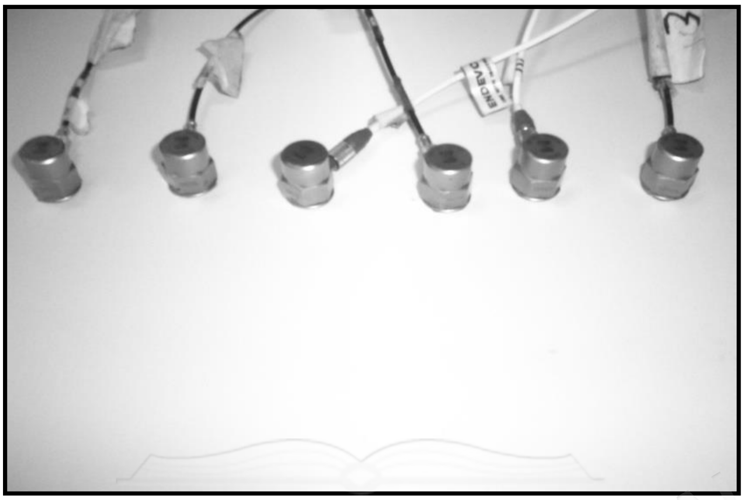

Figure 4.27 The six single axis accelerometers type 750-100

For excitation an Endevco impact hammer type 2302-50 was used. Some relevant physical specifications of this impact hammer are listed in Table 4.10. In order to measure the impact force impacted by the hammer a piezoelectric force transducer is built into the hammer head. Since for this experiment the low frequencies are required, a plastic hammer tip has been chosen. As the tip becomes softer, the pulse becomes broader and lower in peak value. Figure 4.28 shows the impulse shape for various hardness of the hammer tip.

The input excitation frequency range is controlled mainly by the hardness of the tip selected. Thus the tip should be selected such that all the modes of interest are excited by the impact force over the frequency range to be considered. For instance, if the selected tip is too soft, then all the modes will not be excited adequately as seen in Figure 4.29a. In order to get much better frequency response function with much improved coherence function, we strive to have a fairly good and relatively flat input excitation forcing function as seen in Figure 4.29b.

Table 4.10 Physical specifications of the impact hammer

Full scale range	1000 (4448) lbf (N)
Maximum frequency range	Up to 8kHz
Resonance frequency	50 kHz
Sensor sensitivity	5 (1.14) mV/lbf (mV/N)
gain	1
Head mass	100g
Hammer mass	300g

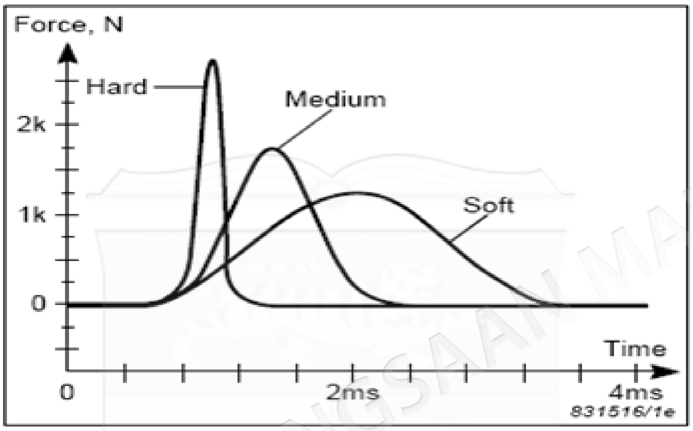

Figure 4.28 Impulse shape for various hardness of the hammer tip.

C

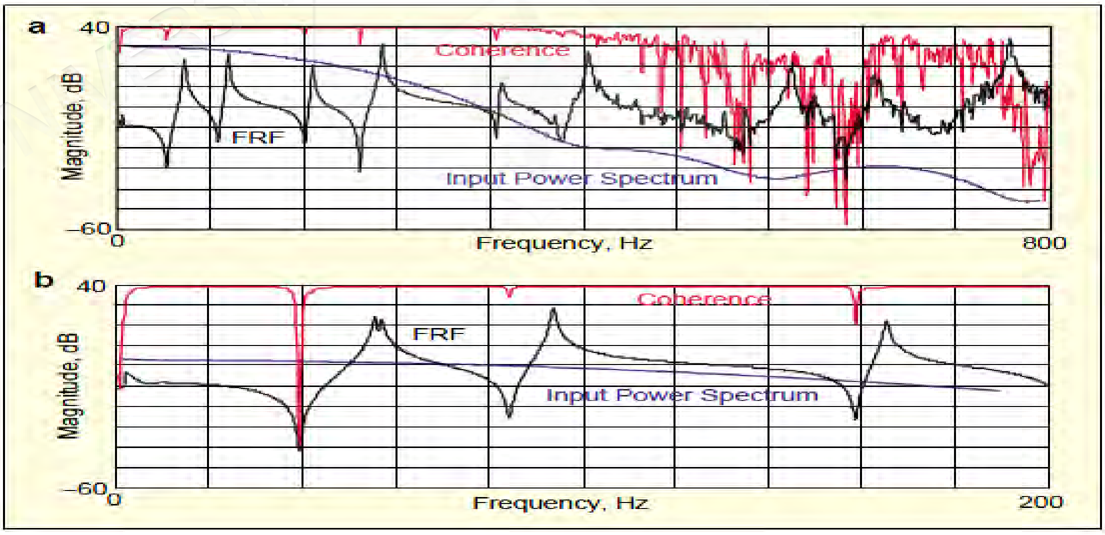

Figure 4.29 a) Hammer tip not sufficient to excite all modes. b) Hammer tip sufficient to excite all modes.

Source: Peter Avitabile 2001.

4.4.4 Dynamic Signal Analyzers

The force and accelerations are measured with two dynamic analyzers B&K 3560C Front End analyzer and B&K 3560B Front End analyzer. The first analyzer contains 3 channels for 3 sensors and the second analyzer contains 4 channels, 3 channels for 3 sensors and one channel for hammer. These two analyzers are connected with D-Link network switch to increase usage of number of channels. The physical properties of the analyzers are given in Table 4.11 and Table 4.12 respectively and the picture is given in Figure 4.30.

The dynamic signal analyzer samples the voltage signals coming from the impact hammer and accelerometers. The sensitivity information of the sensors is used to convert the voltages to equivalent force and acceleration values. The dynamic signal analyzer also performs the transformations and calculations necessary to convert the measured time domain signals into a frequency response function.

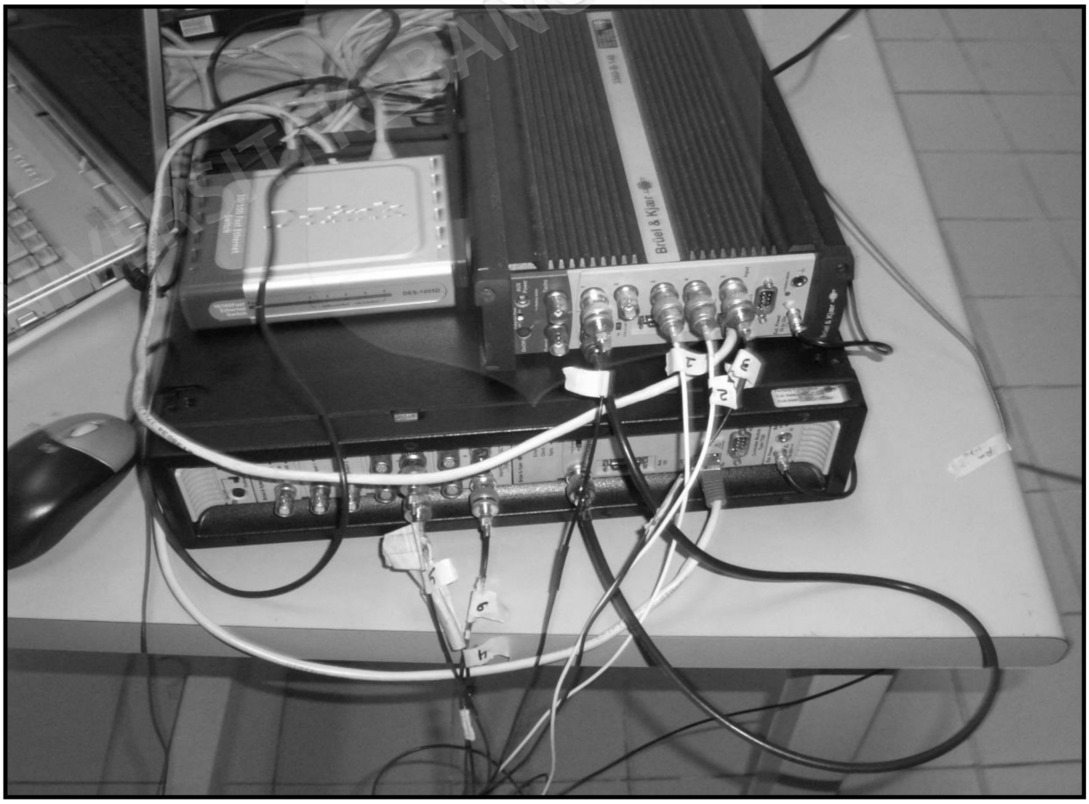

Figure 4.30 Analyzers and D-link used in the experiments

Table 4.11 Signal Analyzer 3560B specifications

Frequency Range	0.1HZ to 25.6 kHz
Dynamic Range	140dB
Accuracy	0.0025%
Maximum Resolution	6400 (FFT)

Table 4.12 Signal Analyzer 3560C specifications

Frequency Range	0.1 HZ to 25.6 kHz
Dynamic Range	140dB
Accuracy	0.0025%
Maximum Resolution	6400 (FFT)

Data was collected in B&K Pulse Labshop Experimental Modal Analysis software then afterwards transferred to ME'scope VES software for further analysis.

Usually commercial transducers are supplied with calibration certificates, but before starting any official test it is strongly recommended to do some tests, because of the following reasons (Dossing 1988):

- To check the integrity of the transducers
- To detect any error in the cables, connectors, conditioning and analyzer.
- To check that all gain, polarity and attenuator settings in the system are correct. In long measurement chains, one setting can easily be forgotten.
- To check that the pair of transducers being used, are matched in the frequency band of interest.

4.4.5 Equipment and measurement setup

The following table lists the equipments used to conduct the experiment measurements for the current research.

Table 4.13 List of equipments

N0	EQUIPMENT NAME	Type	Product principal	Quantity	Remarks
1	Accelerometer Sensor	751-100	B & K	6	DeltaTron Sensor with 10mV/ms-2 sensitivity
2	Impact Hammer	2302-5	B & K	1	Force Sensor with 1.14mV/N sensitivity
3	Front End Analyzer	3506C	B & K	1	Set 3 channels for 3 sensors
4	Front End Analyzer	3506B	B & K	1	Set 3 channels for 3 sensors, 1 channel for hammer
5	Sensor Cables & Connectors		B & K	6	Which includes BNC connectors
6	Network Switch		D-Link	1	To connect 2 Analyzers to increase usage of number of channels
7	Notebook		Compaq	1	Pre-installed B&K Pulse Labshop Experimental Modal Analysis
8	Hammer Cable & Connector		B&K	1	Which includes BNC connectors
9	Sensor Studs		B&K	6	For mounting accelerometer sensor before applying to the car components
10	Bees Wax		B&K	1	Acts as a sticker from the sensor stud to the component surface

The modal analysis experimental setup is shown in Figure 4.31. All equipments used in the test are labeled on the diagram. The necessary equipments and devices descriptions are explained in details in the previous sections of this chapter. Fixed boundary conditions were used in the experimental modal analysis. Therefore, the panels were assembled with the car and the car was suspended on 4 rubber wheels. The panels were excited using impact hammer. Two FFT analyzers with 7 available channels are used. The two analyzers are connected by a router to satisfy the number of channels. Six accelerometers could therefore be used, three of them are connected to the three channels analyzer and the other three accelerometers and a hammer are connected to the other four channel analyzer. Data were collected in the pulse software installed in a Compaq notebook.

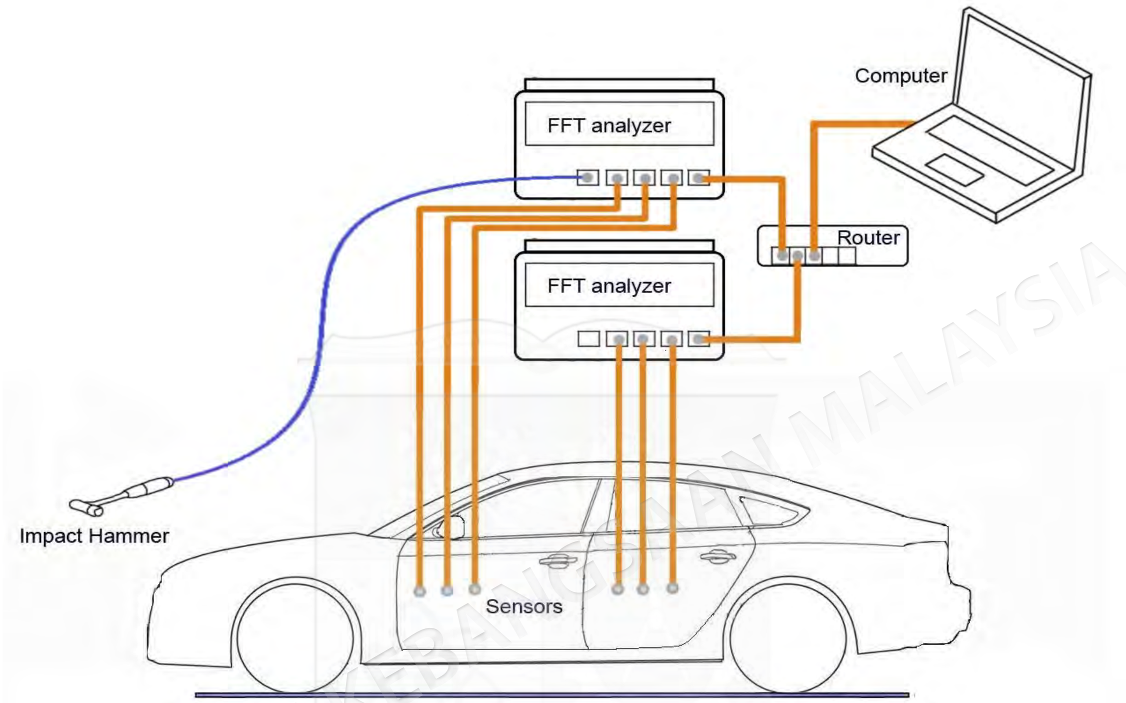

Figure 4.31 Experimental setup

.

4.4.6 Data quality assessment

The quality assessment of the measurement of the frequency response functions is very important, because this leads to the quality of the modal parameters. Therefore some checks are important to ensure that the quality of the measured frequency response functions is sufficient to evaluate the dynamic parameters of the structure.

The first check is the coherence function, it is a frequency dependent indicator that shows which part of the output signal is coming from the real input signal and which part is coming from the additional measurement noise. If the value of the coherence function is near one then a strong linearity exists between the input and output and the influence of the measurement noise is negligible. If the value of the coherence function is far away from one then no linearity exist between the input and output and the spectrum is dominated by the measurement noise. The Figure 4.32 shows the frequency response function and the corresponding coherence measured on the front door panel.

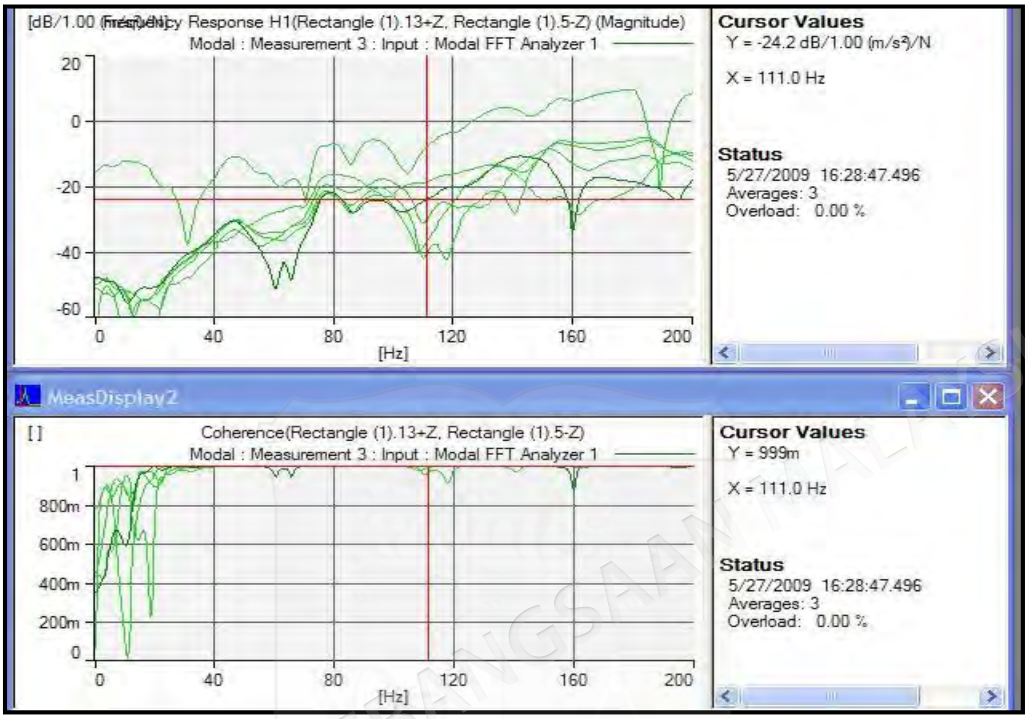

Figure 4.32 Frequency response function and the corresponding coherence

The second check for the quality of measurement is made by evaluating the reciprocity and reproducibility of several measured frequency response functions. In the theory Maxwell's reciprocity i.e $H_{xy}(f) = H_{yx}(f)$ should be the same for all measured frequency response functions. In practice the reciprocity theorem will be valid only for low frequencies. However, for higher frequencies the difference between $H_{xy}(f)$ and $H_{yx}(f)$will be increased. In the impact hammer tests the primary factor that influence the reciprocity is the mounting of accelerometer on the structure. At higher frequencies the extra mass associated with the accelerometer has a relatively large influence on the local dynamics of the structure while at lower frequencies these effects are negligible. The check of the reproducibility of the measured frequency response functions is very important to ensure that the experimental results are valid. The technique is to measure the same frequency response function multiple of times. If the measured frequency function is not remain the same, means there is a problem somewhere in the experimental setup. The problem could be the nonlinearity or the inconsistencies in the measurement directions of excitation and response.

Figures 4.33, 4.34, 4.35 and 4.36 show the frequency response functions measured on the front car panel between two couples of points. Firstly we excite point 5 and take the response at point 6 and vice versa. Secondly we excite point 3 and take the response at point 8 and vice versa. The results showed that the frequency response functions taken from the first couple of points are the same as shown in Figures 4.33 and 4.34. In addition the second couple shows the same frequency functions as well as shown in Figures 4.35 and 4.36. Therefore, we conclude that the reciprocity and reproducibility of the measured frequency response functions is reasonably good.

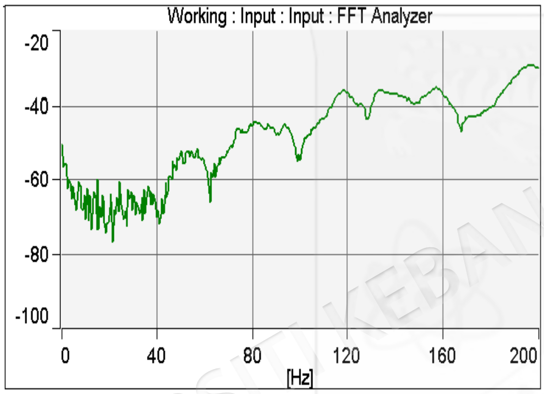

Figure 4.33 Frequency response function between points (5&6)

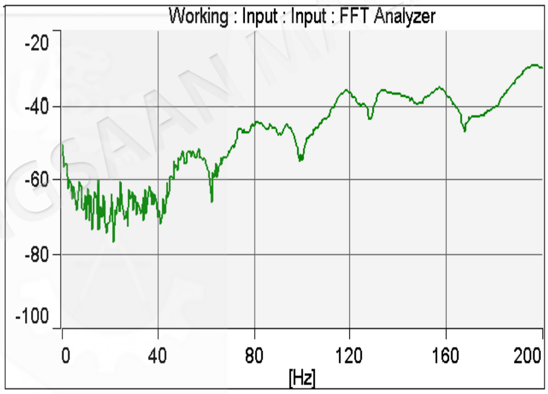

Figure 4.34 Frequency response function between points(6&5)

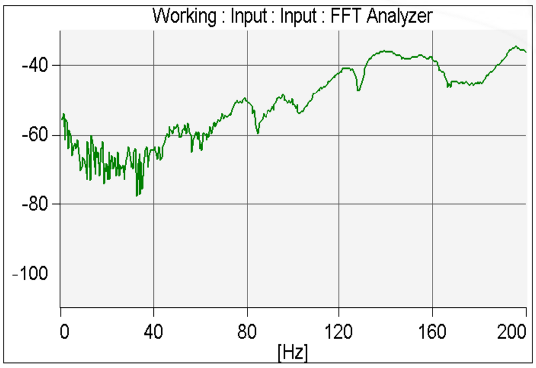

Figure 4.35 Frequency response function between points (3&8)

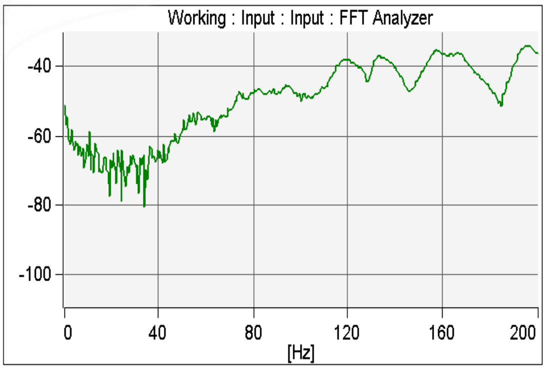

Figure 4.36 Frequency response function between points(8&3)

4.4.7 Triggering

In order to get good results, it is important to capture all of the impulse signal and the response in the sampling window of the FFT analyzer. In other words the inputs of the signal analyzer are triggered. In the pulse software there are three important parameters should be set first to describe the triggering are: triggering level, triggering slope and the pre-trigger delay.

The triggering level is set to a percentage of the maximum input signal and determines the amplitude of the signal at which the measurements are started.
The triggering slope is used to specify whether the measurements should be started at a growing or decaying signal.

The pre-trigger Delay is used to insure that the entire signal is captured. So the analyzer must be able to capture the impulse and response signals prior to the occurrence of the impulse which is usually set to a small percentage of the peak value of the impulse (Verhees 2004).

4.4.8 Windowing

The other important aspect of impact testing is related to the use of the impact window for the response transducer. If the measured signals are not periodic the leakage errors will occur. These errors affect negatively the frequency response function signal. To minimize the effect of the leakage errors, weighting functions are called windows are applied to the measured data. These windows are used to force the data to better satisfy the periodicity requirements of the Fourier Transform process. There are many windowing functions available, each of them has advantages and disadvantages. Two common window functions are usually used in impact excitation are the exponential and the force windows. The exponential window is applied to the response transducer and the force window is applied to the impact force. The exponential and force windows are shown in Figures 4.37 and 4.38 respectively.

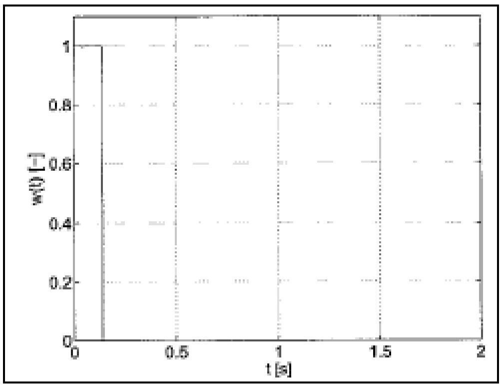

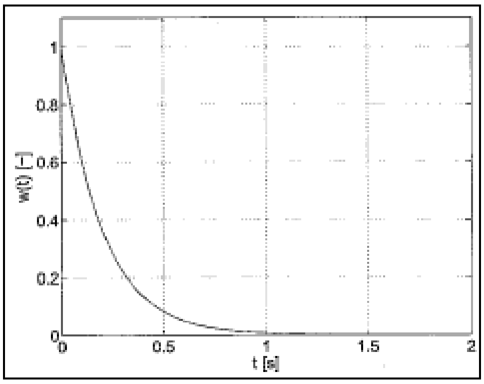

Figure 4.37 the force window

Figure 4.38 The exponential window

Source: Verhees 2004

a) Exponential window

The exponential window is used to reduce leakage in the spectrum of the response. This is achieved by making the measured response signal periodic at the end of the sampling window. The measured response signal is made periodic by bringing it to zero within the time record length. It is also assumed that at the beginning of the time record the measured response is zero. The implementation of the exponential window to minimize leakage is shown in Figure 4.38.

b) Force window

The force window is a rectangular window and is used to remove the noise that is present in the impulse signal. The force window is applied to the impact force signal that is measured through the force sensor in the impact hammer. The impact force signal usually has an impulse like form and is very short in time compared to the total measuring time. Therefore, the leakage errors are not an issue with regard to the impact force signal. The main two reasons for applying the force window are:

Firstly to remove measurement noise that is present on the measured signal after the impact. Secondly to eliminate the additional forces from the measurement signals because they are not exerted on the structure. These additional forces are occurred after the structure hated by the hammer. These forces come originally from noise, placing the hammer on the surface, swinging the hammer, etc.

As shown in Figure 4.37 the force window has a value of one in a time band around the impulse signal and a value of zero elsewhere.

4.4.9 Leakage

If a time signal is not periodic in the transform window, when it is transformed to the frequency domain, a smearing of its spectrum will occur. This is called leakage. Leakage distorts the spectrum and makes it inaccurate. (Brian & Mark 1999).
Signals that are always periodic in the transform window are:

1. Signals that are completely contained within the transform window.
2. Cyclic signals that complete an integer number of cycles within the transform window.

If the response signal in impact test decay to zero or near zero before the end of sampling window, there will be no leakage and no special windowing is required. In the other hand, if the response does not decay to zero before the end of the sampling window, an exponential window must be used to reduce leakage effects in the response spectrum.

4.4.10 Averaging

The accuracy of the frequency response function measurements is mainly determined by the measurement noise present in the system and by the skills of the one doing the measurements. The way to improve the accuracy is to do more measurements on the same point and average the results in the frequency domain. The averaging method will reduce the effect of the random errors, but has no effect on the leakage errors. In all modern FFT analyzers frequency response functions should measured using 3 to 5 impacts per measurement. In these experiments the frequency response functions are measured using 3 impacts at the same point. The pulse has the ability to accept or reject the result of each impact.

The pulse also has some other options available. These options are: the double hit reject and the overload reject. Double hit reject means that frame with more than one impulse are rejected and overload reject means that frames with impacts that exceed the measurement ranges are rejected. These two options save a lot of time during impact testing since we don’t have to restart the measurement process after any bad hit.

4.5 SUMMARY

In this chapter we have discussed the research methodology used in this study to obtain valid computational and experimental modal analysis results. At the beginning we gave in details the computational modal analysis methodology followed by the presentation and discussion of the results. After that a brief survey of the equipments and instruments used in the experimental modal analysis setup was introduced. Afterwards, a detailed description of the experiment conditions such as measurement preparation, measurement points, point of excitation, and considerations and mounting of transducers was presented. Finally, the chapter covered the quality assessment of the measurement of the frequency response function by checking coherence, reciprocity and reproducibility, triggering, windowing, leakage and averaging in order to obtain qualitative results. Any trouble in these parameters produces a low quality frequency response function which leads to low quality of the modal parameters estimation.

CHAPTER 5

COMPARISON OF EXPERIMENTAL AND SIMULATION RESULTS

5.1 INTRODUCTION

The measurement methodology is explained in the previous chapter. This chapter presents the results obtained from the experimental modal analysis and comparison with those obtained from computational modal analysis results. A detailed description and discussion will be also included.

5.2 TRUNK RESULTS

The trunk panel was divided into 108 measurement points distributed equidistance over the panel as shown in Figure 4.16 page 75. This number of points was chosen to cover the all desired modes to be compared with computational results. The Frequency Response Functions (FRFs) were taken on the range 0-200 Hz. The excitation point was fixed at DOF104 Z and the responses were taken at 108 points. The superposed FRF's obtained from all points is shown in Figure 5.1, after that, curve fitting will be applied to obtain the modal parameters of the panel as shown in Figure 5.3. In the upper part of the diagram, each (black) FRF is overlaid with (red) Fit FRF that was synthesized from the curve fitting results and the lower part shows the modal peaks function. Each resonance peak in the diagram gives an indication of the presence of at least one mode. The quality of measurement can be checked from the coherence function as shown in Figure 5.2. It shows a good linearity between the input and output as the coherence is close to 1 over the frequency range of interest.

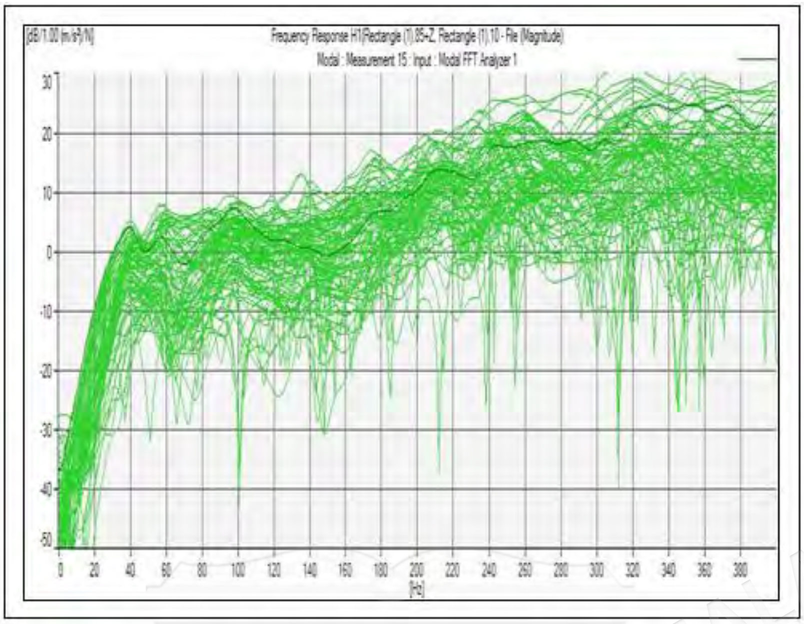

Figure 5.1 The superposed FRF for trunk panel

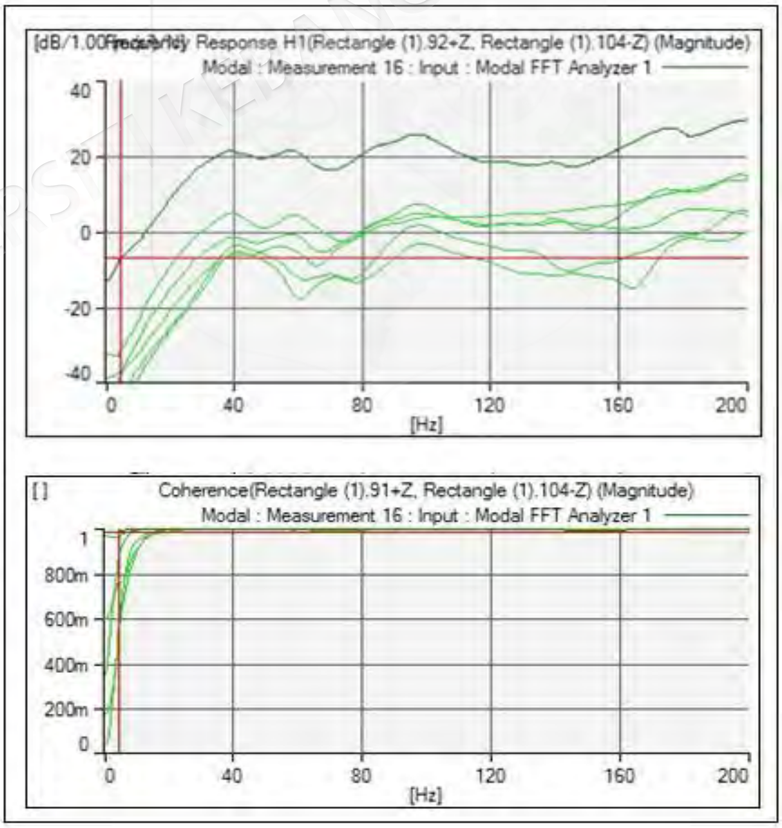

Figure 5.2 FRFs and the corresponding coherences of 6 different points (trunk)

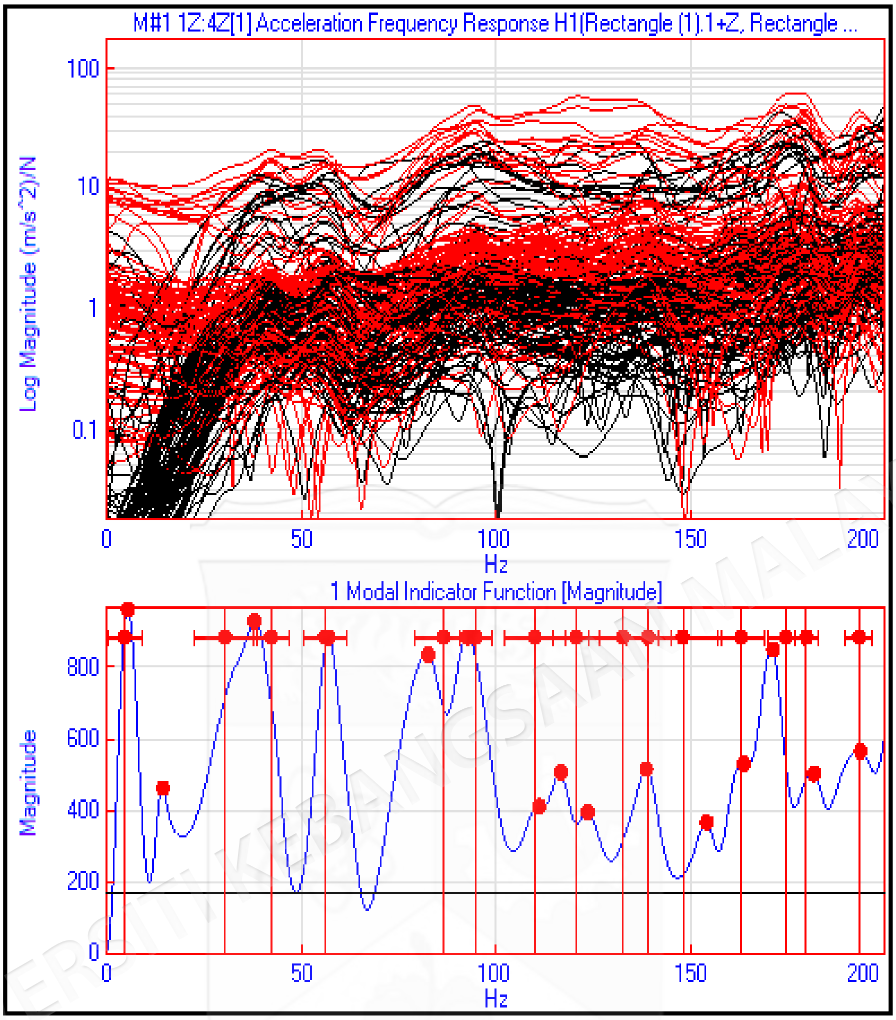

Figure 5.3 Curve fitting results for the trunk panel

The first six natural frequencies and corresponding mode shapes obtained from experimental modal analysis of the trunk panel are shown in Figure 5.4. The other mode shapes are given in Appedix A. This section followed by a short description of the first ten mode shapes.

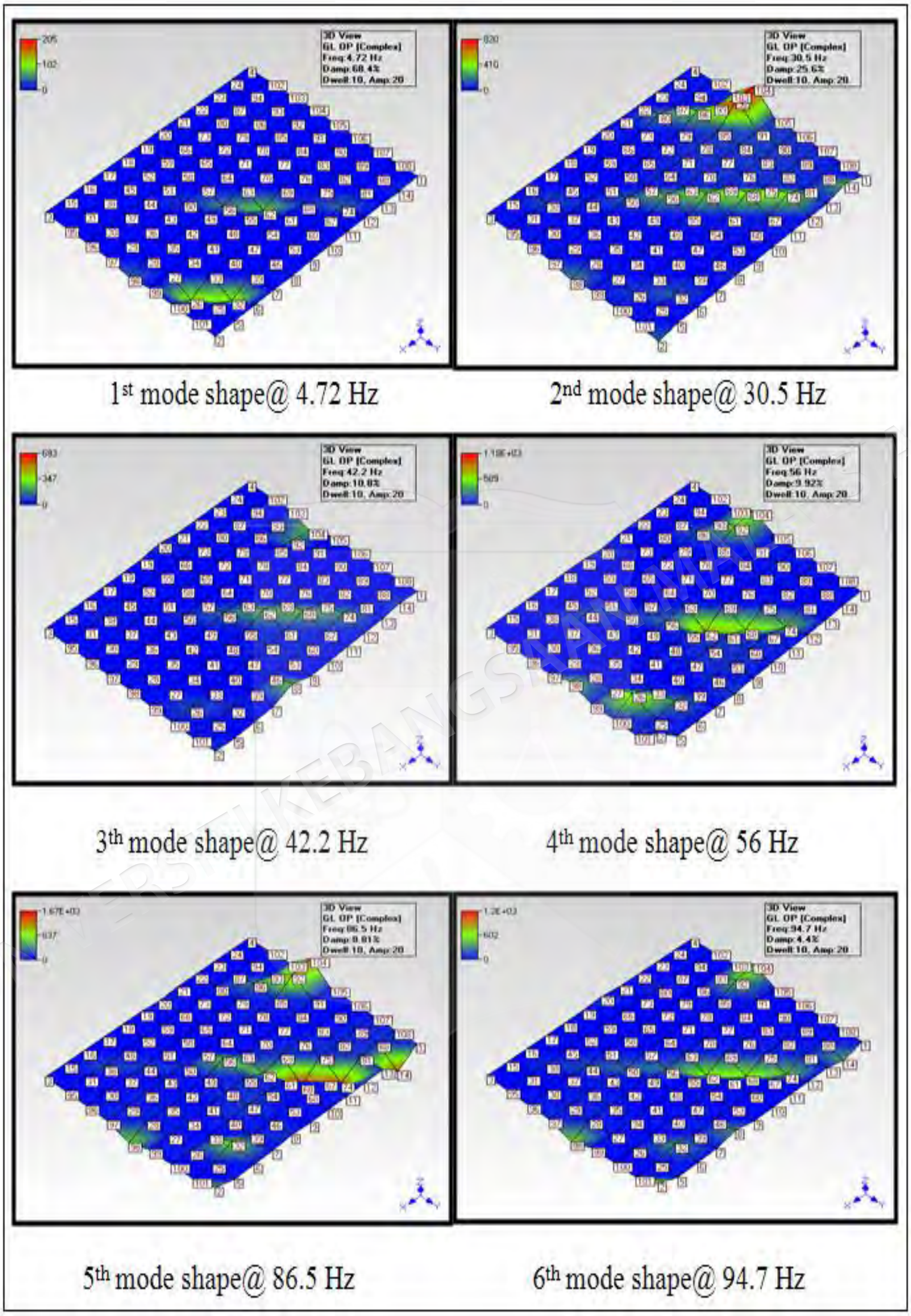

Figure 5.4 Experimental mode shapes for trunk panel

The first mode shape does not show any significant vibration. It shows only low vibration at the middle and corner side of the panel. The second and third mode shapes show almost the same behavior. They show significant vibration at the front of the panel and no vibration at the rear part. The fourth mode shows significant vibration at the front side, rear side and the right side of the panel. The fifth and sixth mode shapes exhibit high amplitude at the front and low amplitude at the back of the panel with slight difference. Mode shape seven and above are shown in Appedix A. Mode number seven shows low vibration at the front and back of the panel but no vibration at the center. At the eighth mode the panel shows significant vibration at the right side and low vibration at the front and back of the panel. The ninth mode shows significant vibration only at the center and at the last mode the panel vibrates at the left edge, the right edge, rear edge and at the center.

The first comparison was made on the trunk panel structure. Table 5.1 shows a comparison between the first ten natural frequencies obtained from experimental modal analysis and those obtained from computational modal analysis over the frequency range 0-200Hz. As we can see in the table, the mode pairs of the experimental and computational frequencies respectively (86.5 Hz,95.40 Hz), (94.7 Hz,101.09 Hz), (110 Hz,105.43 Hz), (120 Hz, 116.74 Hz), (133 Hz, 120.68 Hz) and (139, 133.81) are in good agreement as the difference percentage is less than 9%, whereas the mode pairs (42.2 Hz, 77.53 Hz), (56 Hz,81.13 Hz) are not in good agreement as the difference percentage are 59% and 36% respectively. The remainder modes, such as the first and the second mode pairs at (4.72 Hz, 48.63 Hz) and (30.5 Hz, 71.53) respectively are in very bad agreement as the percentage different is very high. The reason for this discrepancy can be seen in the coherence at this frequency is far from one ($\ll$100%) as shown in figure 5.2, in other words there is no good linearity at this frequency.

In general the comparison between computational and experimental frequencies shown above indicates some discrepancies. This is probably due to some differences in the material properties (using different material density in FE model) between FE model and the actual model or because of the errors in the entering model parameters.

Table 5.1 Comparison between Exp and Simulation frequencies of Trunk panel

Mode no	**Exp.Frq [Hz]**	**Simul. Freq[Hz]**	**Diff %**
1stmode	4.72	48.63	164
2nd mode	30.5	71.94	80
3rd mode	42.2	77.53	59
4th mode	56	81.13	36
5th mode	86.5	95.40	9
6th mode	94.7	101.09	6.5
7th mode	110	105.43	4
8th mode	120	116.74	2.7
9th mode	133	120.68	9
10th mode	139	133.81	3.8

The other useful technique for comparison is to plot the experimental and computational natural frequencies in the same xy -plane as shown in Figure 5.5. It shows also that the two graphs are close to each other especially above the third mode which mains that generally there is a good agreement between the two methods.

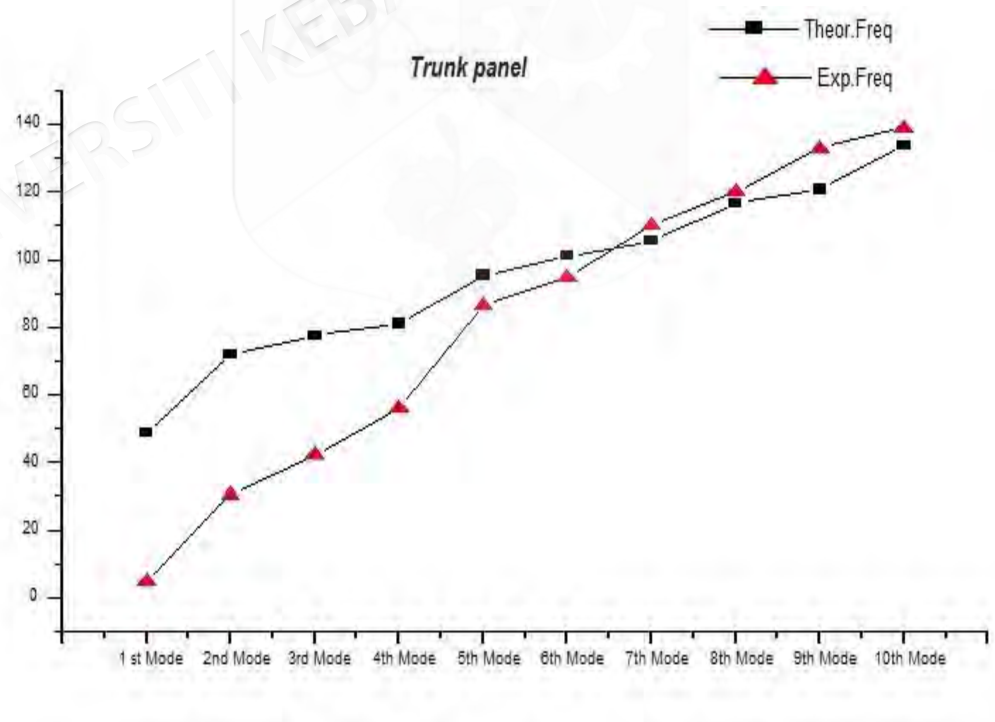

Figure 5.5 Comparison between Exp and Simul frequencies of Trunk panel

In order to satisfy a reasonable comparison between the two methods we should compare the mode shapes as well as shown in Table 5.2. The first two mode shapes do not show any similarity. This is reasonable because their corresponding frequencies are far away from each other as shown above. The third and fourth mode shapes corresponding to frequency pairs (42.2 Hz, 77.53 Hz) and (56 Hz, 81.13 Hz) respectively are exhibit some similarities in their behavior as both showing vibration in front and negligible vibration at the rear part of the panel. The fifth mode shape shows a good similarity between experimental and computational behavior, both of them exhibit significant vibration at the front and rear parts of the panel. The comparison between the experimental and computational mode shape at the sixth mode does not show clear similarity, even though both mode shapes show vibration at the front and rear parts. The comparison between experimental and computational mode shapes at the seven mode and above are represented in Appedix A. The seventh mode shows a good similarity between the experimental and computational behavior as we can see that both are showing significant vibrations at the front and rear sides of the panel. The vibration behavior of the trunk panel at the eighth mode shows a good agreement between the two methods, as both mode shapes showed high vibration at the front center of the front part of the panel. At the ninth mode the panel does not show significant similarity between computational and experimental methods. Mode number ten showing good agreement and its behavior looks like mode number eight.

In conclusion the results obtained from the trunk panel showed a fair agreement between experimental and computational modal analysis in both frequency level and mode shape level. In addition, we have noticed that the computational mode shapes exhibit high amplitude, whereas the experimental mode shapes exhibit low amplitude. Probably this difference occurred because of the damping applied to the surface area of the panels to reduce the vibration amplitude which can affect the excitation and response functions.

Table 5.2 Comparison between exp and Simul mode shapes (Trunk panel)

Mode No	Experimental mode shapes	Simulation mode shapes
1	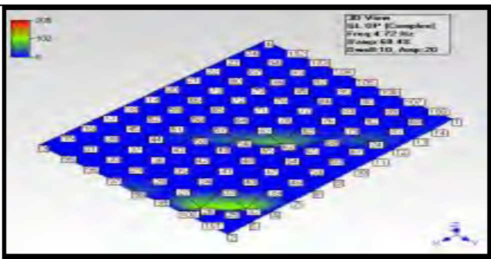	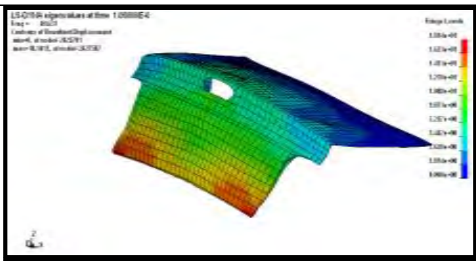
2	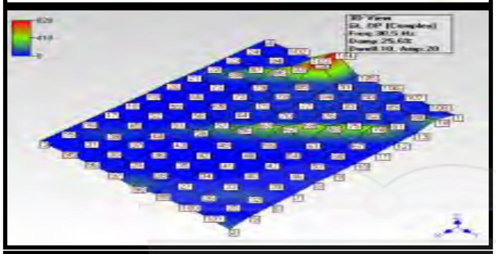	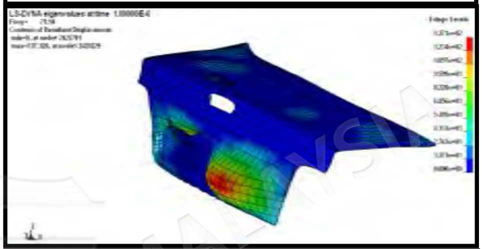
3	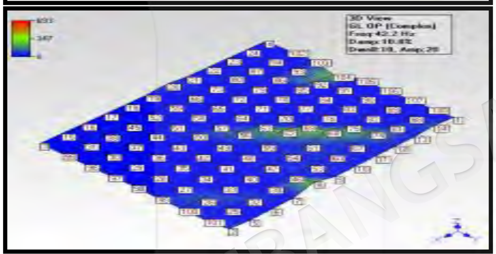	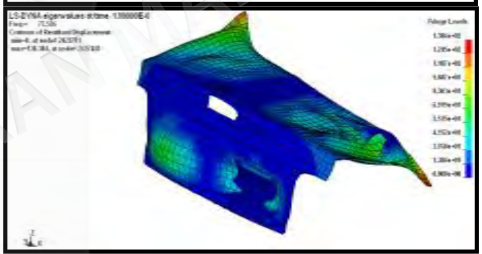
4	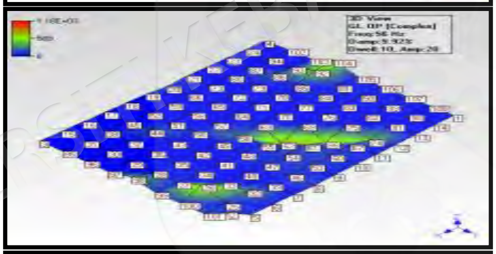	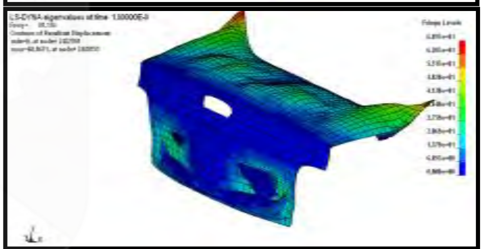
5	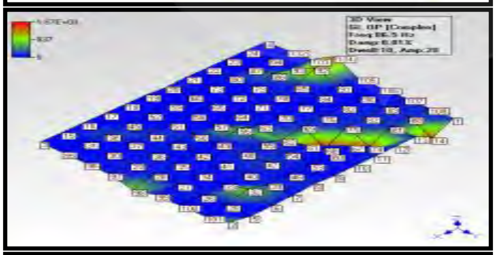	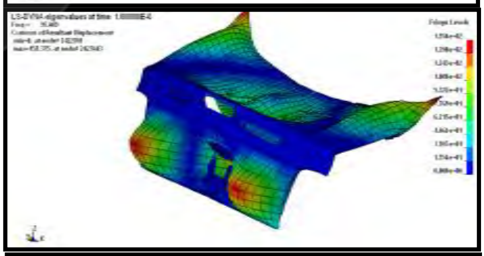
6	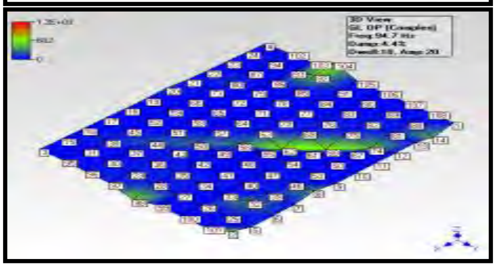	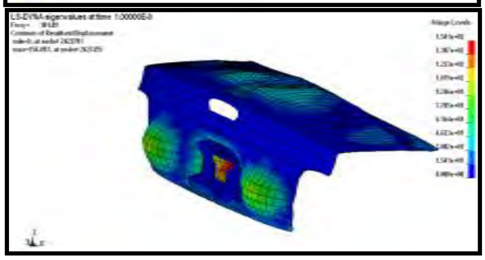

5.3 HOOD RESULTS

The hood panel was divided into 132 measurement points and the excitation point was located at DOF 4Z, as shown in Figure 4.19. The frequency range was taken from 0 to 200Hz and we follow the same procedures used in the previous section. The results obtained from the experiment are shown in Figures 5.6, 5.7, 5.8 and 5.9.

Figure 5.6 shows the superposed measured frequency response functions taken on 132 points. The collected data will be send to ME' scope for further analysis to find the modal parameters of the panel. It was noticed also that the first mode of vibration occurred at 26 Hz as seen in Figures 5.6 and 5.8.

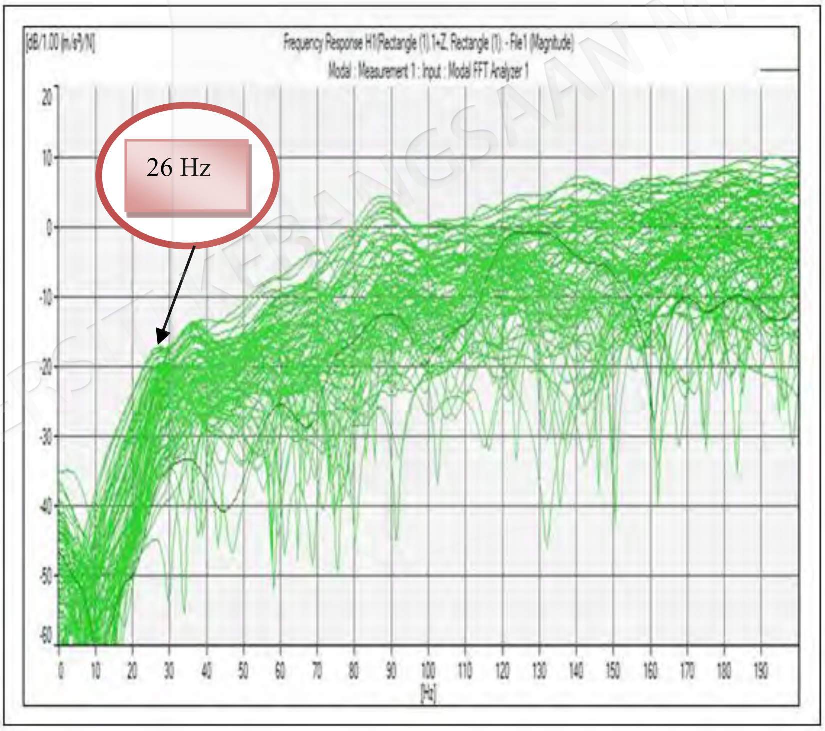

Figure 5.6 The superposed FRF for Hood panel

The frequency response functions and the corresponding coherences taken from a sequence of 6 accelerometers are shown in Figure 5.7. The figure shows that the coherences are good around natural frequency 26 Hz and above, which is relevant to the superposed FRF shown in Figure 5.5. This is a strong prove of the validation of the measurements results taken on the hood panel.

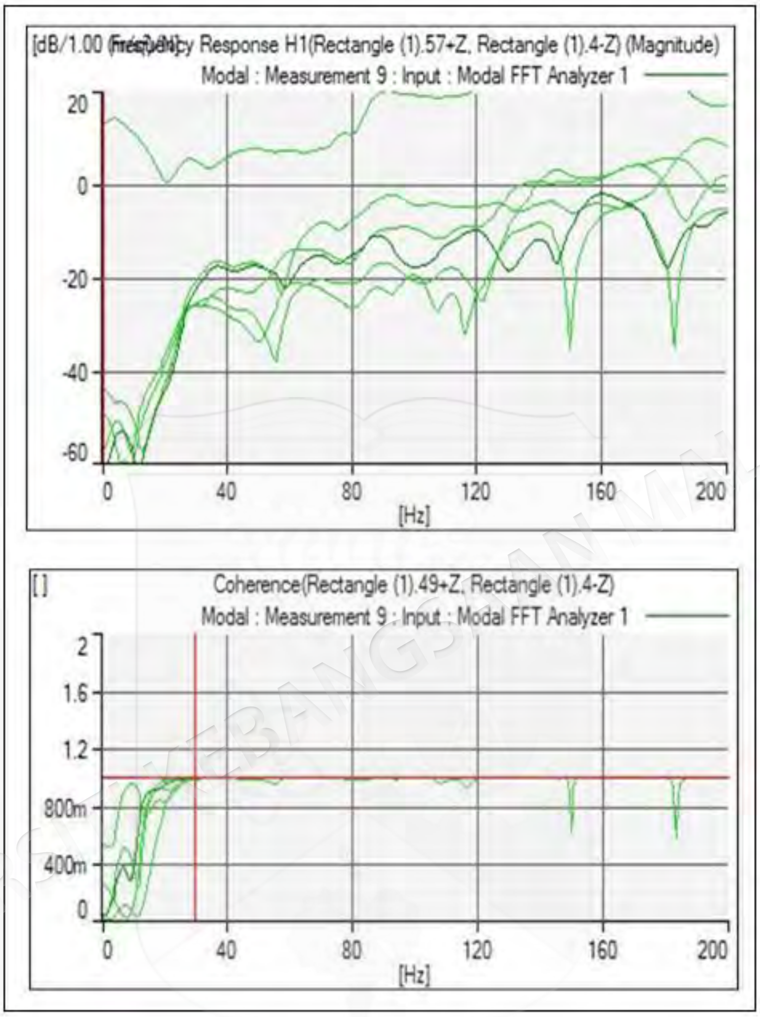

Figure 5.7 FRFs and the corresponding coherences of 6 different points (Hood panel)

Figure 5.8 shows the results obtained from the curve fitting process, which contains the average frequency response function of all frequency response functions taken on 132 points. Furthermore, it shows the possible number of peaks and the amplitude of each peak.

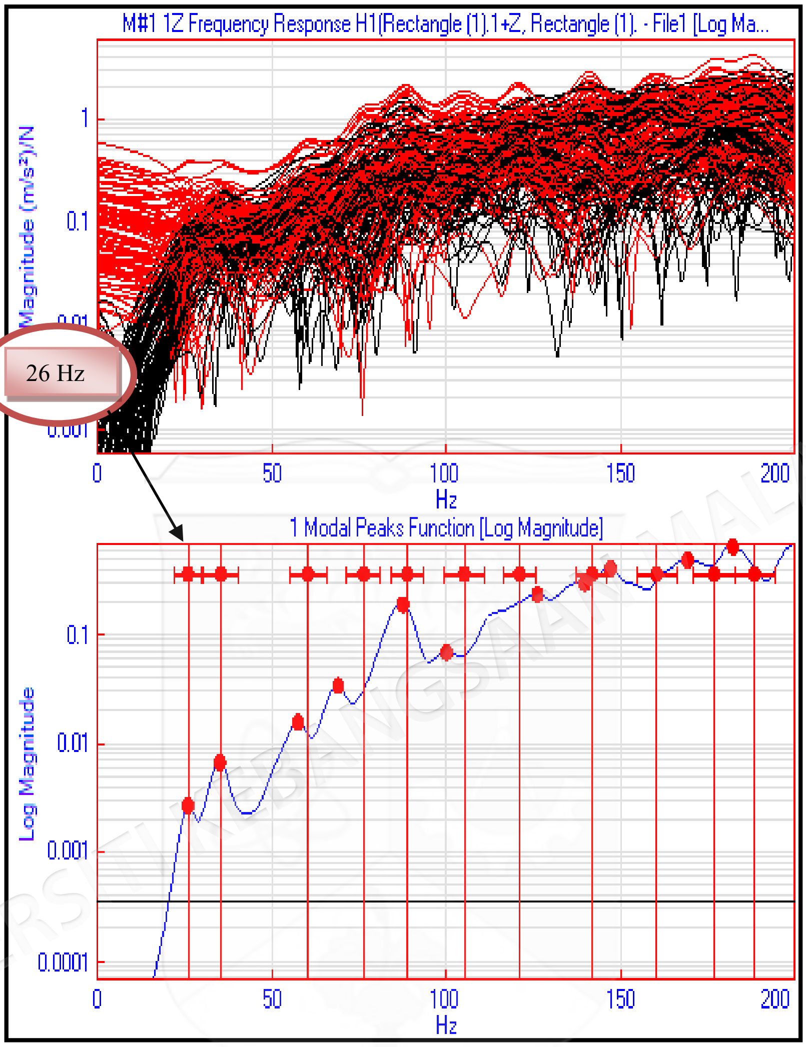

Figure 5.8 Curve fitting results for the Hood panel

The first six natural frequencies and the corresponding mode shapes obtained from the experimental modal analysis of the hood panel are presented in Figure 5.9. The other modes are given in Appendix A. A short description of the behavior of the hood panel at different modes will be given below.

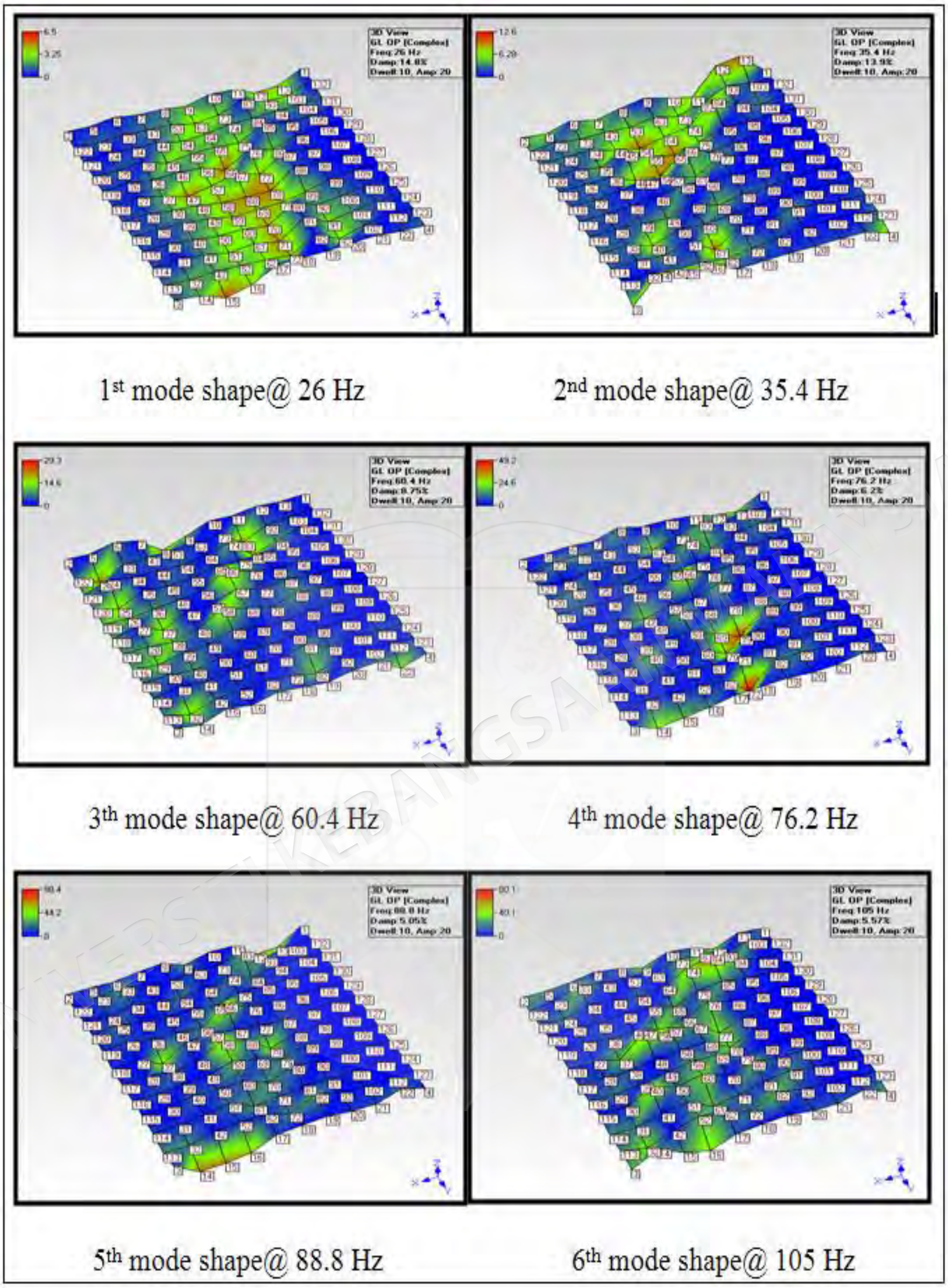

Figure 5.9 Experimental mode shapes for hood panel

The first mode shape shows that the vibration located at the center from left to right, whereas the front and the rear part of the panel do not show any vibration. The second mode shape shows more vibration at the left side and less vibration at the right side of the panel as shown in the figure. The third mode shape shows that the vibration concentrated at the left and rear sides of the panel. At the fourth mode the panel shows significant vibration at the right side and low vibration at the left side. The fifth and the sixth modes showed quit similar behavior. The both modes showed vibration at the diagonal with higher vibration at the two opposite corner of the panel. The 7th mode shows vibration at the center and at the other three corners of the panel. At the 8th mode the hood panel shows significant vibration at the center of the panel. The behavior of ninth mode looks like the 6th mode shape, and at the 10th mode the panel shows more vibration at the rear right quarter side area as shown in Appendix A.

The second comparison was conducted on the car hood panel. Table 5.3 shows the comparison between experimental and computational frequencies. It shows a quite acceptable agreement, except for the first two modes where they show high difference percentage 68% and 49% respectively. It also shows that the fourth, fifth, and sixth modes are in good agreement as the percentage difference is less than 9%. The remaining frequencies correspond to third, seventh, eighth, ninth and tenth modes are in reasonable agreement as the percentage different is less than 33%. So the comparison between experimental and computational frequencies of the hood panel in general shows an acceptable agreement between the two methods. In addition, the two graphs of the experimental and computational frequencies also show acceptable agreement between the two methods as shown in Figure 5.10.

Moreover, to have a good insight on the comparison between the two methods we should also compare the mode shapes. Table 5.4 shows the comparison between experimental and computational mode shapes of the hood panel. The hood panel shows quite similar behavior at the first mode as both showing vibration across the center of the panel, and no vibration can be seen at the front and rear of the panel. At the 2nd mode both mode shapes showing vibration at the front and rear sides of the panel.

Table 5.3 Comparison between Exp and Simulation frequencies of Hood panel

Mode no	Exp.Freq[Hz]	Simul. Freq[Hz]	Diff %
1st mode	26	53	68
2nd mode	35.4	58.83	49
3rd mode	60.4	76	22
4th mode	76.2	84.1	9
5th mode	88.8	86.8	2.2
6th mode	105	100.87	4
7th mode	121	102.89	16
8th mode	142	107.78	27
9th mode	160	117.59	30
10th mode	177	125.68	33

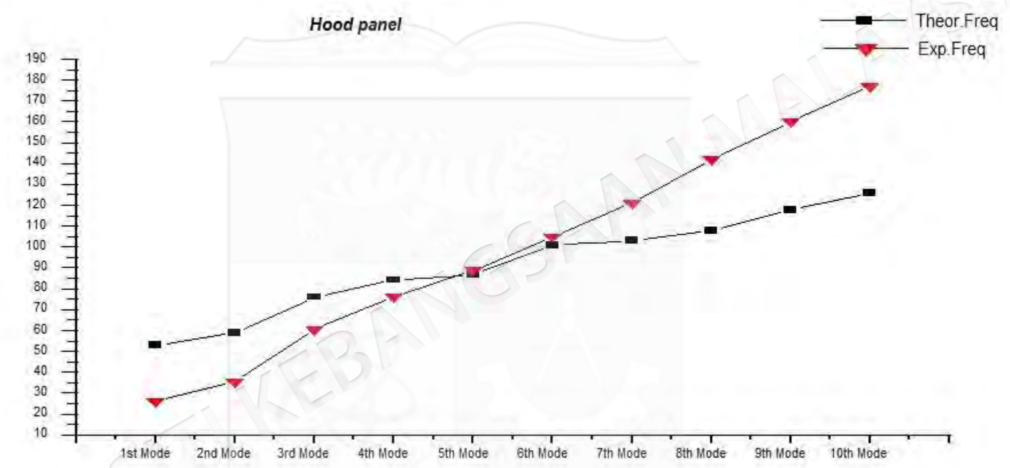

Figure 5.10 Comparison between Exp and Simulation frequencies of Hood panel

The third mode shows quit similarity between the two methods as both showing vibration at the center and the rear part of the panel. The fourth and the fifth modes look very close to each other. The sixth mode does not show clear similarity, even though both mode shapes show vibration at the center. As shown in Appendix A the behaviors of the hood panel at the seventh mode shows a similar vibration between the two methods as both exhibit vibrations at the rear part of the panel. Mode numbers eight and ten do not show significant similarity between the two methods whereas the ninth mode shows a good agreement as shown in Appendix A.

Table 5.4 Comparison between exp and Simulation mode shapes (Hood panel)

Mode No	Experimental mode shapes	Simulation mode shapes
1	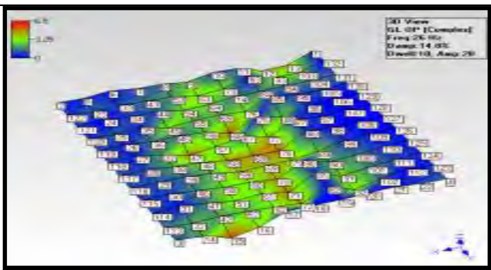	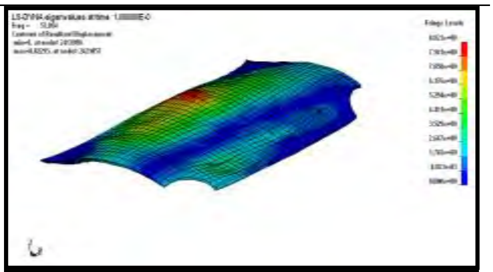
2	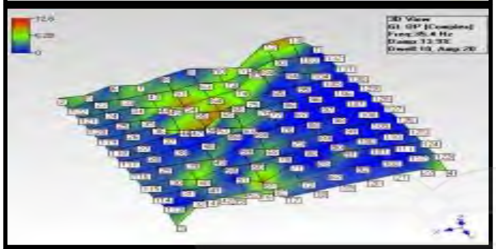	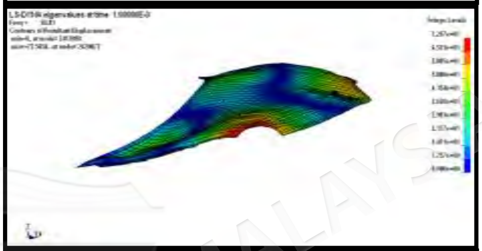
3	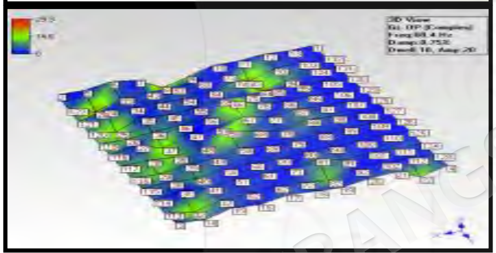	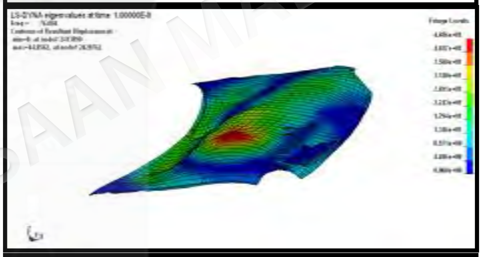
4	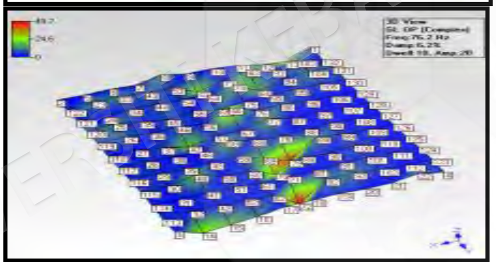	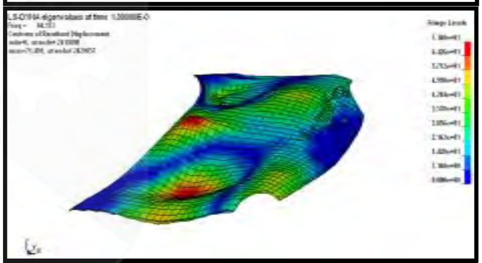
5	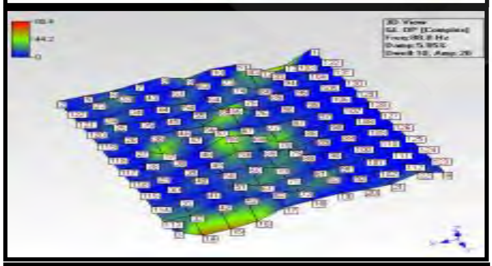	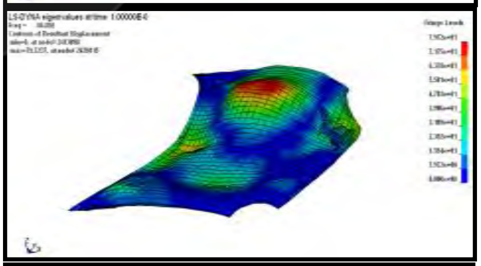
6	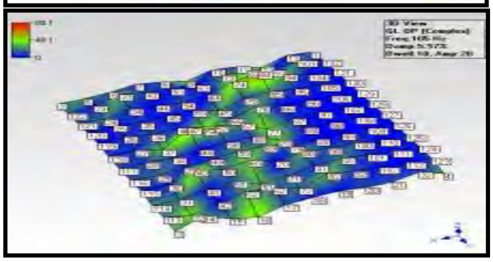	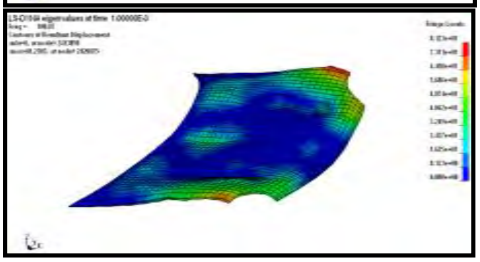

In conclusion the comparison between the experimental and computational frequencies and between experimental and computational mode shapes conducted on the hood panel shows an acceptable agreement between the two methods. However, there are some discrepancies between the two methods results as explained earlier. These discrepancies could be resulted from some differences between the material properties used for FE model and the actual model of the hood panel.

5.4 ROOF RESULTS

120 measurement points are located over the surface of the roof panel and the excitation point was at DOF 1Z as shown in Figure 4.21. Only eight modes can be detected on the frequency range 0 to 200 Hz.

Figure 5.11 shows the frequency response functions taken at 120 points. The six frequency response functions and its corresponding coherences taken from a sequence of six accelerometers are shown in Figure 5.12. It shows a good linearity between input and output forces as we can see that the all six coherences are close to one. The results obtained from the curve fitting process are shown in Figure 5.13. The upper part of the diagram shows each (black) FRF is overlaid with (red) Fit FRF that was synthesized from the curve fitting results. The lower part of the diagram shows the modal peaks function. It shows the possible number of modes can be detected over the frequency range of interest.

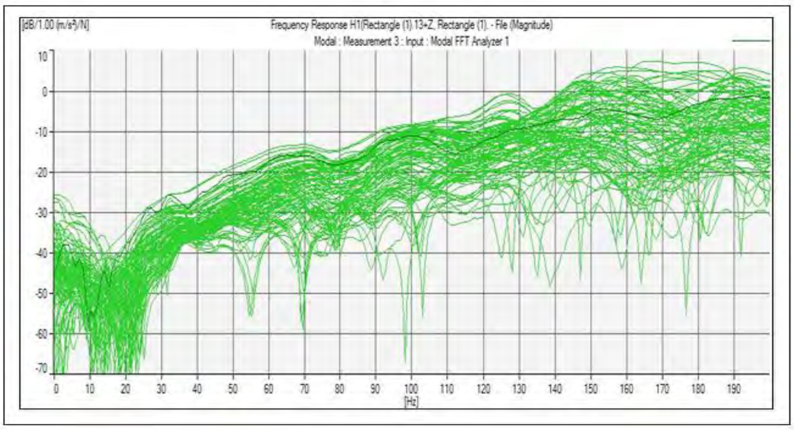

Figure 5.11 The superposed FRF for roof panel

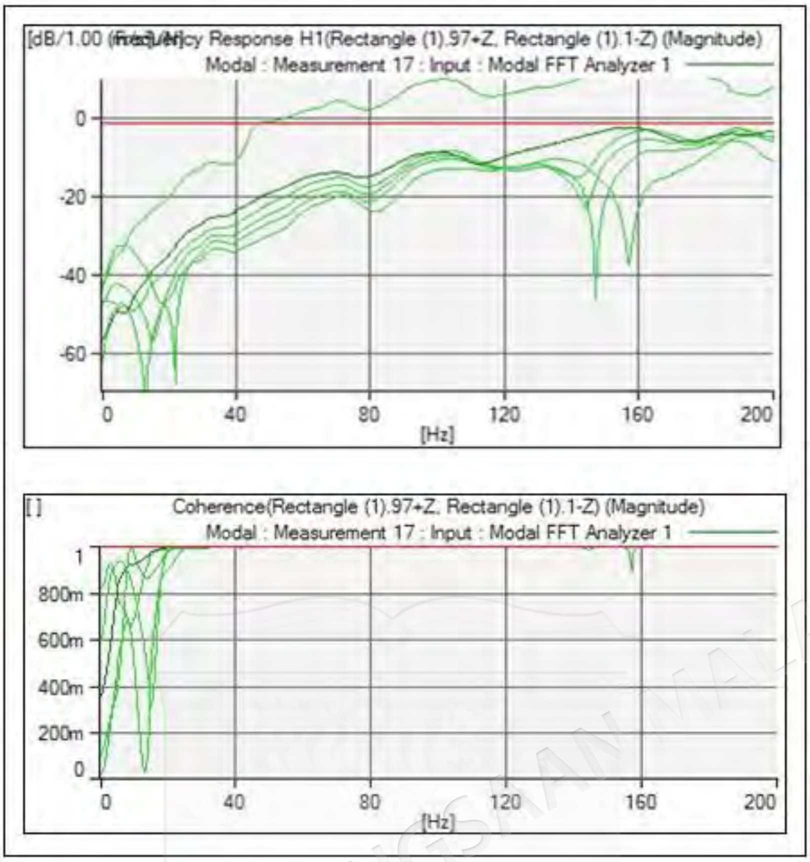

Figure 5.12 FRFs and the corresponding coherences of 6 different points (roof panel)

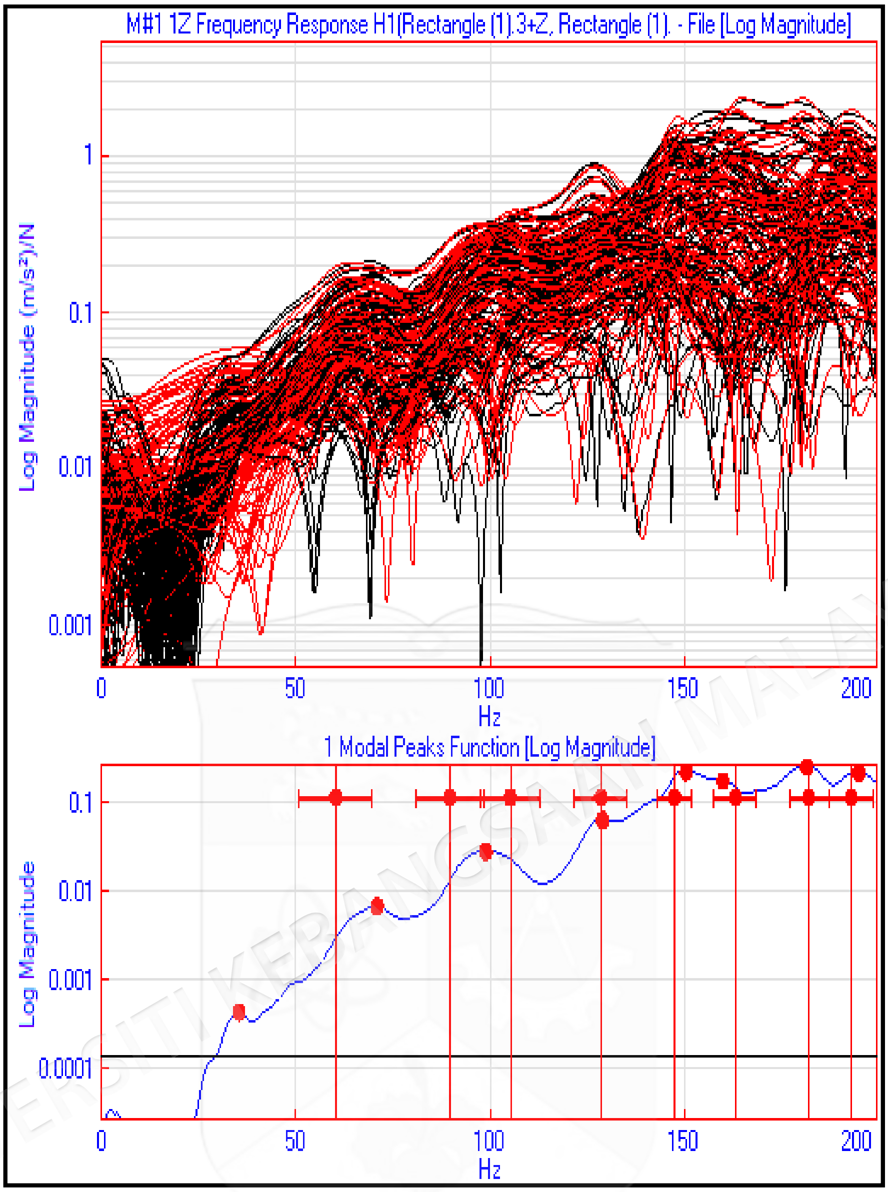

Figure 5.13 Curve fitting results for the roof panel

The natural frequencies and the corresponding modes shapes results t are given in Figure 5.14. At the first mode the panel vibrates at three parts, at the two right corners and the middle of the panel as shown in the figure.

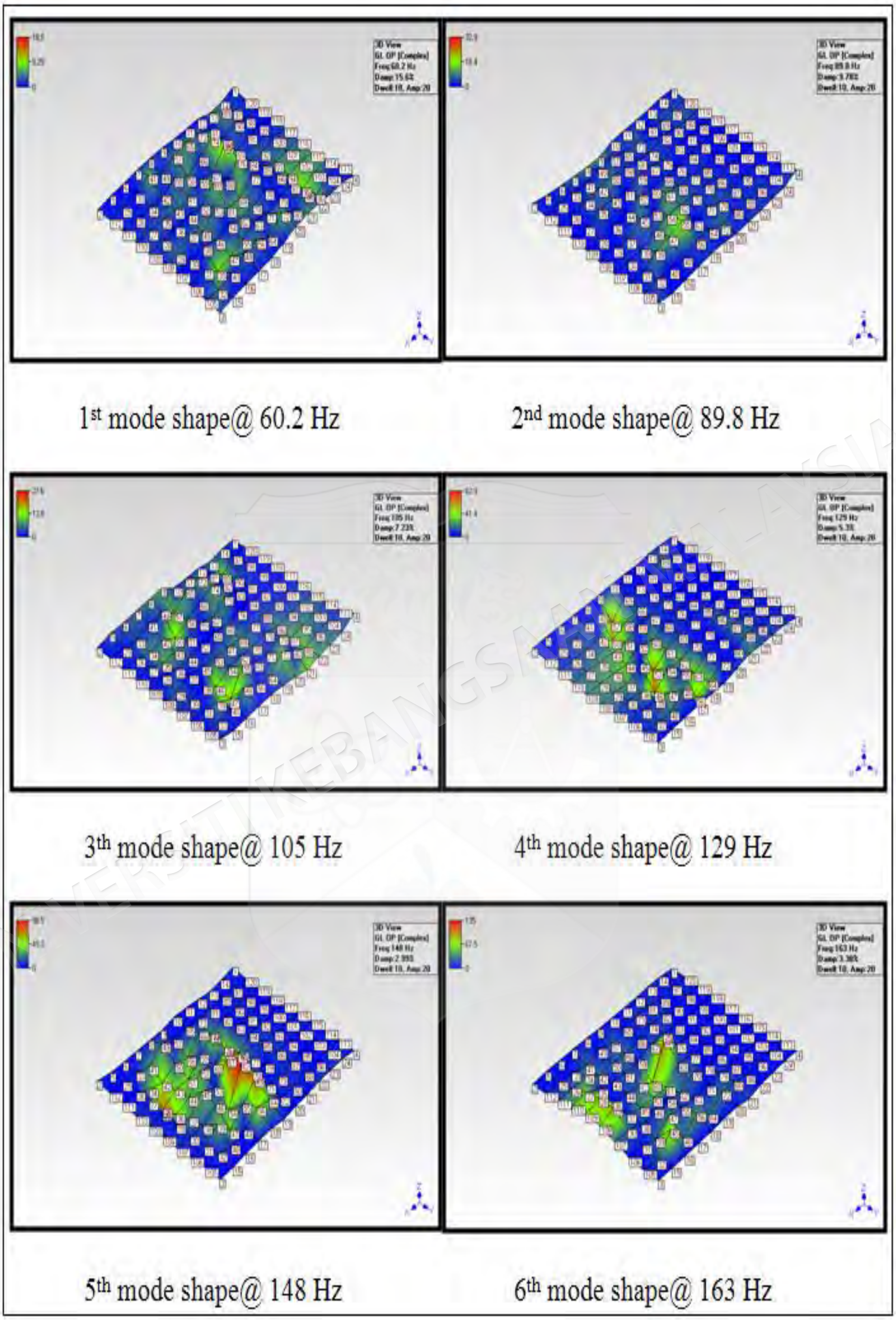

Figure5.14 Experimental mode shapes for roof panel

At the second mode the roof panel does not show significant vibration, it only vibrates around the rear right corner. The third mode showing that the panel vibrates at its four corners. At the fourth mode the panel vibrates at the rear part only at three different locations. However, the front part of the panel does not show any vibrations at all. The fifth mode also shows vibrations at the rear part, but at two locations only. The sixth mode shape shows that the roof panel vibrates at the center and rear parts of the panel. At the seventh mode the roof panel vibrates at the rear part and showing high vibration at the center. At the last mode the panel shows vibration only at the rear part, whereas the front part of the panel does not show any vibrations. The comparison between the experimental and theoretical results conducted on the roof panel will discussed bellow.

Comparison of computational frequencies and mode shapes with those obtained from experimental results indicated poor agreement at the majority of modes as shown in Table 5.5. It shows that the percentage different between the experimental and computational frequencies is more than 50% at all modes.

Table 5.5 Comparison between Exp and Simulation frequencies of roof panel

Mode No	**Exp.Freq [Hz]**	**Simul. Freq[Hz]**	**Diff %**
1^{st} mode	60.2	16.9	111
2^{nd} mode	89.8	32.8	09
3^{rd} mode	105	38.3	09
4^{th} mode	129	73.5	45
5^{th} mode	148	75.4	45
6^{th} mode	163	76.4	21
7^{th} mode	182	97.8	49
8^{th} mode	193	100.5	41
9^{th} mode	-	102.93	-
10^{th}mode	-	104.56	-

In addition Figure 5.15 also shows poor agreement between the two results as we can see that there is a big gap between the graphs of the experimental and computational frequencies.

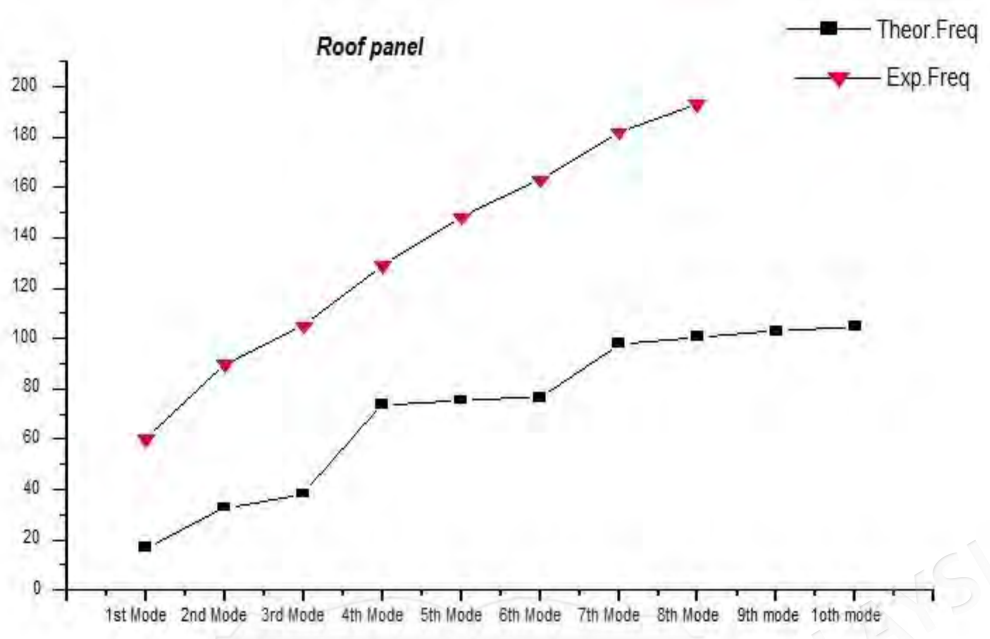

Figure 5.15 Comparison between Exp and Simulation frequencies of Roof panel

The comparison between the experimental and computational mode shapes is shown in Table 5.6. The mode shapes correspond to the second, fourth; fifth, sixth and eighth modes show some similarities. At the second mode both mode shapes presenting vibration at the center of rear part of the panel. The fourth, fifth and sixth modes showed some similarities along the rear part of the panel. At the seventh and eighth modes the panel does not show any significant similarity between experimental and theoretical methods. The last two modes are not detected by the experimental modal analysis test.

Table 5.6 Comparison between Exp and Simulation mode shapes (Roof panel)

Mod e No	Experimental mode shapes	Simulation mode shapes
1	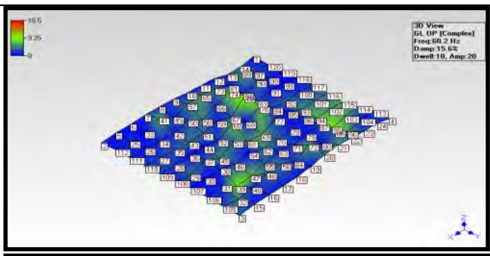	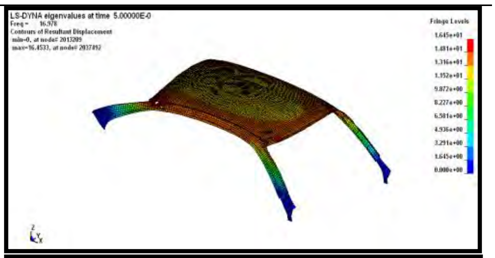
2	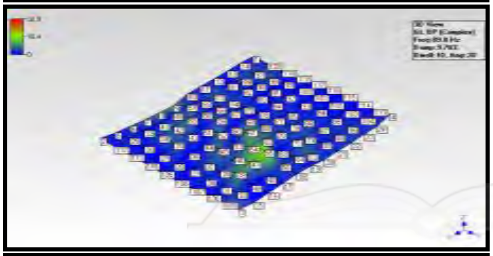	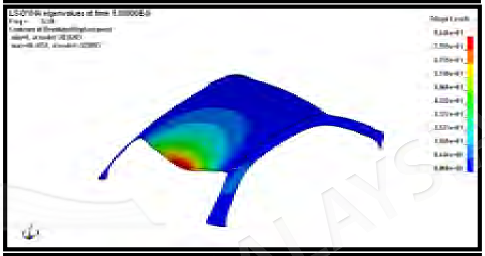
3	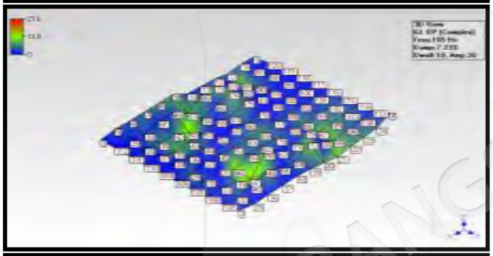	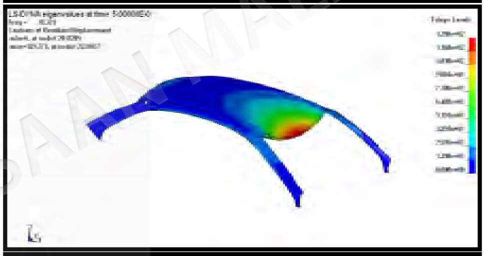
4	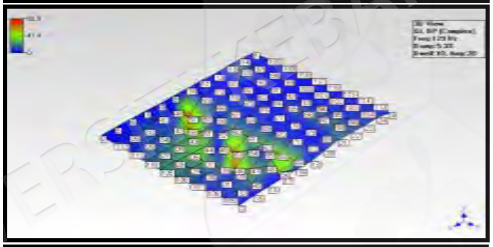	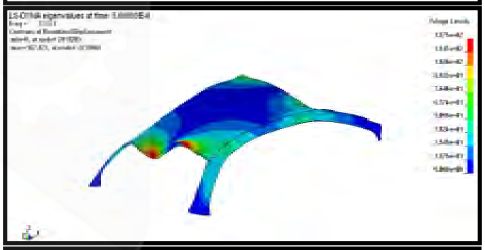
5	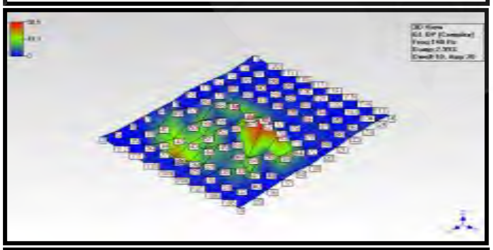	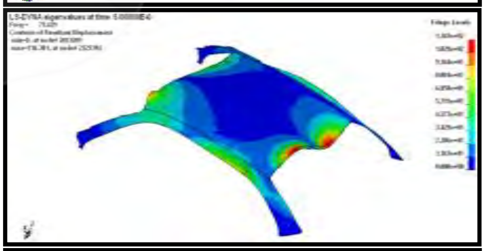
6	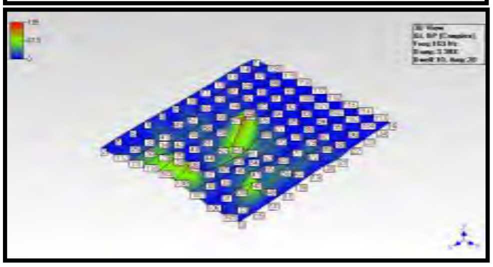	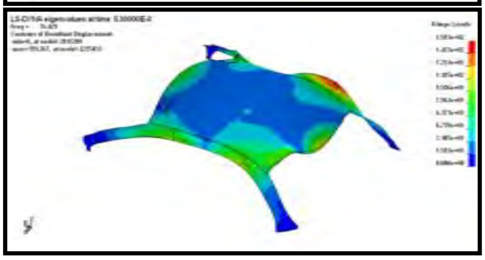

In conclusion the roof panel shows poor agreement between the experimental and computational modal analysis either in frequency level or mode shape level. As can be seen in Table 5.5, there is mismatch between the experimental and computational frequencies (error was more than 50%). Table 5.6 also shows the same discrepancy between the experimental and computational mode shapes although there is some similarities. It has been noted also that the frequencies obtained from the experimental modal analysis are higher from those obtained from computational modal analysis. This is could be because of the stiffness of the material used in FE model is lower than the stiffness of the actual roof panel. Boundary conditions also could have some influence on the vibration modes.

5.5 DOOR RESULTS

Since the four doors are symmetric we have selected the front left door to conduct the experimental modal analysis and compared with the computational modal analysis. We have choose 54 measurement points distributed equally spaced on the door panel as shown in Figures 4.22 and 4.23. The excitation point was fixed at DOF 54Z and the response functions were taken from a sequence of 6 accelerometers roving over the surface of door panel. The results will be discussed bellow

Figure 5.16 presents the total frequency response functions obtained from the experimental modal analysis over the 54 points on the door panel and Figure 5.17 shows an example of six frequency response functions and its corresponding coherences taken from a sequence of six accelerometers at a time. The coherences show good linearity between the input and the output as all coherences are close to one. The results obtained from the curve fitting process are shown in Figure 5.18. The upper part of the diagram shows each (black) FRF is overlaid with (red) Fit FRF that was synthesized from the curve fitting results. The lower part of the diagram shows the modal peaks function.

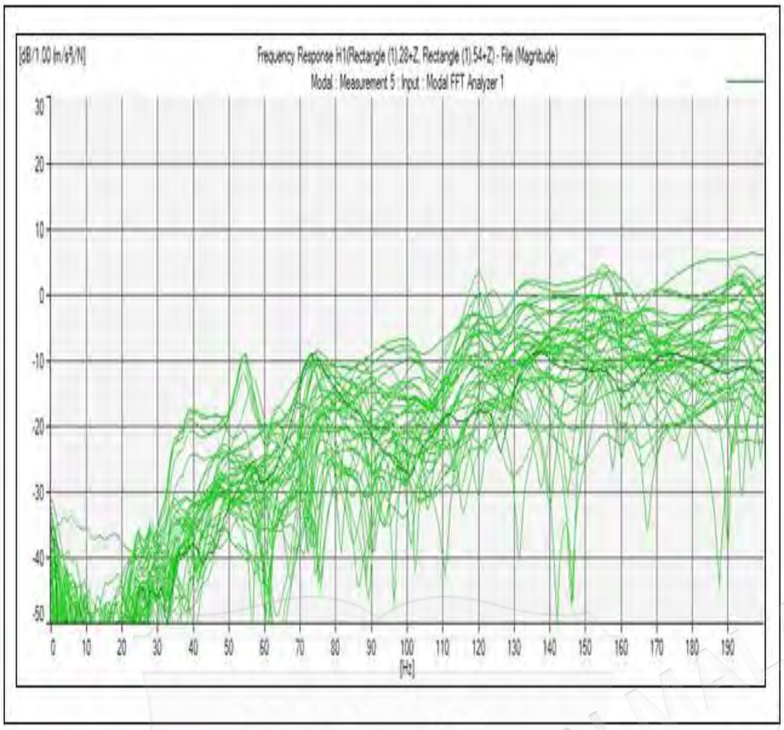

Figure 5.16 The superposed FRF for door panel

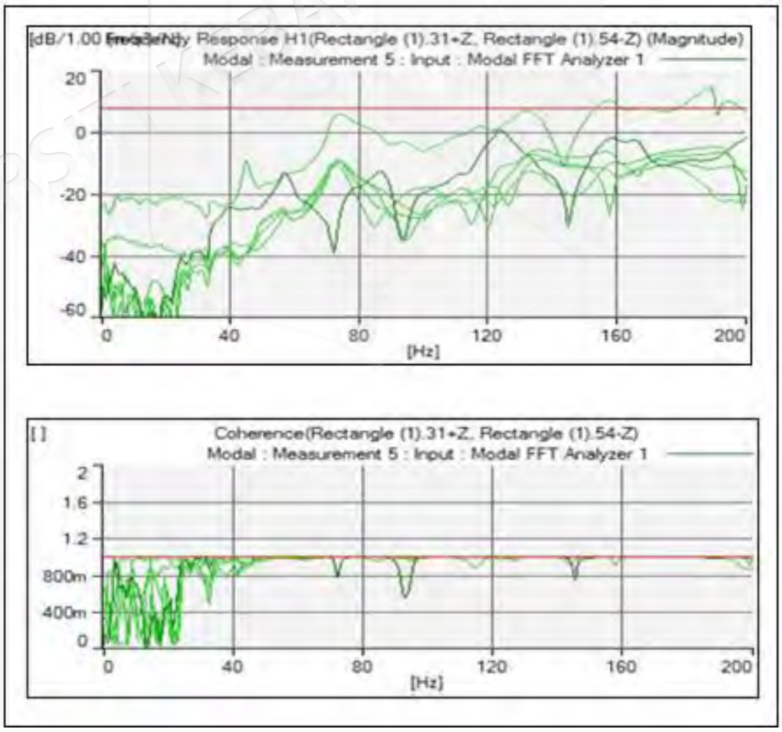

Figure 5.17 Coherences from the response of 6 different points (door panel)

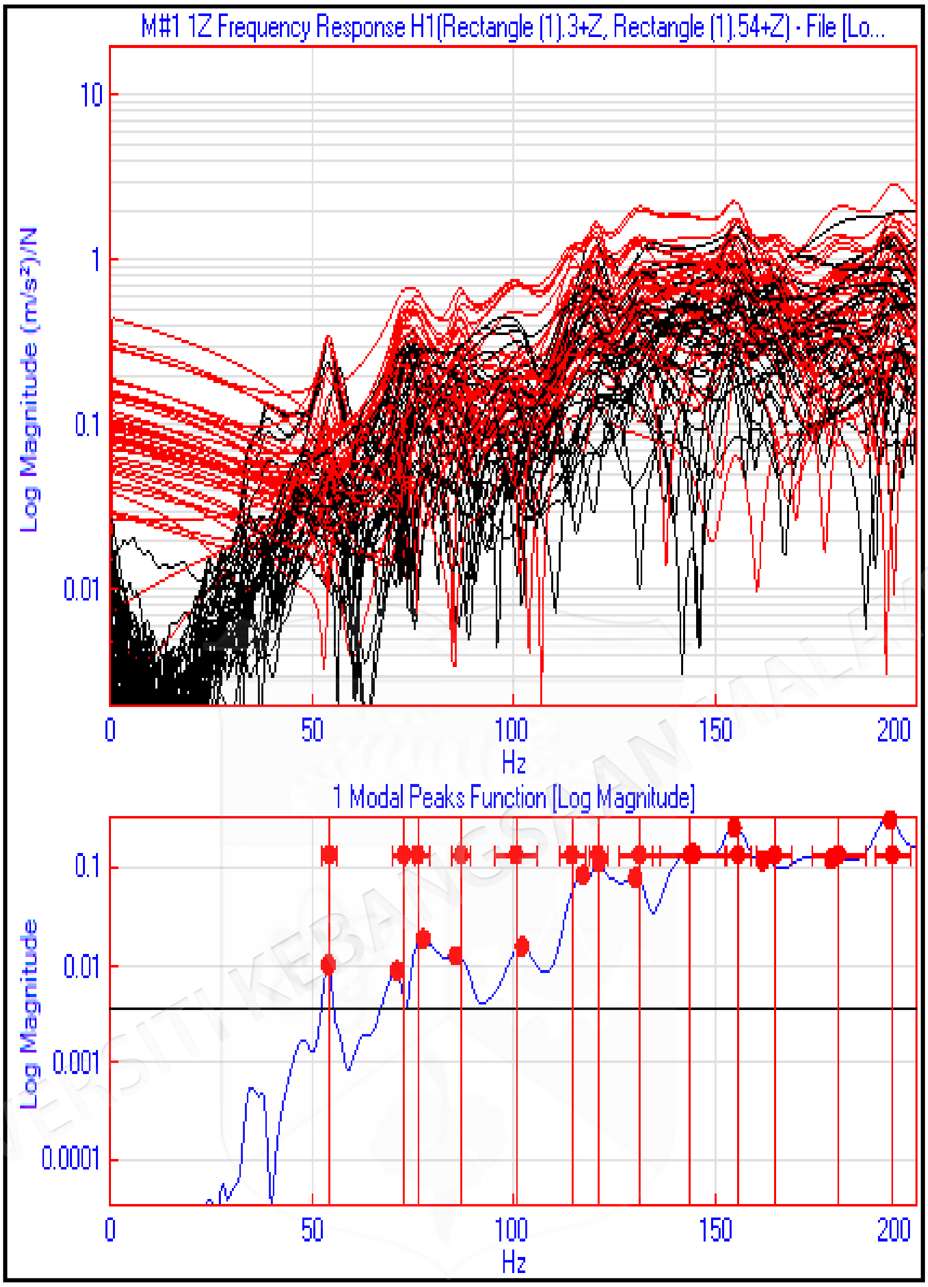

Figure 5.18 Curve fitting results for the door panel

The ten natural frequencies and the corresponding modes shapes of the door panel obtained from the experimental modal analysis test are shown in Figure 5.19.

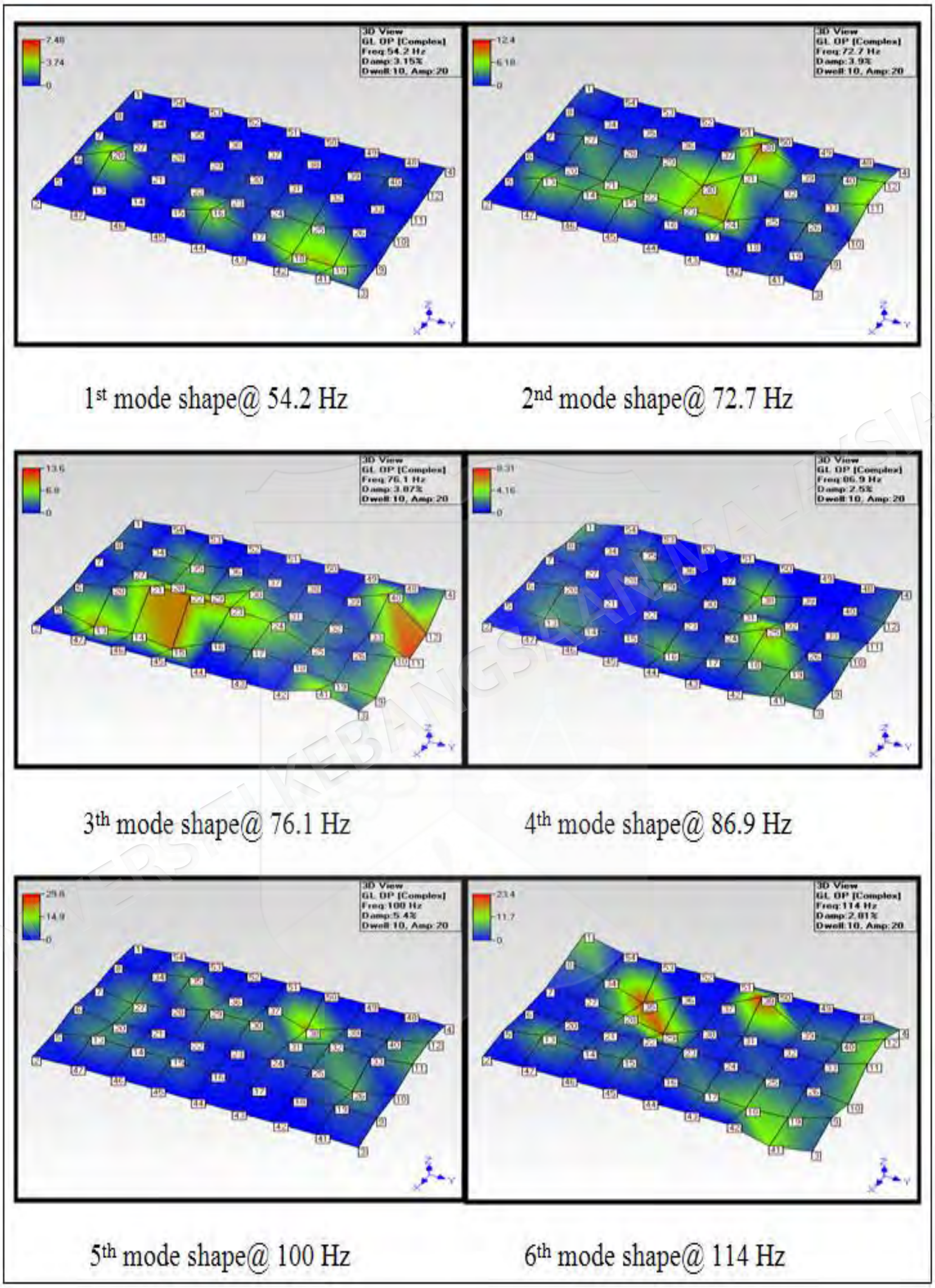

Figure 5.19 Experimental modes shape for door panel

The door panel at the first mode vibrates at three different locations, at rear center and front. At the second mode the panel shows significant vibration at the center and along the lower part of the panel. The third mode shows significant vibration at the lower and rear part of the panel. The fourth and fifth modes are quite similar. At the sixth mode the vibration located at the upper and the front part of the door panel. The seventh mode shows vibration at the front part only. Eighth and ninth modes exhibit quite similar behavior where the panel shows high vibration at the front and less vibration at the rear side. At the tenth mode the door panel shows significant vibration at the front part of the panel.

Finally, the comparison between the two methods was conducted on the front left door panel. Table 5.7 shows the comparison between the experimental and computational frequencies. It shows a fair agreement between the two methods as the percentage difference is vary between 28% and 50%. In addition we have observed that the frequencies of the last eight modes showed almost the same percentage difference between the experimental and computational methods as shown also in Figure 5.20.

Table 5.7 Comparison of frequencies between Exp and Simulation of Door panel

Mode no	**Exp.Freq[Hz]**	**Simul.Freq[Hz]**	**Diff %**
1st mode	54.2	32.7	49
2nd mode	72.7	45	47
3rd mode	76.1	55.7	30
4th mode	86.9	64.9	28
5th mode	100	74	29
6th mode	114	74.3	42
7th mode	121	86.5	32
8th mode	131	94.88	31
9th mode	144	99.37	36
10th mode	155	105.45	38

Comparison of experimental and computational mode shapes is shown in Table 5.8. The first, fourth and sixth modes do not show significant similarity between the two methods. The second mode shows quite similar behavior of the panel between the two methods as illustrated in the Table. It shows that both mode shapes exhibit vibrations at the center and the upper parts of the door panel. At the third mode both experimental and computational mode shapes are in good agreement as both showing

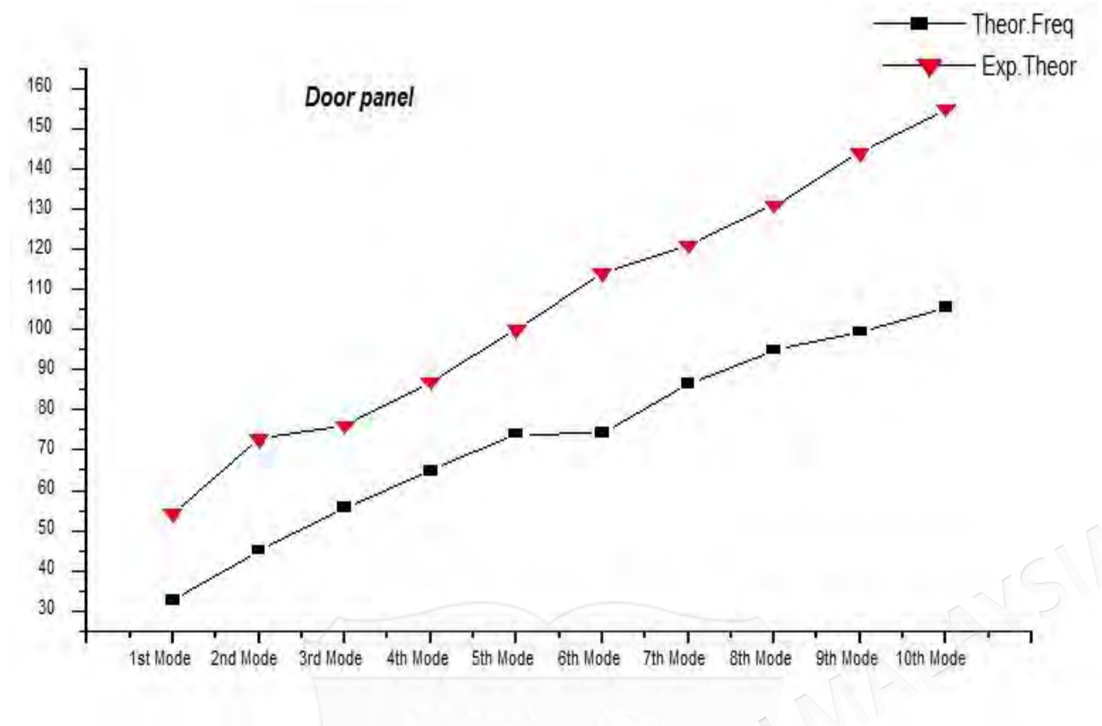

Figure 5.20 Comparison between Exp and Simulation frequencies of Door panel

significant vibrations at the bottom of the door panel. At the fourth mode the door panel does not exhibit significant vibrations either by experimental or computational method. The seventh mode shows a quite good similarity between the experimental and computational behavior, as both mode shapes presenting high vibrations at the rear part and low vibrations at the front part of the panel. Mode number eight also shows quite good agreement between the experimental and computational behavior. At this mode the door panel vibrating along its center. Finally, we compare the mode shapes at the ninth and tenth modes. These two modes showed a fair similarity between the experimental and computational mode shapes as shown in Table 5.8.The ninth mode shows some similarities between the experimental and computational mode shapes especially at the upper rear corner of the panel. At the tenth mode both mode shapes exhibit vibration at the lower part and no vibration can be seen at the upper part of the panel.

Table 5.8 Comparison between Exp and Simulation mode shapes (Door panel)

Mode No	Experimental mode shapes	Simulation mode shapes
1	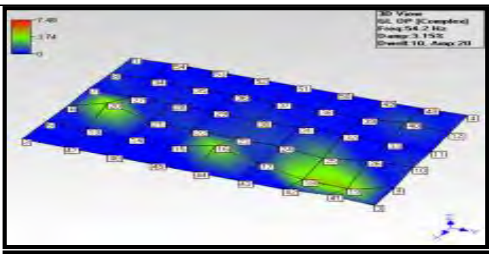	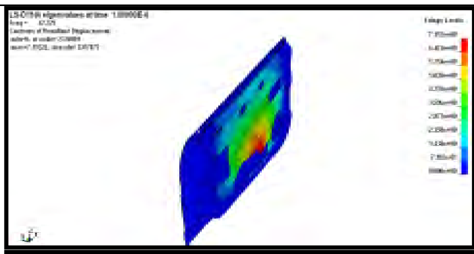
2	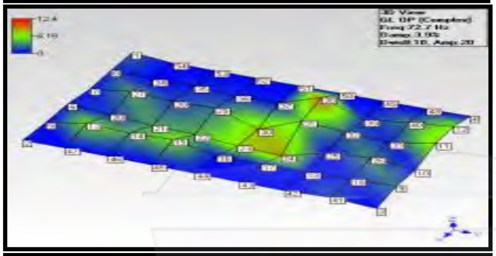	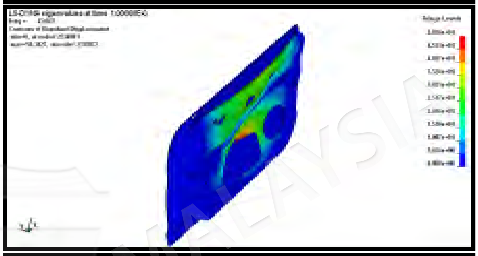
3	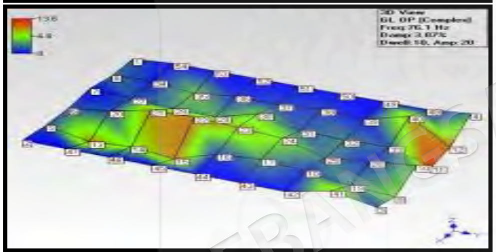	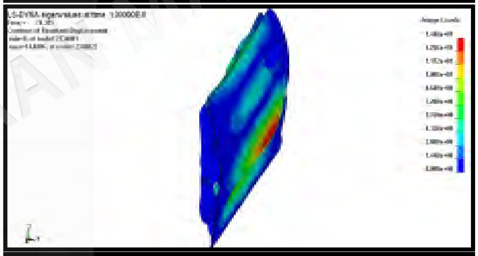
4	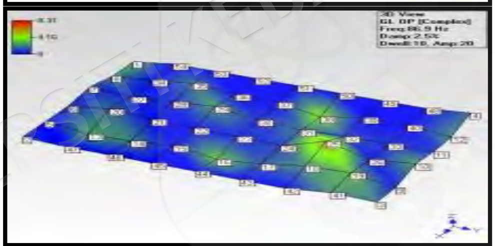	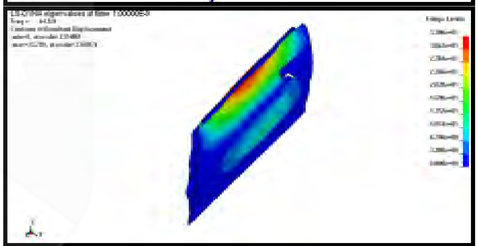
5	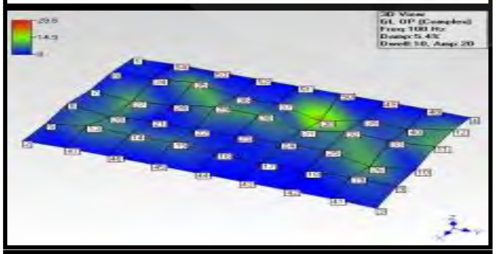	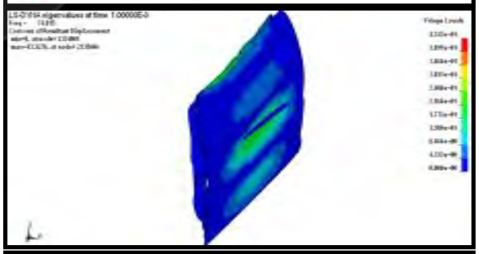
6	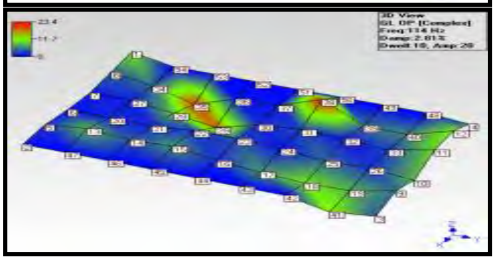	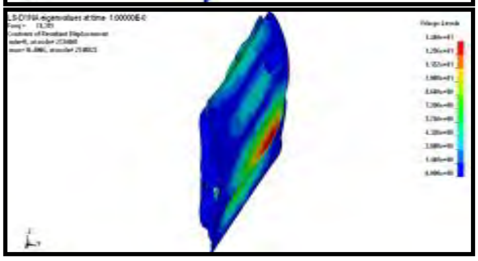

In conclusion the comparison between the experimental and computational frequencies and mode shapes of the door panel shows a fair agreement between the two methods. Even though the frequency difference percentage is around 30% it still can get a good agreement between the mode shapes.

5.6 SUMMARY

The objective of this chapter is to present and discuss the results obtained from experimental modal analysis and compared with those obtained from computational modal analysis in order to validate modal analysis part by part. The results obtained contain modal frequencies and mode shapes. The all FRFs of the panels do not show any rigid body modes. Coherence functions were unity except around anti-resonance points. Peaks resonances frequencies were achieved more precisely using the mode indicator functions. The test has been carried out twice in different time and different places and the results were the same which prove that the results are valid. This part of study addressing the comparison between experimental and computational results obtained from the car panels.

Firstly, the comparison was conducted on the trunk panel. Results indicating that there is a good agreement between the experimental and computational modal analysis in both frequency and mode shape level. The different percentages between the experimental and computational frequencies were good especially after the fourth mode (less than 9%). The second comparison conducted on the hood panel, also the results showed acceptable agreement in both, frequency and mode shape level. The different percentages between the experimental and computational frequencies were varying between 2.2% and 33% except for the first and second modes which the percentage is considered quite high. The third comparison was conducted on the roof panel. Both natural frequencies and mode shape levels show very poor agreement at all modes. It was also noted that the experimental frequencies were substantially higher than the computational values (error more than 50%). However, the comparison of mode shapes still showed some similarity between the two results. The last comparison was conducted on the door panel. It shows a reasonable agreement between experimental and computational results.

Results from the simulation model using modal analysis part by part are in quite good agreement with the experimental modal analysis results within the investigated panels. Slight discrepancies may be accounted for geometric and material approximations made during the simulation of the FE model especially as we know that the simulation FE model is not exactly the same as the actual model.

It has been noticed from the comparison of the results obtained from the experimental and computational modal analysis that the vibration amplitude of the experimental mode shapes is significantly less from those of computational modal analysis. This is obvious because of the extra damping treatment applied on the surfaces of the actual car panels to reduce the strength of the noise and vibration. The numerous damping mechanisms at work in a real structure cannot be easily modeled, so damping is not included in most FEA models. However, mode shapes can still be obtained from model with no damping in it. Mass and stiffness cause resonant vibration, damping only dissipate it (Brain et al. 2006). The other reason could be because of the exciter locations on the panels not been able to excite the all points on panels (complex structure).

As discussed earlier, there is a quite high different percentage in frequency in the first two modes between the two methods. This different could be due to three reasons: 1) the actual structure is stiffer than the FE model; 2) Boundary conditions could have some influence on some or all of vibration modes, and 3) increase thickness due to reinforcement. (Chavan et al. 2013) found that the gearbox natural frequencies derived from the EAM and FEM calculations have the highest error at the second mode (14.25%). In finite element verification for packaged printed circuit board by experimental modal analysis (Ying et al. 2008) found that the first and the second modes have highest frequency discrepancy 4.3% and 7.0% respectively. Jia- Jang (2004) investigated finite element modeling and experimental modal testing of a three-dimensional framework; the results showed that the highest percentage differences between the natural frequencies were at the first mode (23.32%) and second mode (29.89%). The important factor that can have influence on some or all vibration modes is the boundary conditions. Therefore, to overcome this problem we keep try different boundary conditions, which could be an extension work for further research. In addition, the results obtained from experimental modal analysis showed that the coherence at lower modes is far away from one ($\ll 100\%$) which means there is not good linearity between the input and output.

CHAPTER 6

RELATIONSHIPE BETWEEN STRUCTURAL VIBRATION AND THE PASSENGRE'S COMFORT INSIDE THE VEHICLE

6.1 INTRODUCTION

The requirements for comfort and reliability in industrial vehicles have grown much larger in recent years. Owing to the demands of high-speed operation and the use of lightweight and flexible structures in modern machinery, static measurements of stress/strain properties are not sufficient. Noise and vibration testing and analysis measurements are necessary and therefore have widespread use.

In any given situation, there are always, three factors are responsible for the noise and vibration problem:

- Source-where the dynamic forces are generated.
- Paths-how the energy is transmitted.
- Receivers-how much noise/vibration can be tolerated.

Any of these factors can be the cause of the discomfort, and to find the solution of each corresponding problem, each factor should be investigated.

A typical example for this case is the ground vehicle; where the dynamic components, such as engine, ground and wind, would be the sources of noise and vibration, the car body would be the path and the receiver would be the driver's ear. The dynamic components transmit noise and vibration through the structural connection to the body panels that dominate the interior noise.

Automotive researchers perform extensive analysis and testing techniques to determine the dynamical behavior of new car designs which is also one of the goals of this thesis. The results of this analysis and testing frequently lead to design changes that will improve the comfort of the vehicle. For instance there were techniques developed by Sung (1991) to predict the interior noise of the passenger car under broadband excitation by coupling coefficients between the structural vibration modes and the acoustic modes. The results indicated that the boundary panels strongly contributed to the interior noise. A combination of experimental and analytical works was investigated by Werner (1990). The frequency range of interest was up to 200Hz.

(Walter and White 1994) used an approach to define two transfer functions, which are cascaded to produce a transfer function from the valve to driver's ear acoustic pressure. The first transfer function relates the air acoustic source at the intake valve to the acoustic pressure at the snorkel inlet. The second transfer function relates the snorkel acoustic pressure to driver's ear noise. As driving speeds increase, aerodynamic noise sources on ground vehicles are becoming relatively more important. They often dominate at cruising speed as investigated by Feng et al. (1991). Constant et al. (2001) also studied the contribution of tire to the interior noise which is not considered in this study.

The purpose of this study is to investigate the dynamic characteristics of a vehicle and it relation to interior noise comfort. Two types of analysis were carried out, namely:

- Signal analysis-to predict the sources of noise and vibration components problem.
- Modal analysis to determine the dynamic characteristics of the various components of the car, namely, natural frequencies, mode shapes and damping.

The aims of this study are:

- To study the structural vibration in automobile and its relationships with the interior noise.

- To determine the relationship between the interior noise components and modal parameters namely natural frequency, mode shape and damping.
- To establish a complete dynamic characteristics database of the vehicle.
- To establish a useful methodology to reduce noise and vibration level interior the passenger cabin.

6.2 METHODOLOGY

6.2.1 Modal testing

The system used in this investigation is STAR system. It consists of a series of programs, developed for testing and analyzing the dynamics of mechanical structures as shown in Figure 6.1. The system is able to perform measurement display, real-time animated mode shape display, and transfer and save measurement data required with FFT transform, transfer storage and viewing frequency domain measurement data from an FFT analyzer and examining the effects of potential design modifications to a structure.

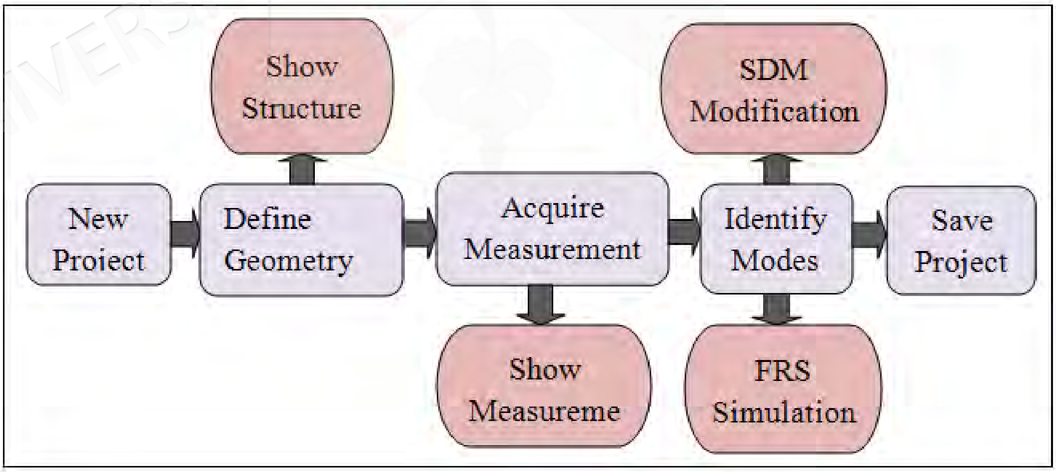

Figure 6.1 Project flowchart

The system can be used for three related types of dynamic analysis, time domain analysis, operating deflection shapes analysis and modal analysis. In this study we have used modal analysis because it is the best tool to fully analyze structural dynamics and to indicate solutions.

6.2.2 Instrumentation

The instrumentations used for the experiments and analysis purposes are consist of:

- Scientific Atlanta SA390 Dual-channel FFT analyzer, used to perform FFT analysis.
- ICP accelerometer (PCB 352A & 352B WR 786c) placed at various points to measure structural acceleration response.
- Charge accelerometers (B & K Type 4371) to measure structural acceleration response.
- Force transducers (B & K Type 8201 & 8200, PCB 086CO3) placed at the tip of the shaker to measure structural force input.
- Vibration shaker (Type IMV VEH-10) to excite the structure with the signal generated by the signal generator.
- Signal Generator (Denon DCD-1015) to generate white noise that will give a similar broad band frequency range.
- Charge amplifier (B & K Type 2635) to preamplify the signal before reach the Analyzer.
- Power supply and Integrator (WILCOXON Research WR P702B) to convert acceleration quantity from acceleration into velocity.
- Sound Level meter (RION Type 1 NA-10A, NA-61 & NA29E) to measure sound pressure level.
- SLM calibrator (Cirrus CRL 511E) to calibrate sound level meters before and after measurement.
- SMS Star modal analysis software, version 5.2 to perform data processing after capturing all necessary measurements.
- Cables to preamplifier connections.

6.2.3 Test descriptions and procedures

The two roads that can be followed for this investigation are namely, Signal analysis and Modal analysis. Data processing technique for determining the response signals of the system due to some generally unknown excitation force is called signal analysis. Knowledge obtained from the signal analysis enables distinct frequency components to be related to specific dynamical component, which could be the source of the noise or vibration problems.

Once the source of noise and vibration has been located, we can concentrate after that on modal analysis technique to determine the dynamic characteristics of the all components, in order to find the natural frequencies and the corresponding mode shapes and damping.

6.2.4 Ramp engine excitation test

The test was done in two stages, noise and vibration tests. They are performed at the vibration laboratory. We have used engine RPM excitation, the engine was ramped from the Idling to approximately 4000 RPM. The goal of the test at this stage is to predict the dominant frequency components that can be contributing to the interior noise of the passenger cabin. The simplest technique is to fix a microphone inside the cabin area at the level of the passengers' ear. The instrumentations set up is shows Figure 6.2.

At the second stage of this test, a similar approach is used to extract the vibration response under the engine excitation at the engine cross-member center. Its vibration energy can be radiated as noise which then expected to be transmitted directly to the interior cabin. An accelerometer was mounted at the center of the front support member in the vertical direction, as shown in Figure 6.3.

Both tests measurements results will be plotted in three-dimensional plots by using dual-channel FFT analyzer to obtain waterfall plots.

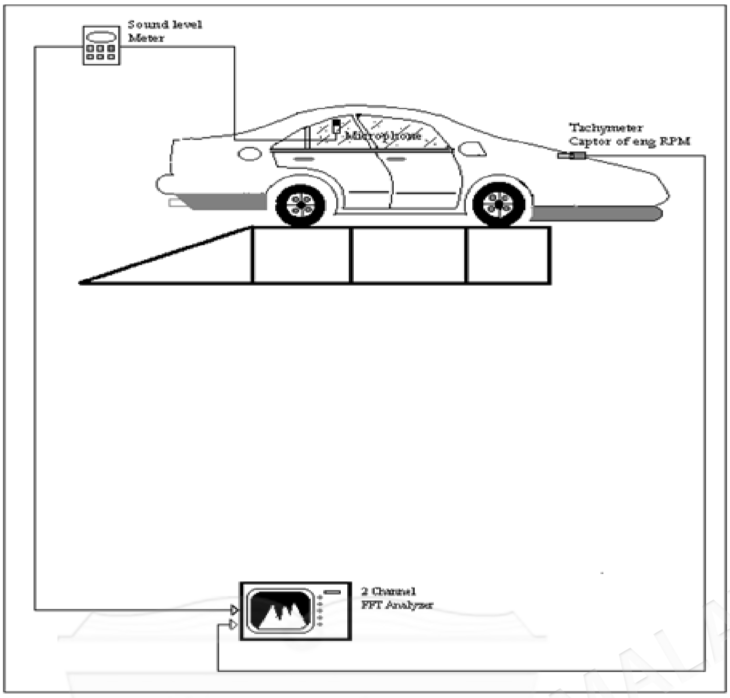

Figure 6.2 Ramp Engine Excitation set up-Noise test for Proton Perdana car

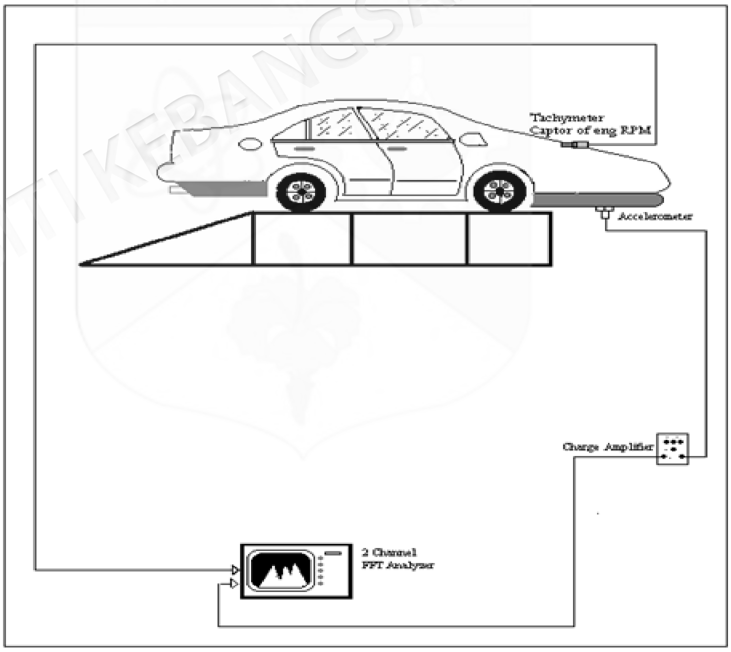

Figure 6.3 Ramp Engine Excitation set up-vibration test for Proton Perdana car

6.2.5 Random excitation

The goal of the noise contour is to predict the dominating sound pressure level component inside the passenger cabin. The test was conducted in the vibration laboratory. The contour of sound pressure level was performed by placing the microphone over the horizontal cross-sectional plane in the interior of the cabin with a grid of 10 X 10. The cross-sectional plane was selected close to the passenger ear. In the first stage of the test, the shaker was mounted at the rear center axle. The second stage the shaker was mounted at the engine center member support. The excitation energy level remained constant during both tests. A microphone was placed to measure the average noise spectra of each point over the cross-plane area. The signals out from the microphone were recorded in the FFT analyzer via a sound level meter. The contours of the dominant frequency components were plotted separately.

6.2.6 Experimental modal analysis

Modal analysis is a way of determining a complete dynamic description of each component of the vehicle body that suspect to be the source of the interior noise. The lower bending modes are required in this investigation because they contribute to the structural noise. All other elastic modes are required also to establish a complete database of the vehicle for further work. The experimental work was done by suspending the vehicle on two simple supports. The car was set into vibration using an Electro-dynamic shaker applied at a bottom away from the nodal lines. An impact hammer was used to excite the vertical components in the horizontal direction. A force transducer was mounted at the excitation point as a reference in order to excite the structure by the signal generated from the signal generator by using the white noise. An accelerometer was moved to each point on a structure (for transient excitation the accelerometer was moving and the hammer was fixed). The force and acceleration signals were fed into a dual-channel FFT analyzer to produce a FRF. SMS Star- modal analysis software- performed data processing after capturing all necessary measurements.

6.3 RESULTS AND DISCUSSION

6.3.1 Ramp engine excitation results

The aim of this test is to determine the source of noise inside the cabin. Two tests were carried out. The first test was to find the dominating noise frequency of the engine and the second test was to find the dominating vibration frequency of the engine. The engine noise and vibration resonance were taken when the engine was speeding up from Idling to 4000 RPM. Figure 6.6 shows the noise waterfall map interior the cabin. Referring to the same figure it can be seen that no dominating engine noise frequency appeared, so the engine noise could not be an important contributor to the internal noise. However, the vibrations test taken on the engine cross-member showed that the engine exhibit high amplitude at 62Hz component as shown in Figure 6.4 and figure 6.5. According to the engine vibration and engine noise results we conclude that the vibration of the engine cross-member extended from the engine vibration could be the main source of the dominating noise inside the passenger cabin. In other words the interior noise can be resulted from the structural vibration of the engine rather than its air born noise.

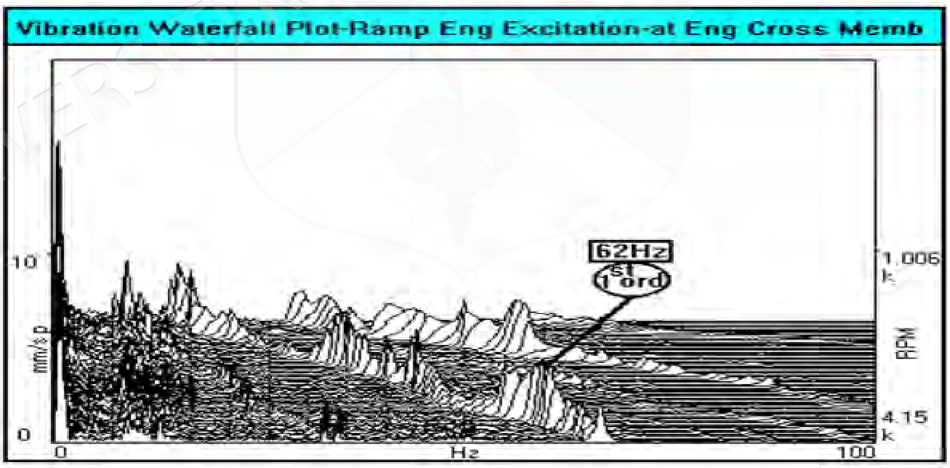

Figure 6.4 Vibration 3-D plot from run-up test on engine Cross-member

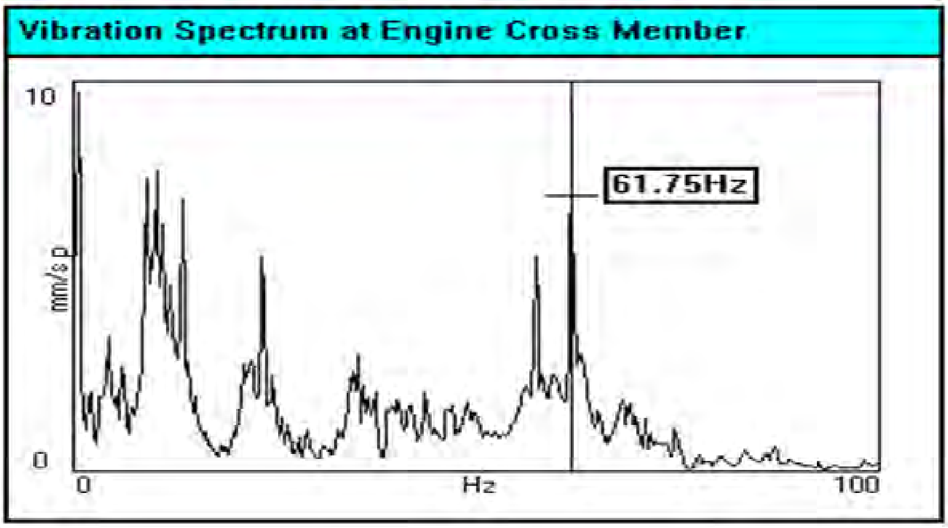

Figure 6.5 Single frequency spectrums taken from the 3D plot

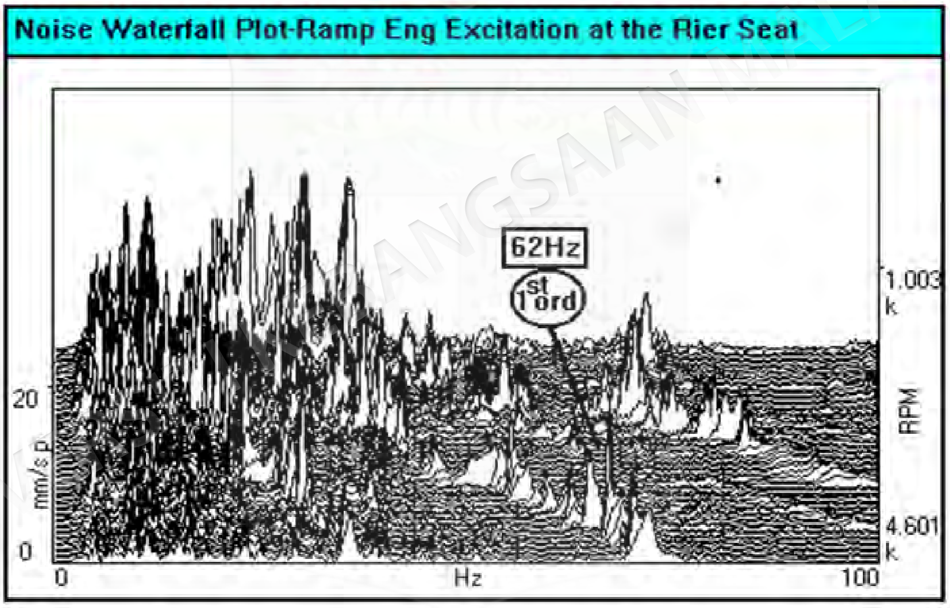

Figure 6.6 noise 3D plots from run-up test interior the passenger cabin.

6.3.2 Noise contour results

The results of the ramp engine excitation tests showed that the structural vibration is the main source contributing to the interior noise. The vibration of the engine cross-member exhibits a dominating component at 62Hz, which was strongly expected to be the main contributor to the interior noise. Noise contour results also shows that the dominating noise component inside the cabin is at 62 Hz as shown in Figures 6.7 and 6.9.

Noise contour plot results were carried out to predict the dominating noise components inside the passenger cabin. The noise spectrum displayed in Figure 6.7 indicates again that the dominating component was at frequency 62Hz when the excitation was at the front center member. When the excitation was at the rear Axle the noise spectrum indicates the presence of other two significant peaks such as 163Hz and 173Hz that could be contribute to the interior noise as shown in Figure 6.8.

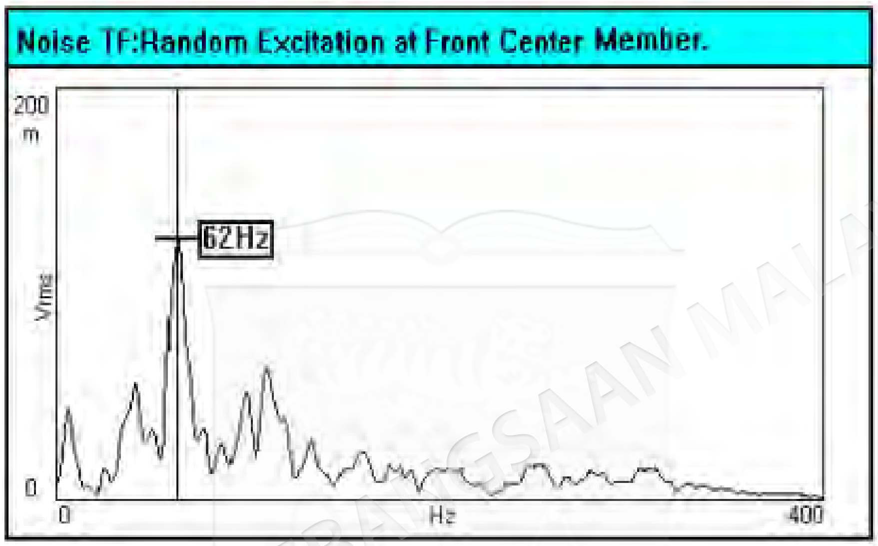

Figure 6.7 Noise transfer function between front center and interior cabin

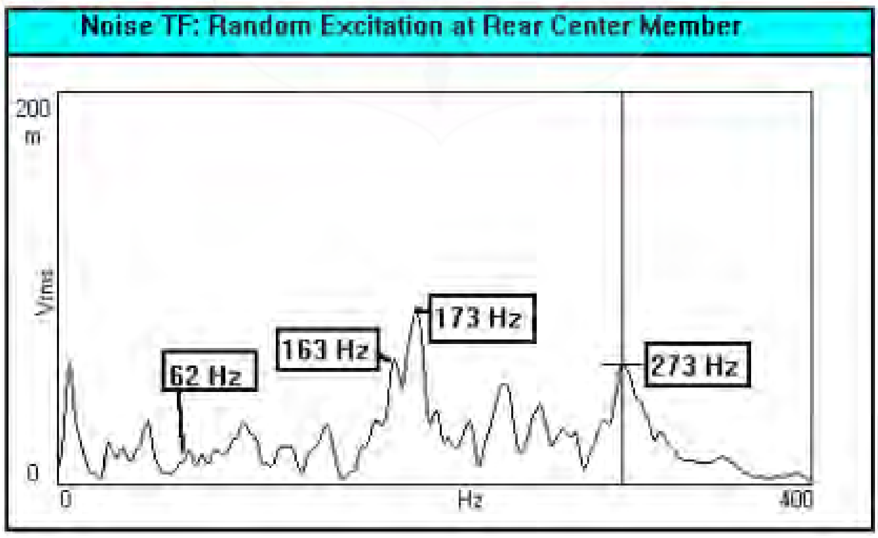

Figure 6.8 Noise transfer function between rear center and interior cabin

The noise contour plots at 62Hz indicate higher sound pressure level at the front seats as shown in the sound pressure plots over the cross-sectional plane inside the cabin as presented in Figure 6.9.The noise contour characteristics of the 163Hz and 173Hz components are also show high amplitudes around the center of the roof which is very close to the roof beam as shown in figures 6.10 and 6.11. These also could be strongly contributed to the interior noise. The noise peak corresponds to 62 Hz is highly possible caused from the bending mode of the suspension, in particular the engine cross and center members. The 163Hz and 173Hz noise components are most probably originated from the cantilever with end twisting mode and twisting mode respectively as will be shown later in modal analysis test. In conclusion the noise and vibration signal analysis results confirm that the front suspension and the roof beam panel were the dominant noise sources to the interior noise. The detailed data for the noise contour of 62 Hz, 163 Hz and 173 Hz are given in Appendices B and C.

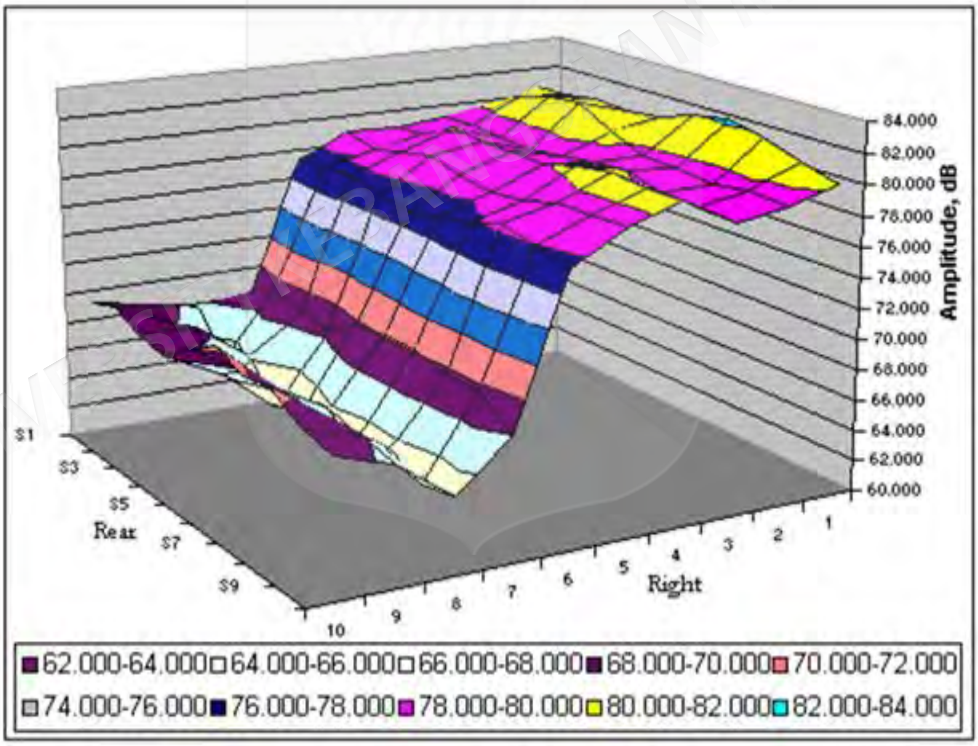

Figure 6.9 Noise contour plots at 62 Hz

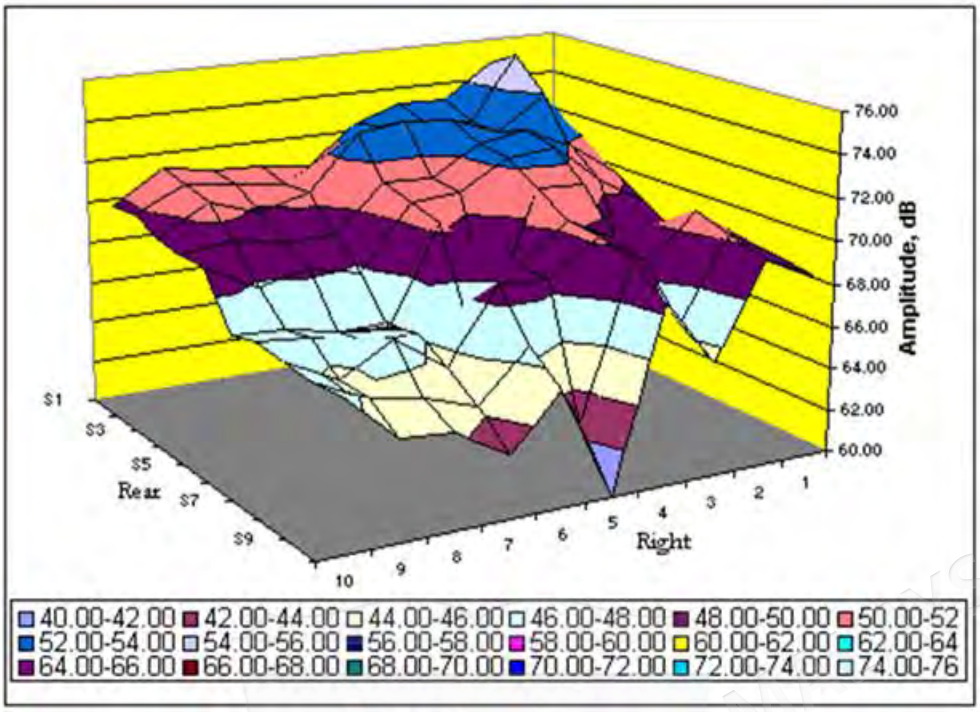

Figure 6.10 Noise contour plots at 163 Hz

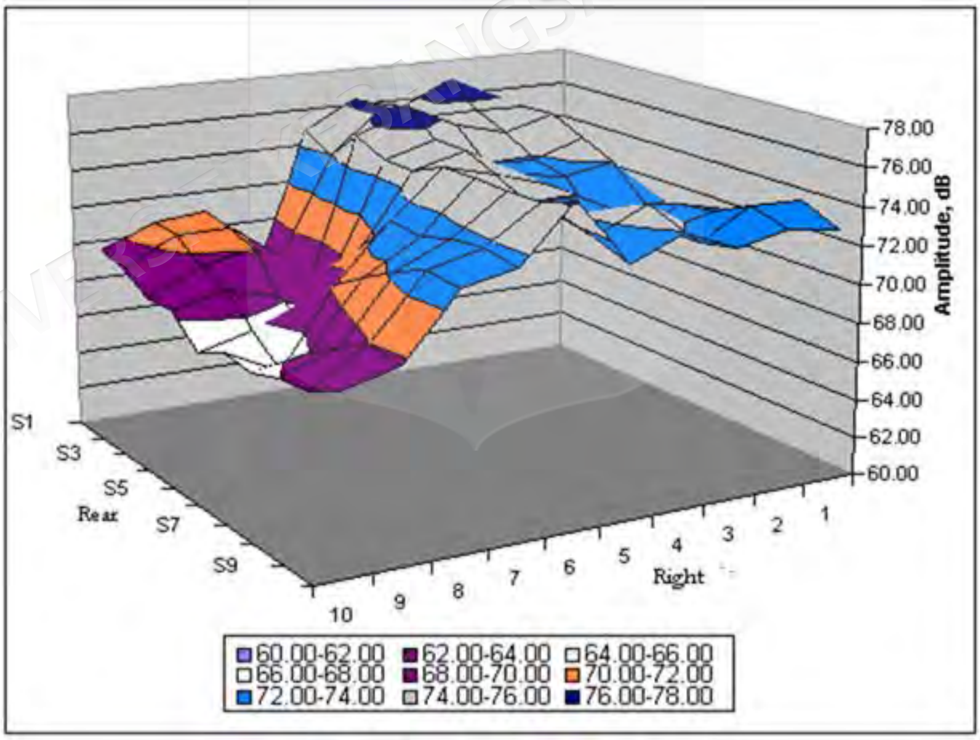

Figure 6.11 Noise contour plots at 173 Hz

6.3.3 Modal analysis results

It was well known that one of the major sources of the internal noise is caused by the front suspension and cross roof beam panel, as investigated by signal analysis. Modal analysis has been proposed to prove the structural vibration for major components of the body and their relationship to the interior noise, by determining their dynamic characteristics, namely, natural frequency, mode shape and damping. As the bending modes equal or close to 62 Hz, 163Hz and 173Hz are suspected to be the main contributors to the interior noise, it is necessary to establish their locations before it is possible to ease them out. The other lower binding modes with lower damping are also taken in consideration to be contributors to the internal noise. The modal analysis results will be presented and discussed in the following sections and the details will be given in the appendix D.

The first modal analysis was done on the rear-right & left window panels. No significant bending modes exist close to 62 Hz, 163 Hz and 173 Hz components, except the first mode of the rear right window at 61.06 Hz with damping 4.55%. This mode can produce minimal noise, as its damping is quite high. Front-right & left window panels do not show any significant bending mode near or coincident with the disturbing frequency components 62Hz, 163Hz and 173Hz. At front windshield there are several bending modes. The first significant bending mode was at 51.94 Hz with 0.136.01% damping, which may contribute to the internal noise, as its damping is low. The other bending modes are far from the disturbing frequencies and their dampings are quite high. Rear windshield presents the first bending mode at 56.73Hz with damping 1.64%. Its contribution to the interior noise is suspected to be quite considerable, as its damping is low. Front right & left door panels showed similar characteristics i.e. natural frequencies and mode shapes. All modes are undesirable except the second bending mode at 60.50 with 1.5% damping, which is very close to the disturbing frequency components 62Hz. So its contribution to the internal noise is expected to be considerable. At the rear right & left door panels it was found that the closest mode to the 62Hz component is appeared in the rear right door panel at frequency 65.96 Hz with 4.12% damping. Since the damping is quite high the bending mode may have minimal contribution to the interior noise. No significant bending modes near or close to 62 Hz, 163 Hz and 173 Hz can be seen on the Roof panel. No significant bending mode near or coincides with the disturbing frequency components can be observed at the floor, engine hood, trunk lid, rear left quarter, front left finder and fuel tank panels, the details are shown in Appendix C. Modal analysis of the exhaust system showed six bending modes. The first bending mode was at 16.69 Hz with 3.49% damping. Its contribution to the interior noise suspected to be minimal since it is below the audible hearing range (20 - 20 kHz). The second mode was observed at 25.22Hz with 4.72% damping. As it is out-of phase bending mode, the noise contribution will be minimal. The third elastic mode was at 40.66 Hz. No significant problem is expected. The forth-bending mode was at 64.30 Hz with 1.68% damping. It is close to 62 Hz. The positions of the front hangers are quite good since they were located at the node points. While the middle and rear hangers were ineffective as they were located at anti-nodes where the vibration can be transmitted through the hungers to the body. Similar characteristics were shown at fifth mode at 76.29 Hz. The last mode was at 123.64 Hz; all hangers were at the nodes.

The front suspension system includes the engine center member, cross members, and left and right arms. The system exhibits five modes; two rigid body modes & three elastic modes. The first and second rigid body modes were at 15.08 Hz & 32.92 Hz respectively. The first mode is avoided because it is below the human audible hearing. The first bending mode occurred at 54.54 Hz with 2.72% damping. A cantilever mode is pivoted at the front roll stopper. The same mode behavior was found at 62.49 Hz. This mode is very close to the disturbing frequency at 62 Hz, which is suspected to be strongly contributes to the interior noise. The last bending mode was at 66.30 Hz, is also near to the disturbing frequency, and has low damping 0.294% with the same behavior as the precedent mode.

Cross roof beam is one of the strong expected contributor to the interior noise as explained in the previous section. The results obtained from modal analysis of the beam exhibit components close to the disturbing frequency components 163 Hz and 173 Hz. The first rigid body mode was at 98.40 Hz. The first bending mode was observed at 150.79 Hz with 2.06% damping. A cantilever mode was detected at 162.79 Hz with a twisted end section. This mode is very close to the disturbing mode i.e. at 163Hz, which suspected to be strongly contributed to the interior noise. The last elastic mode was at 171.25 Hz with 0.92% damping that exhibits a twisting mode. This twisting mode appeared to coincide with one of the disturbing frequencies i.e. at 173HZ. We suspect that this mode is strongly contributed to the interior noise problem, as its damping is very low. Finally, the modal analysis for the rear suspension bar does not give any significant bending mode near or coincides with any of the disturbing frequencies.

6.4 GENERAL DISCUSSION

The objectives of this chapter have been achieved. The responses to the engine and random excitations and the dynamic characteristics of the major vehicle components have been analyzed.

The results of the noise test conducted by using engine excitation showed that no dominating noise frequency can be identified. However, the vibration test results showed that the engine cross-member exhibit high amplitude at 62Hz component. Therefore, the engine vibration could be the important contributor to the internal noise rather than the engine noise. The vibration energy of the engine is passed to the surrounding structures, after which it is radiated as audible sound inside the passenger cabin (structure-borne noise).

In addition the noise contour test has been performed to estimate the localization and the dominating amplitudes of noise level inside the passenger cabin. It was found that by the front excitation the interior noise was dominated by a peaks near or equal 62 Hz components. Therefore, removal of this peak would lower the noise level and then improve the comfort inside the passenger cabin. Furthermore, the vibration measurements indicated that this peak was radiated from the resonating of the engine cross member. Noise contour plots characteristics also exhibit localization of high amplitudes at 62 Hz over the front seats, which is very close to the front suspension and this is a prove that the interior noise comes from the resonance of the front suspension. These findings are confirmed by modal analysis too. It was found that the engine cross member with center member and left & right arms (front suspension) exhibit together the first bending mode at the same frequency component. In short, a good correlation was found between noise contour, vibration measurement and modal analysis at this frequency. Therefore, we conclude that one of the interior noise sources of the interior vehicle passenger cabin is due to the excitation induced by the dynamic of the front suspension system, mainly the cross member and center member, which is transmitted and dominating the interior noise in the form of structural-born noise.

Other significant components were also recorded at 163Hz and 173Hz from the rear excitation. A similar frequency band was recorded on modal analysis transfer function for the cross roof beam. Noise contour plots characteristics for both components i.e. 163Hz and 173Hz also indicated highly localized amplitudes around the cross roof beam area. The beam is fixed near the center of the roof panel. The modal analysis of the beam panel showed two modes near 163 Hz and 173 Hz, are 171.25 Hz and 162.79 Hz respectively. The first is a twisting mode and the second is a cantilever with twisted end section mode. These two modes could be strongly contributed to the interior noise too.

Ultimately the interior noise problem for the passenger vehicle is largely caused by the structural-born noise caused from the vibration of the front suspension and cross roof beam as well. The isolation of these components will improve the comfort inside the passenger’s cabin.

Hence the purpose of modal analysis test is primary to establish complete dynamic characteristics of the vehicle and secondly to find the mode shapes at the disturbing frequencies 62 Hz, 163 Hz and 173 Hz components; extensive measurements have been done on several vehicle components in order to predict the panels that radiate noise at these frequencies. Only two components were found faulty in the test, which are, front suspension and roof cross beam.

6.5 SUMMARY AND CONCLUSION

The objective of this chapter was to investigate the relationship between the structural vibration and the passengers' comfort inside the cabin. The analysis technique used was based on signal analysis and modal analysis methods. Signal analysis method was conducted on sound pressure level and vibration response and modal analysis method conducted on vehicle structural components. The first test conducted to find the main source of the interior noise by studying the vibration response on the front suspension in the vertical direction and the noise inside the cabin under the engine excitation. Secondly, the results were obtained by the noise contour test, which is a contour of sound pressure level, done over the horizontal cross-sectional plane near the passenger's ear inside the cabin. This is carried out under the random excitation, to predict the dominating noise frequencies inside the passenger cabin. Thirdly, modal analysis was used to determine the dynamic characteristics of every component of the vehicle body panels that would expect to contribute to the interior noise. It was found that the interior noise of the car vehicle is mainly caused by the excessive bending mode vibration of the front suspension and twisting mode vibration of the cross roof beam.

In conclusion, from the results and analysis obtained, we can conclude that the dominating noise peaks interior the passenger cabin is associated with the resonance of the front suspension system mainly cross member and center member at 62 Hz and the resonance of the cross roof beam at 163Hz and 173Hz from the rear excitation.

6.6 VALIDATION OF THE RESULTS

It was found that the frequencies contributing most to cabin noise discomfort were at 63 Hz, 163 Hz and 173 Hz. They are associated with the resonance of the front suspension system mainly cross member and center member and the resonance of the cross roof beam respectively. The discomfort factors can be identified from noise, vibration or driver's seat or all together. In this investigation we focused on noise and vibration discomfort. The discomfort can be resulted in different forms such as aural pain, annoyance, loudness, noisiness, effects on communication and psychosocial effects sleep disturbance and mental health etc. There are debates in the literatures regarding the frequency range for discomfort study as shown in Table 6.1.

Table 6.1 Established published data on the frequency range of discomfort.

References	Discomfort frequency range	Effects
1. Mohd Hosseein. 2006	below 200Hz.	Engine vibration was the dominant source of interior noise below 200Hz.
2. Atmosphere and life Bureau of Ministry of environment Japan. 2000	1Hz to 80 Hz	Complaints of rattling ,mental and physical discomfort.
3. Leventhall G. 2007	50Hz to 80Hz	Excite body vibrations such as a chest resonance.
4. Leventhall HG. 2004	10 Hz to 200 Hz	Environmental noise problem (annoyance).
5.Broner & Leventhall (1984); Poulsen (2003)	20 Hz to 90 Hz.	Were rated as sounds 'annoyance and unacceptability.
6. ISO 2631	0 to 80 Hz	Effecting on human body(Resonance in eyeballs at 60 Hz).
7. AFS 2000; Persson et al.(1997; 2001); Buller (2008)	20 Hz to 200 Hz	Lead to fatigue, sleepiness, headache and disturbances.

Complaints of mental and physical discomfort are often caused when people hear a certain frequency in the range of 50 Hz or more, or those in the range of 100 Hz or more (Atmosphere and life Bureau of Ministry of Environment 2000 Japan). Low frequency noise is sometimes confused with vibration. This is mainly due to the fact that certain parts of the human body can resonate at various low frequencies. For example the chest wall can resonate at frequencies of about 50 to 100 Hz (DEFRA 2001). In addition it has been demonstrated that high levels of low frequency sound can excite body vibrations, such as a chest resonance vibration that can occur at a frequency of 50 Hz to 80 Hz (Leventhall 2007).

Furthermore, data presented in figure 6.11 indicate the extensive production of low frequency noise by different passenger cars to which much of population is exposed both inside and outside the vehicles. It has been noted that over the frequency range approximately less than 100 Hz are noteworthy because they present greater levels of subjective reactions such as annoyance and discomfort. However, less levels are presented over the high frequency range for all cars (Birtitta & Peter 1996).

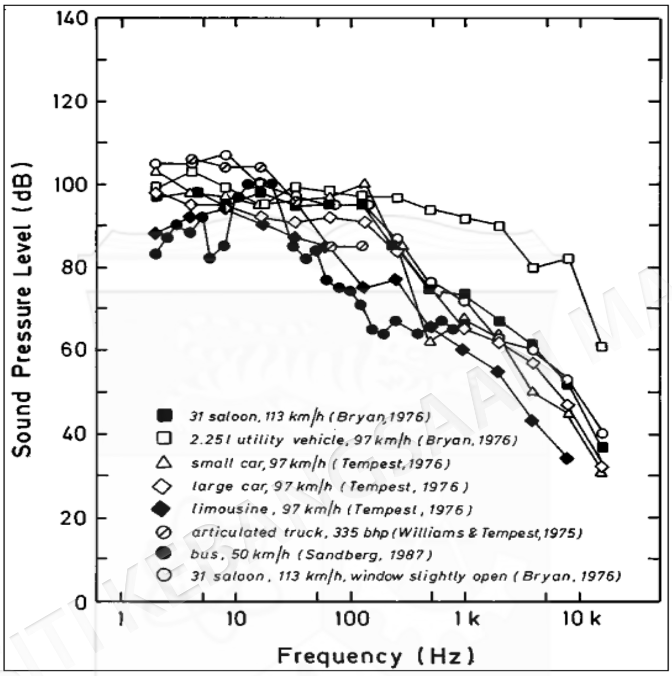

Figure 6.12 Passenger noise exposures in road transportation vehicles as a function of frequency.

Source : Birtitta & Peter. 1996

Moreover, the Atmosphere and life Bureau of ministry of environment in Japan put in the reference values for complaints of mental and physical discomfort as presented in Table 6.2.

Table 6.2 Reference values for complaints of mental and physical discomfort

Frequencies (Hz)	10	12.5	16	20	25	31.5	40	50	63	80
Sound Pressure Level (dB)	92	88	83	76	70	64	57	52	47	41

Source: Atmosphere and life Bureau of Ministry of Environment Japan 2000.

In the other hand, the frequency range from about 10 Hz to 200 Hz, has been recognized as a special environment noise problem which is leading to annoyance and stress, particularly to sensitive people (Leventhall 2004). Moreover, Buller (2005;2008) and Person (1997; 2001) are claimed that frequency range from 20 Hz to 200 Hz is leading to fatigue, sleepiness, headache and disturbances.

Even though, there are debates in the literatures regarding the frequency range of discomfort, the most existing researches are agreed with the discomfort frequency range that is less than 200 Hz, which is in-line with the findings of this study. Finally, this study (Modal analysis part by part) is can be a benchmark for future work to determine the source of the dominant frequencies that contribute to the interior noise and vibration discomfort either in the department level or national level, specially that Malaysia has its own automotive industry. In the other hand, in Malaysian automotive engineering scenario, comfort or discomfort study is still in its infancy stage. Cancellation of noise and vibration sources leads to improve the designs that would increase comfort and reduce the experienced annoyance from excessive vibrations.

CHAPTER 7

GENERAL CONCLUSION AND DISCUSSION

7.1 CONCLUSION OF THE STUDY

This study focused on the measurement of the dynamic characteristics of a Malaysian car structure using a new method called modal analysis part by part. The analysis was done using both experimental and computational methods and then is capped with a comparison between these two methods in order to validate the new method. Finally, this method was applied to discover the relationship between structural vibrations of the car panels with the interior noise comfort inside the passenger cabin. According to the main objectives of this research which are mentioned in the first chapter, conclusions are classified as below:

7.1.1 Computational modal analysis part by part

Firstly, computational modal analysis part by part was carried out on the vehicle structure. In this investigation, the car of interest was Proton Perdana V6 2001. Since no CAD model is provided for this car, we had to search for what we have in terms of the available FEA models. It was found that the closest model to the Proton Perdana car is the Dodge Neon car, which we have done some modifications on it to be exactly following the dimensions and mechanical characteristics of Perdana car as shown in detail in chapter 3.

The initial computational modal analysis tests were carried out using Ansys Workbench since the methodology is relatively simple and easy to follow, as the documentation provided was reliable and robust. However, a problem still remained because Ansys was not completely compatible with Ls-Dyna keyword files, where our car model is of this nature. Later we discovered VPG 3.2 software, which is a very useful program with many libraries that contain vehicle-related components and which uses Ls-Dyna as its processor and solver.

At first we tried to do modal analysis for the whole car. The problem was that this model was designed for crash testing and has several other parameters attached to the car model that are irrelevant to the modal analysis. The fallback plan was to use a new technique called modal analysis part by part. Therefore, we had to extract each part from the FEA model and then carry out modal analysis.

At the beginning, we used LS-PrePost to output the activated parts. The result was that only the geometry was exported while the properties of the parts were not. We then used different software that allowed us to select parts and export the activated parts with their properties. This is where VPG 3.2 came in handy; we could select the parts we wanted and then export them with their full properties.

Results from the computational modal analysis part by part method successfully produced natural frequencies and their associated mode shapes for the passenger car to be compared with the experimental results, which is one of the achievements of this work.

7.1.2 Experimental modal analysis part by part

Experimental modal analysis is one of the useful tools for providing a proper understanding of structure dynamic characteristics, and also can be used as a validation tool for computational modal analysis. The validation consists of a comparison of modal analysis results (natural frequencies and mode shapes) with computational modal analysis results.

The procedures for carrying out experimental modal analysis part by part using the impact hammer excitation technique have been satisfactorily detailed in this study. A single-input multi-output (SIMO) test was conducted using an impact hammer and six accelerometers. The great advantage of this technique was implementing cheap and fast hammer rather than expensive and time consuming shaker. Because, firstly shaker tests need extra measurement equipments such as amplifiers, actuators, etc, that are very expensive compared to hammer price. Secondly it is required to build a structure and hang the object prior to excitation (time consuming). The detailed steps for carrying out experimental modal analysis are explained in details in chapter 4.

7.1.3 Comparison between experimental and computational methods

One of the main objectives of this work is to validate modal analysis part by part. The validation consists in comparing computational and experimental modal analysis of a Malaysian car (Proton Perdana). Modal analysis was performed part by part due to the reasons mentioned in the previous section. It was performed on the natural frequencies and mode shapes of four car panels: trunk, hood, roof and door. A comparison of both computational and experimental modal analysis results showed satisfactory agreement in both frequencies and their corresponding mode shapes except for roof panel.

The first comparison was done on the trunk panel, and the results showed a good agreement as majority modes showed (error less than 9%). However some modes indicate some discrepancies especially the first two modes. In addition, the plots of experimental and computational frequencies of the trunk panel in the same xy plane also showed same agreement. Furthermore, the mode shapes of the panel obtained from experimental and computational methods are also in good agreement.

The second comparison was done on the hood panel for both frequencies and mode shapes. At the frequency level generally the results showed quite acceptable agreement except for the first two modes where they show high difference 68% and 49% respectively. The frequencies of the fourth, fifth and sixth modes are in good agreement (error less than 9%). The remaining frequencies are in reasonable agreement (error less than 33%). In the mode shape level, the results showed similarities at majority of modes.

The third comparison was carried out on the roof panel. Results showed poor agreement at all modes. However, mode shapes still showing some similarities. Finally, results obtained from door panel indicated fair agreement between experimental and computational modal analysis methods. Although the frequency difference percentage is about 30% the mode shape results still showed a good agreement between the two methods,

Generally, it can be concluded that modal analysis part by part is a valid method and can be implemented to determine the dynamic characteristics of any complex structure. The results showed fair agreement between experimental and computational modal analysis. However, still some discrepancies between the experimental and computational results. This could be because of: 1) boundary conditions: wrong boundary conditions can have influence on some or all vibration modes. Therefore, to overcome these problems we keep try other boundary conditions, which could be a further work for this research. 2) linearity between input and output as been noticed from the coherence signals obtained from experimental modal analysis tests for all panels. The results showed that the coherence at low frequencies was far away from one ($\ll 100\%$) which resulted in high error at the first modes. 3) Correspondence between computational model and the real model as the available FE model was not exactly the same as the real model. This can have great effect on the results and must be considered in future research.

7.1.4 Relationship between structural vibration and interior noise discomfort

Noise and vibration quality is among the most important factors that influence the passengers' comfort. The whole passenger cabin (windows, doors, roof, etc.) vibrate and therefore radiate audible sound which can dominate inside the passenger cabin. This is a study case of the importance of the structural vibration analysis of any car component that can be expected to be the source of the interior noise. Therefore, it is an imperative task for automotive manufacturers that firstly, estimate the structural vibration and its effect on the interior noise, and then conduct the appropriate structural modification if needed.

The analysis technique used to achieve this objective was based on signal analysis and modal analysis part by part methods. Signal analysis method was conducted to evaluate the sound pressure level and the transfer functions responses inside the passenger car cabin. The proposed approach (modal analysis part by part) is also applied to the actual car to determine the dynamic characteristics of vehicle components that can be expected to be the source of the interior noise, and the results revealed structural panels that contributed most significantly to the interior noise. The engine and roof cross bean vibrations were found to be the dominant source of interior noise below 200Hz. The first dominating noise peak inside the passenger cabin is mainly caused by the excessive bending mode of the front suspension system at 62 Hz. The second and third dominating noise peaks are mainly resulted from the twisting vibration of the roof cross beam at 163 Hz and 173 Hz. Therefore, cancellation of these components leads to improve the design that would increase comfort and reduce the experienced annoyance from excessive vibrations. Hence, it can be concluded that there is a good relationship between the structural vibration and the interior noise comfort.

Since the results are in line with the literatures as mentioned earlier, this study can be considered a worthy preliminary study for further studies.

7.2 RECOMMENDATION AND FUTURE WORK

The research presented in this thesis provides several interesting directions to be undertaken in the future work. The following are some of these directions:

1. It would be better to have detailed information on the design and materials of the vehicle at hand. This will reduce more the errors.
2. Carry out more modal analysis for other small individual parts of vehicle to confirm the validity of modal analysis part by part method
3. Utilization of signal analysis and modal analysis part by part methods and implementing more vehicles can give deep insights into the structural vibration and its relationship to interior noise comfort.

REFERENCES

Abrams, R. 2008. Formula SAE race car analysis: simulation & testing of engine as a structural member. ATZ *online. Edn*.

Agilent Technologies. 2000. The fundamentals of modal testing. *Application Note* 234-3. U.S.A. 5/00 5954-7957 E.

Allemang, R. J. 1998. An Overview of MIMO-FRF Excitation/Averaging Techniques. *Proceedings, Int Conference on noise and vibration Engineering*, Vol 1, Katholieke Univ Leuven, Belgium, 12 pp.

Allemang. R.J.Vibrations 111. 1999. Experimental Modal Analysis. *UC-SDRL Class Notes*

Allen, R.E. 1975. Limits of Ride Quality through cab isolation. *SAE Paper* No 750165.

Atmosphere and life Bureau of the Ministry of Environment. 2000 Measurement Manual for low frequency Noise.Issued on October 2000 Japan.

Avitable. P. 1998. Is there any difference between a modal test with shaker excitation and impact excitation?. *Society of Experimental Techniques*

Avitable. P. 1998. Which shake excitation is best?. Is there any difference?. *Society of Experimental Techniques*

Avitable. P. 1999. I still Don't Understand Curve fitting?. How do you get Mode Shapes from FRF?. *Society of Experimental Techniques.*

Avitable. P. 2001. Experimental Analysis: A simple non mathematical presentation. *Sound & Vibration Magazine*.

Avitable. P. 2002. Is there any real advantage to MIMO testing?, Why not just use SISO and then move the shaker?. *Society of Experimental Techniques.*

Bathe, K.J. 1996. *Finite Element Procedures in Engineering Analysis.* Prentice Hall.

Binchao Li Qiancheng Zhang &Tianjian Lul. 2008. Dynamic performance of truss core sandwich structures based on modal analysis experiments. *Chinese Journal of Solid Mechanics.2008-* 04.

Birtitta. B & Peter. H. 1996. Sources and effects of low frequency noise. *J. Acoust. Soc. Am.* 99 (5):2985-3002.

Bram De Kraker. 2000. A numerical-experimental approach in structural dynamics. *Class Notes.*

Brian, J., S. & Mark, R. 1999. Experimental modal Aanalysis. *Vibrant Technology. Inc. Jamestown. California*

Brian, J., S & Mark. R. 2006. Using FEA Modes to scale Experimental Mode Shapes. Presented at IMAC XXIV January, 2006.*Vibrant Technology.Inc. Jamestown. California*

Broner, N. Leventhall, H.G. 1984. The annoyance and unacceptablity of lower level low frequency noise. *Journal of Low Frequency Noise and Vibration.* 3(4): 154-166.

Brown, D, Carbon, & Ramsey, K. 1977. Survey of excitation techniques applicable to automotive structures. *Society of Automotive Engineers*. No 770029.

Bruel & Kjaer. 2006. Modal Excitation – Theory: Background and Concept http://www.bksv.com/default.

Brüel & Kjær. 2010. Operating deflection shapes analysis. *www.bksv.com/products/.../operatingdeflectionshapesanalysis.aspx*

Brughman. M, F.Lembregts & Furini. F. 1995. Modal test on the pininfarina concept car body. Ethos 1. MSC. World User' *Conf. Proc.*

Brughman. M, Leuridan. J. & Blauwkamp K. 1993. The application of FEM-EMA correlation and validation techniques on a body-in-white. MSC World Users'*Conf. Proc.,*IMAC XI. February 1-4, 1993 Florida

Buller;. 2008. High noise levels and noise indoor. *National Board of Health and Welfare.* ISBN 978-91-85999-30-9. (translated)

Cantley, C. 2003. Modal testing facility for advanced LIGO. *University of Glasgow, Advanced LIGO SUS Workshop*, LIGO-G 030534-00-K, Caltech.

Carlos, A. 2006. Robust bird-strike modeling using LS-DYNA. *Master Thesis. University of Puerto Rico. Mayaguez Campus.*

Chandrupatla, T.R. & Belegundu, A.D. 1997. *Introduction to Finite Elements in Engineering (3rdEd).* New Jersey Prentice Hall.

Chavan, D.S., Mahale, A.K., and Thakur, A.G. 2013. Modal Analysis of Power Take Off Gearbox. *Int. J of Emerging Technology and Advanced Engineering*. 3(1): 70-76.

Chowdhury, S. 1999. Damping characteristics of reinforced and partially prestressed concrete beams. *PhD. Thesis, Griffith Univ. QLD, Australia.*

Cloutier, P. Avitabile. Shaker/Stinger Effects on Measured FRFs. Structural Dynamic and Acoustic Systems. *University of Massachusetts Lowell. Orlando, Florida.*

Constant, M., Leyssens, J., Penne, F. & Freymann, R. 2001. Tire and Car Contribution and Interaction to low frequency Interior Noise. *Proceedings of the Noise and Vibration Conference, SAE* 2001-01-1528.

Cook, R.D. 1989. *Concepts and Application of Finite Element Analysis.* 3rd ed., New York: John Wiley & Sons.

Cooley, J.W. & Tukey, J.W.1965. An algorithm for the machines calculation of complex fourier series. *Mathematics of Computation*. 19(90): 297-311.

Corbridge, C. & Griffin, M.J.1986. Vibration and comfort: vertical and lateral motion in the range 0.5 to 5.0 Hz. *Ergonomics. 29(2)*: 249-272.

Corbridge, C. & Griffin, M.J. 1991. Effects of vertical vibration on passenger activities:writing and drinking. *Ergonomics.* 34(10):1313-1332.

Corelli, D & Brown D. L. 1984. Impact testing considerations. *proceedings of the* 2nd *Internati Modal Analysis Conference.(IMACII)Florida*, pp 735-742.

Cremona, C. 2004. Dynamic monitoring applied to the detection of structural modifications: A high-speed railway bridge study. *Journal of Eng & Mater*, 6(3):147-161.

Daniel, J. Inman. 2001. *Engineering vibration*. New Jersey *Prentice-Hall International, Inc.*

Dave Corelli. & David L. Brown. 1984. Impact Testing Considerations. *Proceedings of the 2nd International Modal Analysis Conference.*

David, F & Barian, M. 1999. The exponential window. *Sage Technologies Morgan.* Hill.*CA Sound & Vibration*. MacMillan.

DEFRA. 2001. Low frequency noise. *(Department for Environment, Food Rural Afairs) Noise programme. Northern Ireland Scottish Executive, National Assembly for Wales.*

Demic, M., Lukic, J. & Milic, Z. 2002. Some aspect of the investigation of random vibration influence on ride comfort. *Journal of Sound and Vibration*. 253(1):109-129.

Dempsey, T.K., Leatherwood, J.D. & Clevenson, S.A. 1979. Development of noise and vibration ride comfort criteria. *Journal of Acoustical Society of America* 65(1):124- 132.

Dihua Guan, Xiindong & Fang. Z. 2006. Sensitivity analysis of brake squeal tendency to substructures modal parameters. *Journal of Sound & Vibration*. 291(1-2): 72-80.

Donati. P, Grosjean. A, Mistrot. P & Roure. L. 1983. The subjective equivalence of sinusoidal and random whole-body vibration in the sitting position. *Ergonomics*. 26(3):251- 273.

Donders. S, Takahashi. Y, Hadjit.R, Van.T, Brughmans.T & Desmet. W. 2009. A reduced beam and joint concept modeling approach to optimize global vehicle body dynamics. *Finite Elements in Analysis & Design.* 45: 439-455.

Dossing, O. 1988. Structural testing. Part I: Mechanical Mobility Measurements. *Bruel & Kjaer. Technical Note BR*. 0458-12.

ENDEVCO. 2000. Guide to adhesively mounting accelerometers. *Technical paper.*

Ewins, D. J. 1984. Modal: *Theory and Practice*. New York: Research Studies Press.

Ewins, D. J.2000. *Modal Testing: Theory Practice and Application*. Baldock. 2nd Edn. UK. *Research Studies Press.*

Fairley, T.E. and Griffin, M.J. 1988. Predicting the discomfort caused by simultaneous vertical and fore-and-aft whole-body vibration. *Journal of Sound &Vibration* 124(1): 141-156.

Farina, A. & Bozzoli, F. 2002. Measurement of the speech intelligibility inside cars. Presented at the 113th *Convention of the Audio Engineering Society*, California, USA.

Feng, Z., Wang, X & Sun, F. 1991. Experimental modal analysis for bending vibration of automobile power trains. Seoul, Korea*: Korean SAE*, pp. 1031-1034.

Formenti, D. & Richardson, M. H. 1985. Global curve fitting of frequency response measurements using the rational Fraction polynomial method. 3rd *International Modal Analysis Conference*, Orlando, FL.

Formenti, D. & Richardson, M. H. 1986. Global frequency and damping from frequency response measurements. 4th *International Modal Analysis Conference*. Los Angeles.

Friswell, M. I 1995. Finite element model updating in structural dynamics. *Netherlands Boston Kluwer academic Publishers*.

George F. L & Dave, S. 2001. Understanding the physics of electrodynamic Shaker Performance. *Sound and Vibration*, Data Physics Corporation, San Jose, California.

Cenuit, K. 2004. The sound quality of vehicle interior noise: a challenge for the NVH-engineers. *International Jornal of Vehicle Noise and Vibration* 1(1-2):158-168.

Gillespie, T.D. & Karamihas, S.M. 2000. Simplified models for truck dynamic response response to road input. Heavy Vehicle Systems. *International Journal. of Vehicle Design*.7(1): 52-63.

Goldman, D.E.1948. A review of subjective responses to vibratory motion of the human human body in the frequency range 1 to 70 cycles per second. *Naval Medical Research Institute Report* No 1.

Graham, S. Kelly, 2000. Fundamentals of mechanical vibrations. *2nd Edn, McGRAW-Hill Education.*

Guan, D., Su, X. and Zhang, F. 2006. Sensitivity analysis of brake squeal tendency to substructures modal parameters. *Journal of Sound and Vibration*. 291:72–80.

Guinchard, M. 2007. Experimental modal analysis of the CMS Tracker Outer Barrel (TOB). CERN, Geneva, Switzerland, *Technical Note:* TS-001.

Gupta A.D.1999. Evaluation of a fully assembled armored vehicle hull-turret model using computational and experimental modal analyses. *Computers and Structures.* 72:177-183.

Hastings, J, Juds, M.A & Brauer, J.R. 1985. Accuracy and economy of finite element analysis. 33rd *Annual National Relay Conference*.

He, H & Fu, Z. 2001. Modal analysis. *Great Britain Butterworth – Heinemann publishers.*

Herlufsen, H. Modal analysis using multi-reference and multiple-input multiple- output techniques. *Bruel & Kjaer Application note* BO 0505-12.

Herlufsen, H. 1984. Dual channel FFT analysis: Part 1 & 2 *Bruel & Kjaer*. *Technical Review No*. 1 & 2 BV 0014-11.

Herlufsen, H. & Moller, N. Operational analysis of a wind turbine wing using acoustical excitation. *Bruel & Kjaer Application Note* BO 0500-11.

Hewlett-Packard Co, 1986.The fundamentals of modal testing: application note 243-3.

Hieronimus, K. 1977. A Few aspects on the development of structural models. *SAE Technical Paper* 770598.

Hiroaki. H. Sakurai, T. &Takahashi, K. 2003. Vibration reduction in the cabins of heavy-duty trucks using the theory of load transfer paths. *JSAE*. Review. 24 (2):165-171.

Hiroshi,K.,Mnoru,O and Tohru, Y. 1990. Analysis of noise sources and their transfer paths in Diesel Engines. *SAE*: Warrendale, PA. 99(3): 34-41.

Hurlebaus, S, Stobener, U & Gaul, L. 2008. Vibration reduction of curved panels by active modal control. *Journal of Computer & Structures*. 86 (3-4):251-257.

Huseyin Kaya. 2004. Experimental Modal Analysis of a steel Grid Frame. Master Thesis. *Middle East Technical University.*

Irvine, T. 1999. The steady-state response of a single-degree-of-freedom system subjected to a harmonic Force. *Vibrationdata.com* Publications. Murry.

Ishiyama, T. & Hashimoto, T. 2000. An impact of sound quality on Annoyance caused by road traffic noise: An influence of frequency spectra on annoyance. *Journal of Society of Automotive Engineers of Japan* 31(1): 35-39

Jacobsen, N.J. & Hensen, T.F. 2007. *Bruel & K*jaer Seminar on transducer and analyzers for Vibration measurement and analysis, Shah Alam, Malaysia.

Jae-Yeol, Park, & Rajaendra Singh. 2010. Role of spectrally varying mount properties in influencing coupling between powertrain motions under torque excitation. *Journal of Sound & Vibration.* 329 (14): 2895-2914.

Jeong & Singh. 2000. Analytical methods of decoupling the automotive engine torque roll axis. *Journal of Sound and Vibration* 234: 85–114.

Jia-Jang. Wu. 2004. Finite element modeling and experimental modal testing of a three-dimensional framework. *International Journal of Mechanical Sciences* 46: 1245-1266.

Jiang .S.J, Gu, S.N, Wang. Y.J & Yao,Q.H. 1990. A modal parameter identification technique and its application to large complex structures with multiple steady sinusoidal excitations. *Journal of Sound and Vibration*. 138 (2): 221-231.

Jinchun, H. Charles, M.K. &Anil, K.B. 2006. Modeling of automotive drum brakes for squeal and parameter sensitivity analysis. *Journal of Sound & Vibration*. 289(1-2): 245-263.

Jin Y-M. 2000. Analysis and evaluation of minivan body structure. *Proceedings of 2nd MSC worldwide automotive conference,* MSC, 2000.

Johansson. I. & Gustavsson. M. 2000. FE-based vehicle analysis of heavy trucks, Part I: Methods & Models, Proceedings of 2nd MSC. *Worldwide Automotive Conference*, MSC, 2000 Sweden.

Kaewunruen, S & Remennikov, A. M. 2005. Application of Experimental Modal Testing for Estimating Dynamic Properties of Structural Components, *ASEC, Newcastle, Australia,* 11-14 September, [CD ROM].

Kassahun M. 2008. Static and dynamic analysis of a commercial vehicle with van body. University thesis. *Addis Ababa University.*

Kirby, R.A. 2009. Comparison between analytic and numerical methods for modeling automotive silencers with mean flow. *Journal of Sound and Vibration*. 325(3): 565-582.

Kohoutek, R. 1995. Non-destructive and ultimate testing of semi-rigid connections. *Procs of AISC Connections IV*. pp 454-463.

Kung, L.E. Soedel, W. &Yang, T.Y . 1986. On the dynamic response at the wheel axle of a pneumatic tire. J*ournal Sound & Vibration.* 107(2): 195-213.

Lan, J. Chen. & Lin, J. 2004. Comparative analysis for bus side structures and lightweight optimization. *Journal of Automobile Engineering.* 218(10):1067-1075. Part D.

Lee, R.A. & Pradko, F. 1968. Analytical Analysis of Human vibration. *SAE* Paper No. 680091.

Lee, S.K, Kim, B.S., Chae, H.C., Park, D.C. & Jung, S.G. 2005. Sound quality analysis of a passenger car based on rumbling index. *SAE Paper* 2005-01-2481.

Leib, N.S. Nacivet & Thouverez, F. 2010. Experimental and numerical study of a vibro-impact phenomenon in a gearshift cable. *Journal of Sound and Vibration.* 329(3): 289-301.

Leventhall, G. 2004. Low frequency noise and annoyance. *Noise & Health. A Bimonthly Inter-disciplinary Int. J*. 6(23):59-72.

Leventhall, G. 2007. What is infrasound? 2007 Jan-Apr,93(1-3):130 -137. Epub 2006 Aug 4.

Li, S.B., X. Q. Guan, T. L. Lu & Zhang, J.W. 2008. Vehicle modeling with the exhaust system and experimental validation to investigate the exhaust vertical vibration characteristics excited by road surface inputs. *International Journal of Automotive Technology.* 9(4): 483-491.

Liu, P.L. 1999. Identification and damage detection of trusses using modal data. J*ournal of Structure Eng.* 121(4):599-608.

Lopez, I. Rooyaker, W., Vijgen & Nijmeijer, H. 2004:120. Traineeship Report. M.L.J. Verhees. Experimental Modal Analysis of a turbine blade. Eindhoven. .

Mark, H.R. 1997. Is it a mode shape, or an operating deflection shape?. *Sound & Vibration Magazine.* 30th Anniversary Issue.

Mathews, J. (no date). Guide to Accelerometer Installation. *ENDEVCO Technical Paper* No 319.

Mohd Hosseini Foladi.2006. PHD thesis. Faculty of Engineering Universiti Kebangsaa Malaysia.

Mohd, Nor, M,J., Nahvi, H. & Hosseini Foladi, M. 2006. Evaluation of acoustical and vibration comfort indicators inside a passenger car. *Proceedings of the 8th International Symposium of transport Noise and Vibration,* St. Petersburg, Rassia.

Nahvi, H., Mohd. Nor, MJ., Hosseini F, M. & Shahrum Abdullah. 2006. Evaluating automobile road vibrations using BS6841 and ISO2631 comfort criteria. *Proce -edings of the 1st Regional Conference on Vehicle Engineering & technology: RTVET06*, Putra World Trade Centre, Malaysia

National Crash Analysis Centre (NCAC). 2009. www.ncac.gwu.edu. National Instruments. Modal Parameter Extraction. Lab VIEW Vis.

Pandit, S & Jacobson, E. 1988. Data dependent systems approach to modal analysis, Part II:Application to structural modification of a disc-brake rotor. *Journal of Sound & Vibration.* 122(3): 423-432.

Park & Singh. 2008. Effect of non proportional damping on the torque roll axis decoupling of an engine mounting system, *Journal of Sound and Vibration* 313: 841–857.

Persson Waye K, Rylander R, Benton S& Leventhall H G.1997. Effects on performance performance and work quality due to low frequency ventilation noise. *Journal of Sound and Vibration.* 205: 467-474.

Persson Waye K, Bengtsson J, Kjellberg A & Benton S. 2001. Low frequency noise “pollution” interferes with performance. *Noise and Health.* 4:33-49.

Peter Avitabile. Modal Analysis and Controls Laboratory. Mechanical Engineering Department University of Massachusetts Lowell, Massachusetts USA.

Peter. Avitabile. Modal space back to basics. SEM Experimental Techniques.

Peter. Avitabile. 2001. Basics Spectrum Analysis/Measurements and the FFT Analyzer. University of Massachusetts Lowell. Mechanical Engineering – 22.403 Mechanical Lab II. Spectrum Analysis 082702-1.

Poulson , T. 2003. Annoyance of low frequency noise (LFN) in the laboratory assessed by LFN- Sufferers and non-suffers. *Journal of Low Frequency Noise, Vibration and Active Control*. 22(4):191-201.

Pradko, F. 1965. Human Response to random vibration. *Shock and Vibration Buletin, US Naval Research Institute*, WA, Vol. 34(4).

Pradko, F. and Lee, R.A. 1966. Vibration Comfort criteria. *SAE* paper 660139.

Pradko, F., Lee, R.A.,& Kaluza, V. 1966. Theory of Human Vibration Response. ASME *Paper* No. 66WA/BHF-15.

Ralph D, Gary A, R & Ferdinand, W. 2000. Finite element model development and validation for aircraft fuselarge structures. 18th *International Modal Analysis. Conference* San Antonio, Texas February 7-10, 2000.

Repik, E.P. 2003, Historical perspective on vehicle interior noise development. *SAE Paper* 2003-01-1518, Noise and Vibration Conference and Exhibition, Traverse City, Michigan, USA

Richardson, M. H. 1975. Modal analysis using digital test systems. Seminar on Understanding Digital Control and Analysis in Vibration Test Systems, Shock and Vibration Information Center Publication, *Naval Research Laboratory*, Washington.

Robert K.Otnes & Loren D Encochson. 1972. Digital time series analysis. *Wiley, New York.*

Salane, H.J & Baldwin, J. W. 1990. Identification of modal properties of bridges. *ASCE Journal of Structure Eng.* 116 (7): 2008-2021

Salzmann, A. 2002. Damping characteristics of reinforced and prestressed normal- and high strength concrete beams. Ph.D. Thesis, *Griffith Univ.*, QLD, Australia.

Schemitz, Lopez, A & Nijmeijer. 2005:112. Experimental modal analysis of the tyre measurement tower. DCT . *University Eindhoven*.

Schwarz.B & Richardson. M. Using FEA Modes to Scale Experimental Mode Shapes. Vibrant Technology, *Inc.Scotts Valley, California.* Presented at *IMAC XXIV.* January 2006.

Schrijver P.A.R. 2005. Experimental modal analysis of the tyre measuremen tower. DCT 2005.112, *Eindhoven*.

Soliman, A. M.A., Abd Allah, S.A., El-Beter, A. A. & Hamid, M.S. 2001. Effect of suspension spring stiffness on vehicle dynamics. Heavy Vehicle System. *In. J. of Vehicle Design.* 8(3/4): 316-334.

Souza, M. A & Assaid, L. M.B. 1991. A new technique for the prediction of buckling loads from nondestructive vibration tests. *International Journal of Exper Mech.* 31(2): 93-97.

Sparfum Electronics. 2006. View topic- charge amplifier. http://64.106.253.12. *Technical Paper*.

Stone, M.R. & Demetriou, M.A. 2000. Modeling and simulation of vehicle ride and handling performance. *Proceedings of the 15th IEEE International Symposium on Intelligent Control*, Rio, Patras, Greece.

Sung, M-H. 1991. Effective methods for interior noise reduction of a passenger car. *Proceedings of the 6th International Pacific Conference on Automotive Engineering*, Seoul, Korea: Korean Society of Automotive Engineers, Inc., pp. 553-559.

Taylor, R. 1971. *Noise*. Penguin Books Ltd., ISBN-10:0140212337.

Technoblogger, 2009. Mounted resonant frequency of an accelerometer. *Zimbio – Interactive Magzine.*

Teo H, F & Roslan Abd. Rahman. 2007. Statics and dynamics structural analysis of a 4.5 Truck Chassis. *Journal. Mekanikal*. 24: 56-67.

The Modal Shop Modal Shaker – 2100 E11 - 100 lbf. Electrodynamic Exciter and Accessory Kit, Inc.http://www.modalshop.com/test_tmproducts.asp?ID=164

Thomas, R.S., Stanecki, P.J. & Creutz H.P. 1991. A development process to improve vehicle sound quality. *SAE Paper* 911079.

Vander Auweraer, H. 2004. SCORES Workshop. LMS International, Leuven.

Van Deusen, B.D. 1968. Human Response to vehicle vibration. *SAE Paper* No 680090.

Vasconcellos. N, dos Anjos & Argentino. M. 2003. Structural analysis of an exhaust system for heavy trucks. *Debis humaita IT Services* Latin America, Brazil.

Verboven, P. Parloo, E. Cauberghe, B. & Guillaume, P. 2005. Improved modal parameter estimation for lowly damped systems using nonparametric exponential windowing techniques. *Mech. Sys.& Signal Processing.* 19(4): 675-699.

Verboven, P. Guillaume, P. Vanlanduit, S. & Cauberghe. B. 2006. Assessment of nonlinear distortions in modal testing and analysis of vibrating automotive structures. *Journal of Sound and Vibration*. 293 (1-2): 299-319.

Verhees. M.L.J. DCT 2004:120. Experimental Modal Analysis of a turbine Blade. Traineeship report. Eindhoven, December, 2004.

Vibrant Technology. 2005. Introduction to modal curve fitting. *Note #13.* www.vibetech.com.

Vold, H. & Rocklin, G.T. 1982. The numerical implementation of a multi-input estimation method for mini-Computers. *1st International Modal Analysis Conference.* Orlando, FL.

Von Eldik Thieme, H.C. 1961. Passenger Riding Comfort Criteria and Methods of Analysing Ride and Vibration Data. *SAE Paper* No. 610173.

Walter. E & White. J.A. 1994. Transfer Function Techniques for Automotive Interior Interior noise due to the induction system. *PoughKeepsie, NY: Institute of Noise Noise Control Engneering,* pp.123-127.

Werner, D. 1990. Parameter identification for noise prediction in car structures. *SAE,* Warren dale, PA, USA. P1-6.

Wong, J.Y. & Gillespie, T.D.1992. Fundamentals of Vehicle Dynamics" *SAE,*.

Yasar, D. Wolfram, L & Peter, S. 2005. Coupled use of FEA and EMA for the investigation of dynamic behaviour of an injection pump. *World Congress* 2005, Malta.

Ying, C.L., Bor, T.W., Yi, S.L., Chang, L.Y. & Rong, S.C. 2008. Finite element model verification for packaged printed circuit board by experimental modal analysis. *J. Microelectronics Reliability* 48 (2008) 1837-1846.

Zahir Hanouf & Waleed, F. Faris. 2009. Investigation into noise problems in vehicle structure using vibro-acoustic approach. *Int. Journal. Vehicle Noise & Vibratio.* 5(3):238-260.

Zhanwang. Y & Chen. Z. 2000. Dynamic response analysis of minicar changan Star 6350. *Changan Automobile Groupe.*

Ziaei, S.R. 2005. Finite element, modal testing and modal analysis of a radial Flowimpeller. *Iranian Journal of Science & Technology,* Transaction B, Engineering. 29(B2).

APPENDIX A

COMPUTATIONAL AND EXPERIMENTAL MODE SHAPES OF PANELS

a) Computational mode shapes

1. Mode shapes of Trunk Panel

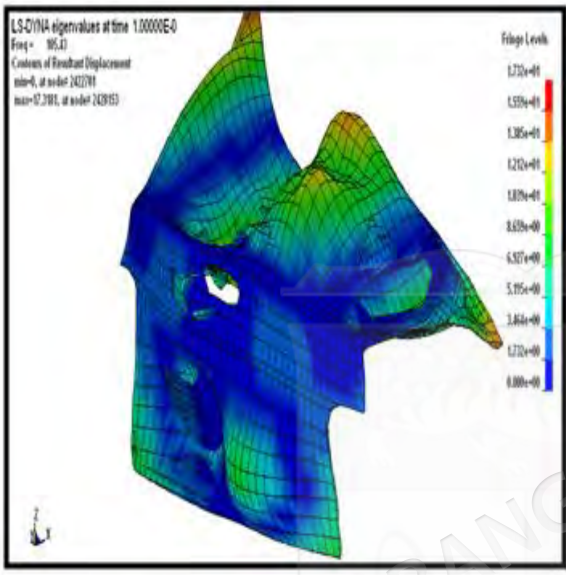

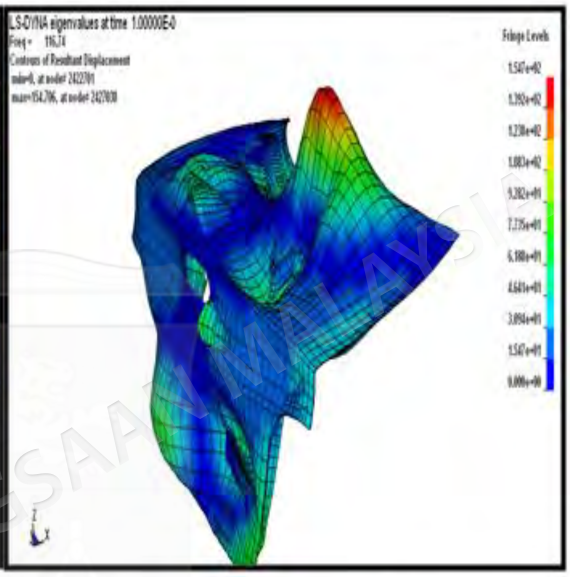

7th mode shape@ 105.43Hz

8th mode shape@ 116.74Hz

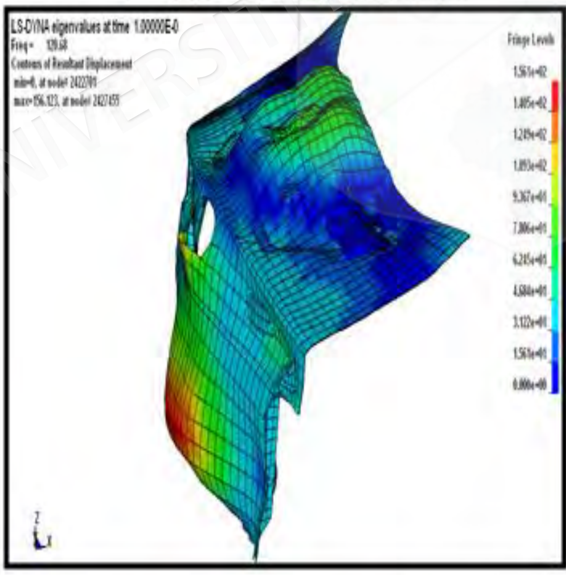

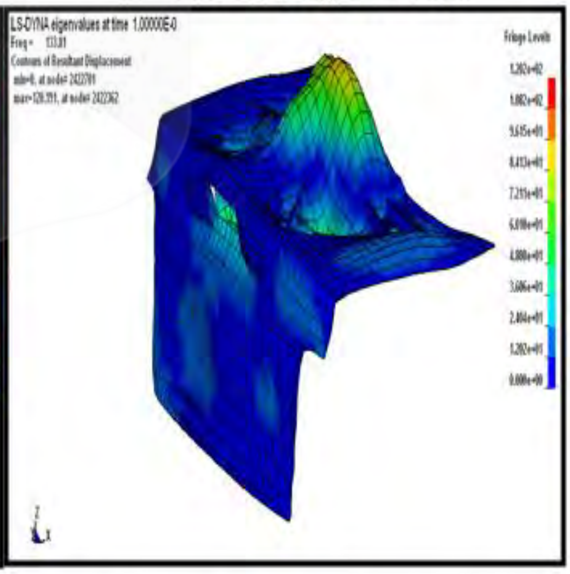

9th mode shape@ 120.68Hz

10th mode shape@ 133.81Hz

2. Mode shapes of Hood panel

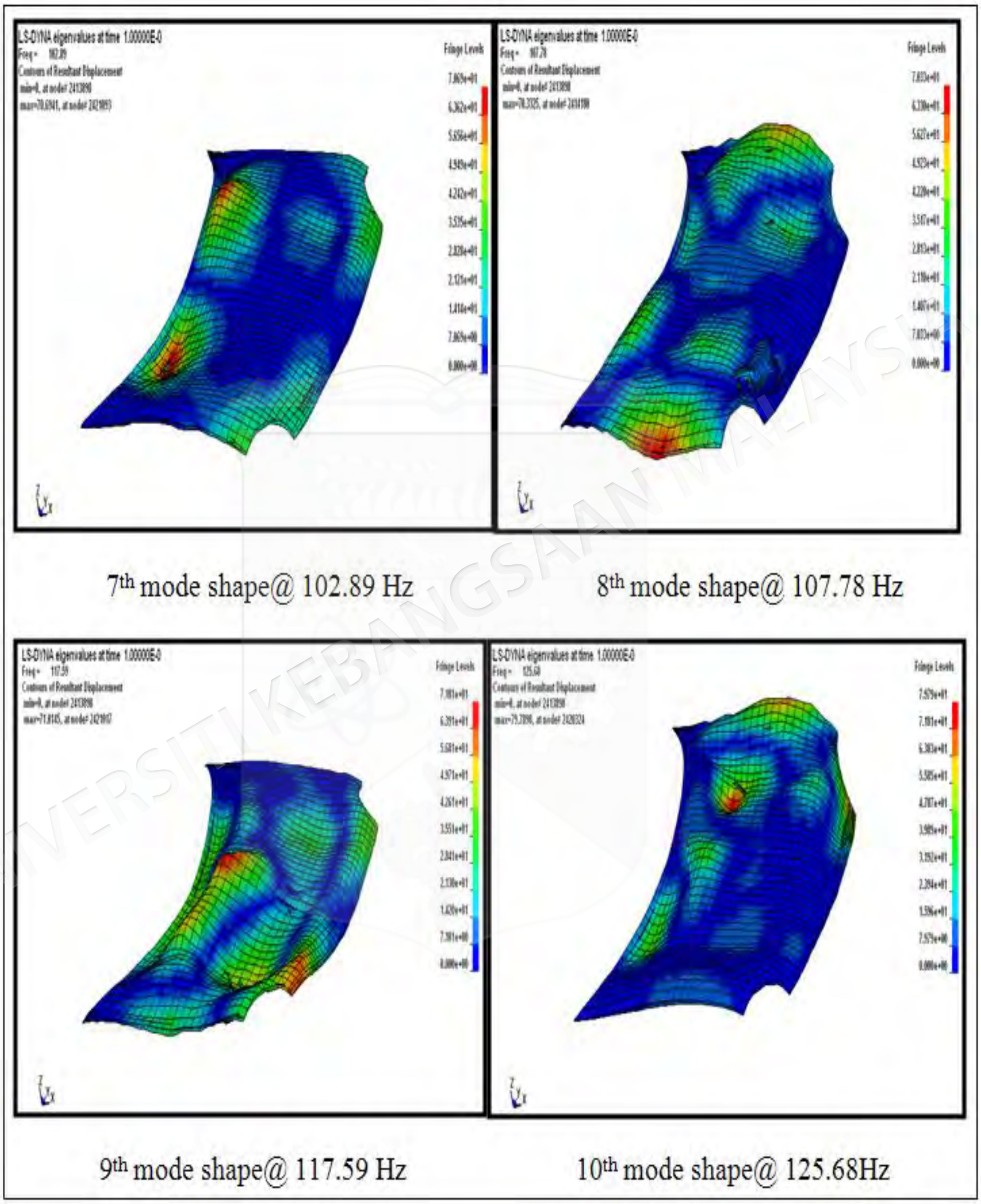

7th mode shape@ 102.89 Hz

8th mode shape@ 107.78 Hz

9th mode shape@ 117.59 Hz

10th mode shape@ 125.68Hz

3. Mode shapes of Roof panel

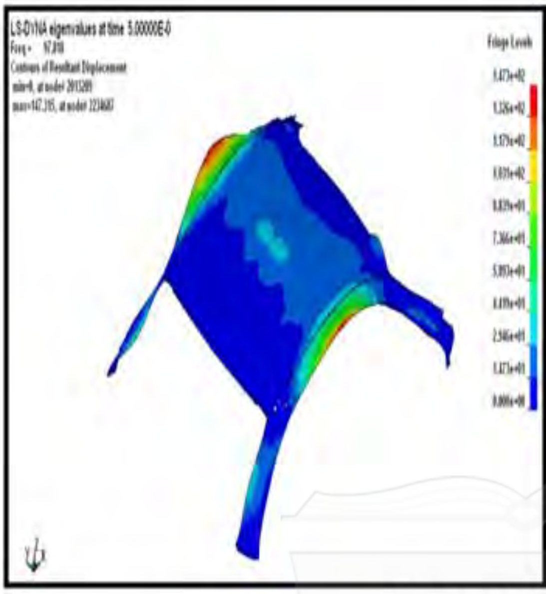

7^{th} mode shape@ 97.81 Hz

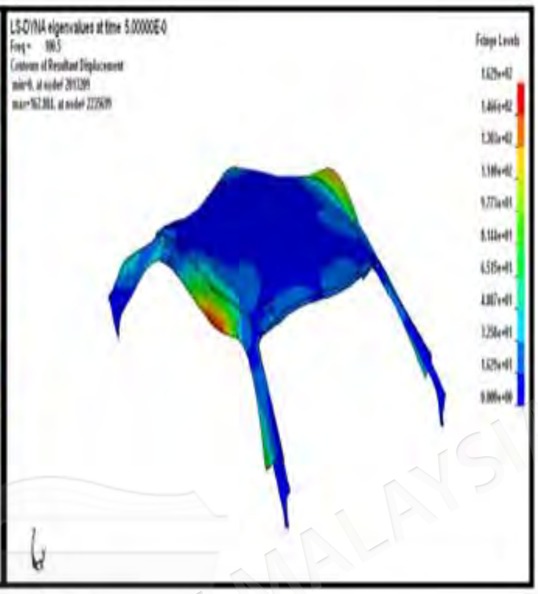

8^{th} mode shape@ 100.5 Hz

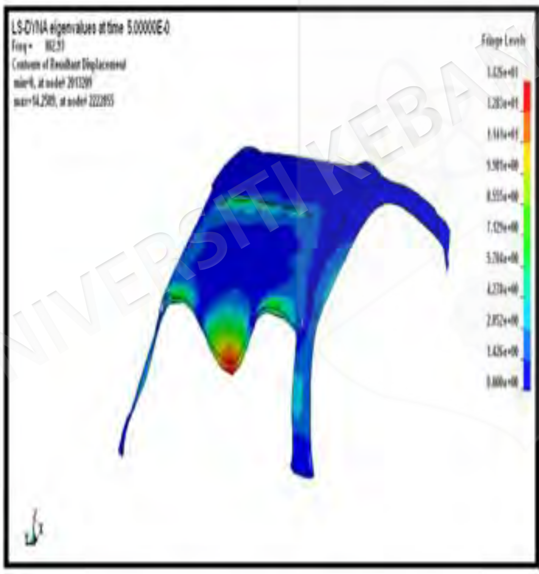

9^{th} mode shape@ 102.93Hz

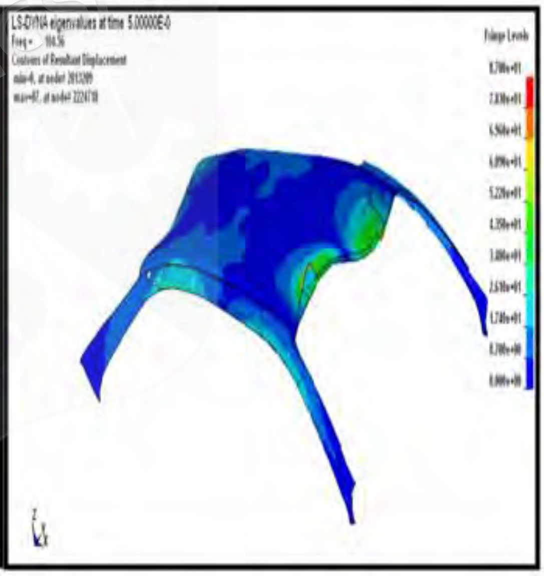

10^{th} mode shape@ 104.56Hz

4. Mode shape of Door panel

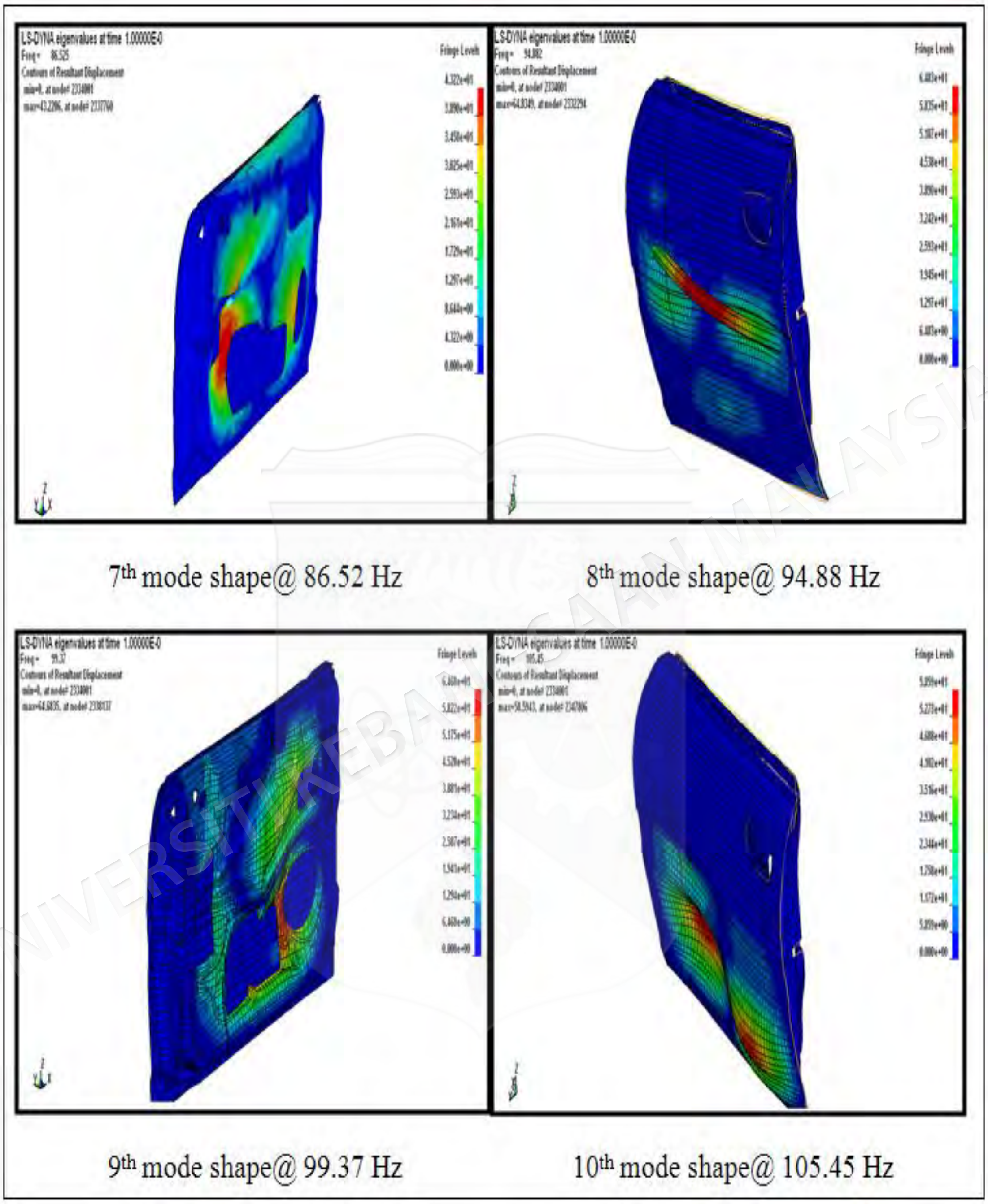

7th mode shape@ 86.52 Hz

8th mode shape@ 94.88 Hz

9th mode shape@ 99.37 Hz

10th mode shape@ 105.45 Hz

5. Mode shapes of Floor panel

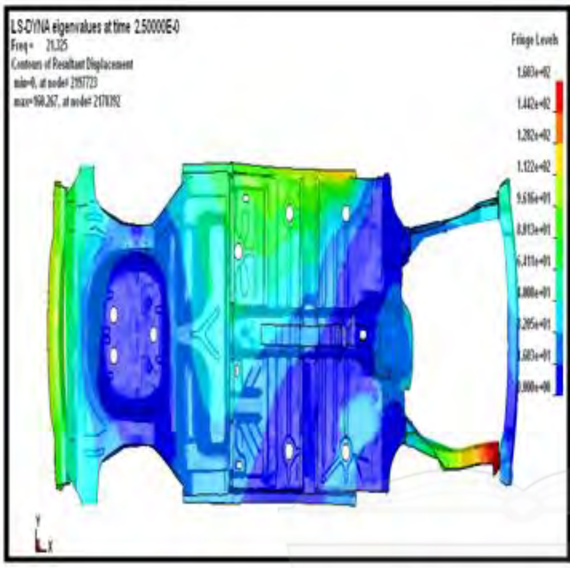

7th mode shape@ 21.32 Hz

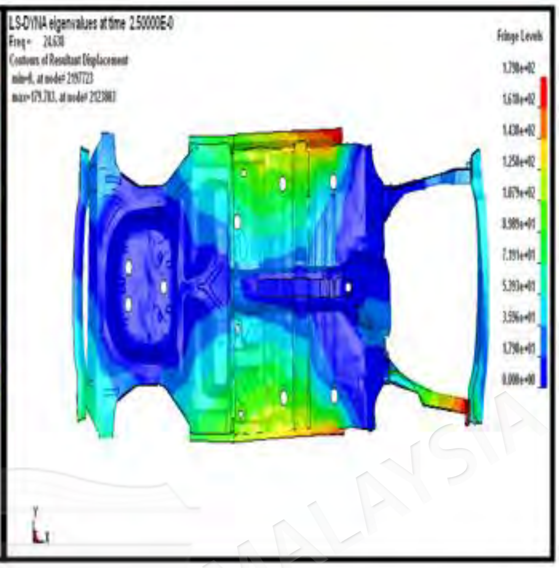

8th mode shape@ 24.63 Hz

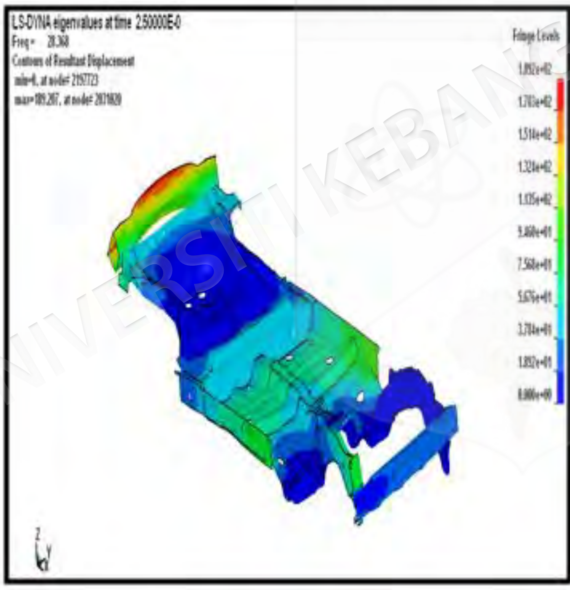

9th mode shape@ 28.36 Hz

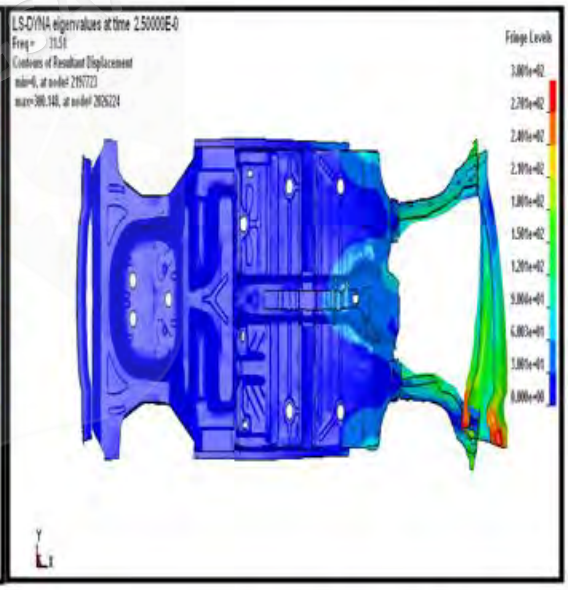

10th mode shape@ 31.51 Hz

b) Experimental mode shapes

1. **Mode shapes of Trunk panel**

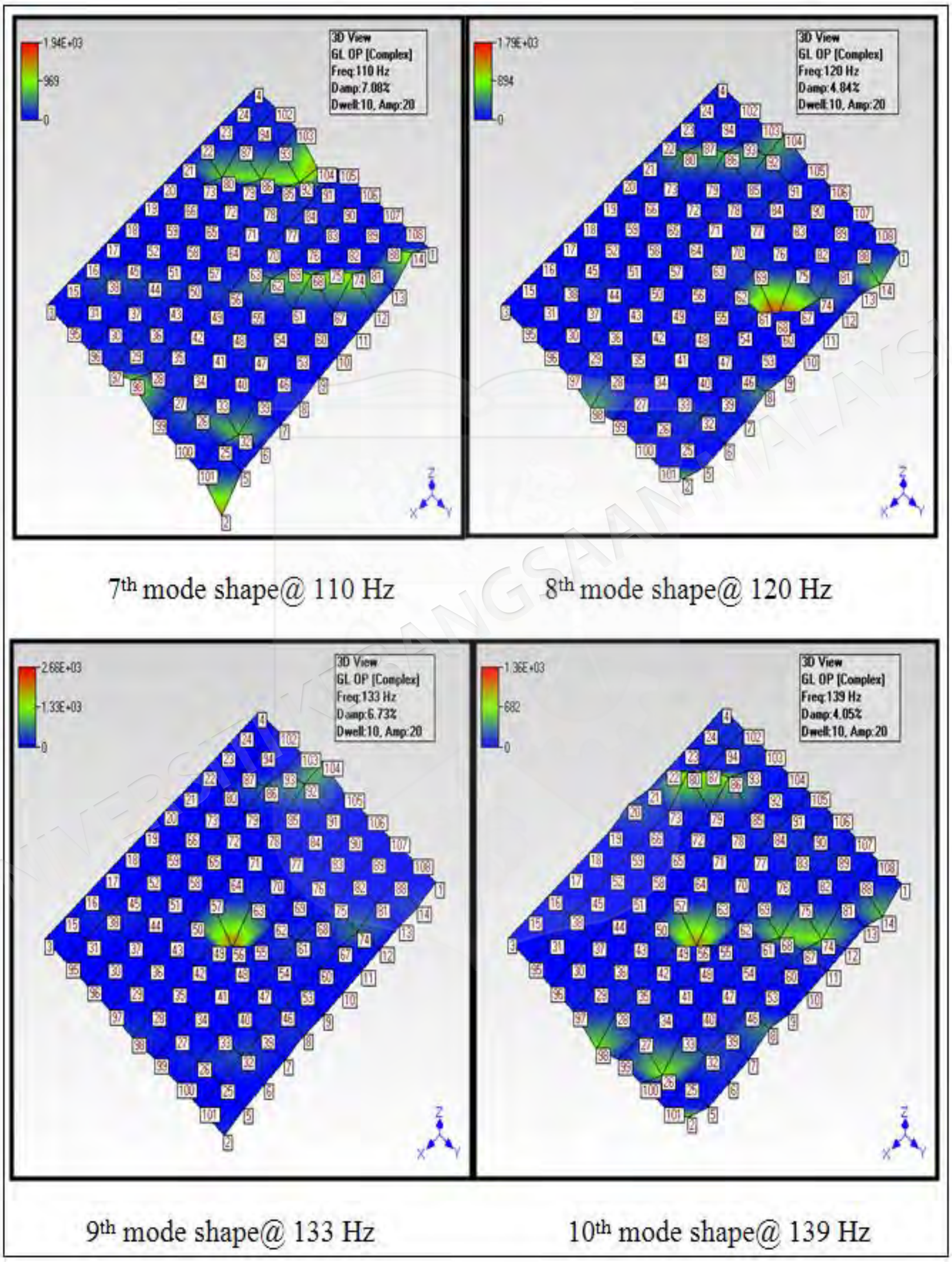

7th mode shape@ 110 Hz

8th mode shape@ 120 Hz

9th mode shape@ 133 Hz

10th mode shape@ 139 Hz

2. Mode shapes of Hood panel

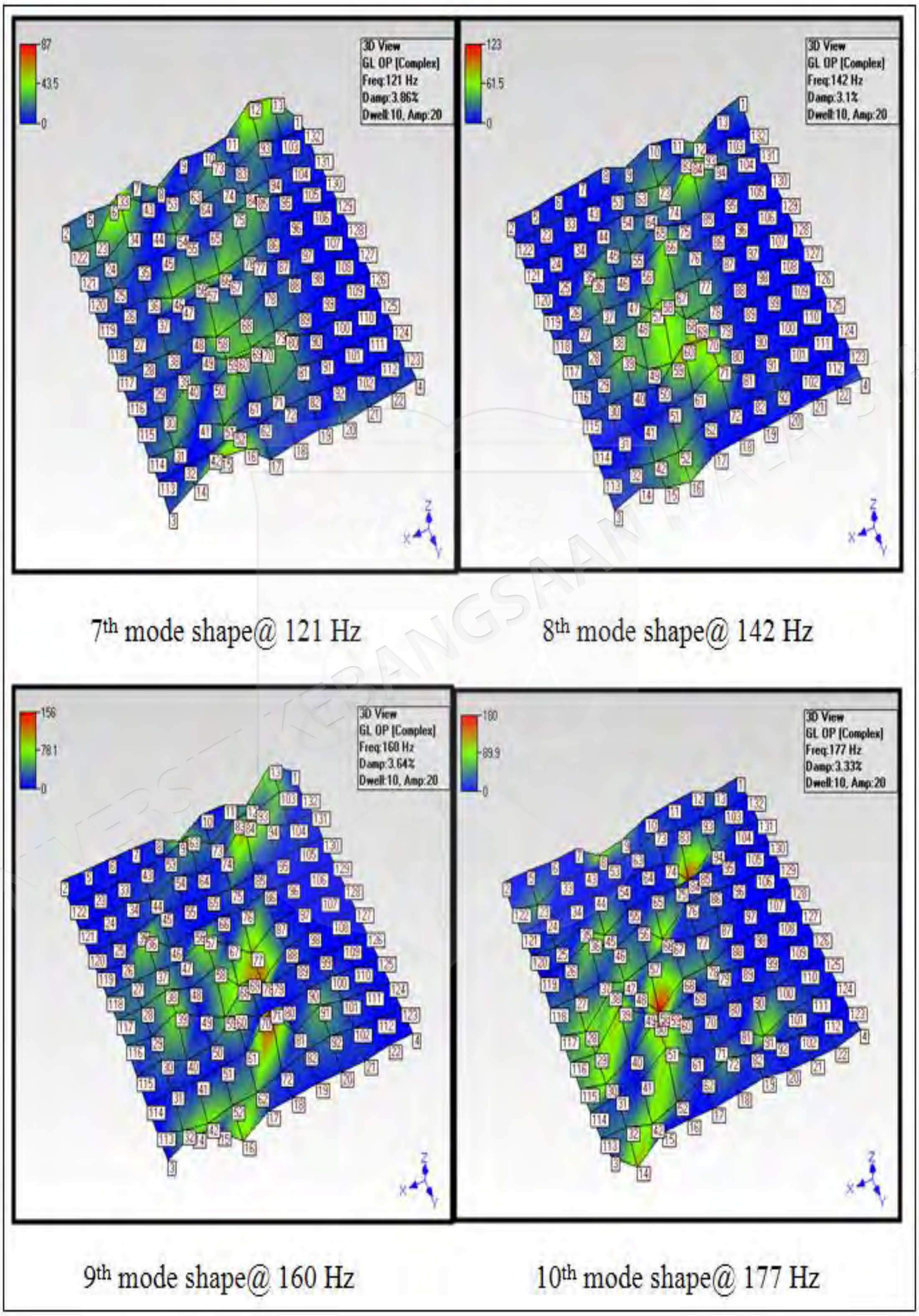

7th mode shape@ 121 Hz

8th mode shape@ 142 Hz

9th mode shape@ 160 Hz

10th mode shape@ 177 Hz

3. Mode shapes of Roof panel

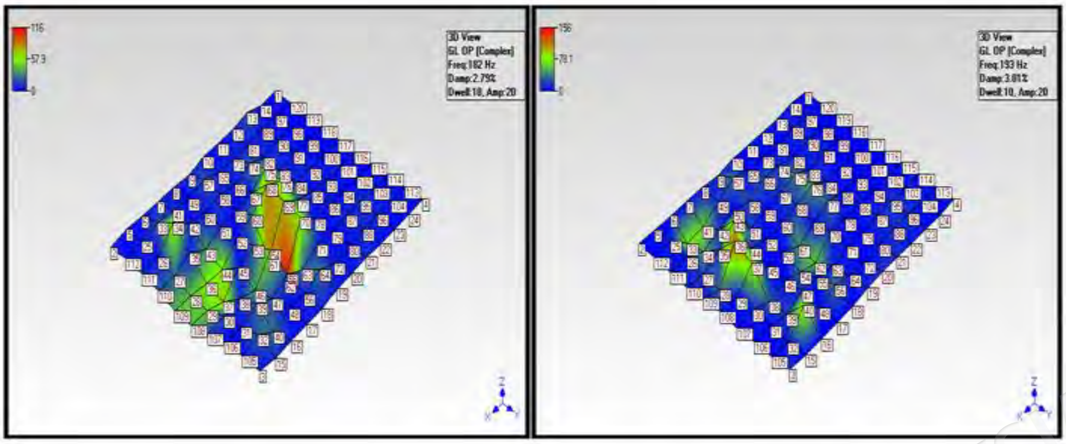

7th mode shape@ 182 Hz   8th mode shape@ 193 Hz

4. Mode shapes of Door panel

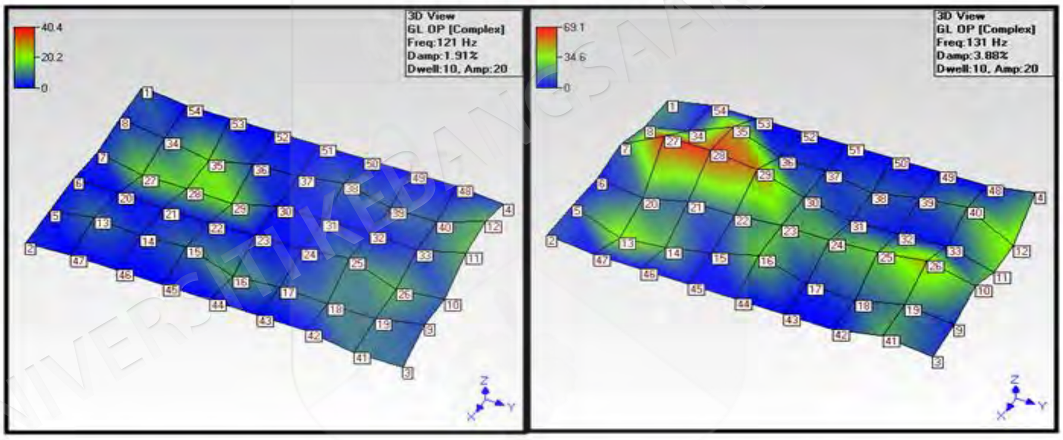

7th mode shape@ 121 Hz   8th mode shape@ 131 Hz

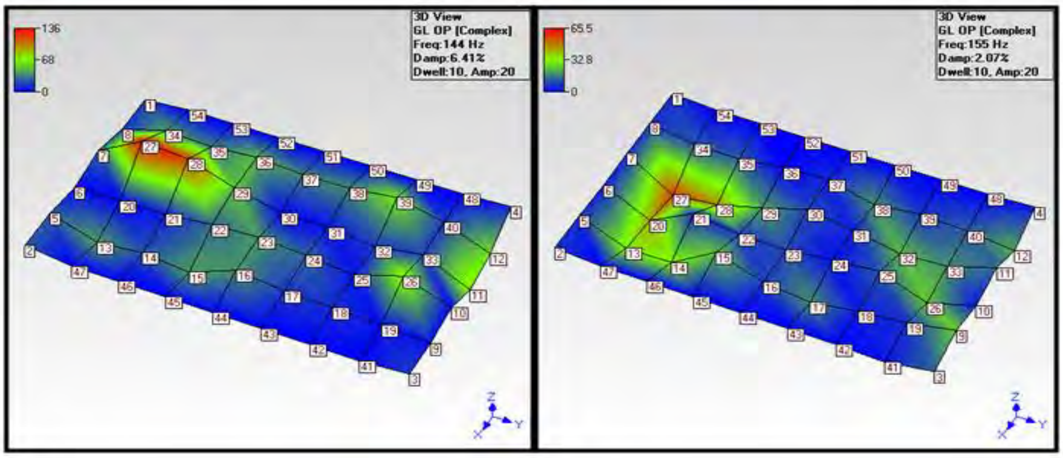

9th mode shape@ 144 Hz   10th mode shape@ 155 Hz

c) Comparison between experimental and computational mode shapes

1. Trunk panel

Mode No	Experimental mode shapes	Simulation mode shapes
7	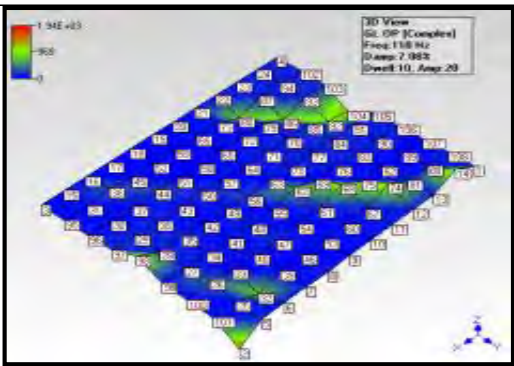	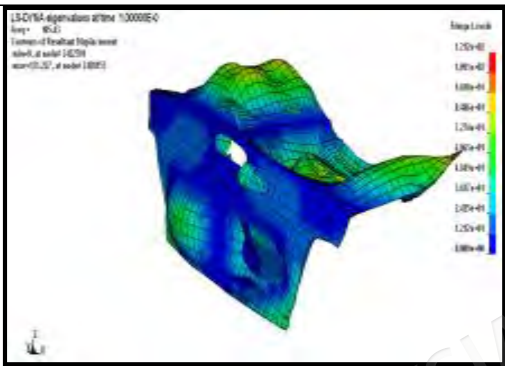
8	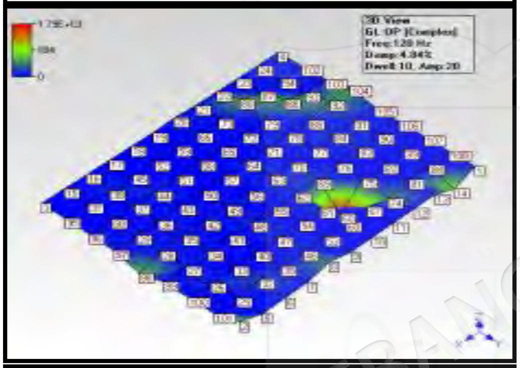	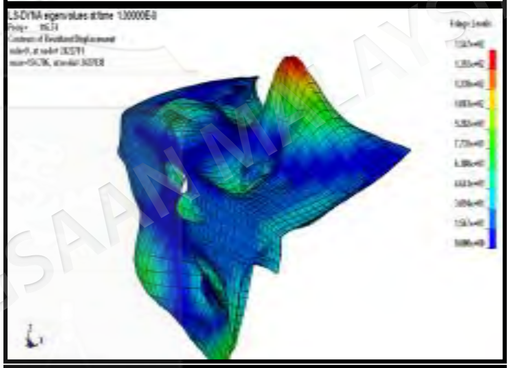
9	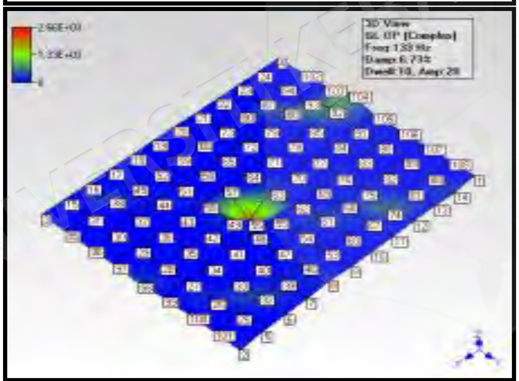	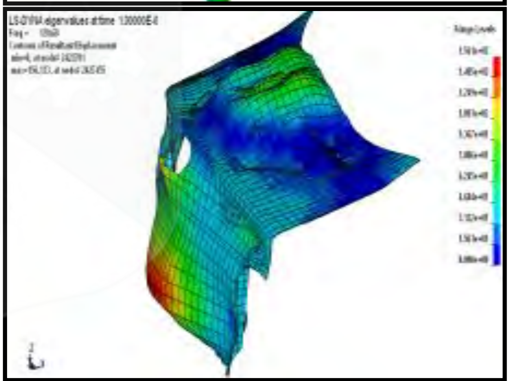
10	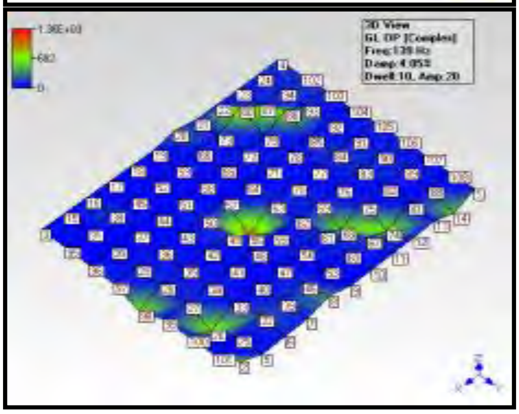	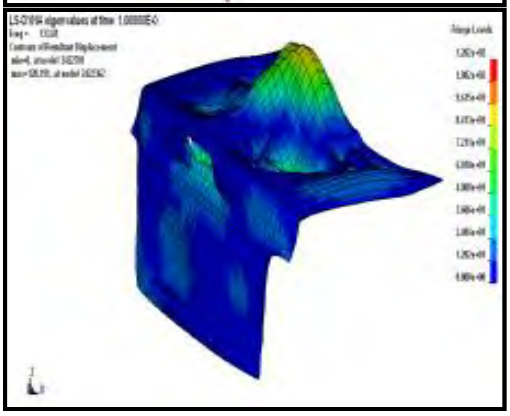

2. Hood panel

Mode No	Experimental mode shapes	Simulation mode shapes
7	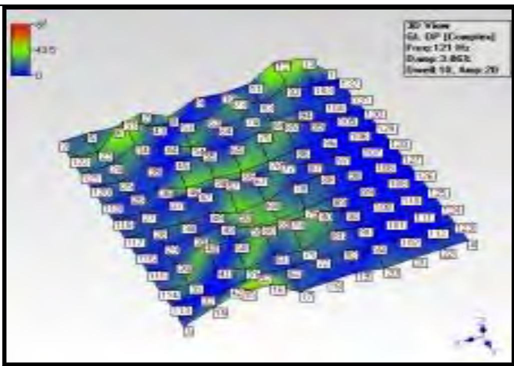	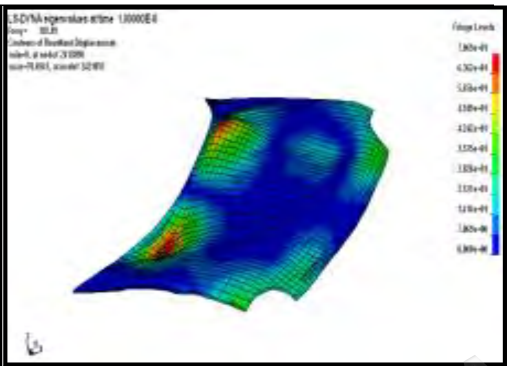
8	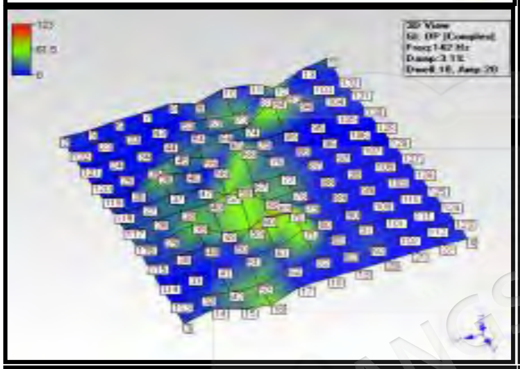	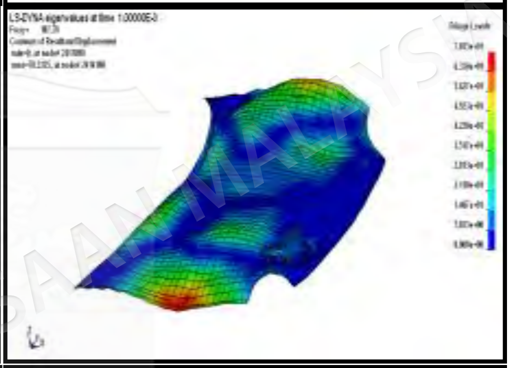
9	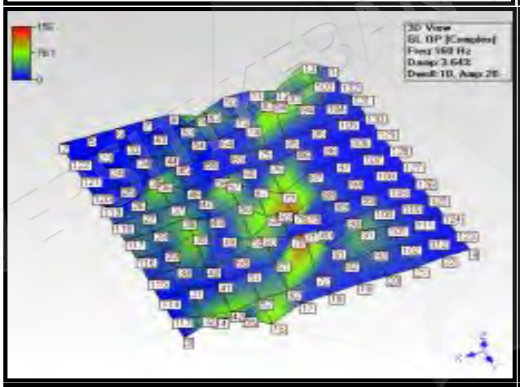	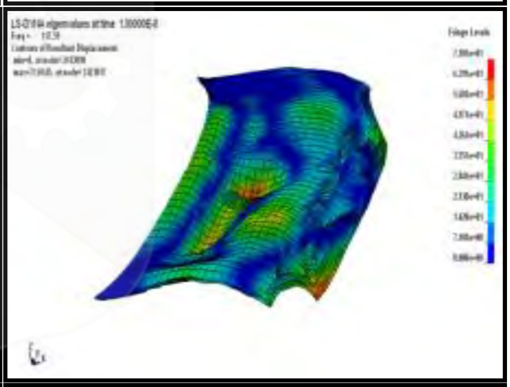
10	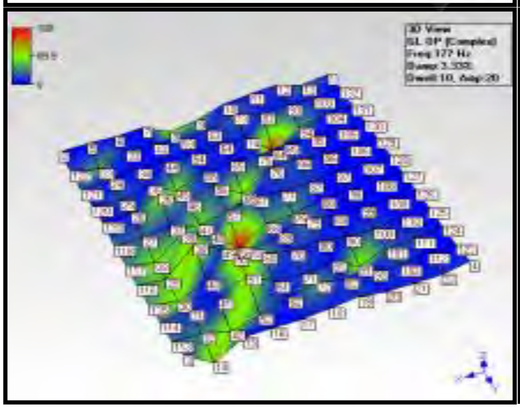	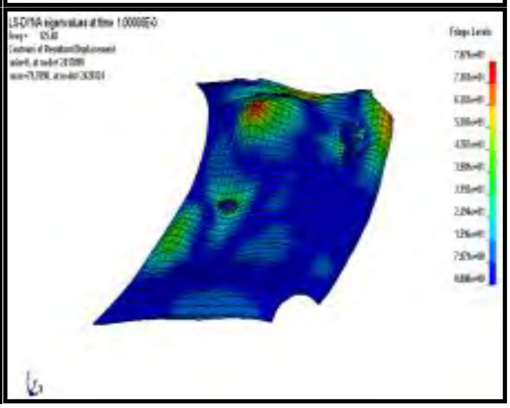

3. Roof panel

Mode No	Experimental mode shapes	Simulation mode shapes
7	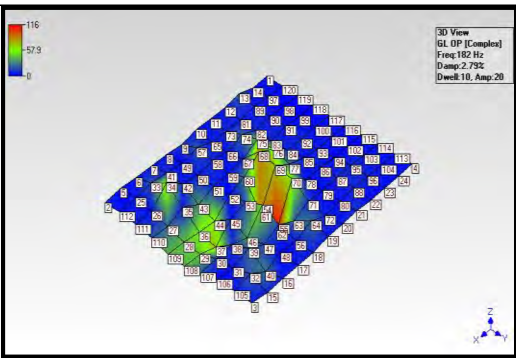	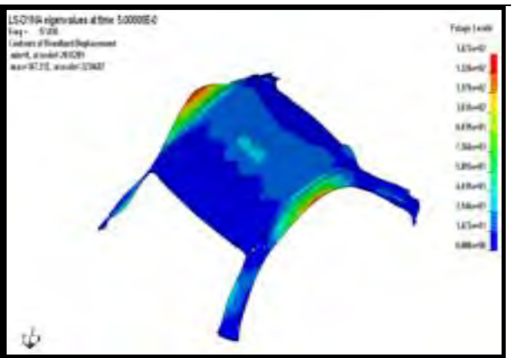
8	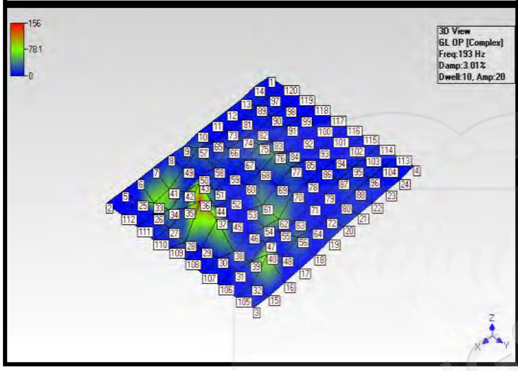	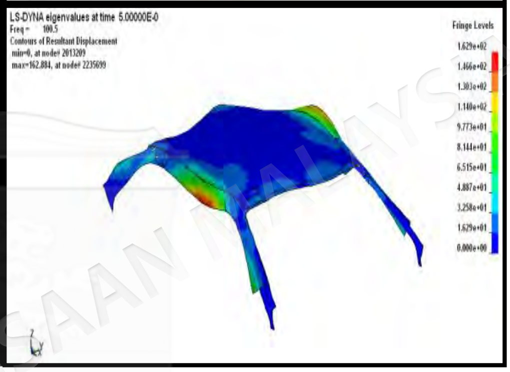

4. Door panel

Mode No	Experimental mode shapes	Simulation mode shapes
7	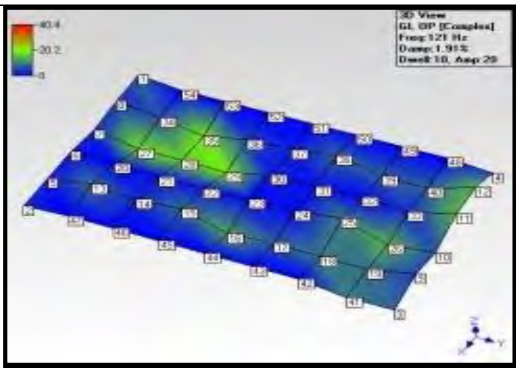	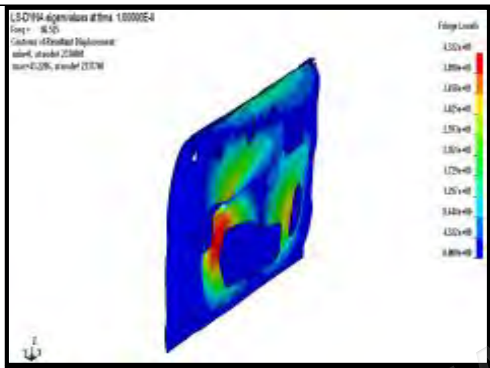
8	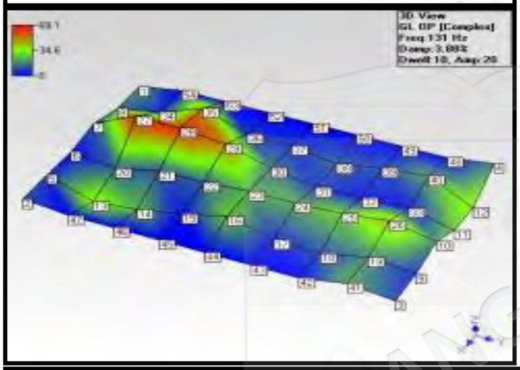	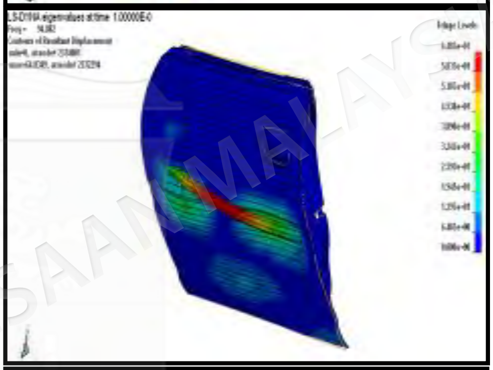
9	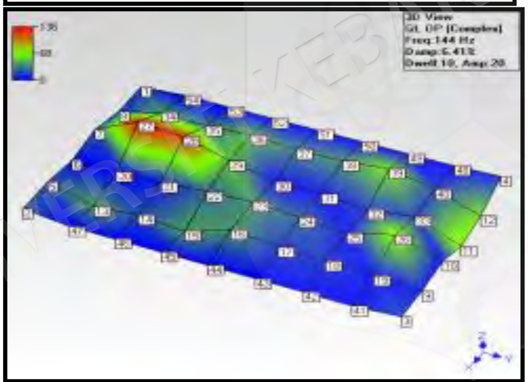	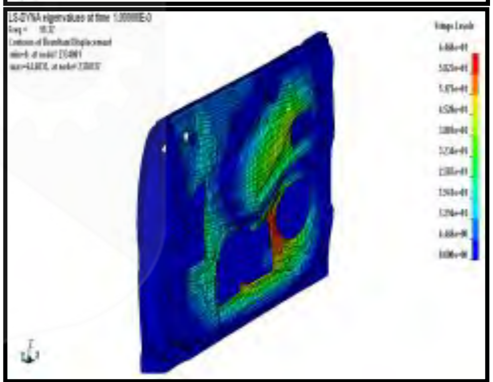
10	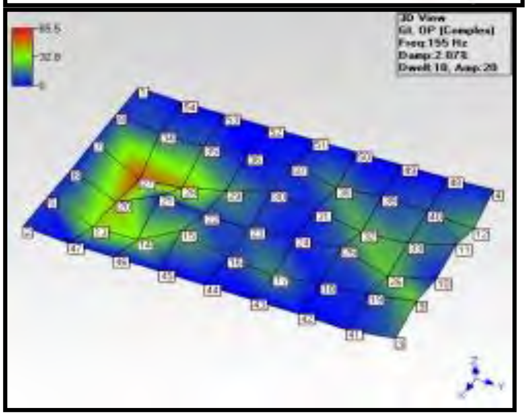	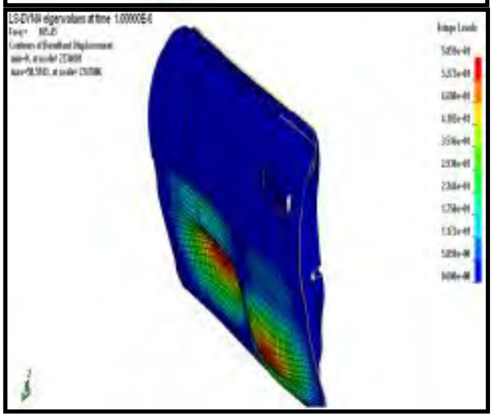

APPENDIX B

NOISE CONTOUR DATA INTERIOR THE CAR
(rear center excitation)

Points		Frequency &	sound level		Overall
1	Freq	163	170	261	0.425
	Sound level	0.077	0.081	0.097	
2	Freq	162	170	264	0.374
	Sound level	0.069	0.083	0.079	
3	Freq	163	169	276	0.338
	Sound level	0.071	0.072	0.046	
4	Freq	162	169	275	0.35
	Sound level	0.065	0.062	0.084	
5	Freq	162	170	276	0.355
	Sound level	0.058	0.062	0.085	
6	Freq	162	173	270	0.4
	Sound level	0.052	0.07	0.09	
7	Freq	163	173	270	0.403
	Sound level	0.053	0.082	0.087	
8	Freq	162	175	269	0.379
	Sound level	0.052	0.089	0.073	
9	Freq	162	175	269	0.384
	Sound level	0.056	0.099	0.056	
10	Freq	162	174	269	0.374
	Sound level	0.054	0.098	0.038	
11	Freq	162	176	276	0.592
	Sound level	0.114	0.124	0.046	
12	Freq	162	174	276	0.596
	Sound level	0.12	0.126	0.055	
13	Freq	162	172	276	0.55
	Sound level	0.103	0.126	0.097	
14	Freq	162	172	276	0.547
	Sound level	0.078	0.11	0.152	
15	Freq	163	172	276	0.59
	Sound level	0.068	0.1	0.176	
16	Freq	164	174	274	0.652
	Sound level	0.039	0.082	0.179	
17	Freq	163	176	273	0.621
	Sound level	0.039	0.088	0.155	
18	Freq	162	175	274	0.525
	Sound level	0.069	0.09	0.128	
19	Freq	159	176	275	0.518
	Sound level	0.065	0.103	0.101	
20	Freq	161	176	-	0.514
	Sound level	0.061	0.094	-	

Points		Frequency &	sound level		Overall
21	Freq	163	174	275	0.468
	Sound level	0.09	0.147	0.055	
22	Freq	163	173	275	0.444
	Sound level	0.083	0.126	0.062	
23	Freq	163	174	275	0.423
	Sound level	0.083	0.11	0.09	
24	Freq	163	173	277	0.456
	Sound level	0.089	0.099	0.128	
25	Freq	163	172	276	0.48
	Sound level	0.085	0.095	0.15	
26	Freq	164	172	276	0.511
	Sound level	0.073	0.076	0.15	
27	Freq	165	173	274	0.497
	Sound level	0.058	0.073	0.13	
28	Freq	163	175	275	0.492
	Sound level	0.054	0.084	0.11	
29	Freq	161	176	274	0.506
	Sound level	0.042	0.084	0.1	
30	Freq	158	176	272	0.52
	Sound level	0.037	0.088	0.107	
31	Freq	163	174	276	0.441
	Sound level	0.091	0.12	0.076	
32	Freq	163	174	276	0.508
	Sound level	0.085	0.122	0.084	
33	Freq	163	174	275	0.497
	Sound level	0.092	0.12	0.11	
34	Freq	163	173	273	0.459
	Sound level	0.085	0.1	0.11	
35	Freq	164	174	277	0.482
	Sound level	0.083	0.1	0.12	
36	Freq	165	174	275	0.48
	Sound level	0.074	0.1	0.129	
37	Freq	164	173	276	0.482
	Sound level	0.066	0.1	0.11	
38	Freq	165	174	275	0.49
	Sound level	0.065	0.099	0.093	
39	Freq	165	172	276	0.509
	Sound level	0.061	0.11	0.094	
40	Freq	165	172	275	0.518
	Sound level	0.053	0.1	0.079	
41	Freq	164	175	276	0.452
	Sound level	0.083	0.13	0.087	
42	Freq	164	175	276	0.444
	Sound level	0.087	0.13	0.078	

Points		Frequency &	sound level		Overall
43	Freq	164	174	275	0.424
	Sound level	0.094	0.14	0.085	
44	Freq	164	174	275	0.41
	Sound level	0.072	0.12	0.083	
45	Freq	165	174	275	0.412
	Sound level	0.071	0.12	0.082	
46	Freq	156	173	276	0.37
	Sound level	0.037	0.11	0.064	
47	Freq	166	173	275	0.4
	Sound level	0.054	0.1	0.068	
48	Freq	-	173	275	0.467
	Sound level	-	0.099	0.066	
49	Freq	161	173	275	0.477
	Sound level	0.027	0.095	0.068	
50	Freq	160	173	270	0.514
	Sound level	0.016	0.088	0.1	
51	Freq	164	174	275	0.427
	Sound level	0.067	0.11	0.093	
52	Freq	164	174	275	0.435
	Sound level	0.078	0.1	0.098	
53	Freq	163	174	275	0.415
	Sound level	0.09	0.12	0.087	
54	Freq	164	174	275	0.391
	Sound level	0.073	0.11	0.069	
55	Freq	164	174	275	0.382
	Sound level	0.069	0.11	0.058	
56	Freq	165	174	274	0.377
	Sound level	0.066	0.12	0.037	
57	Freq	160	174	270	0.373
	Sound level	0.041	0.12	0.048	
58	Freq	165	174	268	0.423
	Sound level	0.055	0.12	0.088	
59	Freq	165	175	270	0.451
	Sound level	0.043	0.12	0.093	
60	Freq	164	175	269	0.49
	Sound level	0.037	0.13	0.12	
61	Freq	162	176	275	0.39
	Sound level	0.069	0.046	0.089	
62	Freq	162	175	275	0.38
	Sound level	0.066	0.054	0.09	
63	Freq	162	175	276	0.385
	Sound level	0.067	0.048	0.075	
64	Freq	161	175	274	0.399
	Sound level	0.056	0.057	0.07	
65	Freq	165	175	275	0.444

Points		Frequency &	sound level		Overall
66	Freq	160	175	274	0.395
	Sound level	0.039	0.091	0.057	
67	Freq	158	174	272	0.42
	Sound level	0.041	0.089	0.067	
68	Freq	159	175	267	0.412
	Sound level	0.037	0.95	0.085	
69	Freq	158	175	270	0.39
	Sound level	0.033	0.097	0.096	
70	Freq	158	175	270	0.44
	Sound level	0.028	0.094	0.1	
71	Freq	162	168	276	0.466
	Sound level	0.07	0.07	0.071	
72	Freq	162	168	275	0.476
	Sound level	0.068	0.068	0.072	
73	Freq	162	168	275	0.534
	Sound level	0.062	0.064	0.071	
74	Freq	162	168	275	0.434
	Sound level	0.056	0.051	0.07	
75	Freq	162	167	274	0.435
	Sound level	0.052	0.044	0.072	
76	Freq	160	174	273	0.420
	Sound level	0.04	0.065	0.07	
77	Freq	158	174	273	0.394
	Sound level	0.041	0.074	0.067	
78	Freq	157	174	271	0.404
	Sound level	0.045	0.082	0.074	
79	Freq	158	174	270	0.385
	Sound level	0.036	0.9	0.076	
80	Freq	158	174	269	0.371
	Sound level	0.033	0.088	0.077	
81	Freq	164	170	276	0.421
	Sound level	0.073	0.068	0.045	
82	Freq	164	169	275	0.454
	Sound level	0.071	0.068	0.05	
83	Freq	164	169	275	0.50
	Sound level	0.068	0.06	0.05	
84	Freq	163	169	276	0.40
	Sound level	0.059	0.056	0.056	
85	Freq	160	169	-	0.384
	Sound level	0.049	0.048	-	
86	Freq	160	169	273	0.353
	Sound level	0.042	0.041	0.047	
87	Freq	160	172	274	0.344
	Sound level	0.044	0.05	0.036	
88	Freq	160	176	277	0.329
	Sound level	0.038	0.056	0.022	

Points		Frequency &	sound level		Overall
89	Freq	161	176	277	0.329
	Sound level	0.038	0.063	0.028	
90	Freq	161	172	277	0.333
	Sound level	0.034	0.061	0.028	
91	Freq	165	170	274	0.326
	Sound level	0.061	0.06	0.038	
92	Freq	164	169	277	0.31
	Sound level	0.062	0.057	0.036	
93	Freq	161	170	275	0.312
	Sound level	0.058	0.052	0.036	
94	Freq	161	170	275	0.325
	Sound level	0.057	0.052	0.035	
95	Freq	161	170	275	0.335
	Sound level	0.057	0.044	0.027	
96	Freq	160	169	-	0.324
	Sound level	0.043	0.048	-	
97	Freq	161	171	-	0.299
	Sound level	0.045	0.047	-	
98	Freq	161	172	277	0.352
	Sound level	0.044	0.05	0.021	
99	Freq	161	172	277	0.367
	Sound level	0.043	0.051	0.036	
100	Freq	161	172	276	0.368
	Sound level	0.044	0.056	0.045	

APPENDIX C

NOISE CONTOUR DATA INTERIOR THE CAR

(front center excitation)

Points	Frequency &	Sound level	Overall
1	Freq	62	0.41
	Sound level	0.215	
2	Freq	62	0.425
	Sound level	0.216	
3	Freq	62	0.416
	Sound level	0.226	
4	Freq	62	0.415
	Sound level	0.22	
5	Freq	62	0.418
	Sound level	0.227	
6	Freq	62	0.432
	Sound level	0.247	
7	Freq	62	0.441
	Sound level	0.259	
8	Freq	62	0.436
	Sound level	0.247	
9	Freq	62	0.424
	Sound level	0.222	
10	Freq	62	0.416
	Sound level	0.206	
11	Freq	62	0.4
	Sound level	0.17	
12	Freq	62	0.409
	Sound level	0.19	
13	Freq	62	0.41
	Sound level	0.2	
14	Freq	62	0.411
	Sound level	0.2	
15	Freq	62	0.409
	Sound level	021	
16	Freq	62	0.426
	Sound level	0.19	
17	Freq	62	0.5
	Sound level	0.188	
18	Freq	62	0.444
	Sound level	0.181	
19	Freq	62	0.453
	Sound level	0.189	
20	Freq	62	0.415
	Sound level	0.186	
21	Freq	62	0.46

Points	Frequency &	Sound level	Overall
22	Freq	62	0.614
	Sound level	0.184	
23	Freq	62	0.419
	Sound level	0.179	
24	Freq	62	0.428
	Sound level	0.177	
25	Freq	62	0.426
	Sound level	0.184	
26	Freq	62	0.421
	Sound level	0.189	
27	Freq	62	0.393
	Sound level	0.196	
28	Freq	62	0.372
	Sound level	0.179	
29	Freq	62	0.388
	Sound level	0.178	
30	Freq	62	0.4
	Sound level	0.175	
31	Freq	62	0.363
	Sound level	0.174	
32	Freq	62	0.36
	Sound level	0.178	
33	Freq	62	0.377
	Sound level	0.203	
34	Freq	62	0.365
	Sound level	0.196	
35	Freq	62	0.356
	Sound level	0.197	
36	Freq	62	0.369
	Sound level	0.197	
37	Freq	62	0.375
	Sound level	0.21	
38	Freq	62	0.391
	Sound level	0.222	
39	Freq	62	0.399
	Sound level	0.215	
40	Freq	62	0.392
	Sound level	0.214	
41	Freq	62	0.36
	Sound level	0.175	
42	Freq	62	0.343
	Sound level	0.163	
43	Freq	62	0.347
	Sound level	0.177	
44	Freq	62	0.385
	Sound level	0.184	

Points	Frequency &	Sound level	Overall
45	Freq	62	0.327
	Sound level	0.174	
46	Freq	62	0.317
	Sound level	0.167	
47	Freq	62	0.33
	Sound level	0.173	
48	Freq	62	0.343
	Sound level	0.185	
49	Freq	62	0.356
	Sound level	0.187	
50	Freq	62	0.371
	Sound level	0.189	
51	Freq	62	0.348
	Sound level	0.146	
52	Freq	62	0.338
	Sound level	0.151	
53	Freq	62	0.353
	Sound level	0.151	
54	Freq	62	0.326
	Sound level	0.146	
55	Freq	62	0.32
	Sound level	0.138	
56	Freq	62	0.302
	Sound level	0.146	
57	Freq	62	0.312
	Sound level	0.154	
58	Freq	62	0.337
	Sound level	0.17	
59	Freq	62	0.35
	Sound level	0.159	
60	Freq	62	0.359
	Sound level	0.151	
61	Freq	62	0.335
	Sound level	0.051	
62	Freq	62	0.321
	Sound level	0.0599	
63	Freq	62	0.341
	Sound level	00.545	
64	Freq	62	0.303
	Sound level	0.061	
65	Freq	62	0.286
	Sound level	0.061	
66	Freq	62	0.291
	Sound level	0.064	

Points	Frequency &	Sound level	Overall
67	Freq	62	0.278
	Sound level	0.0641	
68	Freq	62	0.322
	Sound level	0.06	
69	Freq	62	0.33
	Sound level	0.061	
70	Freq	62	0.359
	Sound level	0.05	
71	Freq	67	0.322
	Sound level	0.0489	
72	Freq	67	0.303
	Sound level	0.0347	
73	Freq	67	0.3
	Sound level	0.041	
74	Freq	62	0.336
	Sound level	0.0308	
75	Freq	62	0.308
	Sound level	0.0339	
76	Freq	62	0.297
	Sound level	0.0391	
77	Freq	62	0.309
	Sound level	0.0362	
78	Freq	62	0.331
	Sound level	0.0377	
79	Freq	62	0.346
	Sound level	0.0334	
80	Freq	62	0.364
	Sound level	0.035	
81	Freq	66	0.31
	Sound level	0.053	
82	Freq	66	0.302
	Sound level	0.0509	
83	Freq	66	0.303
	Sound level	0.0552	
84	Freq	65	0.309
	Sound level	0.0429	
85	Freq	65	0.304
	Sound level	0.05	
86	Freq	62	0.481
	Sound level	0.0497	
87	Freq	62	0.47
	Sound level	0.0494	
88	Freq	62	0.353
	Sound level	0.05	

Points	Frequency &	Sound level	Overall
89	Freq	62	0.341
	Sound level	0.051	
90	Freq	62	0.353
	Sound level	0.048	
91	Freq	62	0.305
	Sound level	0.0565	
92	Freq	67	0.301
	Sound level	0.0614	
93	Freq	67	0.318
	Sound level	0.055	
94	Freq	64	0.632
	Sound level	0.0525	
95	Freq	64	0.313
	Sound level	0.0618	
96	Freq	64	0.316
	Sound level	0.0719	
97	Freq	64	0.313
	Sound level	0.0651	
98	Freq	64	0.334
	Sound level	0.0677	
99	Freq	64	0.356
	Sound level	0.0573	
100	Freq	64	0.368
	Sound level	0.0548	

APPENDIX D
SUMMARY OF MODAL ANALYSIS RESULTS

No	Components	Freq [Hz]	Damp [%]	Mode shapes
1	Rear left wind panel	51.08	1.62	First bending mode
		75.73	1.67	Second bending mode
		94.09	0.072	Third bending mode
		251.91	3.45	Fourth bending mode
		328	2.86	Fifth bending mode
2	Rear right wind panel	61.06	4.55	First bending mode
		79.84	2.14	Second bending mode
		93.87	5.85	Third bending mode
		238.76	3.45	Fourth bending mode
		338.05	2.64	Fifth bending mode
3	Front left wind panel	49.83	3.55	First bending mode
		80.79	4.04	Second bending mode
		117.72	3.04	Third bending mode
		217.27	0.788	Fourth bending mode
4	Front right wind panel	180.36	0.305	First bending mode
		278.67	5.07	Second bending mode
		356.81	4.16	Third bending mode
5	Rear windshield panel	56.73	1.64	First bending mode
		100.79	3.56	Second bending mode
		153.59	4.37	Third bending mode
		314.68	2.32	Fourth bending mode
6	Front windshield panel	51.94	0.136	First bending mode
		106.39	2.82	Second bending mode
		148.31	0.147	Third bending mode
		168.47	3.05	Fourth bending mode
		227.39	6.29	Fifth bending mode
7	Front right door panel	43.42	9	First bending mode
		60.50	1.51	Second bending mode
		77.14	2.49	Third bending mode
		94.51	8.65	Fourth bending mode
8	Front left door panel	43.71	3.9	First bending mode
		60.87	1.63	Second bending mode
		74.11	2.25	Third bending mode
		93.37	2.62	Fourth bending mode
9	Rear right door panel	44.04	3.25	First bending mode
		65.96	4.12	Second bending mode
		91.28	0.94	Third bending mode
		113.90	1.74	Fourth bending mode

No	Components	Freq [Hz]	Damp [%]	Mode shapes
10	Rear left door panel	49.48	3.85	First bending mode
		68.52	2.55	Second bending mode
		93.56	6.53	Third bending mode
		128	3.09	Fourth bending mode
11	Roof panel	26.73	0.967	First bending mode
		55.50	5.76	Second bending mode
		98.12	5.42	Third bending mode
		132.41	3.3	Fourth bending mode
		166.29	2.87	Fifth bending mode
12	Floor	34.69	5.64	First bending mode
		50.04	7.87	Second bending mode
		58.10	3.73	Third bending mode
13	Engine hood	27.41	5.02	First bending mode
		37.81	2.96	Second bending mode
		66.00	2.77	Third bending mode
		95.47	4.46	Fourth bending mode
		195.29	2.79	Fifth bending mode
14	Trunk lid	29.84	5.55	First bending mode
		49.95	6.69	Second bending mode
		84.96	3.08	Third bending mode
		121.92	2.05	Fourth bending mode
15	Rear left quarter panel	53.64	2.73	First bending mode
		99.37	2.20	Second bending mode
		187.92	0.68	Third bending mode
		234.72	1.02	Fourth bending mode
16	Front left fender	85.49	5.85	First bending mode
		106.89	2.16	Second bending mode
		215.62	1.86	Third bending mode
		312	2.81	Fourth bending mode
17	Fuel tank	23.54	1.72	First bending mode
		32.99	1.41	Second bending mode
		108.68	1.8	Third bending mode
		130.45	0.406	Fourth bending mode
18	Exhaust system	16.69	3.49	First bending mode
		25.22	4.72	Second bending mode
		40.66	2.74	Third bending mode
		64.30	1.68	Fourth bending mode
		76.29	2.52	Fifth bending mode
		123.64	1.32	Sixth bending mode

No	Components	Freq [Hz]	Damp [%]	Mode shapes
19	Front suspension	15.08	6.56	First rigid body mode
		32.92	3.46	Second rigid body mode
		54.54	2.72	First bending mode
		62.49	6.34	First bending mode
		66.30	0.294	First bending mode
20	Rear suspension bar	187.48	2.63	Fist elastic mode
		235.61	0.42	Second elastic mode
		243.40	0.79	Third elastic mode
		260.38	2.65	Fourth elastic mode
21	Roof beam	98.40	2.06	First rigid body mode
		150.79	2.06	First bending mode
		162.79	4.73	Cantilever+twist end mode
		171.25	0.92	Twisting mode